NASA Contractor Report 172428

248p.

Propeller Aircraft Interior Noise Model

Utilization Study and Validation

L.D. Pope

L.D.POPE, PH.D., P.E./CONSULTING ENGINEER
The Woodlands, TX 77380

32756

CONTRACT NAS1-17281
September 1984

NASA
National Aeronautics and
Space Administration

Langley Research Center
Hampton, Virginia 23665

NASA Contractor Report 172428

Propeller Aircraft Interior Noise Model

Utilization Study and Validation

L.D. Pope

L.D.POPE, PH.D., P.E./CONSULTING ENGINEER
The Woodlands, TX 77380

CONTRACT NAS1-17281
September 1984

NASA
National Aeronautics and
Space Administration

Langley Research Center
Hampton, Virginia 23665

TABLE OF CONTENTS

TABLE OF CONTENTS (Continued)

TABLE OF CONTENTS (Continued)

LIST OF FIGURES

LIST OF FIGURES (Continued)

LIST OF FIGURES (Continued)

LIST OF TABLES

LIST OF TABLES (Continued)

1.0 SUMMARY

This report considers the utilization and the validation of a computer program designed for aircraft interior noise prediction. The program, entitled PAIN, permits (in theory) predictions of sound levels inside propeller driven aircraft arising from sidewall transmission. The objective of the present work is to determine the practicality of making predictions for various airplanes and the extent of the program's capabilities. The ultimate purpose is to discern the quality of predictions for tonal levels inside an aircraft occurring at the propeller blade passage frequency and its harmonics. This effort involves three tasks:

1) program validation through comparisons of predictions with scale-model test results,

2) development of utilization schemes for large (full scale) fuselages, and

3) validation through comparisons of predictions with measurements taken in flight tests on a turboprop aircraft.

Findings should enable future users of the program to efficiently undertake and correctly interpret predictions.

2.0 INTRODUCTION

PAIN (an acronym for Propeller Aircraft Interior Noise) is a computer program that has been developed for predicting sound levels inside an airplane caused by the rotation of a propeller (of any design) alongside. PAIN can calculate the tonal levels in the cabin space occurring at the propeller blade passage frequency and its harmonics.

PAIN mechanizes an analytical model that can be found in Reference (1). The program's Users' Manual, Ref. (2), contains a basic overview of the mechanization and specifies the input data requirements. There are some features of the PAIN model that make it unique in interior noise work:

1) it requires a precise description of the propeller noise signature (pressure field) on the fuselage skin,

2) fuselage sidewall dynamic restraint offered by a structurally integral stiffened floor in a ring-stringer stiffened cabin shell is included, and

3) the acoustic modes of the complex cabin configuration (with floor partition) are utilized; cabin acoustic and fuselage structural modal losses are computed using the sidewall trim properties.

Theoretical developments, experiments, and validation studies that preceded PAIN and culminated in its invention are documented in Refs. (3) through (6). Some preliminary validation of PAIN for propeller noise prediction is given in Appendix E of Ref. (1). However the work reported herein should be considered the fundamental validation of the model. Here, the quality of PAIN interior noise predictions is explored through more extensive comparisons with scale-model and flight tests' results. The primary goal is to develop insight into the use of PAIN as a tool to make reliable full-scale aircraft predictions.

2.1 The PAIN Model

The elements of the PAIN model include a fuselage and a propeller (Figures 1 and 2). The fuselage consists of a cylinder stiffened by ring frames and stringers, and a floor that is structurally an integral part of the fuselage. The interior surface of the cabin (sidewall) is finished out with a trim consisting of insulation covered with a lining. The propeller rotates about an axis parallel to the center line of the fuselage. PAIN will predict the space average sound pressure levels in the cabin space at each of the harmonics of the propeller (up to a maximum of ten (10) harmonics).

PAIN works with the pressure time histories (signatures) as defined over the fuselage at a number of closely spaced points on a grid that lies in the fuselage skin (Fig. 3). The pressures can be specified at up to 160 points on the upper quarter surface of the fuselage nearest the propeller. Fourier series are used to define the amplitudes and phases of each harmonic (at each location). PAIN then generates data for an identical grid on the lower quarter surface of the fuselage nearest the propeller (using the data input for the upper grid). The propeller data must be generated with a propeller noise prediction program such as PROPFAN (7) or NASA ANOPP (Aircraft Noise Prediction Program) (8).

Structural properties of the cylinder and floor are required as input data to compute the fuselage structural modes

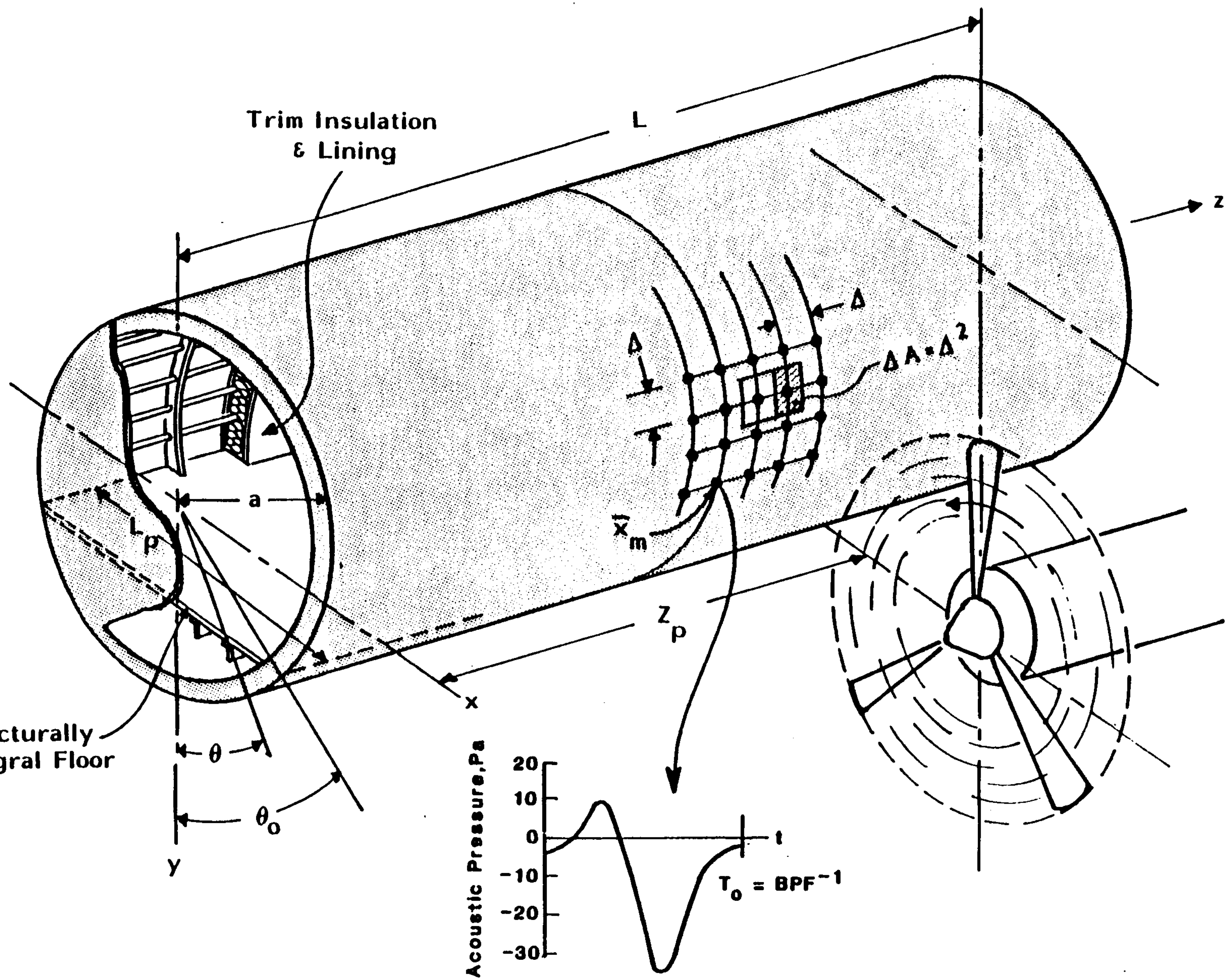

FIGURE 1. PROPELLER AIRCRAFT INTERIOR NOISE MODEL [1]

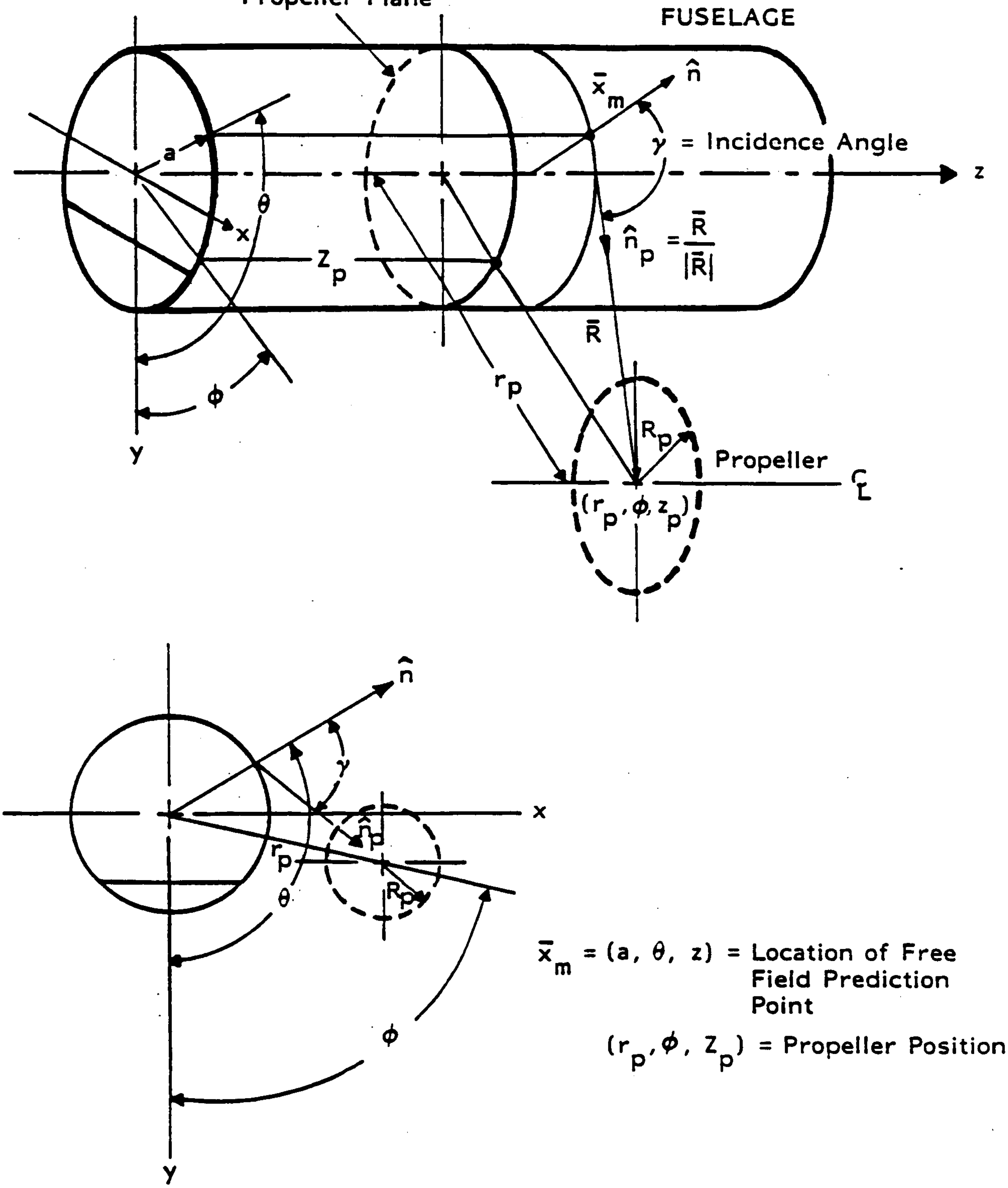

FIGURE 2. PROPELLER AND FUSELAGE SURFACE POINT GEOMETRY [1]

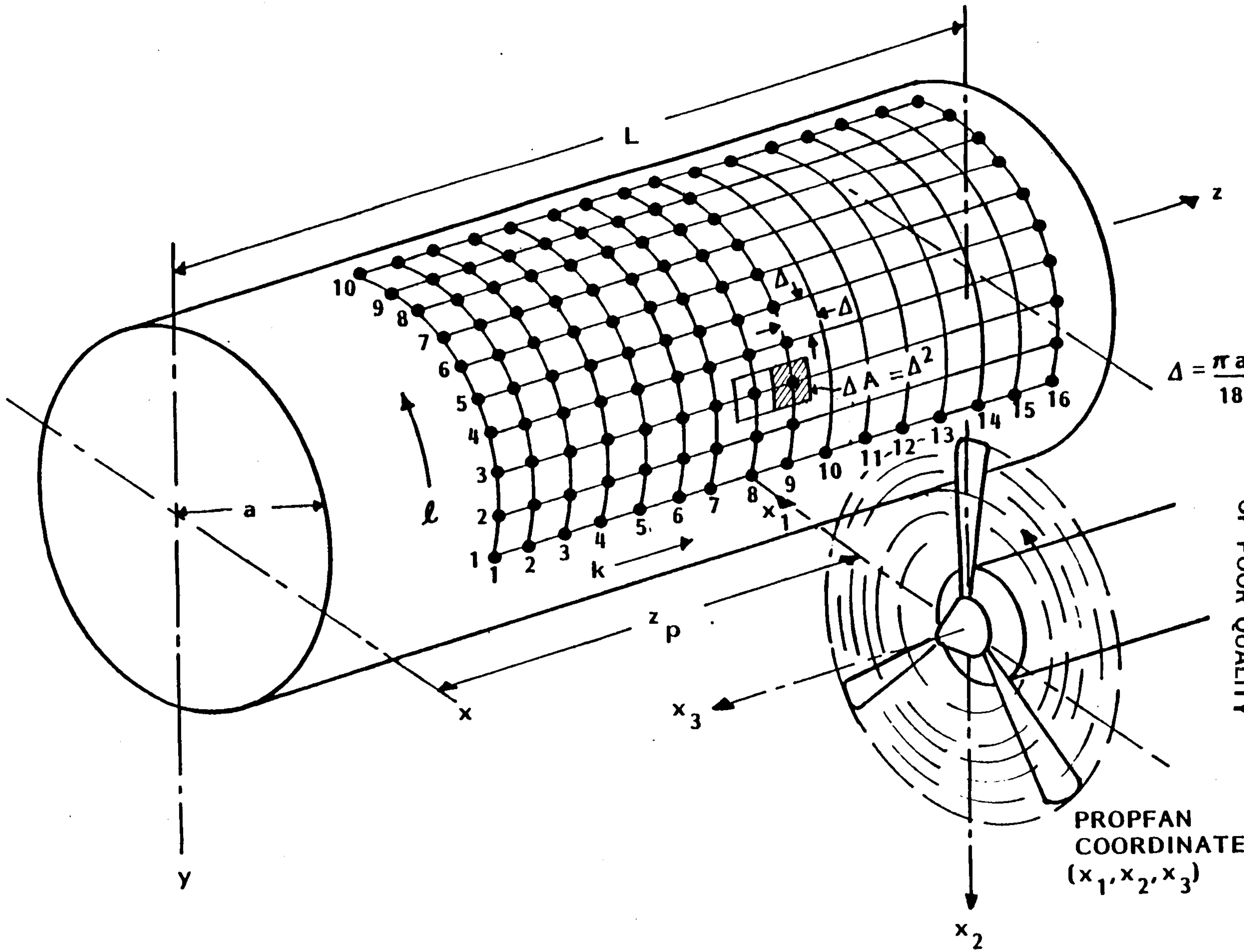

ORIGINAL PAGE IS
OF POOR QUALITY

FIGURE 3. GRID USED FOR PROPELLER NOISE PREDICTIONS [1]

(resonance frequencies and mode shapes). Associated structural loss factors must be input if the cabin is bare, but if trim is installed, the required modal loss factors are computed for the particular trim installation (estimates for the bare fuselage may still be input).

Similarly, acoustic modal properties of the cabin space (resonance frequencies, mode shapes, and loss factors) are calculated from input data specifying the cabin shape (floor angle, θ_0, of Figure 1, and the cabin length) and the trim properties.

Transmission and absorption characteristics of the trim (at a given frequency) are computed using input data for the wave impedance and complex acoustic wavenumber in the insulation, and the trim lining surface weight and its loss factor (theoretically as measured installed).

A step-by-step procedure to be followed in parameterizing the interior noise model is given in Section 3.0 of Ref. (2). Elaboration on the procedure and on the preparation of input data for full scale aircraft predictions is a major focus of this report.

2.2 PAIN Program Description

The main program PAIN computes and outputs the interior sound levels. It requires (as input) data that are generated by four auxiliary programs. One of the auxiliary programs calculates the acoustic modal properties of the cabin, two other programs the structural modal properties of the fuselage, and a fourth the propeller noise field.

The acoustic modes are calculated with the program CYL2D which determines the two-dimensional (cabin cross-section) modal characteristics (floor present), conditions the results and writes the data on a file (tape) for recall by the main program. PAIN uses the data to generate the complete three-dimensional modal set required for the noise predictions.

The structural modal data are generated with a program called MRPMOD whose output is also to a file (tape) read by PAIN. In addition to its own input data, MRPMOD reads two files (tapes) that are used for output from the fundamental structural program MRP. MRP computes the mode shapes and resonance frequencies, and must be run twice, once for the symmetric modes and once for the antisymmetric modes. The two files (tapes) created by these runs are read by MRPMOD, which conditions these data for PAIN.

As stated, the propeller noise data must be calculated with a propeller noise prediction program, such as the NASA Langley PROPFAN (7) program or that of ANOPP (8). This auxiliary program is not part of PAIN as are the programs CYL2D, MRP, and MRPMOD.

Section 4.0 of Ref. (2) should be consulted for an expanded overall program description with accompanying flow chart. Sections 5.0 and 6.0 of Ref. (2) deal with the input data requirements and control cards.

2.3 Report Organization

In this report, comparisons are first made between predictions and measurements from a set of scale model experiments. Next consideration is given to the application of the PAIN program to real aircraft, and to the development of utilization schemes that will allow its efficient use on a full scale airplane. Comparisons are then made between PAIN predictions and flight test results for a particular propeller-driven airplane.

3.0 SCALE-MODEL TESTS AND COMPARISONS

The tests considered in this section provide results for the most direct type of comparison of PAIN predictions and measurements. All of the basic elements of the analytical model are present in the test hardware and the test rig. Nothing is present that does not have an analytical counterpart. The PAIN model (Figure 1) is a propeller excited segment of a cylindrical fuselage stiffened by rings and stringers, with an integral stiffened floor and sidewall trim (lacking wings and empennage). This is exactly the description of the scale-model hardware and test configuration shown in Figures 4 through 7.[1] When PAIN is applied to real aircraft, the problem of fuselage modeling must be addressed; effects of non-uniformity of cross-section, presence of wings and empennage, etc., may need to be examined. Here, however, a simple question is asked: "How good are the interior predictions given that the computer creates counterparts of all elements of the test?".

In the present tests, the propeller tones are much higher around the propeller plane than near the end caps. The transmission to the interior is overwhelmingly dominated by sound passing through the cylinder wall. Because of this, the tests are free of problems introduced by the end caps. It is evident that the tests simulate, in a realistic physical manner, the transmission of propeller noise into an airplane cabin. The basic physical mechanisms of propeller tone transmission are, in fact, being duplicated in the test. It

---

[1] Illustrations of tests and hardware based on sketches provided by C.M. Willis, NASA Langley Research Center.

ORIGINAL PAGE IS
OF POOR QUALITY

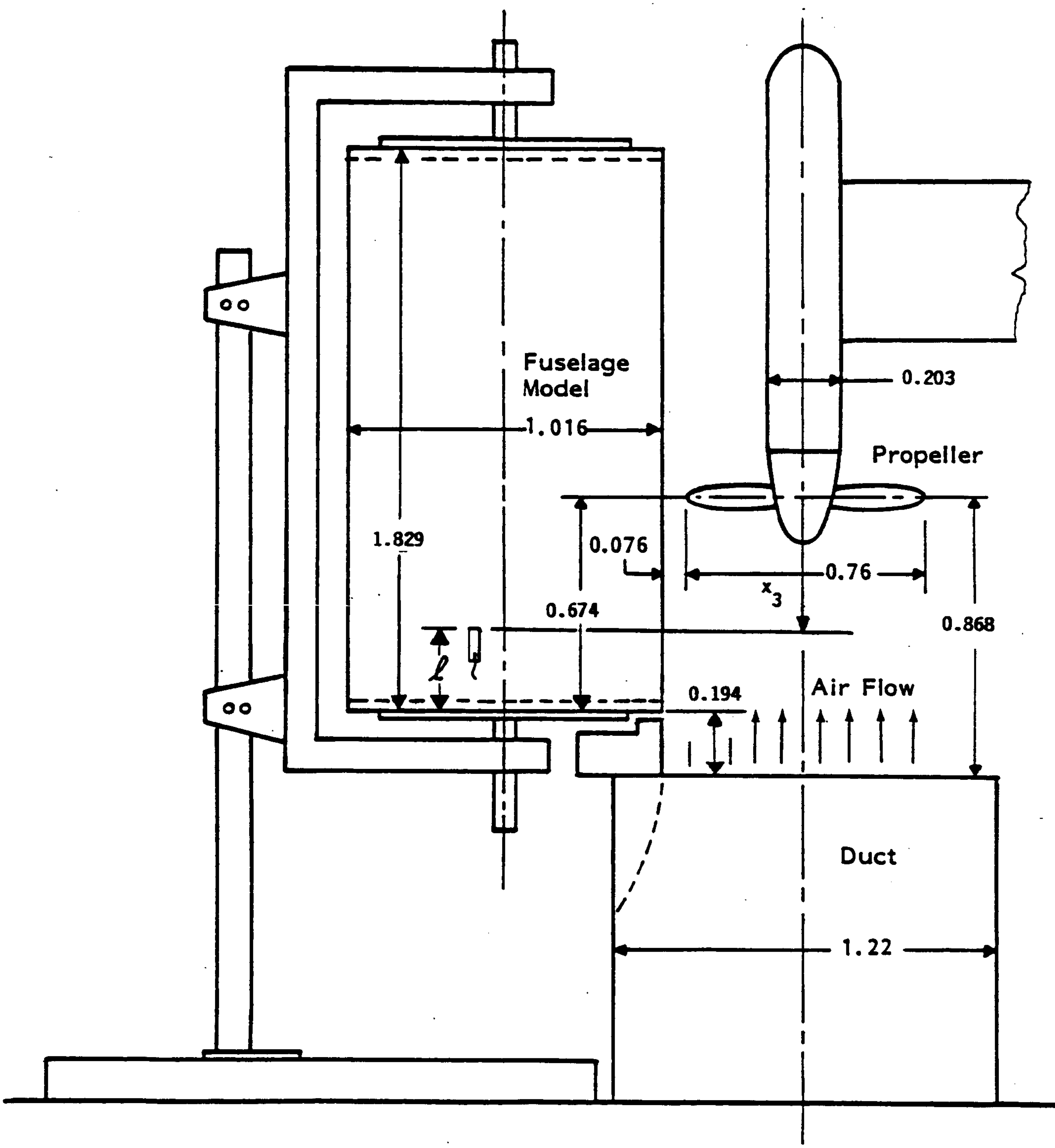

FIGURE 4. MODEL TEST FACILITY [1]
(Dimensions in meters)

ORIGINAL PAGE IS
OF POOR QUALITY

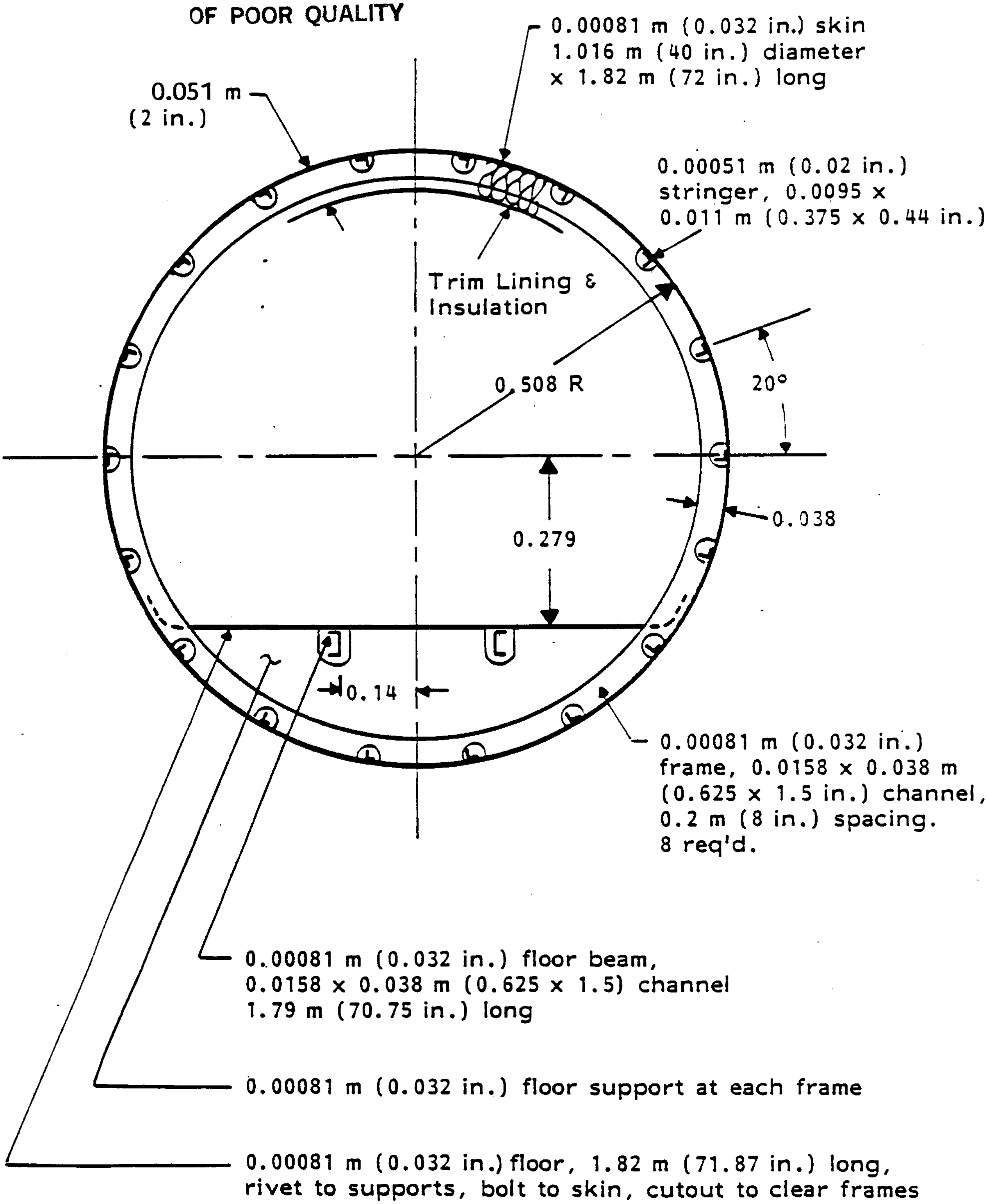

FIGURE 5. FUSELAGE MODEL [1]

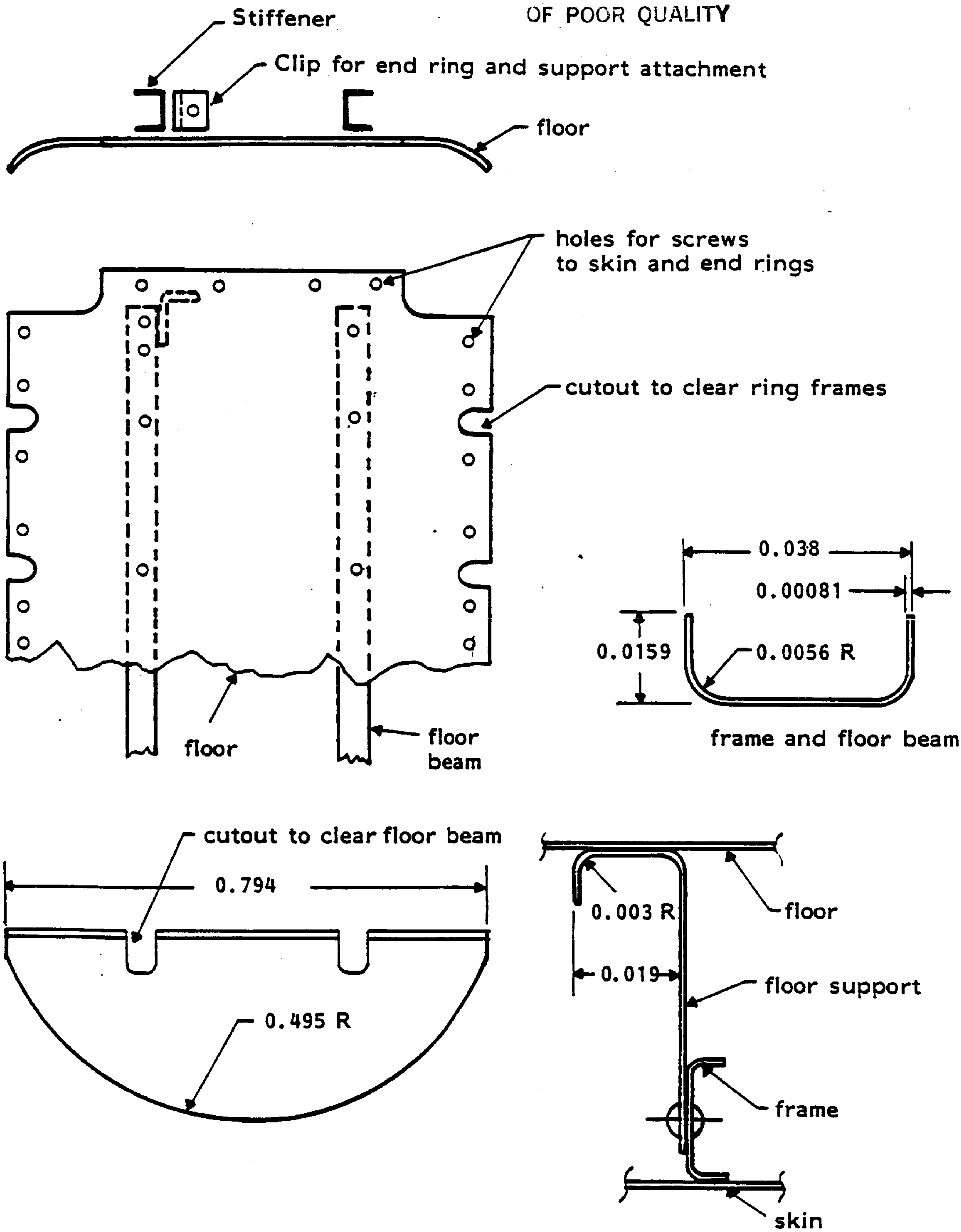

FIGURE 6. FLOOR ASSEMBLY [1]
(Dimensions in meters)

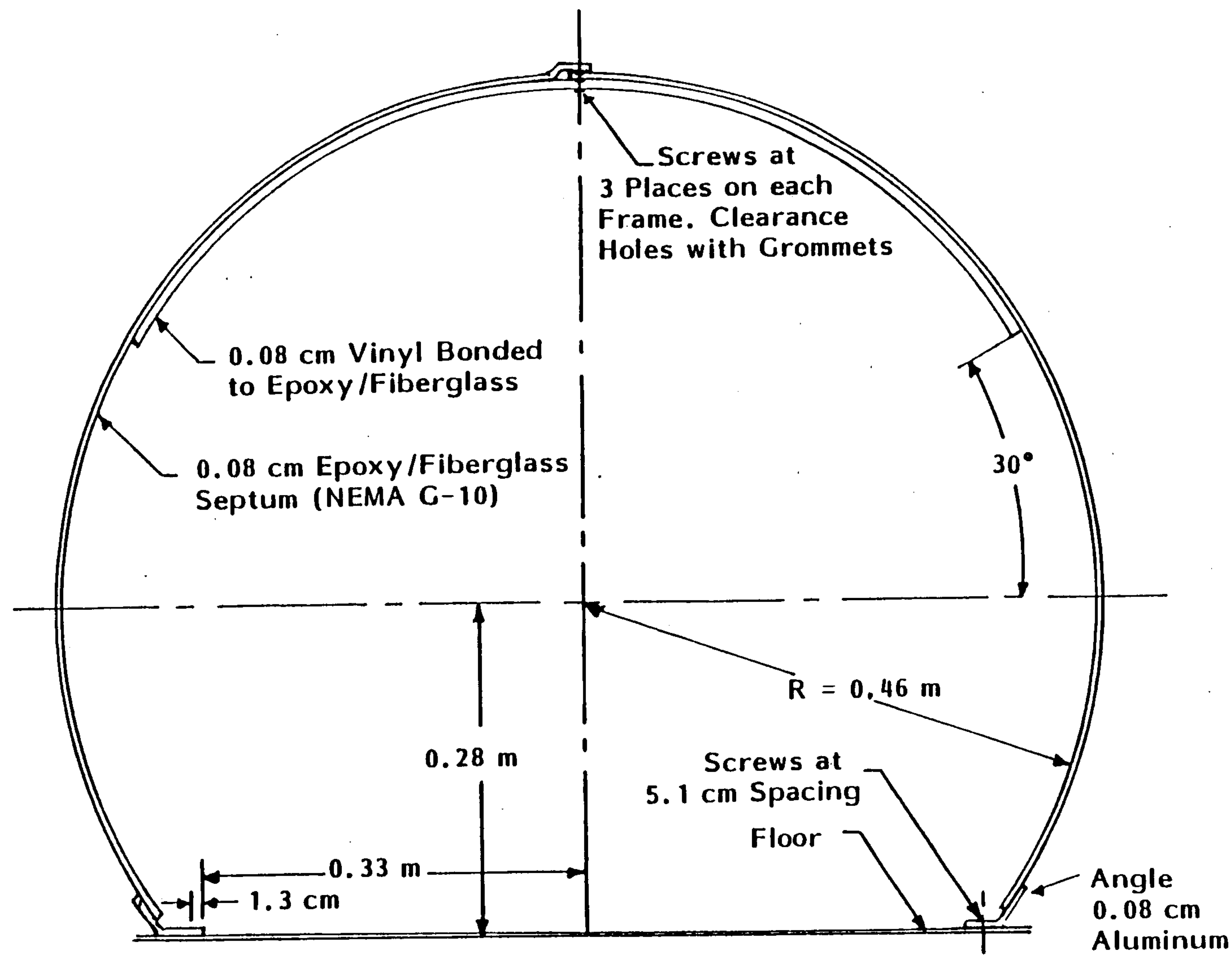

FIGURE 7. CROSS-SECTION OF TEST CYLINDER SHOWING TRIM [1]

is reasonable, therefore, to expect good predictions with PAIN only if good physical modeling has been achieved, i.e., with respect to the coupling of the propeller pressure field with the sidewall and sidewall with the trim. Also the sidewall and floor response must be properly predicted and their coupling to the interior acoustic space adequately described. The rapid decay of the pressure field away from the propeller plane leads to the above conclusions.

3.1 Test Configuration

The test configuration is shown in Figure 4. The fuselage and propeller are located downstream of a duct that supplies air to simulate airplane forward velocity.

3.1.1 Fuselage[2]

The fuselage (Fig. 5) is a cylinder 1.83m (72 in.) long and 1.02m (40 in.) in diameter. The skin is 0.00081m (0.032 in.) thick and is stiffened by eighteen (18) stringers spaced on 20° centers. The stringers are 90° angles having dimensions of approximately 0.00953 x 0.00953 x 0.00051m (3/8 x 3/8 x 0.020 in.). They are riveted to the inside of the skin and pass through cut-outs in eight (8) internal ring frames that are spaced along the cylinder every 0.2m (8 in.) The frames are aluminum channels with dimensions of approximately 0.016 x 0.038 x 0.00081m (5/8 x 1-1/2 x 0.032 in.).

The floor of the cylinder (Fig. 6) consists of a 0.00081m

---

[2] Most of the descriptive information in this section can also be found in Appendix E of Ref. 1.

(0.032 in.) plate stiffened by supports of the same thickness spaced every 0.2m (8 in.). The supports extend downward from the floor to the bottom of the cylinder. There are also two floor beams (channels of the same dimensions as the cylinder ring frames) that run longitudinally, each located approximately 0.14m (5.5 in.) from the center of the floor. The width of the floor is 0.848m (33.4 in.) leading to a floor angle θ_0 of 56.6 degrees (see Fig. 1). The outer edge of the floor is bolted to the cylinder wall. The cylinder is closed by 0.013m (1/2 in.) thick end caps that are used to support the cylinder in the NASA Langley propeller test rig. The entire fuselage assembly is constructed of 2024-T3 aluminum.

3.1.2 Trim

The end caps are lined (inside) with one layer of 0.0127m (1/2 in.) thick Owens-Corning PF-105 Fiberglas having a density of 9.61 kg/m^3 (0.6 lb/ft^3) with a 0.00005m (0.002 in.) thick vinyl film facing. The circumference (or sidewall) is lined with four layers of the same material; three layers between frames and the fourth covering the frames. The unfaced surface of the fiberglass insulation is exposed inwardly. The finish trim is a sheet of epoxy/fiberglass material with properties of a National Electrical Manufacturers Association (NEMA) G-10 (equivalent to Mil. Spec. 18177, GEE). The thickness is 0.00079m (0.032 in.) and its surface mass is 1.465 kg/m^2 (0.3 lb/ft^2). The trim is hard mounted to the floor and attached to the rings by nine soft mounted screws (Fig. 7). A 120° sector of the trim surface is covered with a sheet of vinyl (similar to automobile upholstery) of the same thickness. The total weight of the trim is 6.58 kg (14.51 lb) with a surface area of 3.624 m^2 (39 ft^2) which averages out to 1.815 kg/m^2 (0.371 lb/ft^2).

The 120° sector of vinyl on the trim simulates a similar treatment in a well-known light aircraft. Its presence introduces a small (and undesirable) discontinuity in the surface weight of the trim but benefits the test by providing some damping of the hard epoxy/fiberglass trim. The PAIN model is designed to include a dissipative trim lining.

3.1.3 Propeller

The propeller is a three-bladed, 0.3 scale Hartzell for a Twin Otter aircraft with a diameter of 0.76m (30 in.). It is driven by a 30 kw (40 horsepower) variable speed electric motor capable of turning it up to 8000 rpm. The propeller blades are Series 16 airfoils. The clearance between the blade tip and cylinder wall is 1/10 of the propeller diameter or 0.076m (3 in.). In all tests the blade pitch is fixed at 20°.

3.2 Description of Tests[3]

The primary tests of concern here are those where the interior noise was measured as the propeller turned at different speeds. In the present study, three speeds are considered: 3000, 4000, and 5000 rpm. The airflow velocity in all three cases is 23.8 m/s (78 ft/sec), or about 46 knots.

In the propeller tests, with the model fuselage in place, the only acoustic measurements were of the sound levels inside the cylinder. These were taken with an array of eleven (11) micro-

---

[3] Tests reported herein were performed at NASA Langley Research Center.

phones spaced along a cylinder diameter to represent measurements over equal annular areas (Figure 8). The array was positioned at four axial stations, ℓ/L = 0.125, 0.375, 0.625, and 0.875, representing the center of four subvolumes (segments) of the interior. At each of the four axial stations, there were 49 sampled locations obtained by positioning the array at $\phi = 0^\circ$, $\pm 51.5^\circ$ and $\pm 103^\circ$. (Note, for all tests, the angle θ in Figure 8 was 90°. θ and ϕ in Figure 8 are not to be confused with PAIN θ and ϕ of Figure 2.) A total of 196 measurement locations were sampled from which the space-average interior levels are obtained for each harmonic.

Supplementary tests were performed to assist in diagnostic work related to the determination (and/or evaluation) of PAIN input data and intermediate output. The PAIN program presently uses propeller noise predictions made for a free field condition, then applies a correction to account for the cylinder's presence. This is done because the blocked pressures are not available from present propeller noise prediction programs (it is the author's understanding that NASA Langley has begun work on this problem; PAIN can be easily modified to accept the new type data when available - see Section 3 of Ref. (2)).

Free field measurements of the propeller noise field were made to compare against the PAIN propeller noise input data created with ANOPP. This was done to permit the determination of the extent of "biasing" of interior noise predictions by inaccurate exterior noise predictions from ANOPP. Figure 9 shows the test configuration. Measurements were made (with the cylinder absent) for the three propeller speeds used in the interior noise tests. The microphones were positioned such that predicted and measured data along the grid line

M	r/R
1,9	.250
2,10	.433
3,11	.559
4	.661
5	.750
6	.829
7	.901
8	.968

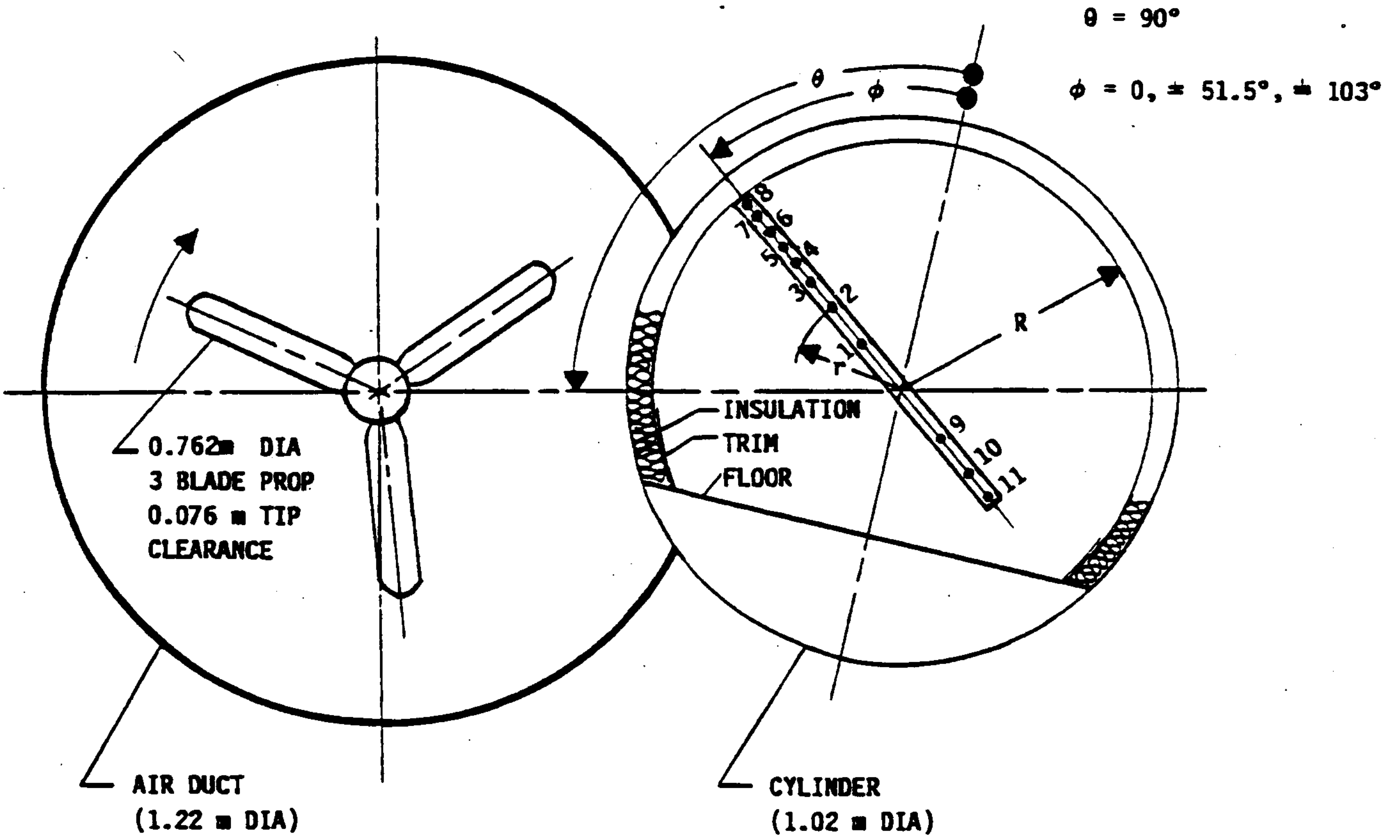

FIGURE 8. PROPELLER TESTS

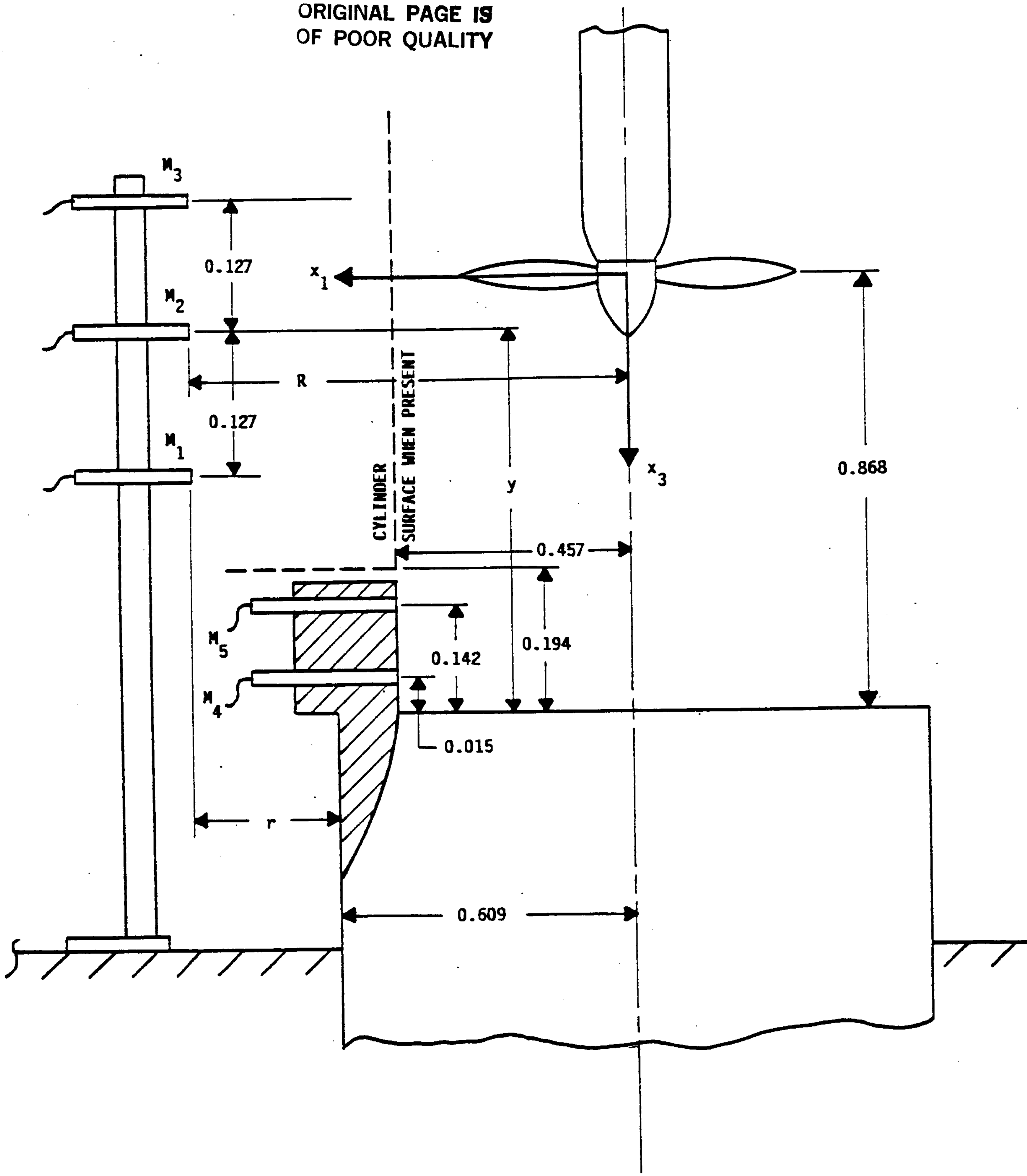

FIGURE 9. FREE FIELD MEASUREMENTS
(Dimensions in meters)

$\ell=1$ of Figure 3 could be compared.

A 0.508m (20 in.) diameter hardwood cylinder with flush-mounted microphones in its surface was used to measure blocked pressure levels along the grid line $\ell=1$ to determine the increase in sound pressure levels arising from surface reflections (the fact that the hard cylinder is only one-half the diameter of the model fuselage is probably not too serious a problem for measurements taken along $\ell=1$). The test configuration is shown in Figure 10.

Finally, measurements were made of acoustic and structural loss factors. As usual for these types of measurements, data are spotty, generally taken at whatever frequencies they could be reliably interpreted and generally unidentified with respect to particular modes.

3.3 Measurement Results

3.3.1 Loss factors

Acoustic and structural loss factors for the outfitted model fuselage are given in Table 1. All of the numbers are based on reverberation decay times of terminated excitation tones. The decay of the sound level inside the model fuselage's cabin determined the acoustic loss factor, η_n. The structural loss factors of the fuselage skin and of the finish trim are given respectively by η_r' and η_T. The loss factors are computed using the relation

$$\eta = 2.2/fT_{60} \quad ,$$

where f is the frequency of the excitation and T_{60} is the time for a 60 dB decay.

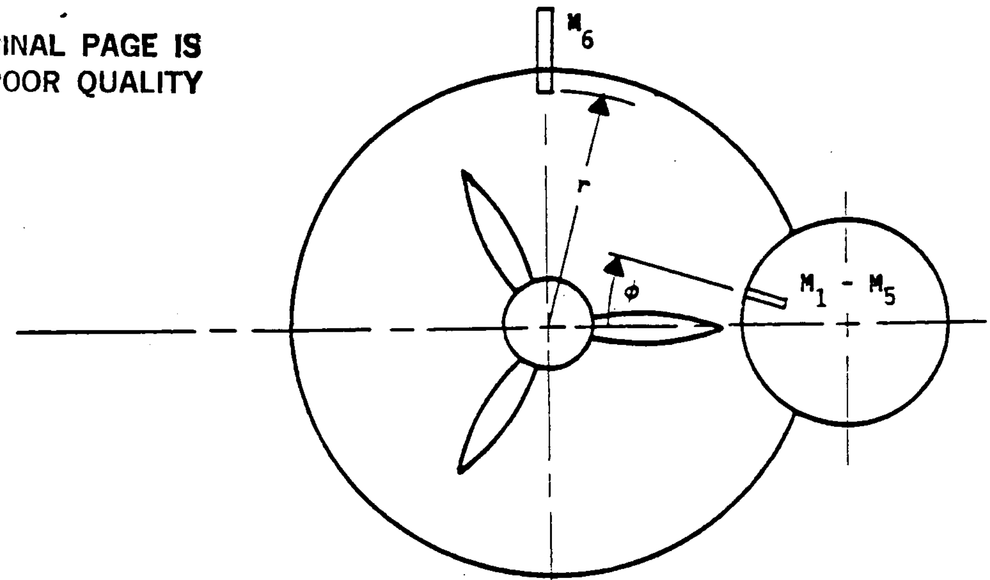

$\phi = 0°$

M	x_3(m)
1	0.508
2	0.102
3	0.0
4	-0.102
5	-0.508

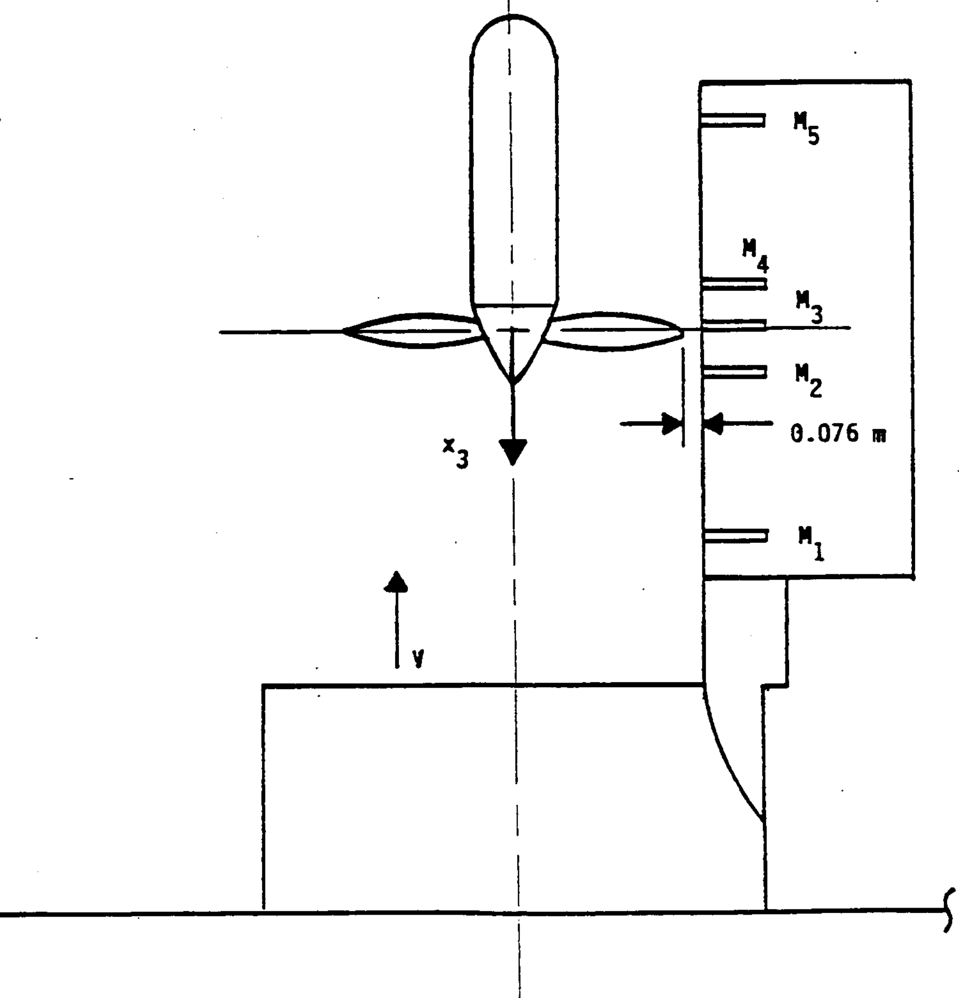

FIGURE 10. MICROPHONE LOCATIONS FOR BLOCKED PRESSURE MEASUREMENTS

Table 1. Measured Acoustic and Structural Loss Factors

Cabin (Micro.)		
Freq. (Hz)	T_{60} sine	η_n
93	1.2	0.020
115	0.61	0.031
142	0.46	0.033
192	0.27	0.042
289	0.40	0.019
301	0.21	0.034
377	0.53	0.011
452	0.19	0.025
512	0.33	0.013
655	0.37	0.009
702	0.13	0.024
755	0.058	0.050
865	0.048	0.053
932	0.094	0.025
942	0.078	0.029
1010	0.15	0.015
1260	0.11	0.016
1355	0.10	0.016
1700	0.10	0.013
1755	0.04	0.031
1770	0.021	0.059
1965	0.029	0.038
2000	0.032	0.034
2000	0.008	0.137
2037	0.018	0.060
2162	0.017	0.060
5625	0.089	0.004
5725	0.034	0.011

Trim (accel.)		
Freq. (Hz)	T_{60} trim	η_T
45	0.462	0.105
88	0.442	0.056
110	0.091	0.219
170	0.065	0.199
216	0.065	0.156
290	0.065	0.116
400	0.065	0.085
500	0.039	0.113
650	0.035	0.097
825	0.042	0.063
1000	0.030	0.073
1150	0.021	0.091
1400	0.027	0.058
1500	0.025	0.059
1800	0.014	0.087
2100	0.032	0.015
2300	0.015	0.064
2800	0.015	0.052
3400	0.019	0.034
4100	0.038	0.014
4600	0.023	0.020

Fuselage (accel.)		
Freq. (Hz)	T_{60} panel	η_T'
127	0.30*	0.057
500	0.041*	0.107
890	0.043	0.057
1345	0.031*	0.053
1465	0.041	0.037
2337	0.047	0.020
2710	0.026*	0.031
4225	0.017*	0.031

* ring and stringer

* stringer

3.3.2 Propeller noise

The measured free field propeller noise levels are shown in Figures 11 through 13. The data are for the grid line $\ell=1$ as previously noted in Section 3.2. In the figures, the plotted values are one-third octave band levels for those bands in which the propeller blade passage frequencies and their harmonics lie. These are to be considered the true tonal levels where it is evident that the tones clearly dominate (for instance near the propeller plane). Broad-band noise appears to be present in measurements at large distances from the plane of rotation. Figure 14 shows a typical measured spectrum. Comparison of measurements in Figure 14 with the data plotted in Figure 13 (Run No. 8113, Microphone 1), shows that the peaks correspond to the third-octave levels at least out to the fourth harmonic.

Phase measurements that were made in the 4000 and 5000 rpm cases are shown in Figures 15 and 16. The arrows indicate the approximate phase differences measured with microphone pairs (1,3) and (2,3) in runs 8112 and 8113.

3.3.3 Interior sound levels

Sound pressure levels at the blade passage frequencies and their harmonics are given in Tables 2, 3, and 4. The interior measurements were analyzed in one-third octave bands and the band levels for those bands containing the tones were taken as the tonal levels. The first three harmonics were sufficiently high on the inside to clearly dominate the broad-band noise background. Narrow band analyses of a few records indicated that the fourth and higher harmonics were so far down in the noise that data for those harmonics were defective. Figure 17 shows a typical interior spectrum illustrating the problem with

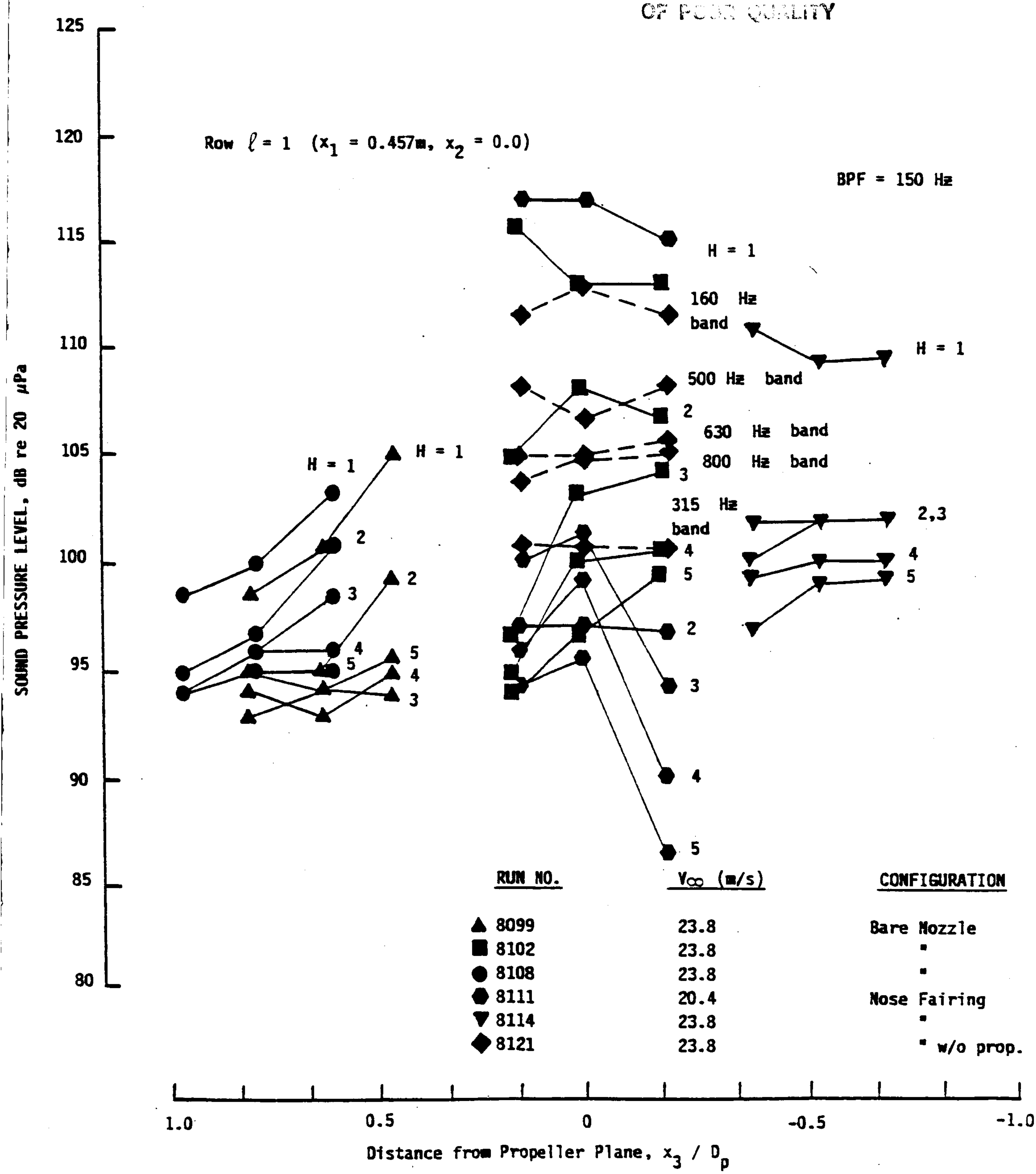

FIGURE 11. MEASURED FREE FIELD NOISE - PROPELLER AT 3000 RPM

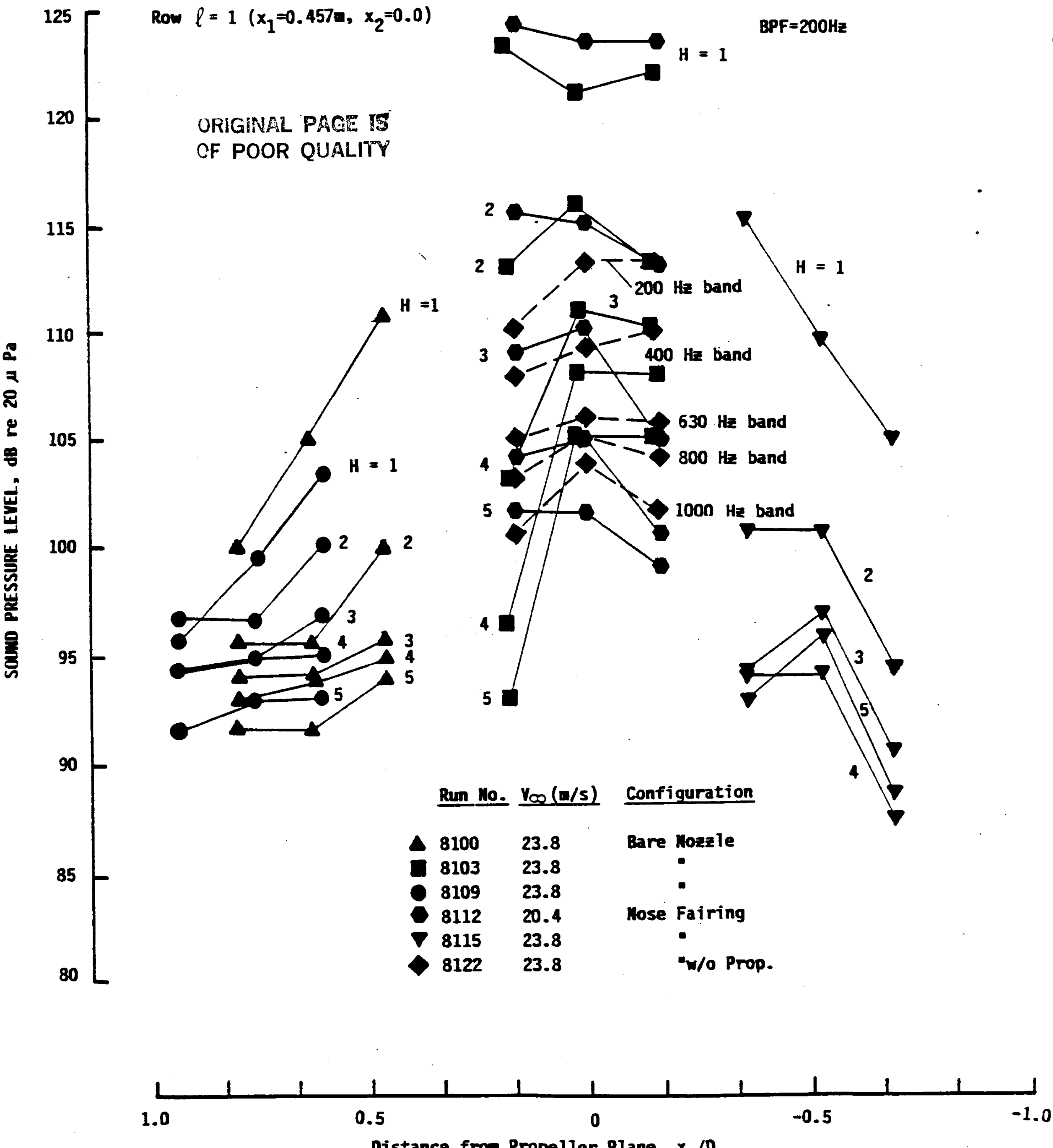

FIGURE 12. MEASURED FREE FIELD NOISE-PROPELLER AT 4000 RPM

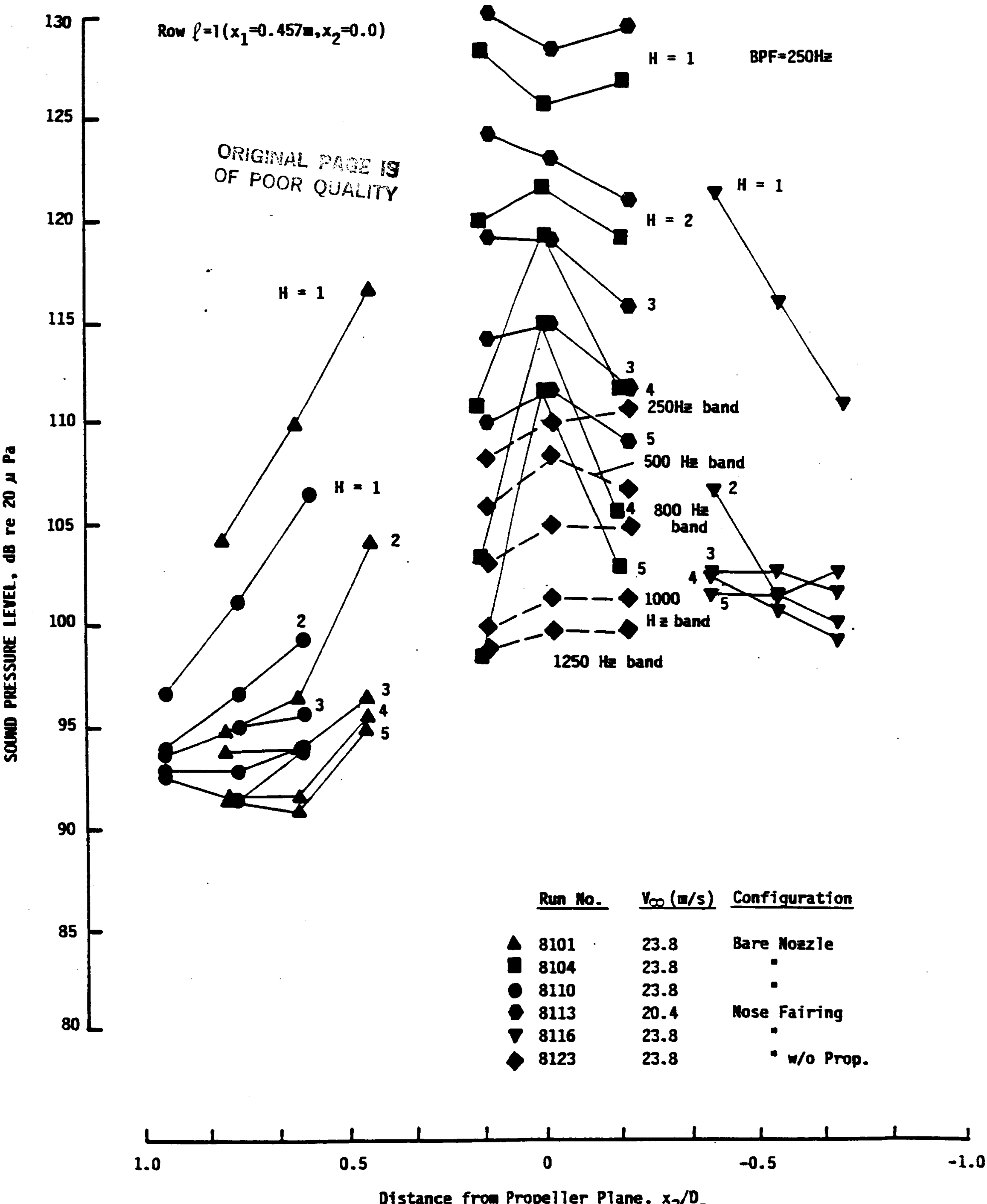

FIGURE 13. MEASURED FREE FIELD NOISE-PROPELLER AT 5000 RPM

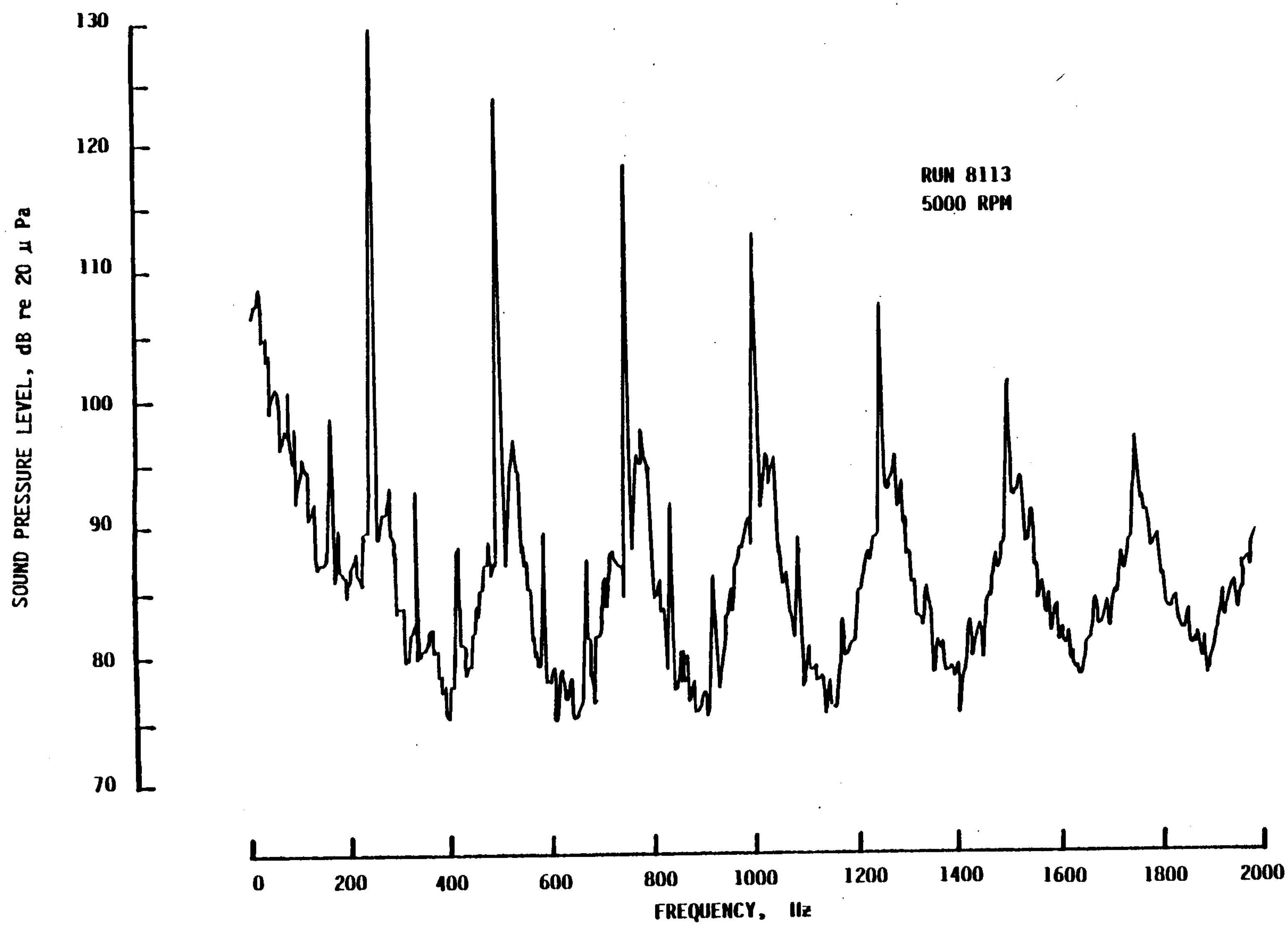

FIGURE 14. SPECTRUM OF FREE FIELD PROPELLER NOISE AT MICROPHONE 1.

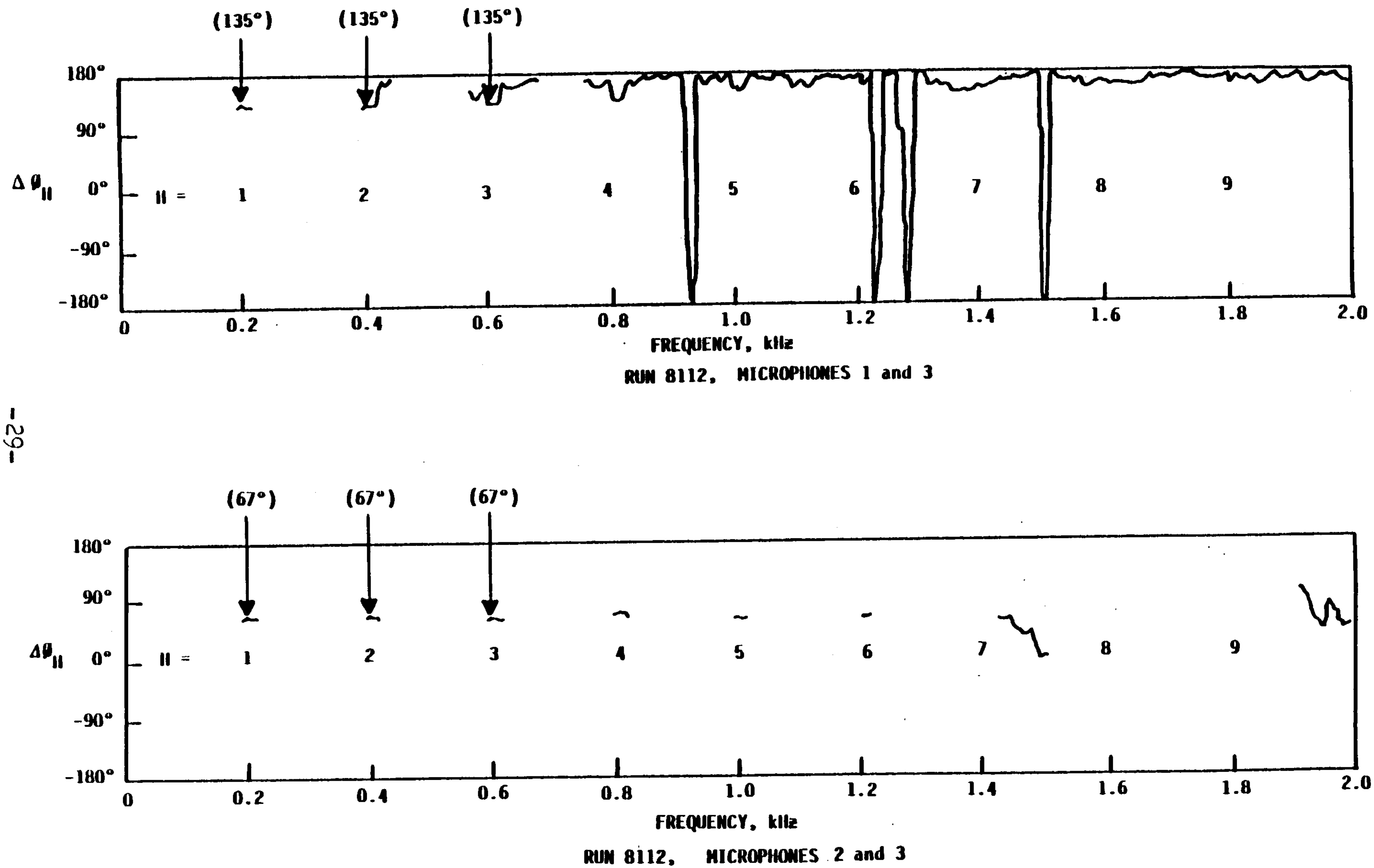

FIGURE 15. PHASE MEASUREMENTS, 4000 RPM
( ) = APPROXIMATE PHASE DIFFERENCE

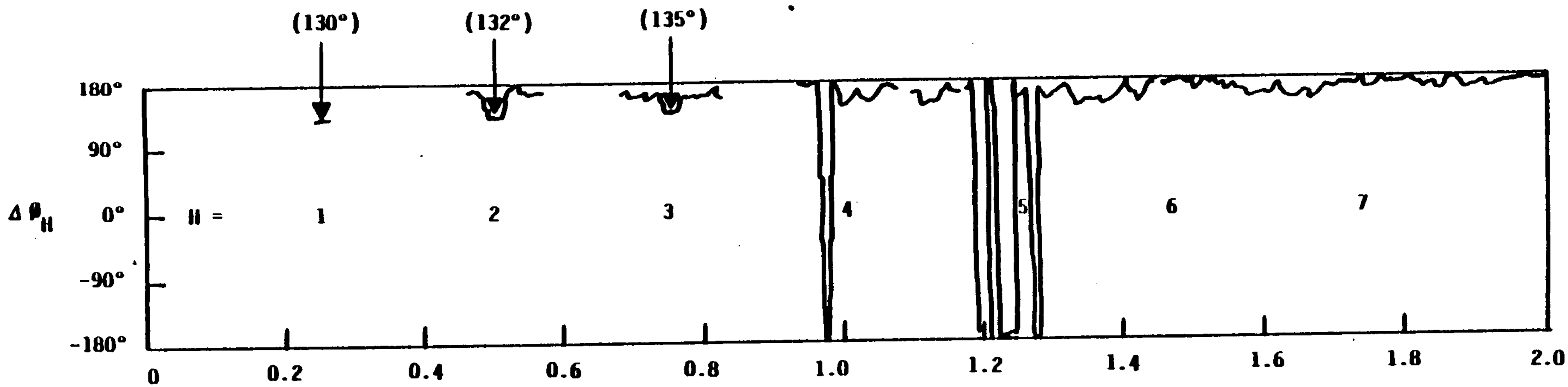

RUN 8113, MICROPHONES 1 and 3

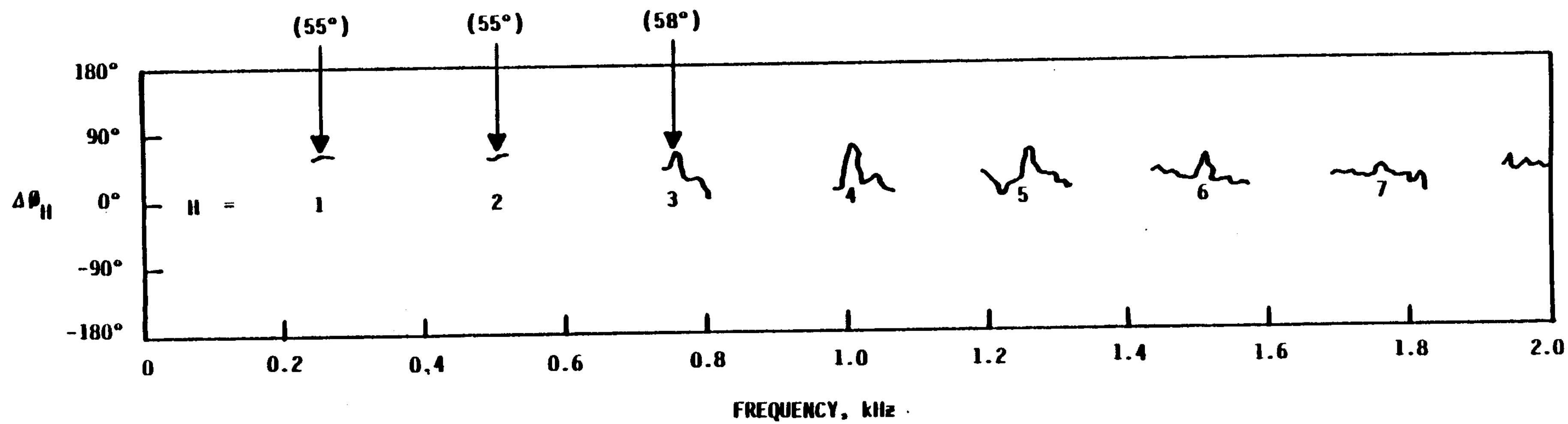

RUN 8113, MICROPHONES 2 and 3

FIGURE 16. PHASE MEASUREMENTS, 5000 RPM
( ) = APPROXIMATE PHASE DIFFERENCE

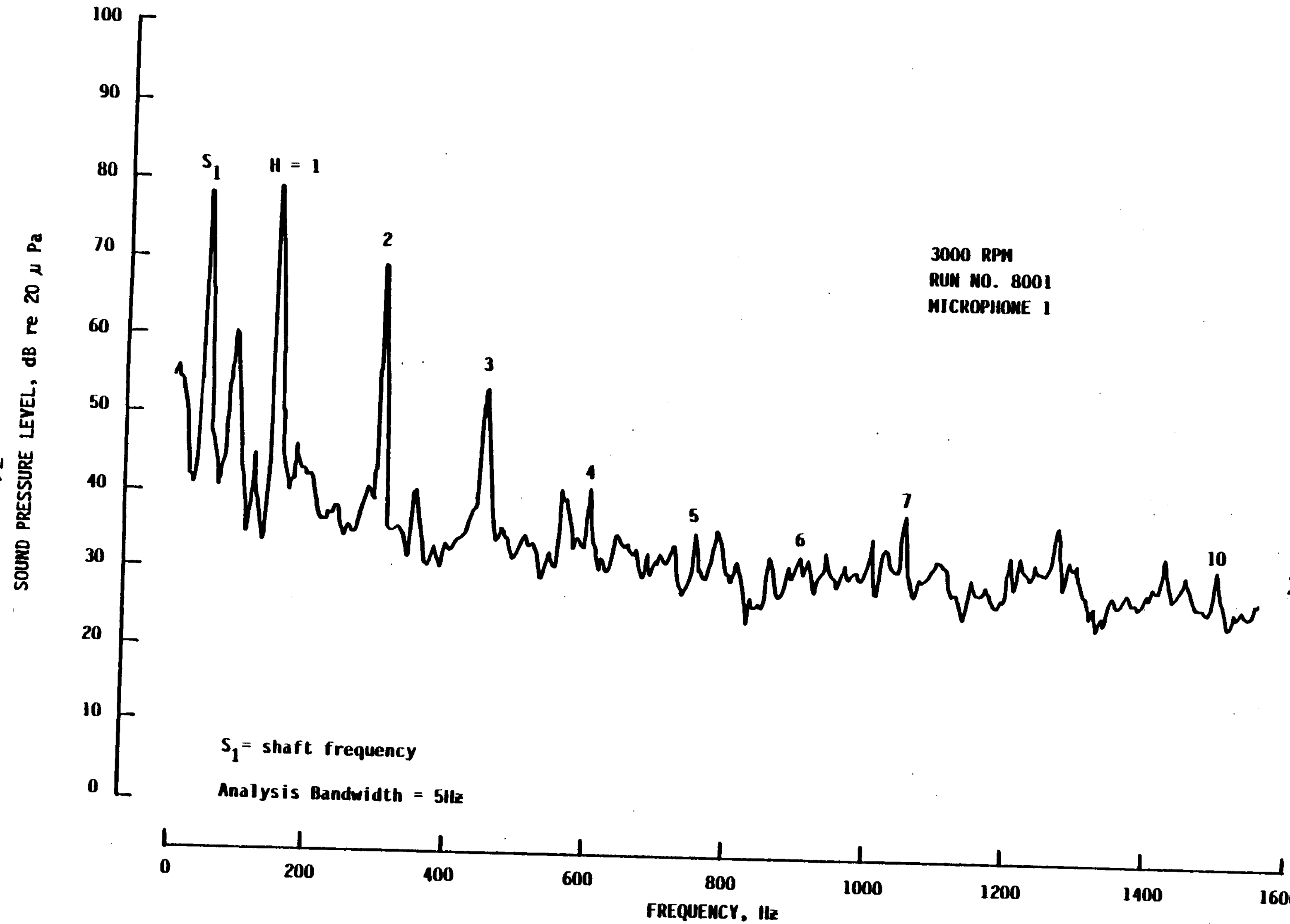

FIGURE 17. TYPICAL INTERIOR SPECTRUM

Table 2. Interior Measurements -
3000 RPM, Harmonic No. 1 (150 Hz)*

Run	x_3/R_p	$\phi°$	M_1	M_2	M_3	M_4	M_5	M_6	M_7	M_8	M_9	M_{10}	M_{11}
			Sound Pressure Level, dB re 20 μPa										
8018	+1.17	-103	82	83	85	83	83	83	83	83			
21		-51.5	83	84	85	86	86	87	87	87	80	80	*
24		0	80	80	80	79	79	*	79	79	81	82	*
27		51.5	78	77	75	73	71	71	70	70	82	82	*
30		103	77	77	76	77	77	78	78	79			
14	-.03	-103	76	76	*	78	79	79	*	82			
11		-51.5	73	73	*	77	79	79	*	81	79	81	*
8		0	75	72	71	69	69	69	*	*	*	81	*
5		51.5	78	78	79	79	80	79	*	80	*	78	*
1		103	80	81	81	82	83	83	*	85			
51	-1.23	-103	78	79	79	80	82	82	82	*			
48		-51.5	75	74	75	76	77	78	80	81	*	82	83
45		0	77	76	76	75	74	74	75	75	*	84	86
42		51.5	80	81	81	81	82	82	82	83	*	81	82
33		103	80	81	82	82	82	83	83	84			
54	-2.43	-103	80	81	82	82	83	83	84	84			
57		-51.5	81	82	83	84	85	86	86	86	*	81	82
60		0	80	80	80	79	79	79	79	78	80	82	83
63		51.5	79	77	76	75	74	73	72	*	80	81	81
66		103	78	78	78	79	79	79	80	80			

* 160 Hz Band

* = data judged to be of poor quality and discarded

Table 2. (Continued). Interior Measurements - 3000 RPM, Harmonic No. 2 (300 Hz)*

Run	x_3/R_p	$\phi°$	M_1	M_2	M_3	M_4	M_5	M_6	M_7	M_8	M_9	M_{10}	M_{11}
			Sound Pressure Level, dB re 20 μPa										
8018	+1.17	-103	62	65	72	65	64	63	62	60			
21		-51.5	61	65	66	68	68	69	69	69	67	70	*
24		0	48	54	58	60	57	*	58	57	64	65	*
27		51.5	62	65	67	66	69	67	68	67	60	62	*
30		103	66	70	71	72	72	72	73	73			
14	-.03	-103	68	67	*	62	64	62	*	70			
11		-51.5	61	61	*	61	61	61	*	61	61	61	*
8		0	68	68	68	69	69	70	*	*	*	72	*
5		51.5	68	66	66	67	66	67	*	67	*	67	*
1		103	69	69	69	68	68	66	*	63			
51	-1.23	-103	52	51	51	51	52	51	51	*			
48		-51.5	51	51	52	52	52	52	52	52	*	62	62
45		0	64	68	69	70	71	71	71	72	*	64	67
42		51.5	62	62	62	62	62	62	62	62	*	58	60
33		103	54	54	56	58	64	61	63	65			
54	-2.43	-103	61	61	61	61	61	61	61	61			
57		-51.5	60	59	64	67	68	69	69	69	*	74	73
60		0	64	72	75	76	78	78	78	79	76	78	79
63		51.5	62	65	68	69	71	70	71	*	74	76	77
66		103	69	68	68	67	66	66	64	62			

* 315 Hz Band

Table 2. (Concluded). Interior Measurements - 3000 RPM, Harmonic No. 3 (450 Hz)*

Run	x_3/R_p	$\phi°$	M_1	M_2	M_3	M_4	M_5	M_6	M_7	M_8	M_9	M_{10}	M_{11}
			Sound Pressure Level, dB re 20 μPa										
8018	+1.17	-103	50	47	63	45	47	49	50	50			
21		-51.5	51	50	52	53	52	54	54	54	51	49	*
24		0	50	44	44	48	52	*	53	54	52	50	*
27		51.5	51	50	50	51	54	53	53	53	51	52	*
30		103	52	48	51	53	55	56	57	58			
14	-.03	-103	47	45	*	51	55	55	*	54			
11		-51.5	51	52	*	54	56	54	*	55	54	53	*
8		0	49	45	47	51	52	52	*	*	*	47	*
5		51.5	50	45	46	49	53	52	*	53	*	51	*
1		103	54	53	52	51	53	55	*	61			
51	-1.23	-103	44	50	54	56	55	58	58	*			
48		-51.5	46	49	52	54	56	57	57	58	*	55	57
45		0	44	42	45	48	50	52	51	52	*	55	55
42		51.5	44	50	54	56	59	58	57	57	*	50	54
33		103	51	50	51	51	51	51	52	52			
54	-2.43	-103	48	45	48	51	54	55	56	57			
57		-51.5	51	52	52	52	53	53	56	53	*	52	54
60		0	50	48	46	44	47	49	49	51	51	49	50
63		51.5	48	44	45	48	50	50	51	*	48	49	52
66		103	51	48	45	44	47	45	46	47			

* 500 Hz Band

Table 3. Interior Measurements - 4000 RPM, Harmonic No. 1 (200 Hz)*

Run	x_3/R_p	$\phi°$	Sound Pressure Level, dB re 20 μPa										
			M_1	M_2	M_3	M_4	M_5	M_6	M_7	M_8	M_9	M_{10}	M_{11}
8019	+1.17	-103	87	92	*	94	95	96	96	97			
22		-51.5	88	91	92	92	93	93	93	93	80	87	91
25		0	76	81	84	86	87	*	90	91	71	70	*
28		51.5	77	82	84	85	86	85	85	85	86	90	*
31		103	87	91	93	93	94	94	94	95			
15	-.03	-103	84	86	*	87	88	87	*	91			
12		-51.5	87	88	*	90	91	90	*	90	87	90	94
9		0	85	86	*	87	87	88	*	89	*	87	*
6		51.5	86	83	87	77	74	75	*	*	*	87	91
3		103	87	90	92	93	94	94	*	95			
52	-1.23	-103	87	89	89	90	90	89	89	89			
49		-51.5	87	89	90	91	91	92	92	92	*	89	91
46		0	86	87	87	88	89	90	90	91	*	86	85
43		51.5	82	76	65	79	83	84	86	87	*	87	87
34		103	87	91	*	94	95	96	96	97			
55	-2.43	-103	80	83	85	85	85	86	85	85			
58		-51.5	79	86	88	90	91	91	92	92	84	87	89
61		0	82	85	87	88	89	89	90	90	77	78	79
64		51.5	85	89	90	92	93	94	94	*	67	74	77
67		103	85	90	92	93	94	94	95	96			

*200 Hz Band

Table 3. (Continued). Interior Measurements - 4000 RPM, Harmonic No. 2 (400 Hz)*

			Sound Pressure Level, dB re 20 μPa										
Run	x_3/R_p	$\phi°$	M_1	M_2	M_3	M_4	M_5	M_6	M_7	M_8	M_9	M_{10}	M_{11}
8019	+1.17	-103	62	68	*	78	79	79	81	80			
22		-51.5	72	75	78	79	79	81	80	81	75	79	76
25		0	70	71	71	70	65	*	71	71	74	76	*
28		51.5	64	73	79	82	84	84	85	86	67	74	*
31		103	72	73	75	78	79	80	81	81			
15	-.03	-103	73	69	*	69	75	71	*	71			
12		-51.5	72	75	*	79	79	78	*	69	75	70	65
9		0	72	72	*	75	75	77	*	78	*	78	*
6		51.5	74	74	81	77	78	79	*	*	*	78	76
3		103	74	70	70	71	73	73	*	79			
52	-1.23	-103	77	77	78	79	78	80	80	80			
49		-51.5	72	67	76	79	81	82	84	84	*	66	68
46		0	76	76	77	77	74	79	77	78	*	81	82
43		51.5	75	72	71	73	75	72	74	76	*	82	82
34		103	68	70	*	82	82	84	85	86			
55	-2.43	-103	78	78	81	82	84	85	85	85			
58		-51.5	74	75	81	84	86	86	86	86	85	84	86
61		0	77	75	75	75	75	76	76	76	85	84	84
64		51.5	77	79	83	85	86	87	87	*	80	80	82
67		103	79	77	80	82	82	84	85	85			

* 400 Hz Band

Table 3. (Concluded). Interior Measurements - 4000 RPM, Harmonic No. 3 (600 Hz)*

Run	x_3/R_p	$\phi°$	M_1	M_2	M_3	M_4	M_5	M_6	M_7	M_8	M_9	M_{10}	M_{11}
			Sound Pressure Level, dB re 20 μPa										
8019	+1.17	-103	64	62	*	59	62	65	66	67			
22		-51.5	63	62	62	63	65	67	68	68	57	62	65
25		0	64	61	56	50	56	*	62	64	59	61	*
28		51.5	62	61	60	60	60	60	58	56	63	64	*
31		103	59	60	60	61	62	65	67	69			
15	-.03	-103	59	60	*	64	64	64	*	63			
12		-51.5	64	61	*	59	62	62	*	64	68	69	71
9		0	69	67	*	66	66	66	*	67	*	66	*
6		51.5	67	62	68	69	72	74	*	*	*	56	61
3		103	68	67	70	64	65	66	*	72			
52	-1.23	-103	66	64	63	64	66	68	69	69			
49		-51.5	67	67	66	65	65	63	63	63	*	62	61
46		0	63	60	58	57	58	61	63	67	*	65	64
43		51.5	61	64	67	68	69	70	70	69	*	65	63
34		103	61	60	*	57	57	62	65	68			
55	-2.43	-103	65	64	63	62	63	64	64	64			
58		-51.5	66	66	65	64	64	64	65	65	64	64	64
61		0	65	64	61	58	57	59	61	62	67	69	68
64		51.5	60	57	62	65	67	68	69	*	64	65	64
67		103	52	54	51	54	58	62	63	65			

*630 Hz Band

Table 4. Interior Measurements -
5000 RPM, Harmonic No. 1 (250 Hz)*

Run	x_3/R_p	$\phi°$	M_1	M_2	M_3	M_4	M_5	M_6	M_7	M_8	M_9	M_{10}	M_{11}
			Sound Pressure Level, dB re 20 μPa										
8020	+1.17	-103	86	93	97	97	98	98	98	98			
23		-51.5	92	99	102	101	101	102	103	103	97	101	*
26		0	90	94	97	98	98	*	100	100	92	95	*
29		51.5	95	97	99	100	101	101	101	101	83	92	*
32		103	98	101	103	103	104	103	103	103			
16	-.03	-103	90	*	*	100	102	101	*	102			
13		-51.5	*	*	*	*	*	*	*	*	*	*	*
10		0	85	91	*	94	95	95	*	95	*	96	*
7		51.5	94	95	*	95	94	94	*	*	*	95	*
4		103	99	102	104	105	105	105	*	105			
53	-1.23	-103	80	*	94	96	98	98	100	100			
50		-51.5	92	99	99	100	100	101	101	101	*	102	*
47		0	91	97	99	100	101	101	101	101	*	97	98
44		51.5	89	85	85	77	81	83	*	*	*	*	*
35		103	87	90	*	104	104	*	*	*			
56	-2.43	-103	86	*	94	96	96	97	97	*			
59		-51.5	93	98	100	102	102	103	103	104	99	102	103
62		0	92	97	100	101	*	*	*	*	*	97	97
65		51.5	94	96	98	99	100	101	102	102	*	*	89
68		103	99	101	104	105	106	106	106	106			

* 250 Hz Band

Table 4. (Continued). Interior Measurements - 5000 RPM, Harmonic No. 2 (500 Hz)*

Run	x_3/R_p	$\phi°$	M_1	M_2	M_3	M_4	M_5	M_6	M_7	M_8	M_9	M_{10}	M_{11}
			Sound Pressure Level, dB re 20 μPa										
8020	+1.17	-103	90	81	77	83	87	90	91	91			
23		-51.5	94	92	92	89	88	87	87	88	89	75	*
26		0	93	84	82	91	94	*	97	97	88	81	*
29		51.5	94	92	92	91	92	91	92	92	89	79	*
32		103	90	81	81	84	87	89	89	89			
16	-.03	-103	86	*	*	87	88	86	*	96			
13		-51.5	*	*	*	*	*	*	*	*	*	*	*
10		0	79	80	*	91	93	94	*	94	*	87	*
7		51.5	83	85	*	89	90	91	*	*	*	81	*
4		103	80	62	85	83	85	86	*	90			
53	-1.23	-103	89	*	86	88	89	90	92	90			
50		-51.5	91	88	82	84	87	89	90	90	*	90	*
47		0	91	88	88	91	92	94	94	94	*	89	89
44		51.5	91	92	93	93	94	94	*	*	*	*	*
35		103	80	75	*	89	91	*	*	*			
56	-2.43	-103	96	*	74	87	92	94	95	*			
59		-51.5	99	97	95	93	91	90	90	90	95	74	91
62		0	99	91	84	96	*	*	*	*	*	82	70
65		51.5	99	97	95	93	91	90	88	87	*	*	91
68		103	96	87	75	87	92	93	94	94			

*500 Hz Band

Table 4. (Concluded). Interior Measurements - 5000 RPM, Harmonic No. 3 (750 Hz)*

Run	x_3/R_p	$\phi°$	M_1	M_2	M_3	M_4	M_5	M_6	M_7	M_8	M_9	M_{10}	M_{11}
			Sound Pressure Level, dB re 20 μPa										
8020	+1.17	-103	71	64	71	67	69	70	72	71			
23		-51.5	74	75	73	70	70	70	71	73	73	69	*
26		0	77	75	73	73	76	*	78	79	65	71	*
29		51.5	76	74	71	72	74	75	75	74	59	71	*
32		103	74	71	71	75	77	78	78	78			
16	-.03	-103	63	*	*	64	66	67	*	70			
13		-51.5	*	*	*	*	*	*	*	*	*	*	*
10		0	76	73	*	67	72	75	*	78	*	75	*
7		51.5	79	76	*	74	77	78	*	*	*	64	*
4		103	77	74	74	75	77	79	*	83			
53	-1.23	-103	73	*	72	74	76	78	77	78			
50		-51.5	77	72	68	70	75	78	80	80	*	63	*
47		0	77	74	70	67	68	70	70	71	*	77	78
44		51.5	75	69	65	66	71	75	*	*	*	*	*
35		103	61	65	*	67	68	*	*	*			
56	-2.43	-103	71	*	65	64	66	67	68	*			
59		-51.5	75	73	69	64	68	71	72	72	75	72	74
62		0	74	71	68	72	*	*	*	*	*	69	72
65		51.5	69	67	68	70	71	72	73	73	*	*	71
68		103	69	64	65	68	70	71	72	73			

* 800 Hz Band

the higher harmonics.

Space-average sound pressure level (Harmonic H)

PAIN predicts the interior space-average sound pressure level for each harmonic. The equivalent measured interior space average needed for comparison, and the standard deviation of the mean square pressure are given below.

$$\overline{SPL}_H = 10 \log(\langle p_i^2 \rangle_{s,t}^H / p_o^2) \quad ,$$

where the space-average mean square pressure for harmonic H is

$$\langle p_i^2 \rangle_{s,t}^H = (1/V) \sum_j^N \langle p_i^2 \rangle_j^H V_j \quad .$$

V is the volume of the cylinder above the floor (or if data for some sampled subvolumes V_j are considered bad and not used, the total volume of all subvolumes V_j used, i.e., $V = \sum V_j$). N is the number of subvolumes with good microphone data.

In the present case

$V_j = 0.014LR^2$ for microphones 1 through 8, $\phi = \pm 103^o, \pm 51.5^o, 0^o$
$= 0.014LR^2$ for microphones 9 through 11, $\phi = 0^o$
$= 0.007LR^2$ for microphones 9 and 10, $\phi = \pm 51.5^o$
$= 0.0225LR^2$ for microphone 11 when $\phi = \pm 51.5^o$

In the relations above,

$$\langle p_i^2 \rangle_j^H = p_o^2 \cdot 10^{SPL_j^H/10}$$

SPL_j^H = Sound pressure level measured in subvolume j, harmonic H

p_o = reference pressure $= 2 \times 10^{-5} nt/m^2 (20 \mu Pa)$.

The standard deviation of the mean square pressure is defined by

$$s_H=\left\{(1/N-1)\sum_{j=1}^{N}(<p_i^2>_j^H-<p_i^2>_{s,t}^H)^2\right\}^{\frac{1}{2}} \quad .$$

Since the sampled subvolumes V_j are not identical the mean and standard deviation are calculated in the following manners. Let

$$x_H^j=(10^{SPL_j^H/10}\cdot V_j\cdot 10^{-6})/LR^2 \quad .$$

Define $\bar{x}_H$ as the average over N subvolumes of x_H^j

$$\bar{x}_H=(LR^2/V)\sum_{j=1}^{N}x_H^j \;=\; LR^2\sum_{j=1}^{N}x_H^j/\sum_{j=1}^{N}V_j \quad .$$

Also let the primed quantity be defined

$$\bar{x}'_H=\bar{V}\bar{x}_H/LR^2 \quad ,$$

where $\bar{V}$ is the average subvolume's volume

$$\bar{V}=(1/N)\sum_{j=1}^{N}V_j \quad .$$

Then the measured mean sound pressure level (average in space) for harmonic H is given by the exact result

$$\overline{SPL}_H=60+10\log\,\bar{x}_H \quad .$$

The standard deviation is defined and computed with

$$s'_H=\left\{(1/N-1)\sum_{j=1}^{N}(x_H^j-\bar{x}'_H)^2\right\}^{\frac{1}{2}} \quad .$$

The above is a sufficiently close approximation to the true sample standard deviation.

Finally, set

$$s_H = s'_H LR^2/\bar{V} \quad .$$

The (1- α)% confidence intervals of the space average sound pressure level at harmonic H are computed by using $\bar{x}_H$ and s_H:

$$SPL_H^{1-\alpha} = 60 + 10\log(\bar{x}_H + s_H t_{m;\alpha/2}/\sqrt{N}) \quad ,$$

where $t_{m;\alpha/2}$ is the $\alpha/2$ percentage point of the Student t - distribution with m = N-1 degrees of freedom. In the present case, a value of α equal to 0.01 is selected and the 99% confidence limits computed.

Figures 18, 19, and 20 show the axial variations of the average sound pressure levels in the four major (axial) subvolumes sampled. Note that very little axial variation is present, however, the third harmonics of the 4000 and 5000 rpm cases do have a slightly apparent peak near the propeller plane.

Table 5 summarizes the reduced interior noise levels. Figure 21 gives the same results in graphical form. It is the basic plot upon which the PAIN predictions can be directly overlaid.

3.4 Computer Simulation of Scale-Model Tests

This section begins with a brief discussion of some of the details of the modeling of the fuselage and trim. Next the propeller modeling requirements are considered. Then the ANOPP propeller noise predictions used as input data to the PAIN program are scrutinized.

ORIGINAL PAGE IS
OF POOR QUALITY

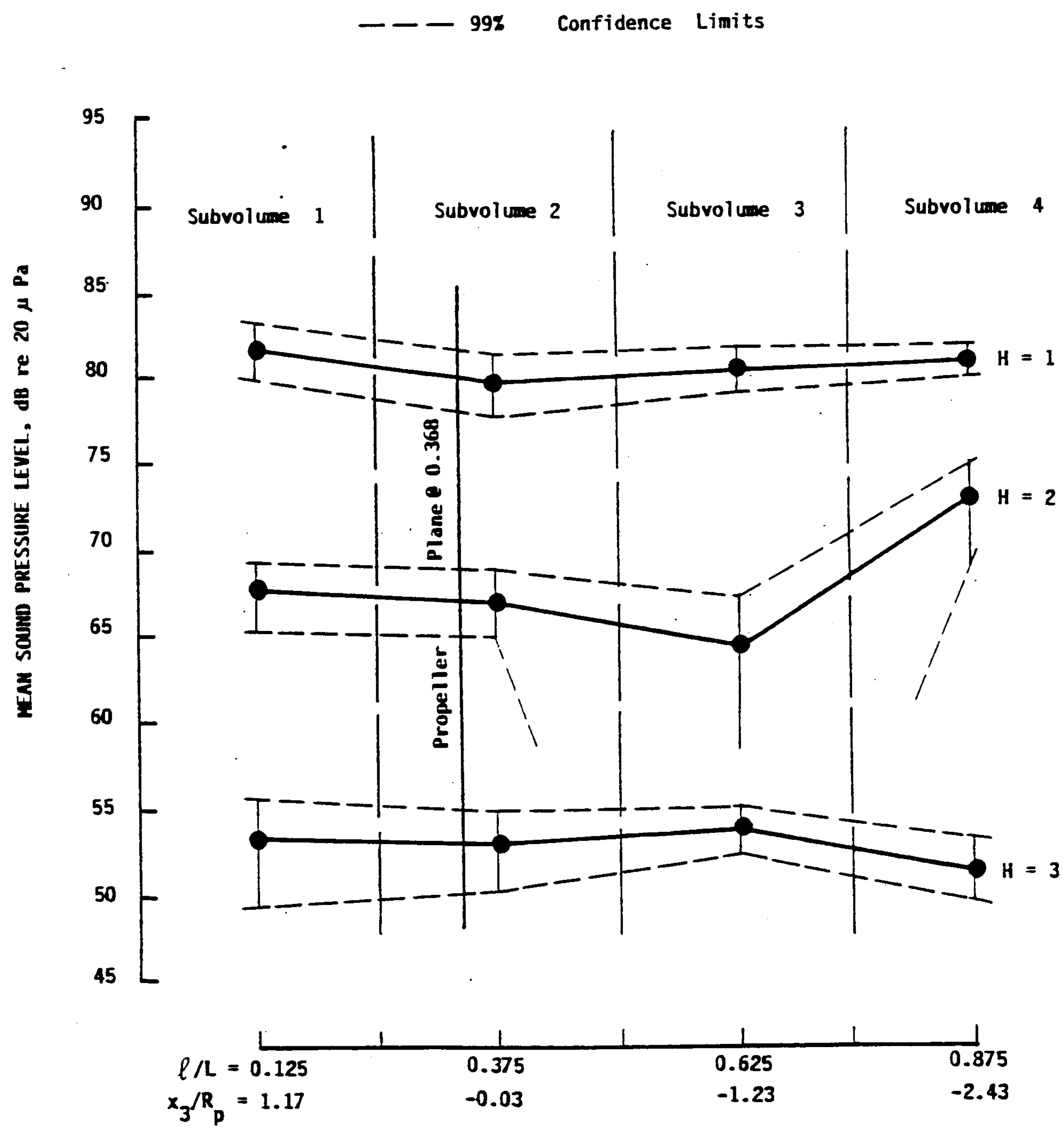

FIGURE 18. AXIAL VARIATION OF AVERAGE SOUND PRESSURE LEVEL BY MAJOR SUBVOLUME (3000 RPM)

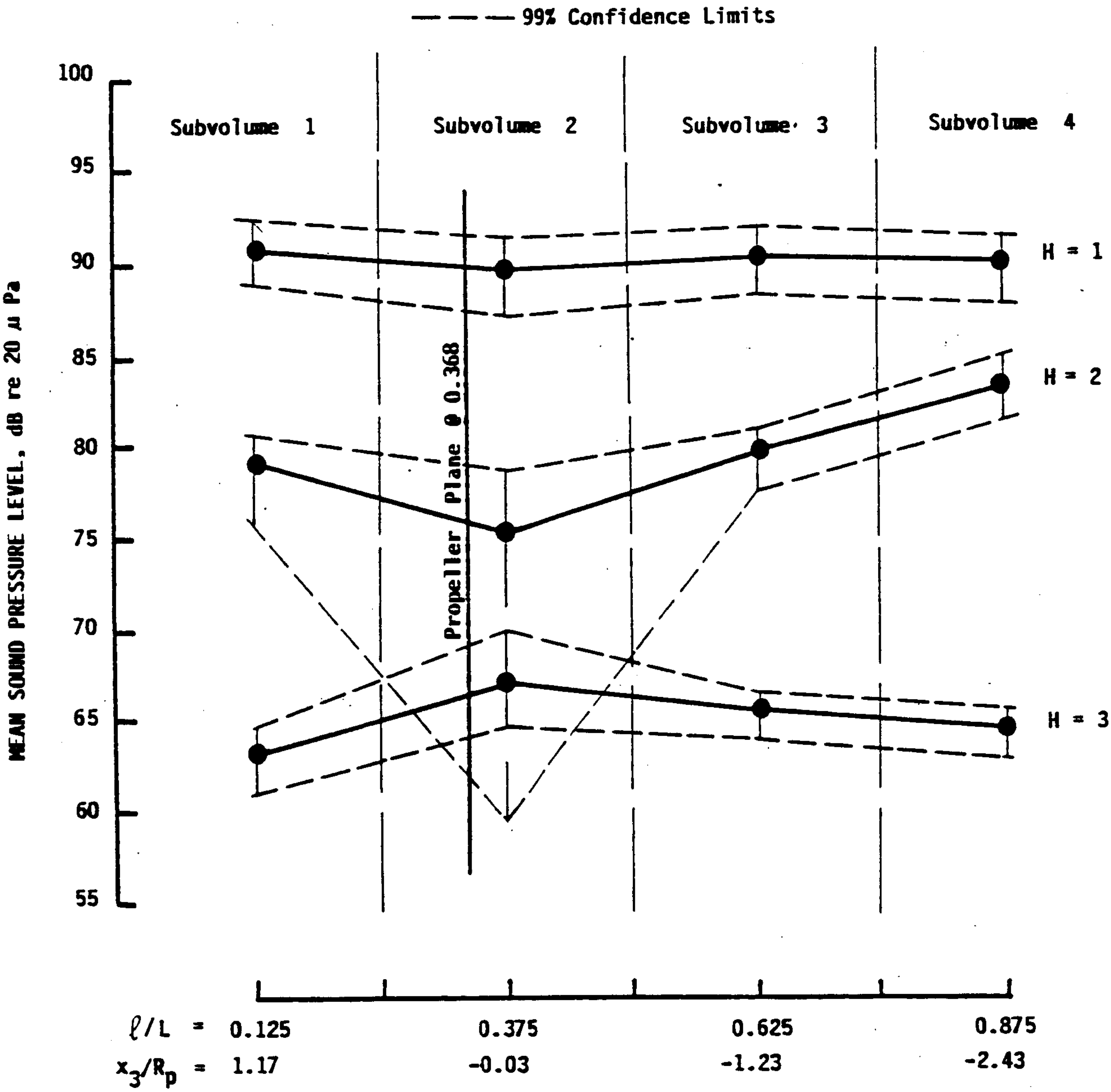

FIGURE 19. AXIAL VARIATION OF AVERAGE SOUND PRESSURE LEVEL BY MAJOR SUBVOLUME (4000 RPM)

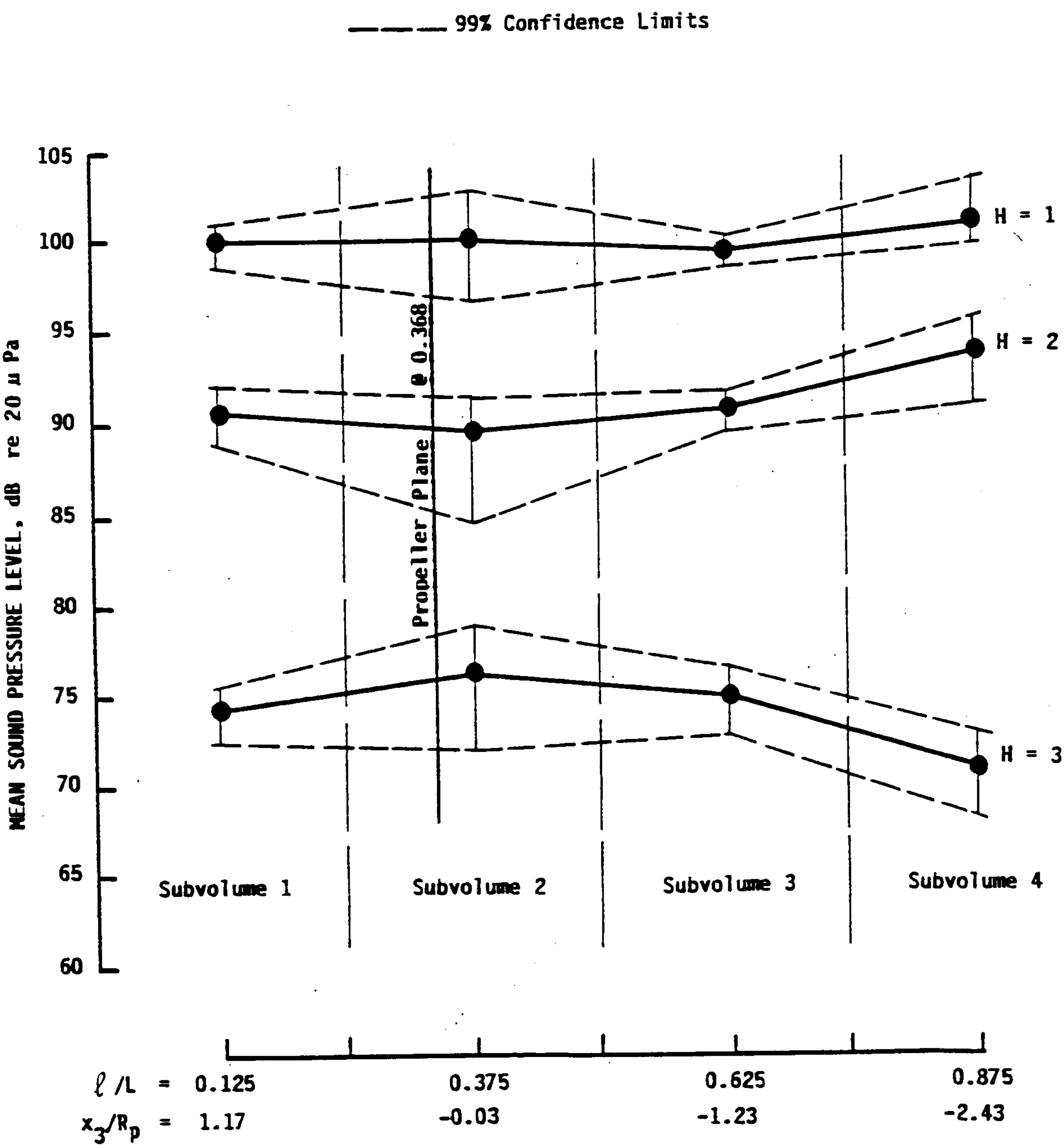

FIGURE 20. AXIAL VARIATION OF AVERAGE SOUND PRESSURE LEVEL BY MAJOR SUBVOLUME (5000rpm)

Table 5. Measured Space Average Sound Pressure Levels, Entire Cabin Space (Above Floor)

RPM	Harmonic, H	Freq. (Hz)	$\overline{SPL}_H$ *	SPL_H^{99} ⋆
3000	1	150	81.0	80.2-81.7
	2	300	69.1	67.1-70.4
	3	450	52.9	51.8-53.8
4000	1	200	90.3	89.3-91.0
	2	400	80.3	79.1-81.1
	3	600	65.2	64.2-65.9
5000	1	250	100.2	99.3-100.9
	2	500	91.5	90.3-92.4
	3	750	74.0	72.9-74.9

* calculated mean

⋆ 99% confidence that true mean lies in this band

ORIGINAL PAGE IS
OF POOR QUALITY

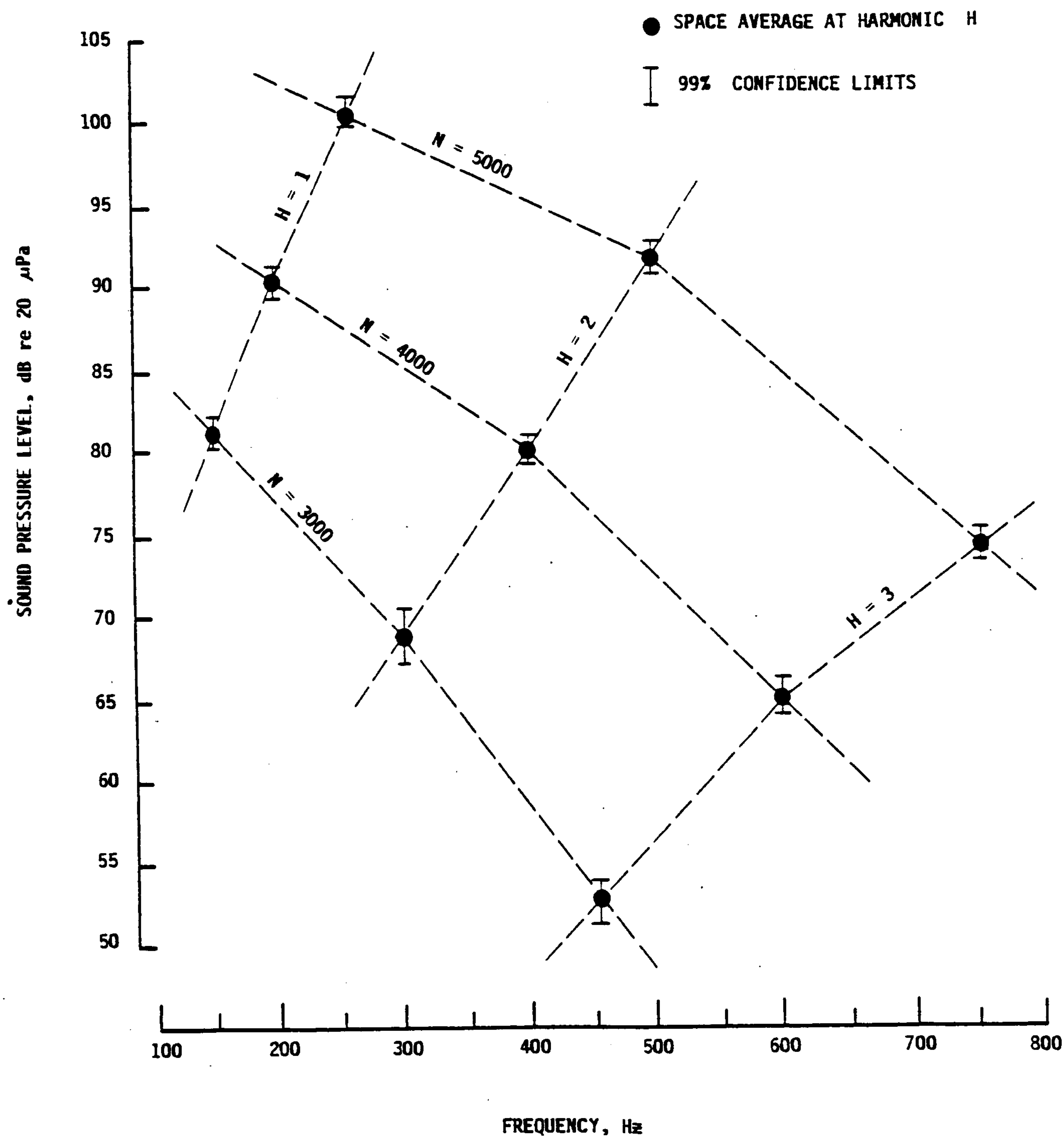

FIGURE 21. MEASURED SOUND LEVELS INSIDE MODEL FUSELAGE INDUCED BY PROPELLER

3.4.1 Fuselage modeling

The scale model fuselage is basically the same as the analytical model, having ring frames and stringers on the shell and longitudinal and transverse floor beams as stiffeners. As part of the input data file for the program MRP, there are four quantities to be specified that are used in the calculation of the modes of the stiffened shell and which define the characteristics of the stiffeners: D_{xs}, the bending rigidity of the shell stringers divided by the stringer spacing; $D_{R\theta}$, the bending rigidity of the shell frames divided by the frame spacing; D_{xp}, the bending rigidity of the longitudinal floor beams divided by the floor beam spacing; D_{yp}, the bending rigidity of the transverse floor supports divided by the support spacing. The procedure to be followed to calculate these quantities is: 1) compute the moment of inertia of a single stiffener about the inner surface of the shell (or lower surface of the floor), 2) multiply by the elastic modulus, and 3) divide by the stiffener spacing. The calculation of the moment of inertia of a transverse floor beam (support) requires special attention.

Figures 5 and 6 show that the transverse floor beams (supports) extend from the bottom of the floor down to the shell frames where they are attached. It is assumed that about 0.038m (1.5 in.) of the total depth of the support actually provides bending rigidity to the floor. This is arbitrarily chosen since the longitudinal floor beams are themselves 0.038m (1.5 in.) deep and because part of the floor support provides stiffening to the shell since it is attached to the frame. This is admittedly an unknown complicating factor in the test which is assumed not to be serious, as the upper part of the shell is felt not likely to be overly restrained by the actual supports as compared to their assumed (computer) configuration.

The input data for the model fuselage (required by programs MRP and MRPMOD) are given in Table 6. In addition to the data shown, the floor must be specified (alphamerically) as being rigidly connected to the shell.

Also given in Table 6 are the input data for programs CYL2D and PAIN. In the latter case, the table is used to specify sources or models used. For instance, no measurements were made of the structural loss factors of the bare fuselage (i.e., without trim), so a simple model was assumed ($\eta_r=2/f_r$). The measured values of η_r with trim installed, i.e., η_r' are given in Table 1 and since PAIN computes the loss factors with the trim installed, a comparison of predictions with measurements is possible and will be presented later. The acoustic loss factors are taken as zero to force PAIN to compute them.

The trim panel mass per unit of area has two values shown. The first corresponds to the total mass of the trim divided by the surface area (including as part of the mass, the 120° sector of vinyl) and the second the mass per unit of area locally where the propeller blade tip passes nearest the structure and where the most intense exterior sound is realized. The latter value is selected as the more correct one to use although either value leads to approximately the same final result. The trim loss factor is set to 0.13 which is the average value of the measured η_T (trim installed) over the frequency range of interest. The properties of the fiberglass insulation are those in Figure A-2 of Appendix A in Ref. (1). Finally, the cavity length is slightly larger than the shell's because of the construction.

Table 6. Input Data Used To Simulate Scale Model Tests

Program		Description	Input Value
MRP	D_{xs},	bending rigidity of shell stringers divided by stringer spacing	62.35 nt-m
	$D_{R\theta}$,	bending rigidity of shell frames divided by frame spacing	1.20×10^4 nt-m
	D_{xp},	bending rigidity of longitudinal floor beams divided by beam spacing	8.63×10^3 nt-m
	D_{yp},	bending rigidity of transverse floor supports divided by support spacing	5.42×10^3 nt-m
	t^s,	equivalent skin thickness of shell (including smeared-out stiffener areas)	0.001153 m
	t^p,	equivalent thickness of floor (including smeared-out stiffener areas)	0.00127 m
MRP, MRPMOD	m_s,	shell mass per unit area including smeared-out stiffener masses	3.113 kg/m^2
	m_p,	floor mass per unit area including smeared-out stiffener masses	3.446 kg/m^2
MRP, MRPMOD PAIN	a,	radius of shell	0.508 m
	L,	length of shell	1.803 m
MRP, MRPMOD CYL2D, PAIN	θ_o,	floor angle	56.6°

Table 6. (Continued). Input Data Used To Simulate Scale Model Tests

Program		Description	Input Value
PAIN	η_r,	structural loss factors of bare fuselage (assuming a mode exists at the resonance frequency, f_r)	$2/f_r$
	η_n,	acoustic loss factors of bare fuselage	0.0
	m_T,	trim panel mass per unit area	1.82 kg/m^2 (1.46)
	η_T,	trim loss factor	0.13
	L_c,	cavity length	1.829 m
	r_p,	propeller radial location	0.962 m
	z_p,	propeller axial location	0.662 m
	ϕ ,	propeller circumferential location	90^o
	B,	number of blades	3
	Direction of rotation (counter-clockwise, looking aft)		+1

3.4.2 Propeller modeling

The propeller is located radially and relative to the front of the structure by r_p and z_p (see Figures 1 and 2). The circumferential position is given by ϕ (Figure 2). Table 6 shows the values corresponding to those of the test. The direction of propeller rotation is defined as counter-clockwise because the top half of the cylinder is swept by the blade tip before the bottom half (or floor).

The grid (Figure 3) is positioned by placing the propeller at k=8. In the present test rig, each grid point (k,ℓ) lying in the fuselage surface has coordinates defined by the equivalence relation

$$(k,\ell) \sim (x_1^\ell, x_2^\ell, x_3^k) \quad ,$$

where (in meters):

$$x_1^\ell = 0.457 + 0.508\{1-\cos[(\ell-1)\cdot\pi/18]\}$$

$$x_2^\ell = -0.508\sin[(\ell-1)\cdot\pi/18] \quad ,$$

and

$$x_3^k = 0.622 - 0.089(k-1) \quad .$$

This grid covers all of the upper quarter surface of the cylinder forward of the propeller and a somewhat greater surface area behind it.

Because of the lengthy calculations involved in the propeller noise prediction programs, the data for the lower quarter of the cylinder seen by the propeller are obtained from the data for the top quarter with the relation (imagining an identical grid below the centerline)

$$p(x_1^\ell, x_2^\ell, x_3^k, t) = p(x_1^\ell, -x_2^\ell, x_3^k, t - \tau_{k\ell}) \quad ,$$

where $\tau_{k\ell}$ is a time delay given in milliseconds by the result

$$\tau_{k\ell} = 333.33\alpha_{k\ell}/N \quad .$$

N is the propeller rpm and $\alpha_{k\ell}$ is in degrees and is given by the result

$$\alpha_{k\ell} = \tan^{-1}\left[\,|x_2^\ell|/x_1^\ell\,\right] \quad .$$

The propeller harmonic amplitudes at corresponding points above and below the centerline are given by

$$A_H^{k\ell}\Big|_{above} = A_H^{k\ell}\Big|_{below} \quad ,$$

and the corresponding phases (in degrees) are related by

$$\phi_H^{k\ell}\Big|_{below} = \phi_H^{k\ell}\Big|_{above} + \tau_{k\ell} H x 360/T_1 \quad ,$$

where $T_1 = BPF^{-1}$ is in milliseconds and H is the harmonic index. This can also be written as

$$\phi_H^{k\ell}\Big|_{below} = \phi_H^{k\ell}\Big|_{above} + 2BH\alpha_{k\ell} \quad ,$$

where B is the number of propeller blades.

Conversion to the coordinate system used in Figures 1 and 2 is with the relations

$$z_k = z_p - x_3^k \quad ,$$

and (using $\phi = \pi/2$ in Fig. 2)

$$\theta_{\ell} = \pi/2 + \tan^{-1}\left\{\frac{-x_2^{\ell}}{r_p - x_1^{\ell}}\right\} = \phi + (\ell - 1)\cdot\pi/18 \quad .$$

The coordinates of the grid point (k,ℓ) are given by the equivalence statement

$$(k,\ell) \sim (a,\theta_{\ell},z_k) \quad .$$

The selected grid has spacing Δ of 0.089m (3.5 in.). This spacing is sufficiently close to assure a relatively smooth change in phase for each propeller harmonic from grid point-to-point.

The free field propeller noise predictions needed at the grid points were made with NASA ANOPP (8). The predictions for the 3000, 4000, and 5000 rpm cases were computed at NASA Langley and provided to the contractor. As required for PAIN input, the predictions are the Fourier representations of the actual pressure time histories (the first 10 harmonics are used). Section 3.4 of Ref. (1) should be consulted for an expanded discussion of the input model. As stated previously, after being read-in, the free field pressure amplitudes of the various harmonics are increased in proportion to the incidence angle γ (Figure 2) to simulate the blocked pressures. The phases computed with the propeller program are not modified.

Creation of the input data with the propeller noise program is a separate problem not of concern in this report. However the quality of the predictions made with that program is of concern due to the potential for introducing bias errors in PAIN predictions. Appendix E of Ref. (1) presents a basic overview of the requirements for input data to the ANOPP program and it should be consulted for any further basic information. Appendix B of Ref. (1) deals with propeller noise theory and should be referred to if a more in-depth treatment of propeller noise predictions is desired.

In the present tests, the data used to define the particular geometrical characteristics of the propeller are proprietary and thus are not included. It is simply noted here that the angle of attack, chord, and blade thickness are specified as a function of the distance out along the pitch change axis via a data list which is then interpolated as required to fix these variables at all locations on the blade.

Figure 22 shows (for an example) a typical predicted pressure time history and the corresponding PAIN model used. The particular case shown, from the 5000 rpm run, is the pressure at grid location $(k,\ell) = (7,1)$. It represents only one of 160 such time histories in the PAIN input data file.

3.4.3 Propeller noise predictions and comparisons

There are two fundamental questions concerning the exterior pressure field that have to be answered before comparison of interior predictions should be attempted. First, are the free field propeller noise predictions made with ANOPP reasonable, when compared to the measurement results of Section 3.3.2? Also, are the predicted blocked pressures correct? Equation (43) of Ref. (1) is the PAIN model used to adjust free field pressures to blocked pressures. Is it a good representation?

To answer the first question, consider the propeller noise predictions in Tables 7, 8, and 9. Results for the grid line $\ell = 1$ are given (first 5 harmonics only, although 10 harmonics are available). The sound levels in these tables are

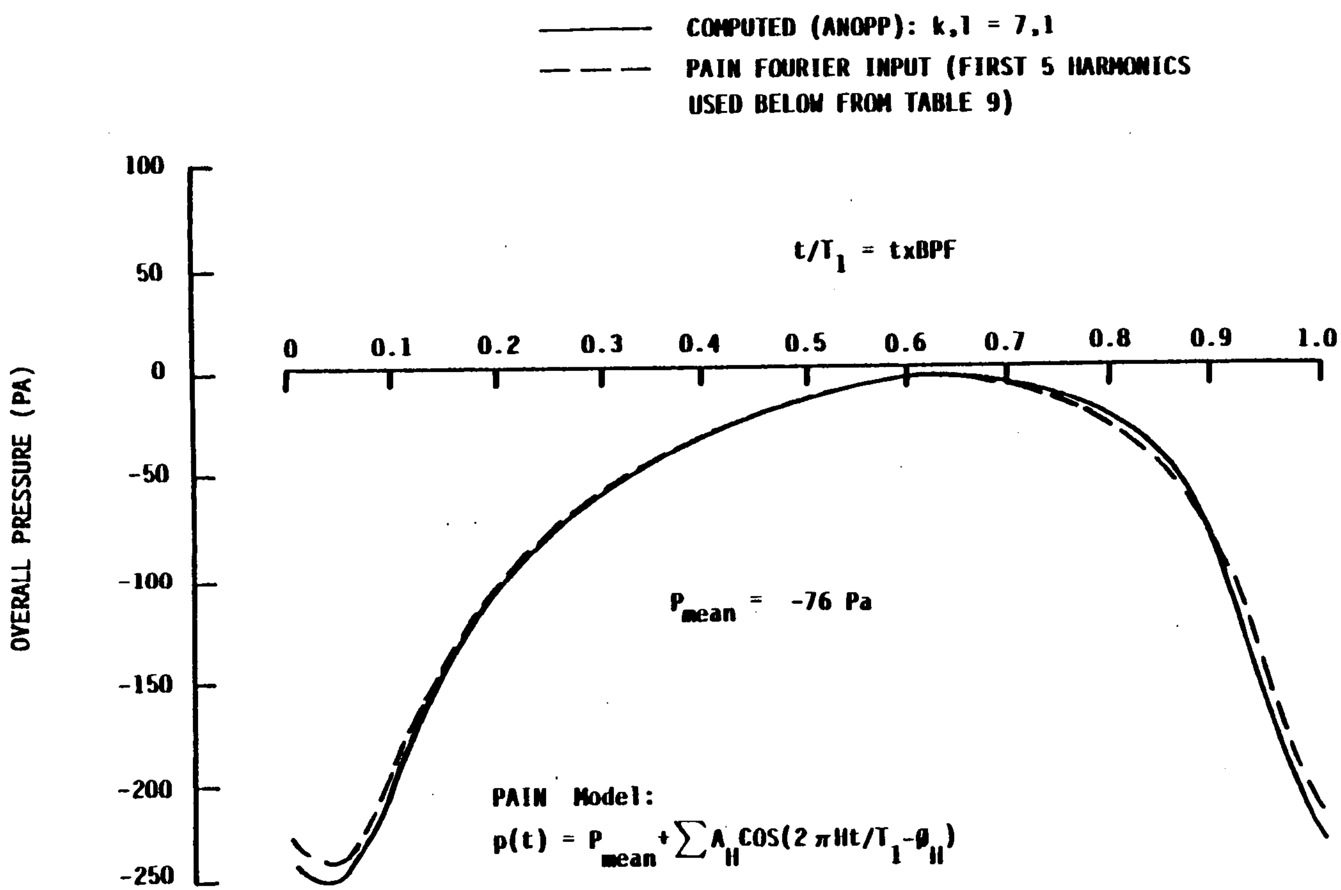

FIGURE 22. TYPICAL PRESSURE SIGNATURE AND THE PAIN PROGRAM FOURIER REPRESENTATION

Table 7. ANOPP Predictions of Propeller Noise, Grid Line ℓ = 1
0.762 m Dia., 3 Bladed Hartzell Propeller @ 3000 rpm

Harmonic H	k=1	2	3	4	5	6	7	8
	Sound Pressure Level, dB re 20 μPa							
1	90.1	95.5	100.5	106.3	112.1	117.4	120.2	114.9
2	57.0	66.2	74.9	85.1	95.6	105.5	112.5	108.3
3	24.2	37.0	49.2	63.9	78.9	93.5	104.8	101.9
4	-8.1	7.8	23.6	42.6	62.3	81.5	97.0	95.8
5	5.3	10.8	16.7	27.5	46.7	69.7	89.4	90.0
	Phase, ϕ_H (degrees)							
1	-148.1	-151.2	-153.6	-155.8	-157.4	-158.0	-153.9	-86.1
2	-144.2	-148.3	-151.4	-154.4	-156.8	-158.3	-155.7	-92.1
3	-146.1	-147.1	-149.4	-152.6	-155.8	-158.1	-156.7	-97.7
4	-142.3	-142.5	-145.6	-150.0	-154.2	-157.6	-157.4	-103.3
5	-148.5	-151.4	-152.9	-152.3	-153.5	-157.2	-158.0	-108.7

Harmonic H	k=9	10	11	12	13	14	15	16
	Sound Pressure Level, dB re 20 μPa							
1	119.3	116.0	110.6	104.8	99.1	94.2	89.0	84.3
2	110.4	102.9	92.8	82.3	72.1	63.5	54.4	46.3
3	101.5	89.7	74.9	59.9	45.3	33.0	20.3	9.0
4	92.6	76.5	57.1	37.4	18.5	2.8	-12.8	-24.8
5	83.7	63.5	40.9	23.8	14.8	9.5	4.2	-.5
	Phase, ϕ_H (degrees)							
1	-27.6	-24.1	-24.8	-26.5	-28.7	-30.8	-33.1	-35.3
2	-28.5	-25.8	-27.4	-30.2	-33.5	-36.8	-40.7	-44.5
3	-29.6	-27.6	-30.0	-33.4	-36.8	-39.0	-39.0	-33.5
4	-31.1	-29.8	-33.3	-37.9	-42.5	-45.3	-42.9	-31.3
5	-33.0	-31.8	-34.1	-31.4	-29.3	-30.5	-32.7	-34.9

Table 8. ANOPP Predictions of Propeller Noise, Grid Line $\ell = 1$
0.762 m Dia., 3 Bladed Hartzell Propeller @ 4000 rpm

Harmonic H	Sound Pressure Level, dB re 20 μPa k=1	2	3	4	5	6	7	8
1	97.6	102.5	107.2	112.6	118.1	123.1	125.7	120.6
2	68.5	76.4	84.0	93.2	102.8	112.0	118.6	114.4
3	39.3	50.2	60.8	73.7	87.4	100.9	111.3	108.4
4	10.6	24.1	37.5	54.2	72.0	89.7	104.1	102.7
5	12.9	18.5	25.1	37.9	57.2	78.7	96.9	97.2
	Phase, ϕ_H (degrees)							
1	-139.5	-144.9	-148.8	-152.5	-155.2	-156.4	-152.7	-86.0
2	-128.9	-138.1	-144.4	-149.8	-153.9	-156.5	-154.5	-92.8
3	-121.6	-133.1	-140.6	-147.1	-152.2	-155.9	-155.6	-98.8
4	-111.5	-126.3	-135.6	-143.5	-149.9	-155.0	-156.1	-104.5
5	-139.2	-143.4	-144.6	-144.4	-148.3	-154.0	-156.5	-110.0

Harmonic H	Sound Pressure Level, dB re 20 μPa k=9	10	11	12	13	14	15	16
1	124.9	121.8	116.8	111.5	106.4	102.1	97.8	93.9
2	116.5	109.5	100.2	90.7	81.8	74.6	67.5	61.2
3	108.1	97.1	83.5	69.9	57.2	47.2	37.5	29.2
4	99.7	84.8	66.9	49.2	32.7	19.9	7.7	-2.3
5	91.3	72.6	51.3	33.4	23.0	17.7	13.0	9.1
	Phase, ϕ_H (degrees)							
1	-29.3	-26.1	-27.2	-29.1	-31.0	-32.2	-32.6	-31.6
2	-31.0	-29.1	-31.7	-35.5	-39.1	-41.2	-41.0	-37.1
3	-32.8	-31.9	-35.9	-41.0	-46.1	-48.7	-46.6	-37.3
4	-35.0	-35.1	-40.4	-47.4	-54.6	-58.9	-56.2	-42.8
5	-37.6	-38.2	-43.0	-42.0	-35.7	-33.4	-32.6	-31.2

Table 9. ANOPP Predictions of Propeller Noise, Grid Line $\ell = 1$
0.762 m Dia., 3 Bladed Hartzell Propeller @ 5000 rpm

Harmonic H	Sound Pressure Level, dB re 20 μPa							
	k=1	2	3	4	5	6	7	8
1	104.5	108.9	113.1	118.1	123.2	127.8	130.2	125.5
2	80.1	86.9	93.5	101.4	109.9	118.1	123.9	120.0
3	56.1	65.2	73.9	84.7	96.4	108.2	117.4	114.6
4	32.6	43.8	54.6	68.1	82.9	98.3	110.9	109.4
5	18.4	27.2	37.9	52.4	69.7	88.4	104.5	104.5
	Phase, ϕ_H (degrees)							
1	-126.7	-135.2	-141.5	-147.1	-151.4	-153.7	-150.4	-85.1
2	-98.2	-116.6	-129.5	-140.4	-148.1	-152.8	-152.0	-93.4
3	-68.6	-98.1	-118.2	-134.4	-145.2	-151.9	-153.1	-100.1
4	-37.6	-78.7	-106.6	-128.4	-142.1	-150.6	-153.7	-106.2
5	-110.1	-101.7	-109.5	-125.6	-139.4	-149.2	-153.9	-111.8

Harmonic H	Sound Pressure Level, dB re 20 μPa							
	k=9	10	11	12	13	14	15	16
1	129.7	127.0	122.5	117.9	113.5	109.9	106.2	102.8
2	121.9	115.8	107.8	100.0	92.9	87.1	81.3	75.9
3	114.2	104.6	93.1	82.1	72.4	64.8	56.9	49.6
4	106.6	93.5	78.3	64.3	52.2	42.6	32.6	23.3
5	98.9	82.4	64.0	48.0	36.4	29.1	23.0	18.3
	Phase, ϕ_H (degrees)							
1	-31.0	-27.8	-28.5	-29.2	-28.7	-26.7	-22.5	-16.1
2	-34.4	-32.9	-35.3	-36.7	-34.4	-28.1	-16.0	0.8
3	-37.1	-37.3	-41.8	-44.2	-39.8	-28.5	-7.8	19.5
4	-40.2	-41.9	-48.7	-52.6	-46.3	-29.8	-0.3	38.0
5	-43.7	-46.4	-54.3	-55.4	-42.5	-27.5	-16.5	-11.1

plotted in Figures 23, 24, and 25 against the measurements of Figures 11, 12, and 13.

In general it can be stated that the comparison is good for the first three harmonics, certainly near the propeller plane where the tones rise well above the broad-band noise. Although the measurement and grid (prediction) positions do not correspond precisely, it is observed that, at least in the 4000 and 5000 rpm cases, within 0.25m (10 in.) either side of the propeller plane, the predictions are quite good. There is some indication that the propeller noise predictions might exceed the actual levels either side of the propeller plane. This cannot be confirmed because measurements were not made at those locations.

The phase predictions (given in the tables) are plotted in Figures 26, 27, and 28. Measurements are available for comparison in the 4000 and 5000 rpm cases. The phase itself cannot be compared, but the phase difference $\Delta\phi_H^{mm'}$ between grid points m and m'. This is the quantity required when calculating the modal forces (see Eq. (41) of Ref. (1)). In Figures 27 and 28, the predicted phase differences are indicated between those positions (along grid line $\ell = 1$) where the microphones were located in Runs 8112 (4000 rpm case) and 8113 (5000 rpm case) which produced the phase measurements of Figures 15 and 16. As can be seen the calculated phase differences and the measured phase differences compare quite well for the first three harmonics (within 10 to 15 degrees usually).

In summary, it can be stated that ANOPP certainly does a good job of predicting the exterior field. While there are indications that the levels may be over-predicted slightly in the regions just fore and aft of the propeller plane, there is no

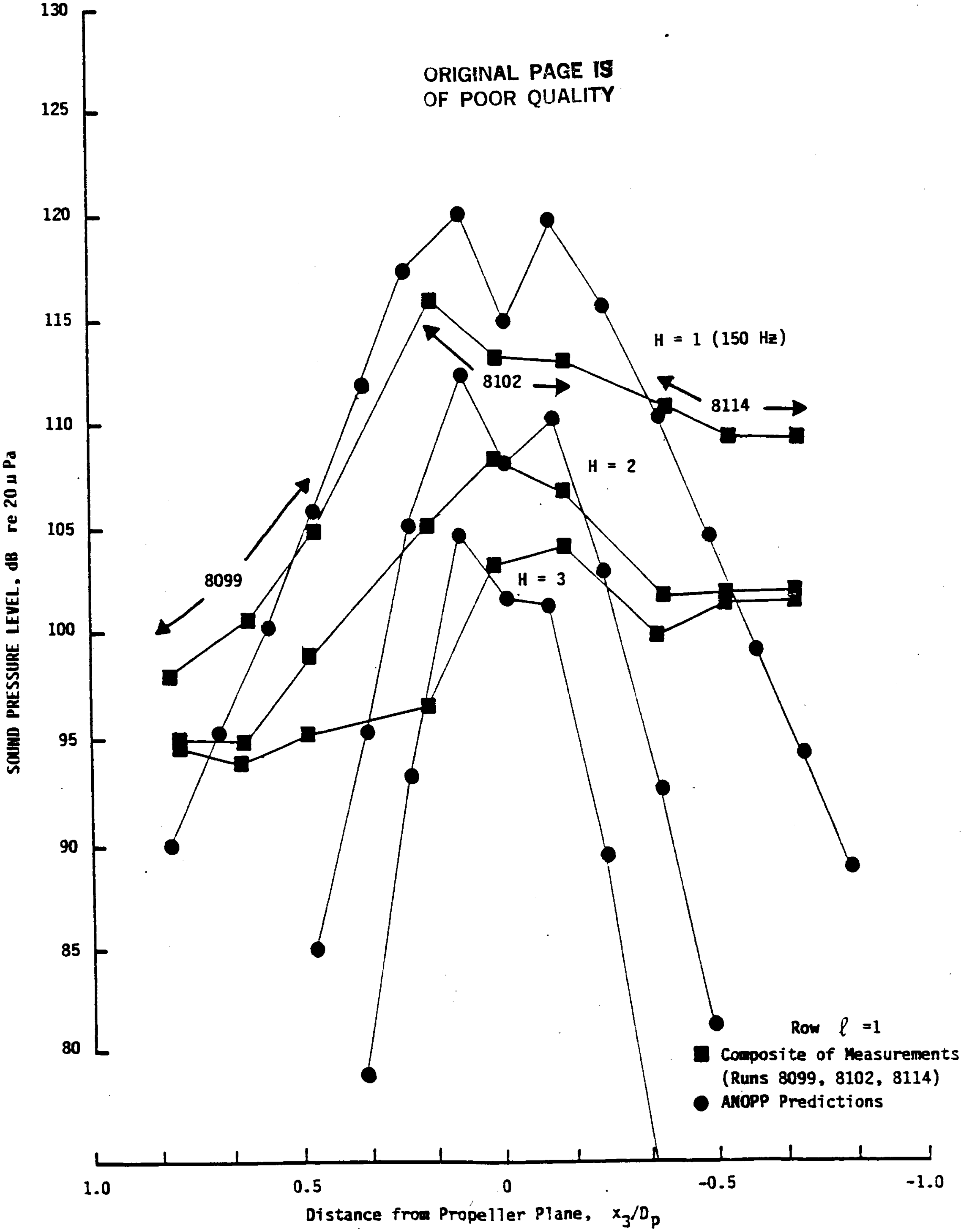

ORIGINAL PAGE IS OF POOR QUALITY

FIGURE 23. COMPARISON OF PROPELLER NOISE PREDICTIONS AND MEASUREMENTS, 3000 RPM

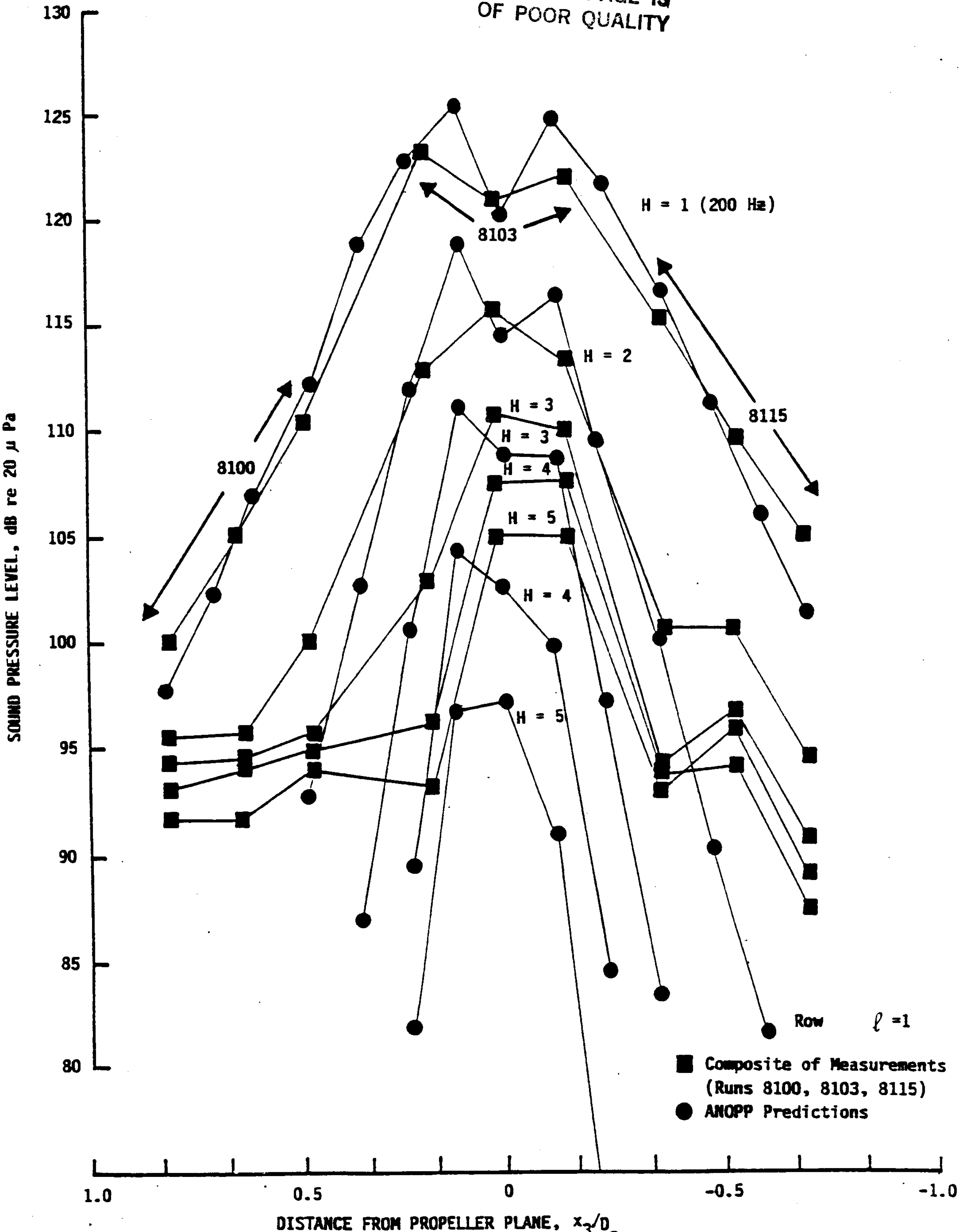

FIGURE 24. COMPARISON OF PROPELLER NOISE PREDICTIONS AND MEASUREMENTS, 4000 RPM

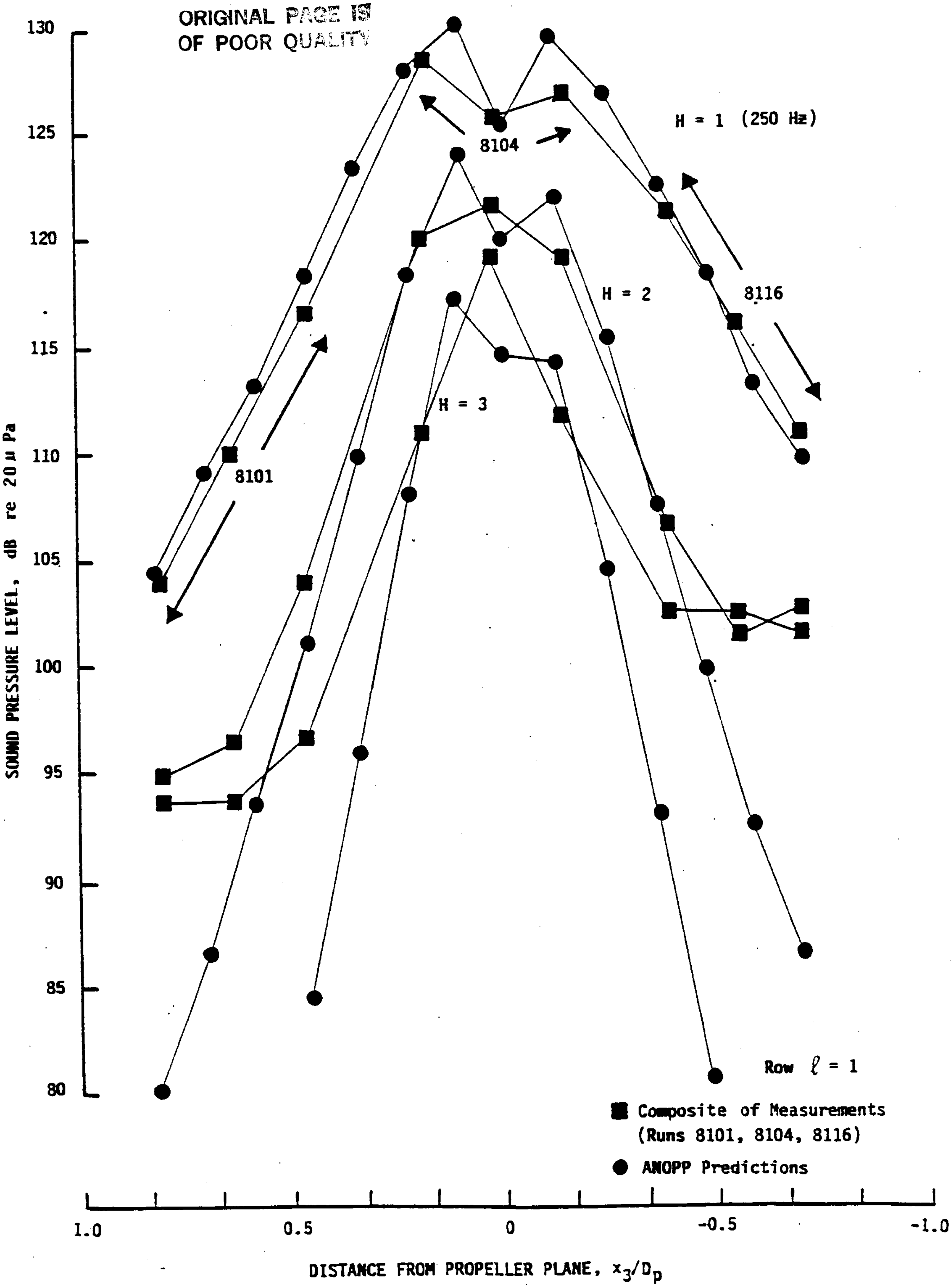

FIGURE 25. COMPARISON OF PROPELLER NOISE PREDICTIONS AND MEASUREMENTS, 5000 RPM

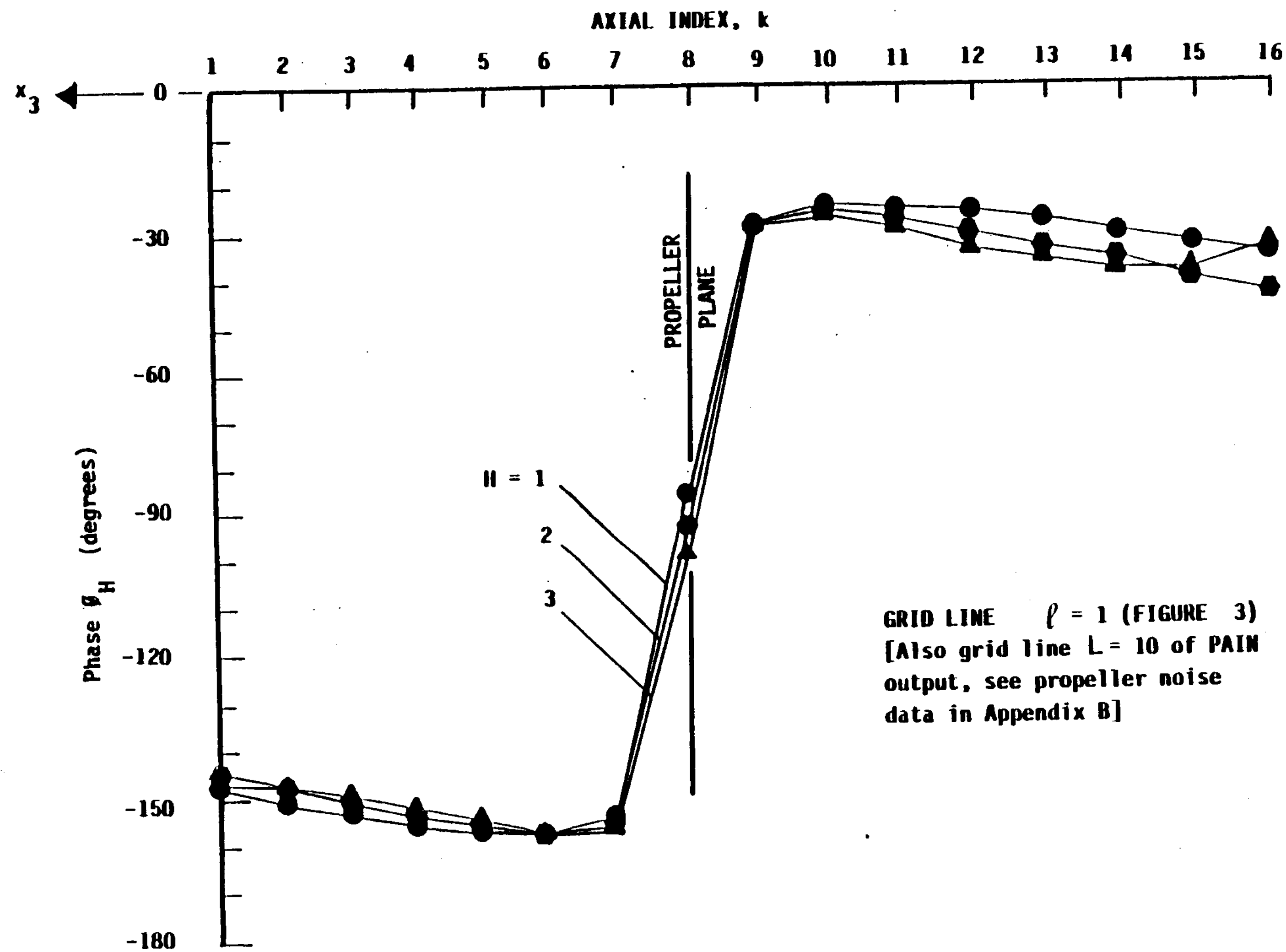

FIGURE 26. PROPELLER TONES PHASE PREDICTION, 3000 RPM

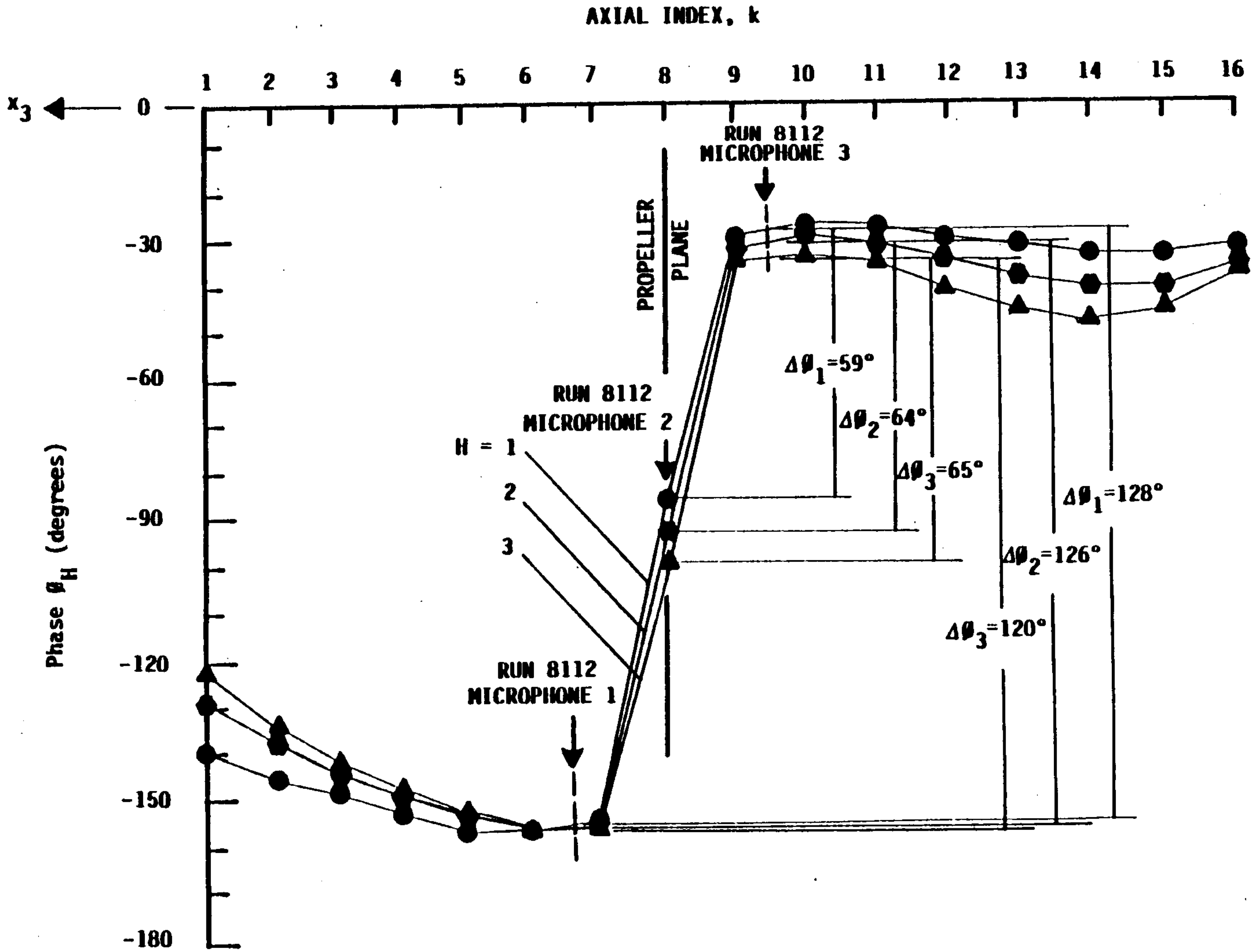

(GRID LINE ℓ = 1)

FIGURE 27. PROPELLER TONES PHASE PREDICTION, 4000 RPM.

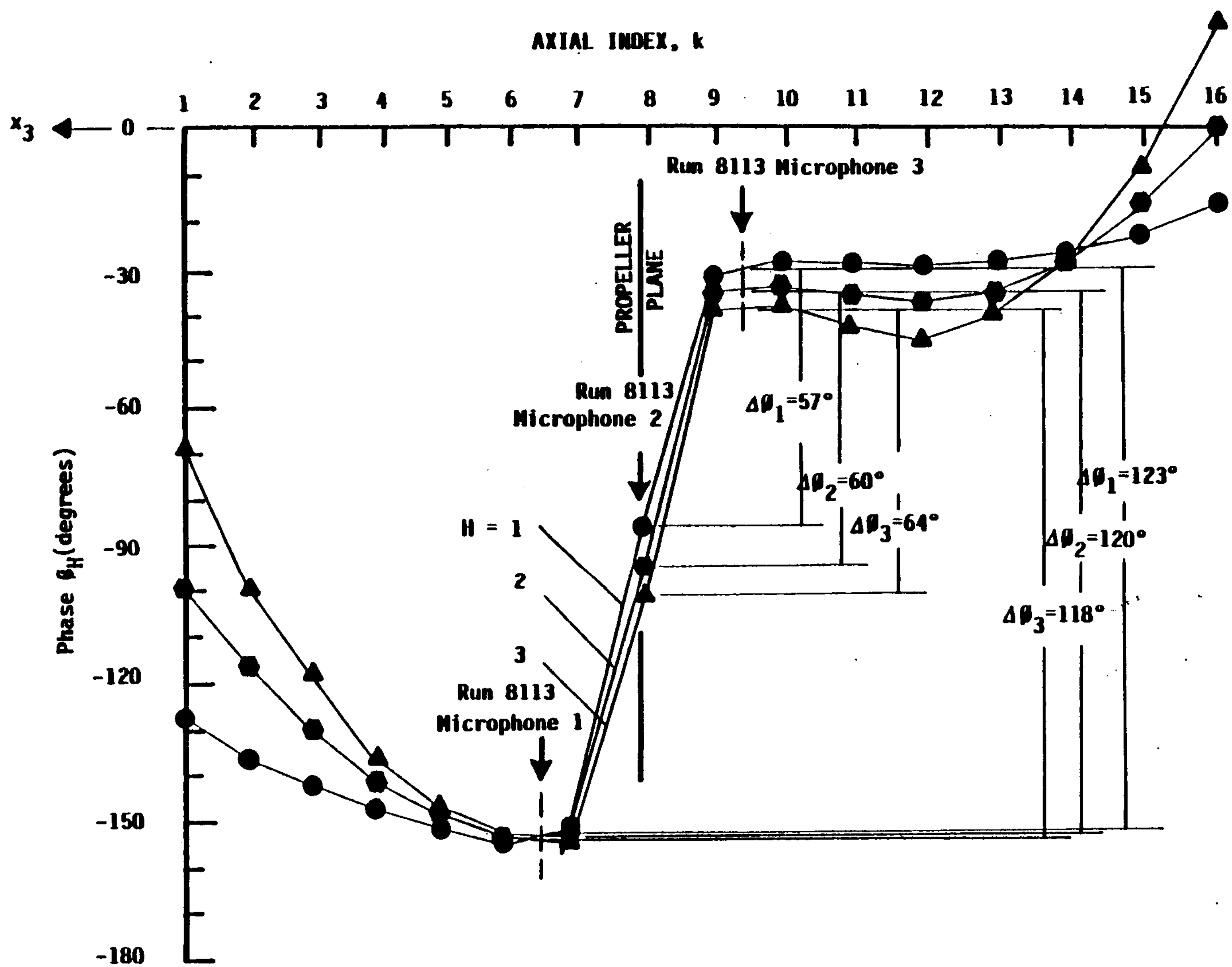

(GRID LINE ℓ =1)

FIGURE 28. PROPELLER TONES PHASE PREDICTION, 5000 RPM

way of proving it from the available data. It is reasonable, at least until future measurements can disprove the assumption, to take the free field predictions as being correct.

Blocked Pressures

To answer the question about the PAIN model used to adjust free field levels to blocked levels, it is necessary to briefly review the basic type of prediction given by Eq. (43) of Ref. (1). If γ (Fig. 3) is zero, the blocked pressure is 6 dB greater than the free field. The ratio remains close to 6 dB for γ less than or equal to about 30°, drops only slightly to 5.75 dB at 50°, 5.4 dB at 60°, 4.75 dB at 70°, 3.3 dB at 80° and finally to zero at 90°. For all practical purposes, the predictions are then for a 5 to 6 dB increase for measurements within a propeller radius either side of the propeller plane along the grid line $\ell=1$.

How much do the pressures actually increase? Figure 29 gives measurement results from the free field and blocked pressure tests (Figures 9 and 10) that show that the pressures increase (near the propeller plane) anywhere from 3 to 4 dB. As one moves away from the plane of rotation the reflection effects appear to dissipate faster than the PAIN model predicts. This implies that perhaps the PAIN model (which is based on some measurements by Magliozzi (9)) should be modified. However the data base is not a large one, and the measurements are not for the same diameter cylinder used in the interior noise study.

Next, the measurements on the hardwood cylinder can be compared to the present PAIN predictions made using the ANOPP free field calculations (Figure 30). The predictions are basically the data in Table 8 increased by 6 dB. These clear-

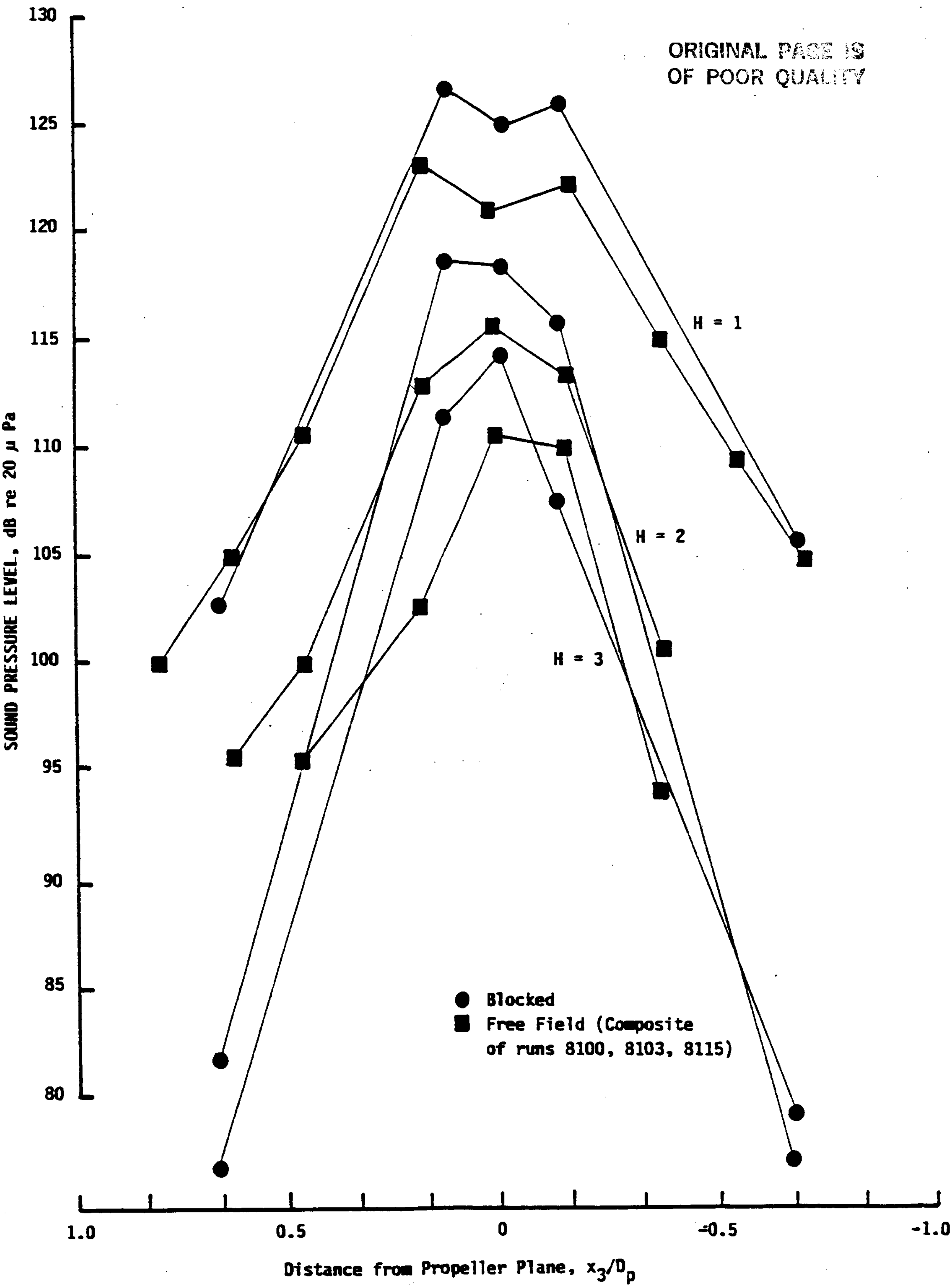

FIGURE 29. MEASURED FREE FIELD AND BLOCKED SOUND LEVELS INDUCED BY PROPELLER

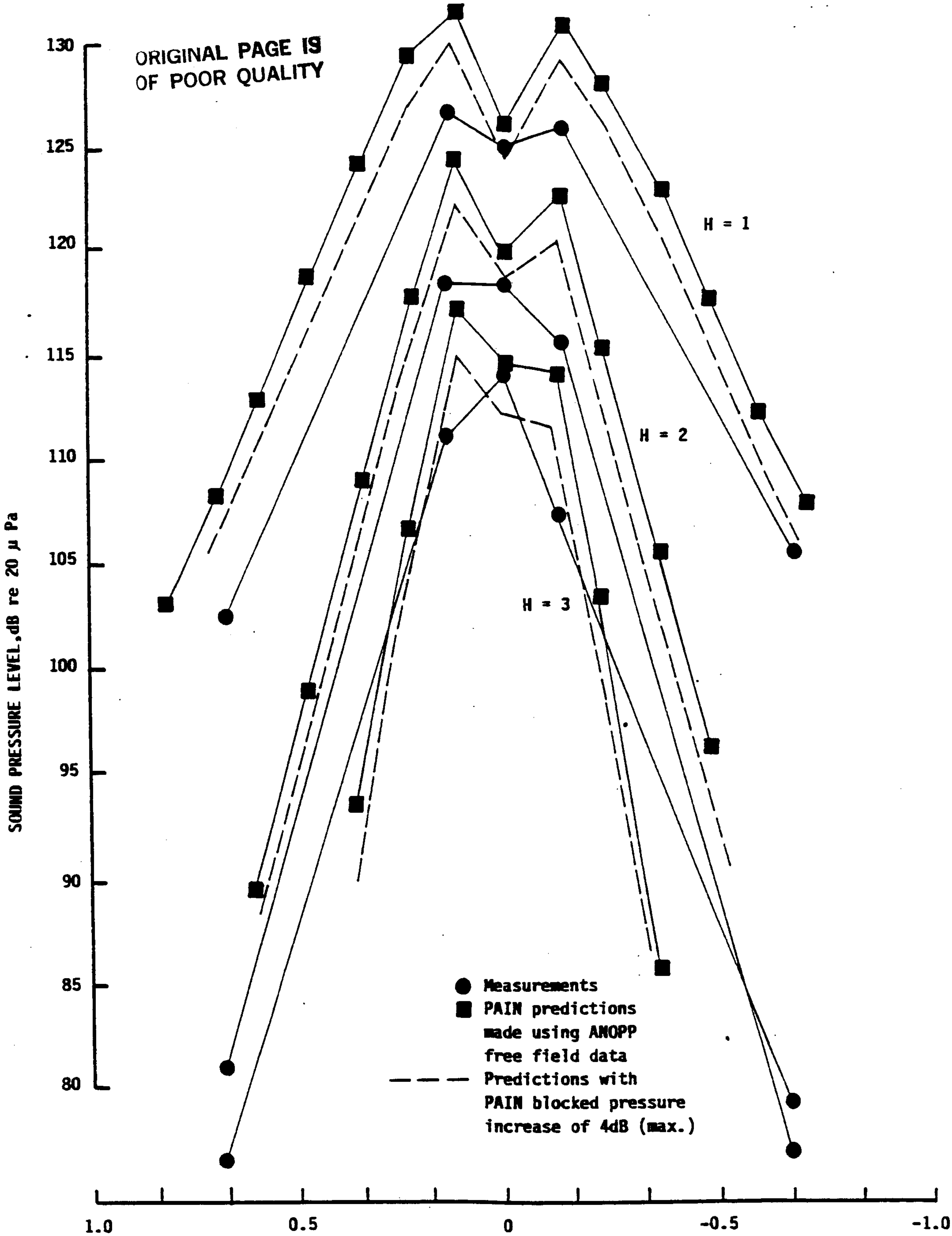

FIGURE 30. MEASURED AND PREDICTED BLOCKED SOUND LEVELS INDUCED BY PROPELLER ON TEST CYLINDER

ly show an overprediction.

For consistency with the measurements of Figure 29, the PAIN predictions can be modified to limit the increase to 4 dB (instead of 6 dB). For convenience these predictions are also shown in Figure 30.

3.5 Test Comparisons

The propeller noise blocked pressure model is temporarily assumed to be suitable as originally programmed in PAIN. To begin, the acoustic and structural loss factors (which are an intermediate output from PAIN) can be compared with measurement data (Table 1). It is necessary first to concentrate on the structural damping model and to correct certain deficiencies known to be present in it.

3.5.1 Structural damping

As previously noted, the structural loss factors of the fuselage modes are calculated for the particular trim installation. For structural mode r, the loss factor is η_r' and is calculated with Eq. (82) of Ref. (1). That equation has been found to be slightly defective.

Modification of η_r' [4]

In Appendix A of this report, it is shown that η_r' of Eq. (82) should be given by

$$\eta_r' = \left\{ \frac{|C_w|^2}{\bar{m}_r^2 \omega_r^4} - \frac{2C_w^I \eta_r}{\bar{m}_r \omega_r^2} + \eta_r^2 \right\}^{\frac{1}{2}} ,$$

[4] Nomenclature used below is consistent with that of Ref. (1).

where $\bar{m}_r$ replaces m of the original result, and

$$\bar{m}_r = mM_r / M_r^X \quad .$$

M_r is the total modal mass and M_r^X is given by

$$M_r^X = \int_X m\psi^{r2}(\bar{x})\, d\bar{x} \quad ,$$

X being the sidewall area covered with trim. The above change is necessary because the original analyses in Refs. (1) and (6) inadvertently led to calculations of structural loss factors premised on total coverage of the model fuselage by trim, and also failed to take into account the fact that significant modal energy of lower order structural modes could be in axial and circumferential stretching motion of the skin (non-bending). The PAIN programming change required is given in Appendix A.

Interpretation of PAIN output

Predicted structural loss factors (output by PAIN) are to be taken from the "Structural Modes" list only. Loss factors, ETA R', listed following "Band-Average Loss Factors" and next to "Trim Factor, dB" are averages over the bands indicated and are wholly fictitious where no modes exist. For the scale-model, the predicted first structural mode is 188.5 Hz and no band average should be shown below 200 Hz.

Comparisons

Predicted loss factors and measurements are compared in Figure 31. The calculated (band average) values shown are heavily weighted at the low end of the modal spectrum by the

ORIGINAL PAGE IS
OF POOR QUALITY

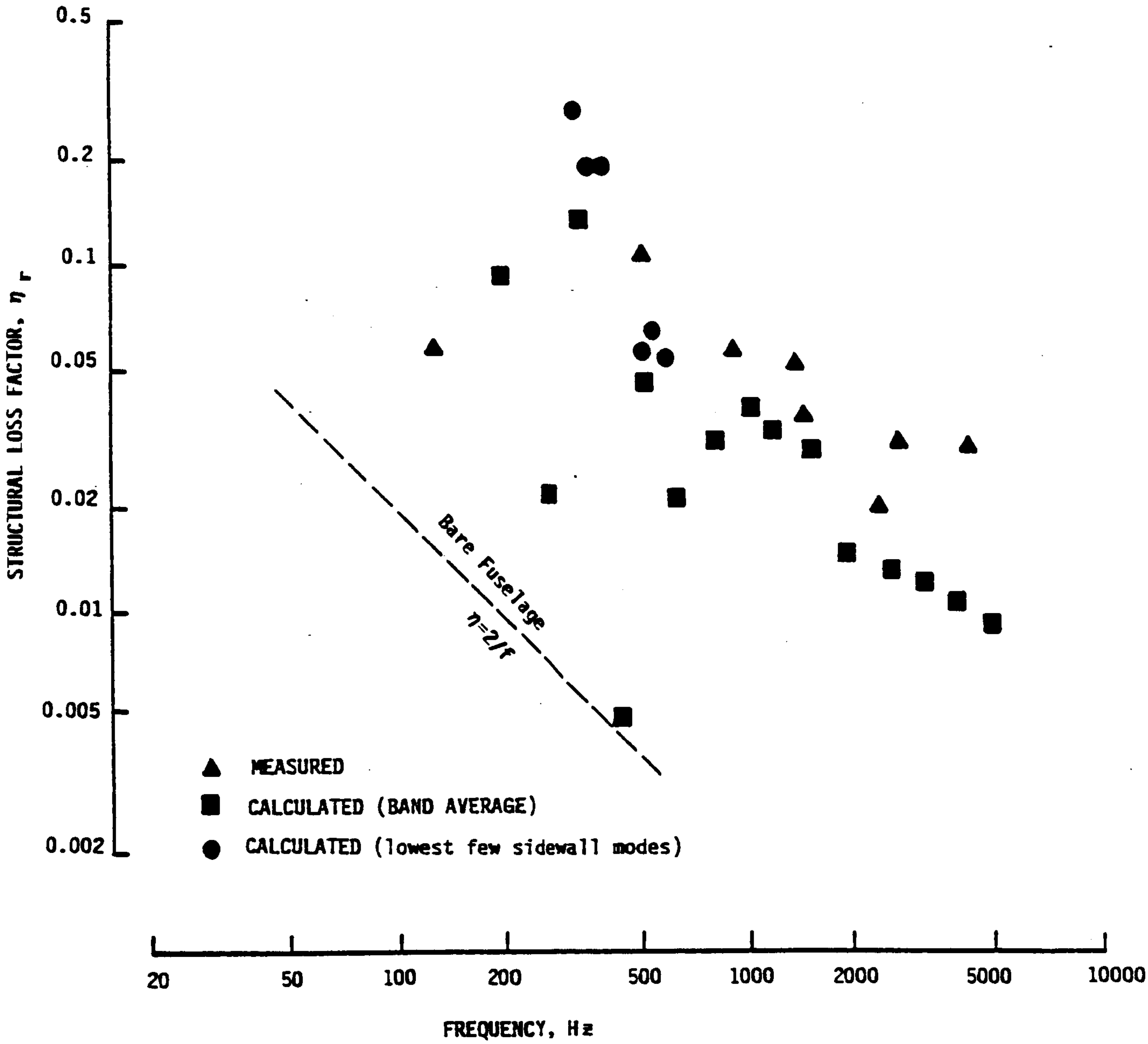

FIGURE 31. PREDICTED AND MEASURED STRUCTURAL LOSS FACTORS OF FUSELAGE WITH TRIM INSTALLED, $\eta_T = 0.13$

loss factors of the floor modes (PAIN predictions are that the scale model fuselage has mostly floor modes at the low end of the modal spectrum). The predicted lowest bona fide shell (cylinder wall) mode is 301.9 Hz. Calculated values of the structural loss factor for the lowest few shell modes are given by the solid circles. Basically the sidewall modes have (predicted) damping values that begin with the solid circles in the range 0.2-0.3 and follow the solid circles and the averages on out to 5000 Hz. These predictions are satisfactory when compared to measurements in the frequency range of interest.

Finally, it is noted here that the modification of η_r' , as detailed previously, alleviates the need to arbitrarily limit its value at low frequencies as assumed in Appendix E of Ref. (1). Also Fig. 31 of this report is the corrected version of Fig. E-15 of Ref. (1).

3.5.2 Acoustic loss factors

The measured and predicted acoustic loss factors are shown in Figure 32. The calculated band average values are plotted upon the scattered individual measurements from Table 1. Predictions are considered satisfactory. Certainly the acoustic loss factor prediction model needs to be applied to a number of different types of trim installations before the quality of the model can be ascertained.

Figure 32 also shows the predicted acoustic loss factors for a heavily damped (almost critically damped) trim lining. Damping is seen to suppress the tendency to predict the upward excursion at about 250 Hz. This is the frequency where the trim model predicts a resonance of the lining on the insulation (see Ref. (6) for some examples of similar predictions).

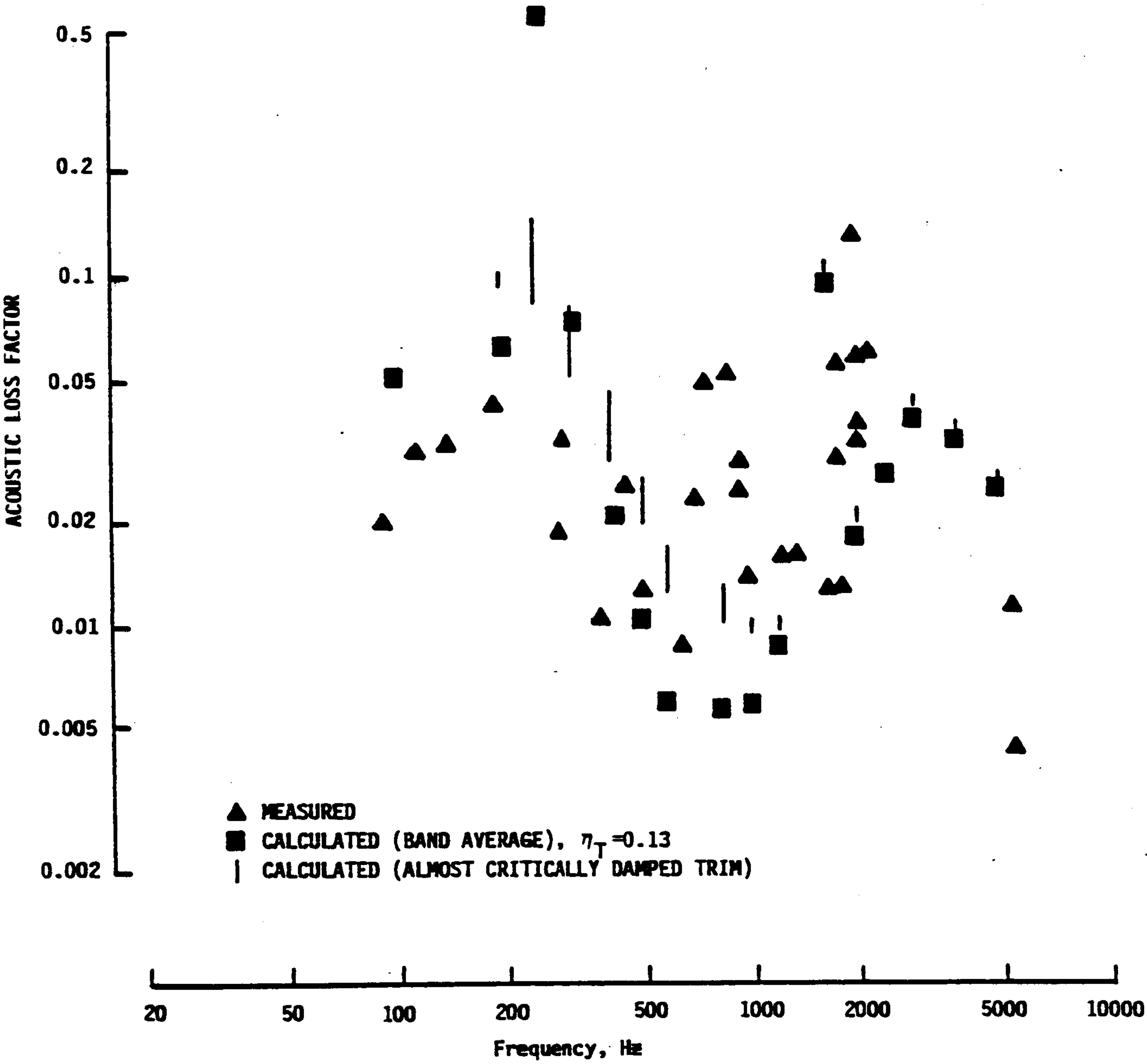

FIGURE 32. PREDICTED AND MEASURED ACOUSTIC LOSS FACTORS

Since the trim transmission loss is also at its predicted maximum negative value, there remains a question as to whether or not this predicted behavior should be suppressed by choosing a large η_T. An answer will be given after the interior noise predictions are examined.

3.5.3 Interior sound levels

Figures 33 and 34 give the predicted interior sound levels. They are plotted on the measurements from Figure 21 (and Table 5). In both cases the input data used are from Table 6. However the original PAIN blocked pressure model (that of a 6 dB increase) was used for the predictions in Figure 33 and the pressure increase was limited to 4 dB in Figure 34. This latter model is more consistent with the results of Figure 29 and thus the latter predictions are those that will be compared with the measurements. The differences between the predictions and the measurements that are plotted in Figure 34 are shown in Table 10.

Statistical Evaluation

Of interest is whether there is a statistically significant difference on the average between the predictions and measurements. Stated another way, are the predictions biased? To determine this, the differences Δ_i, i = 1, 2, ..., n between the predictions and the measurements are computed and their mean $\bar{\Delta}$ and standard deviation s determined. Next a standard hypothesis test is performed (10). The hypothesis is that the true mean difference μ_Δ ($\bar{\Delta}$ is its estimator) is zero, i.e.,

$$H_o : \mu_\Delta = 0 \quad .$$

ORIGINAL PAGE IS
OF POOR QUALITY

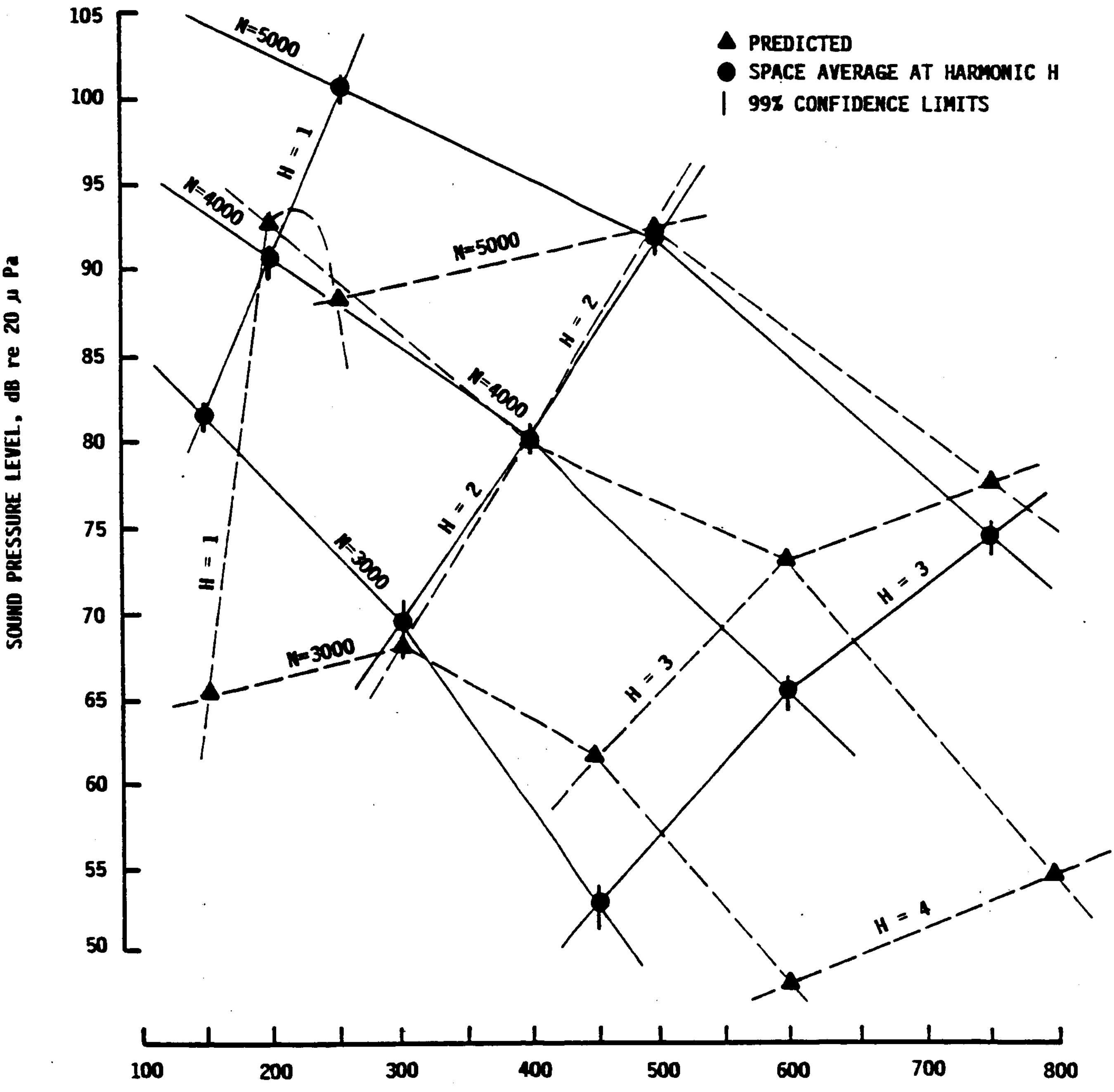

FIGURE 33. MEASURED AND PREDICTED LEVELS INSIDE MODEL FUSELAGE INDUCED BY PROPELLER

ORIGINAL PAGE IS
OF POOR QUALITY

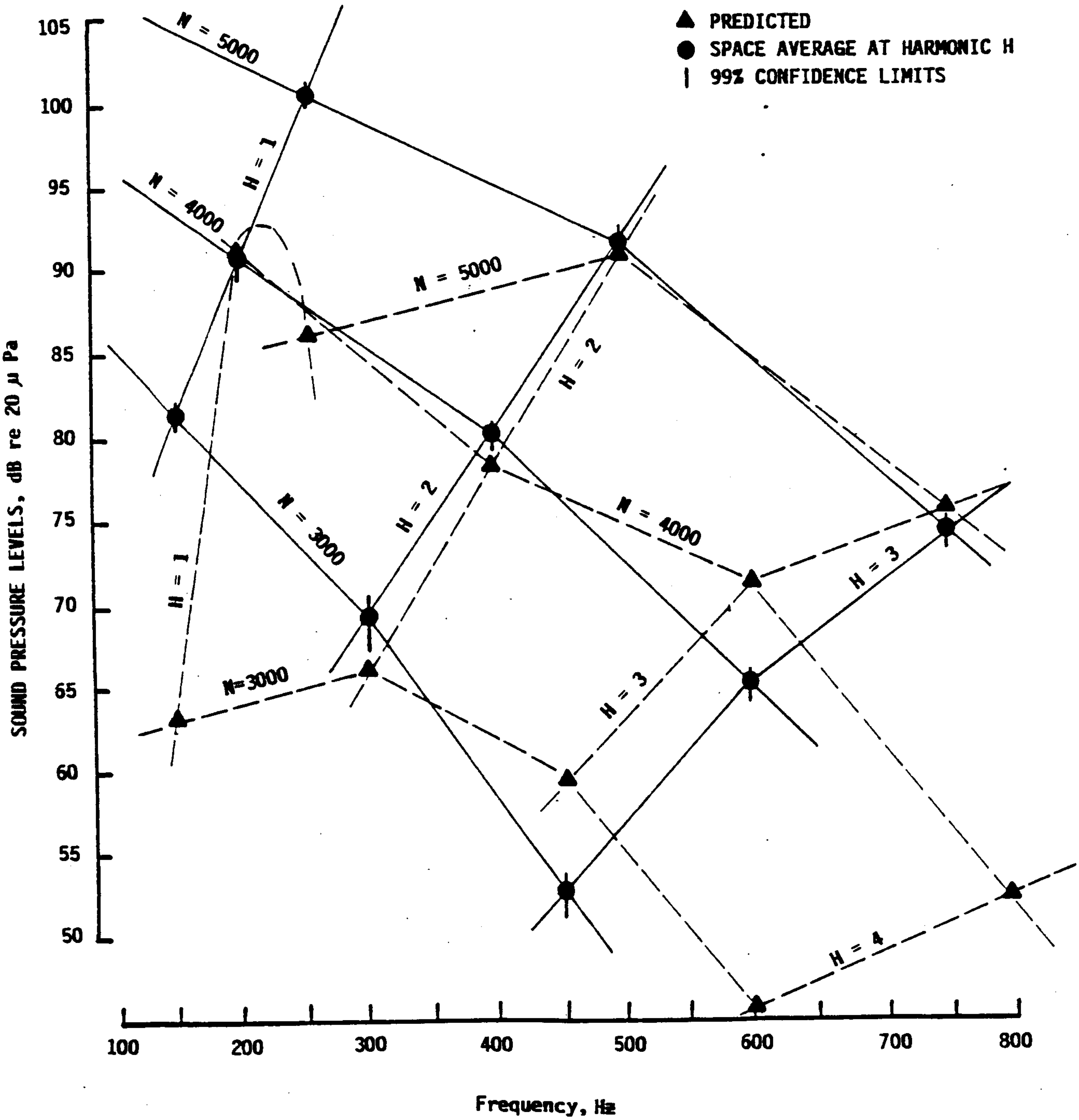

FIGURE 34. MEASURED AND PREDICTED SOUND LEVELS, BLOCKED FIELD LIMITED TO 4dB MAXIMUM INCREASE

Table 10. Predicted Versus Measured Space Average Sound Pressure Levels

RPM	Harmonic H	Freq. (Hz)	$\overline{SPL}_H$ (dB) Predicted*	Measured*	Δ_i
3000	1	150	63.3	81.0	-17.7
	2	300	66.2	69.1	-2.9
	3	450	59.5	52.9	6.6
4000	1	200	91.7	90.3	1.4
	2	400	78.2	80.3	-2.1
	3	600	71.3	65.2	6.1
5000	1	250	86.4	100.2	-13.8
	2	500	91.1	91.5	-0.4
	3	750	75.7	74.0	1.7

* From Fig. 34, η_T=0.13
* From Table 5

Here the sampling distribution of $\bar{\Delta}$ is

$$\bar{\Delta} = s t_{n-1}/\sqrt{n} \quad ,$$

where t_{n-1} is the Student "t" variable with n-1 degrees of freedom. For a two-sided test at the α level of significance, $\bar{\Delta}$ must fall within the acceptance region given by

$$-s t_{n-1;\alpha/2}/\sqrt{n} \leqslant \bar{\Delta} \leqslant s t_{n-1;\alpha/2}/\sqrt{n} \quad .$$

In the present case, the region of acceptance will be taken quite narrow by first selecting $\alpha = 0.1$. Selection of this high level of significance increases the possibility of a so-called Type I error where the hypothesis may be rejected when in fact it is true.

The hypothesis test is performed a number of different ways. First, all of the data are pooled providing a sample size n = 9 (3 rpm x 3 harmonics). The sample mean and standard deviation are computed to be

$$\bar{\Delta} = -2.32 \text{ dB} \; ; \; s = 8.32 \text{ dB} \quad .$$

For the two-sided test at the $\alpha = 0.1$ level of significance

$$t_{8;0.05} = 1.86 \quad ,$$

and the acceptance region for the hypothesis is

$$-5.15 \text{ dB} < \bar{\Delta} < 5.15 \text{ dB} \quad .$$

Since the sample mean $\bar{\Delta}$ (= -2.32 dB) falls within the acceptance region, the hypothesis is accepted. It is also accepted if the level of significance is increased to $\alpha = 0.2$ (Table 11).

Next the hypothesis is tested by considering the data for each propeller speed and harmonic separately. In these cases, the sample size is $n = 3$ and $t_{2;0.05} = 2.92$. The values of $\bar{\Delta}$ and s and the acceptance regions are given in Table 11. Results for $\alpha = 0.2$ level of significance are shown for these tests also.

For the test where all nine datum are considered, there is not a statistically significant difference on the average between predictions and measurements. However, there is a substantial random error indicated by a standard deviation of 8.32 dB. A discrepancy of more than 8 dB can be expected for about one out of three predictions.

When the test is performed by rpm, the hypothesis is accepted in all cases. However, there is also significant random error.

Testing by harmonics leads to acceptance of the hypothesis for $H = 1$, and rejection for $H = 2$ and $H = 3$ at the highest level of significance (each test by harmonic leads to acceptance at a lower level of significance say $\alpha = 0.05$). Rejection of the hypothesis for $H = 2$ and $H = 3$, is an admission of bias being present. However the sample mean error and standard deviation are small.

If data for $H = 2$ and $H = 3$ are pooled ($n = 6$), the hypothesis is accepted even at the $\alpha = 0.2$ level of significance.

Discussion of Results

Although the hypothesis tests have led to the conclusion that

Table 11. Sample Statistics and Acceptance Regions for Interior Sound Levels (Table 10)

Hypothesis Test on	Sample Statistics $\bar{\Delta}$(dB)	Sample Statistics s(dB)	Level of Significance α	Acceptance Region (±dB)	Accept?
All 9 datum (3 rpm x 3 harmonics)	-2.32	8.32	0.1	5.15	yes
			0.2	3.87	yes
3000 rpm (3 harmonics)	-4.67	12.24	0.1	20.63	yes
			0.2	13.32	yes
4000 rpm (3 harmonics)	+1.8	4.38	0.1	7.36	yes
			0.2	4.76	yes
5000 rpm (3 harmonics)	-4.10	8.47	0.1	14.27	yes
			0.2	9.22	yes
H=1 (3 propeller speeds)	-10.0	10.09	0.1	16.99	yes
			0.2	10.98	yes
H=2 (3 propeller speeds)	-1.8	1.28	0.1	2.15	yes
			0.2	1.39	no
H=3 (3 propeller speeds)	-4.86	2.58	0.1	4.33	no
			0.2	2.80	no
H=2 + 3 (3 propeller speeds)	+1.53	4.08	0.1	3.40	yes
			0.2	2.46	yes
8 datum (H=1, 3000 rpm excluded)	-0.4	6.41	0.1	4.28	yes
			0.2	3.20	yes

there is some bias in the predictions, the error that has been identified is not large and is considered an acceptable error at this time (after flight comparisons, its acceptability will be re-examined). The large random error is due to inaccurate predictions of the interior levels at the blade passage frequencies. Now a discrepancy of 4 or 5 dB might (barely) be tolerated for one out of three predictions, but 8 or 9 dB cannot be tolerated. To determine whether further modifications are necessary (beyond those of Appendix A), it is necessary to closely examine PAIN predictions.

Appendix B contains the basics of the PAIN output for the three propeller speeds. The first 48 structural modes are listed (out of 300 total used); also the first 48 acoustic modes (out of 400 total). The distribution of modes in one-third octaves is then given. Next the calculated trim properties are presented. The Trim Factor, dB, is a transmission loss (negative implies an increased transmission). Following these data the propeller noise input is tabulated for the first three harmonics. Data input for the grid of Figure 3 are used to create the data for the large (16 x 19) grid as discussed in Section 3.4.2. Note $L=\ell+9$, so the data for $\ell=1$ to 10 of Figure 3 are found in L=10 through 19. The tone transmission predictions come next followed by a tabulation of the five highest contributing pairs of acoustic and structural modes that make up the predictions. The propeller noise data and the interior predictions for the 3000, 4000, and 5000 rpm cases are given in sequence.

The lowest computed structural mode occurs at 188.5 Hz. From the values of the generalized mass, it can be seen that this is a floor mode since most of the contributing energy is in the floor (the output of MRP can be used to see the mode shape if desired). Note that the first true cylinder (shell) mode occurs at 301.9 Hz, followed by another at 318.7 Hz and another at 346.7 Hz and 470.5 Hz, etc. Since the first harmonics (blade passage frequencies) occur at 150 Hz, 200 Hz, and 250 Hz, all shell (sidewall) modes are being driven below their resonance frequencies (primarily because the model cylinder is too short) and respond in "stiffnesslike" fashion for H=1. However, the frequencies of the second and third harmonics are at 300 Hz or above and in these cases, resonance and mass controlled structural modes are usually dominant contributors.

Consider the cases for H=1. Floor modes dominate transmission at 3000 and 4000 rpm. The shell mode at 301.9 Hz is contributing substantially at 5000 rpm, as is another shell mode (number 8) at 318.7 Hz. Both are stiffness controlled.

The H=2 cases are as follows: At 3000 rpm, the shell mode at 301.9 Hz is resonant and dominates the transmission. A mass controlled shell mode at 346.7 Hz dominates at 4000 rpm. A mass controlled mode at 470.5 Hz dominates at 5000 rpm. The latter mode has significant sidewall and floor motion.

The H=3 cases (all rpms) are a "mixed-bag" in that the predictions are dominated by structural modes having significant sidewall and floor motion.

Now consider the predicted trim TL. Note that at 150 Hz it is about -7 dB, at 200 Hz, -17.3 dB, and at 250 Hz, -4.8 dB. The large negative value might at first appear to cause the prediction for H=1 (at 4000 rpm) to be better than it would have been had this behavior not been predicted. However the trim model compensates for this and when the resonance effect is forced to disappear by increasing η_T, the prediction for the 4000 rpm, H=1 case changes only slightly (as will be seen shortly).

Note the acoustic mode dominating the transmission. For H=1 at 4000 rpm, it is mode 3 (q=2,i=0) at 187.6 Hz. This mode dominates only for small η_T. Also note that acoustic modes 6, 7, and 8 have very high loss factors (0.6-0.7). These high loss factors will be predicted only when and where the trim resonance is predicted. Now if η_T is increased significantly, say to 2, the trim resonance effect will disappear (the trim TL changes to +1.2 dB at 160 Hz, +4.6 dB at 200 Hz, and +8.7 dB at 250 Hz). Simultaneously, the high values of the acoustic loss factors of modes 6, 7, and 8 will fall. η_n is reduced to 0.088 for mode number 6, 0.077 for mode 7, and 0.081 for mode 8. Moreover, with the larger η_T, the prediction for H=1 at 4000 rpm is dominated by the response of modes 7 and 8 (not 3 anymore). Yet even with these dramatic differences, the predicted interior level is about the same (91.2 dB as opposed to the original 91.7 dB).

The predicted results for the case of η_T=2 are given in Figure 35 and Table 12. As can be seen the errors (compared to those in Table 10) remain about the same. However the H=1, 5000 rpm prediction is significantly better. As before, the H=1, 3000 rpm prediction has the largest discrepancy. This particular datum is unique in that the blade passage frequency lies in a region where non-resonant behavior of the cavity is necessary (150 Hz lies between the first and second acoustic modes). It is not felt to provide a good test for the PAIN model, and for this reason, the H=1, 3000 rpm datum is tossed out. The other eight remain (a case could probably be made for throwing out the data for all of the H=1 cases because of the known difficulty of making predictions in the stiffness-controlled region).

Now when the hypothesis test is performed on the data in Table 10 (with the H=1, 3000 rpm datum excluded), the mean error and standard deviation are found to be

$$\bar{\Delta} = -0.4 \text{ dB} \; ; \quad s = 6.4 \text{ dB} \quad ,$$

Table 12. Predicted Versus Measured Space Average Sound Pressure Levels

RPM	Harmonic H	$\overline{SPL}_H$ (dB) Predicted*	Measured	Δ_i
3000	1	62.1	81.0	-18.9
	2	65.5	69.1	-3.6
	3	56.9	52.9	4.0
4000	1	91.2	90.3	0.9
	2	73.8	80.3	-6.5
	3	67.4	65.2	2.2
5000	1	92.9	100.2	-7.3
	2	89.6	91.5	-1.9
	3	74.0	74.0	0.0

* η_T =2.0 to suppress predicted trim resonance

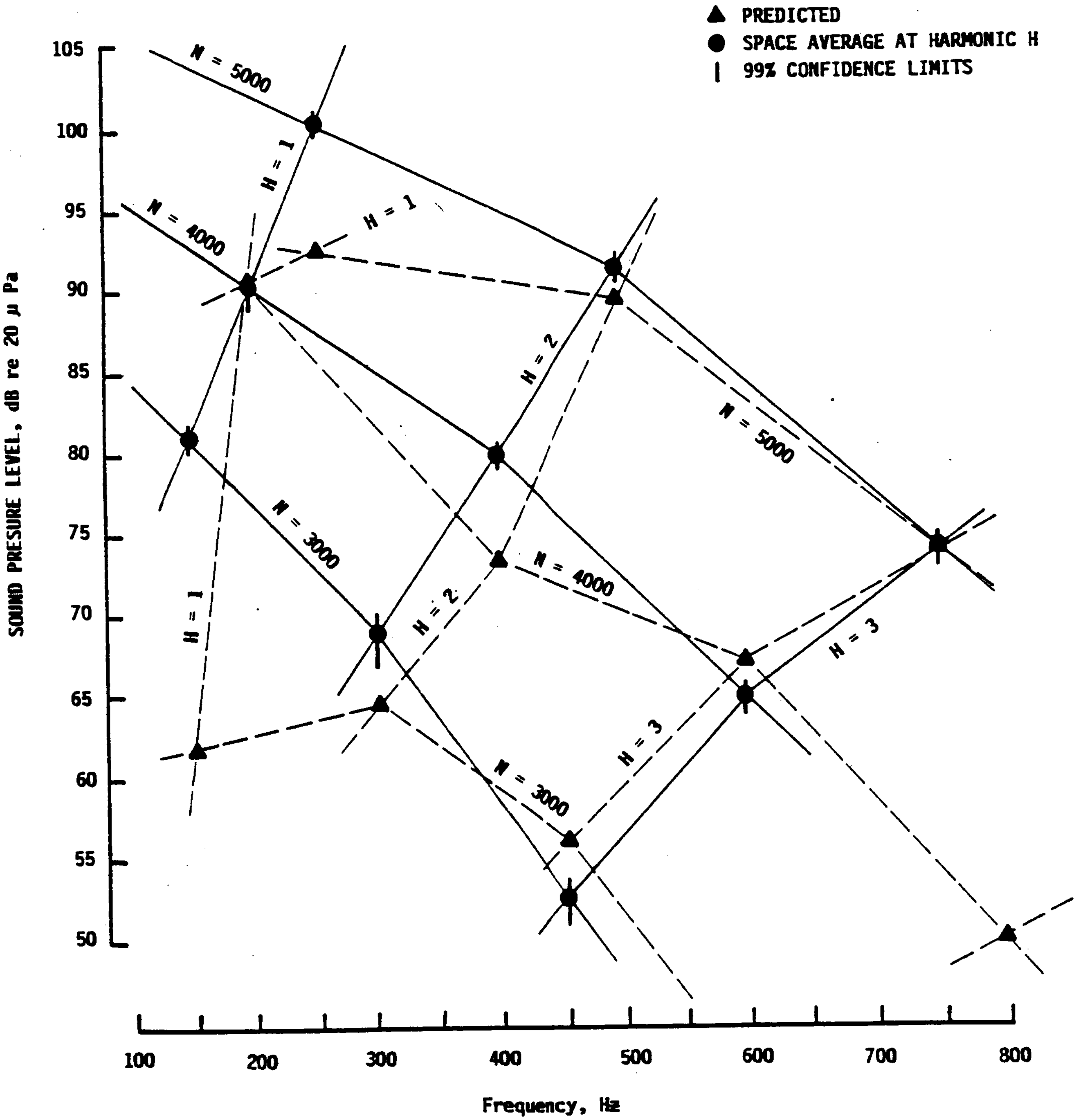

FIGURE 35. MEASURED AND PREDICTED SOUND LEVELS, BLOCKED FIELD = 4dB (MAX), CRITICALLY DAMPED TRIM PANEL

and the acceptance region is ± 3.2 dB at the $\alpha = 0.2$ level of significance. The hypothesis is still accepted, and the random error is almost tolerable. Performing the hypothesis test on the data of Table 12 with the H=1, 3000 rpm datum excluded, the mean error and standard deviation are found to be

$$\bar{\Delta} = -1.5 \text{ dB} \; ; \; s = 4.05 \text{ dB} \quad ,$$

and the acceptance region (for $\alpha = 0.2$) is ± 2.0 dB. In this case also the hypothesis is accepted. Moreover here, the random error is felt to be (barely) tolerable (s=4 dB).

It can now be safely stated that the PAIN model seems to work. It has done a reasonably good job of predicting the scale-model test results, and its testing in application to real aircraft is needed next.

4.0 PROGRAM UTILIZATION: FULL SCALE AIRCRAFT

Capabilities and limitations of the PAIN software for flight predictions in the case of real aircraft are considered in this section. Basically the focus here is on learning about some of the types of problems that a user will be confronted with when a particular aircraft is selected for study. As will be shown, PAIN has some limitations. But in many respects these are not major problems for the user. The software is capable of making predictions for practically any aircraft configuration. There are limits as to the number of propeller harmonics that should be attempted, and there are circumstances where the propeller noise field on the fuselage may decay too slowly (spatially, away from the propeller plane) for the user to be assured that a valid prediction is being made.

4.1 Modeling of the Aircraft

A useful approach to the modeling of an aircraft is to begin with a sketch such as shown in Figures 36, 37, or 38. Here three aircraft are used to illustrate the type of geometric information that must be generated. For instance, the length of the fuselage cylinder must be defined. This can be taken as the actual length of the cylindrical section. It should be kept in mind that there is room for judgement here. It may be confirmed in the future that the cylinder should be longer than the cylindrical section of the fuselage (i.e., that better predictions will be made if it is assumed to be). But presently this length is chosen on the premise that details pertaining to the termination of the cylinder are going to wash out in the frequency range where the tone transmission is of concern. That is, some errors in the modal characteristics in the low frequency range will be accepted, assumed inconsequential as to

ORIGINAL PAGE IS
OF POOR QUALITY

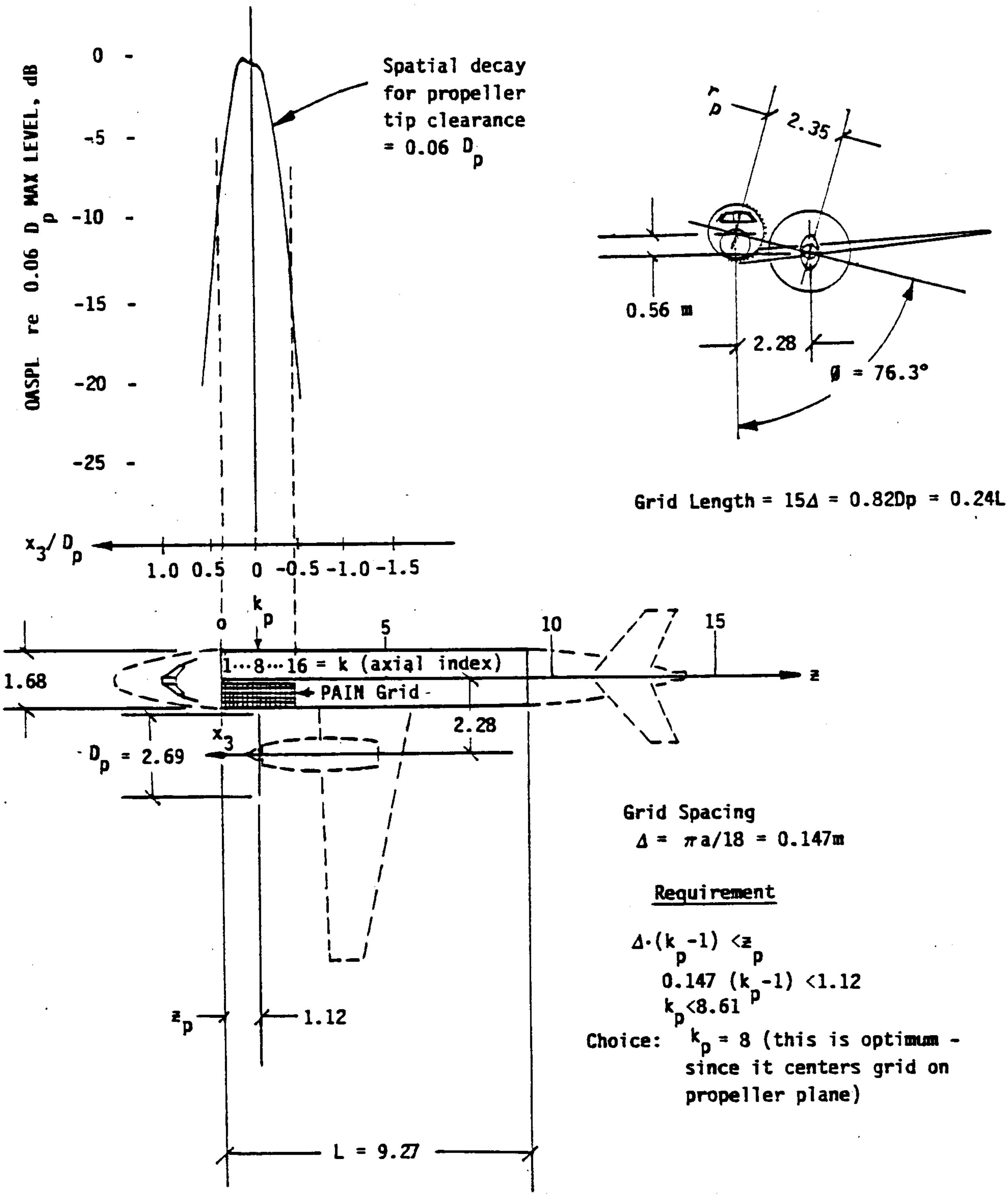

SCALE: 1 in = 5m

FIGURE 36. BUSINESS/COMMUTER AIRCRAFT

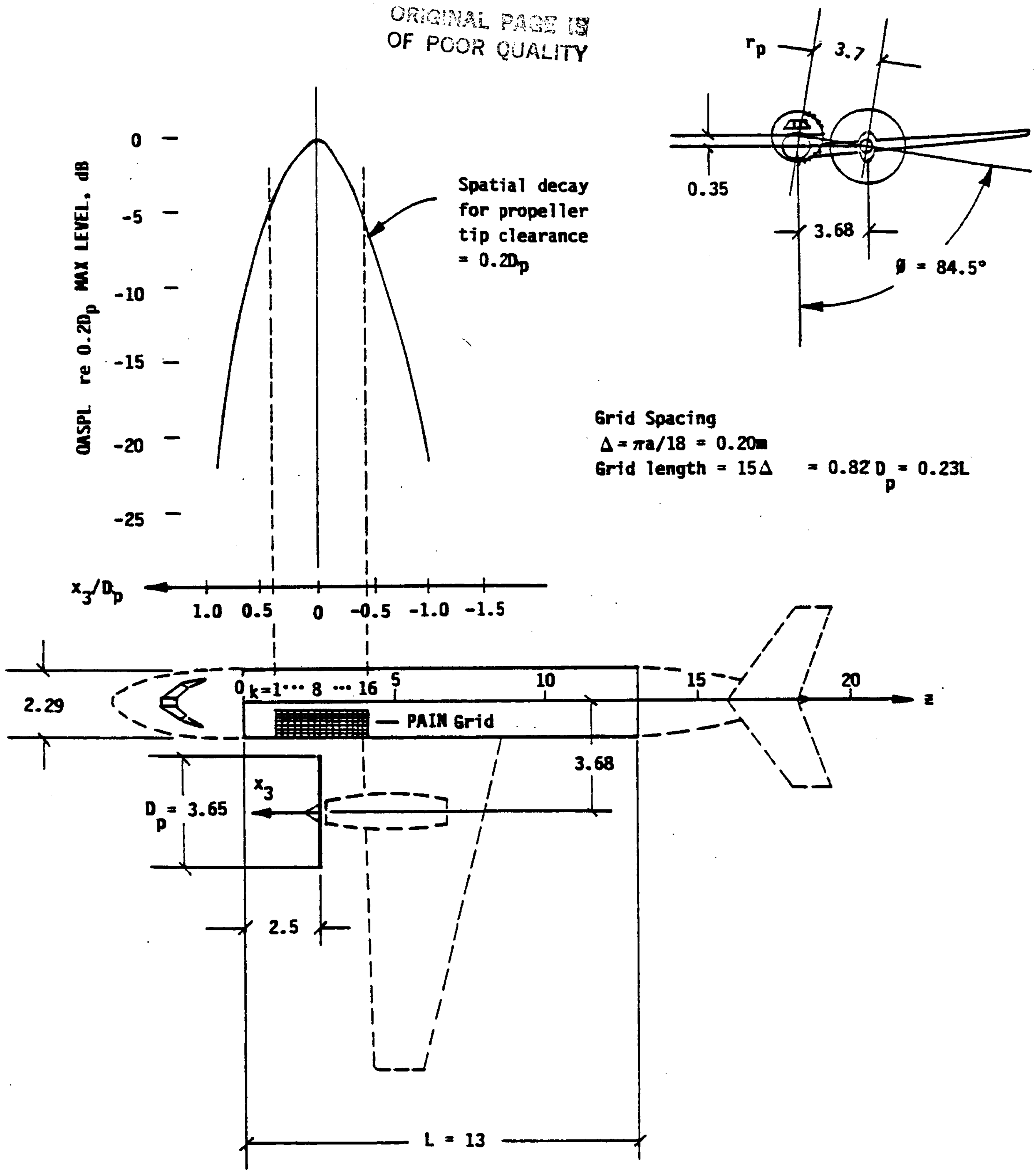

Scale: 1 in = 5m

FIGURE 37. SMALL BODY AIRCRAFT

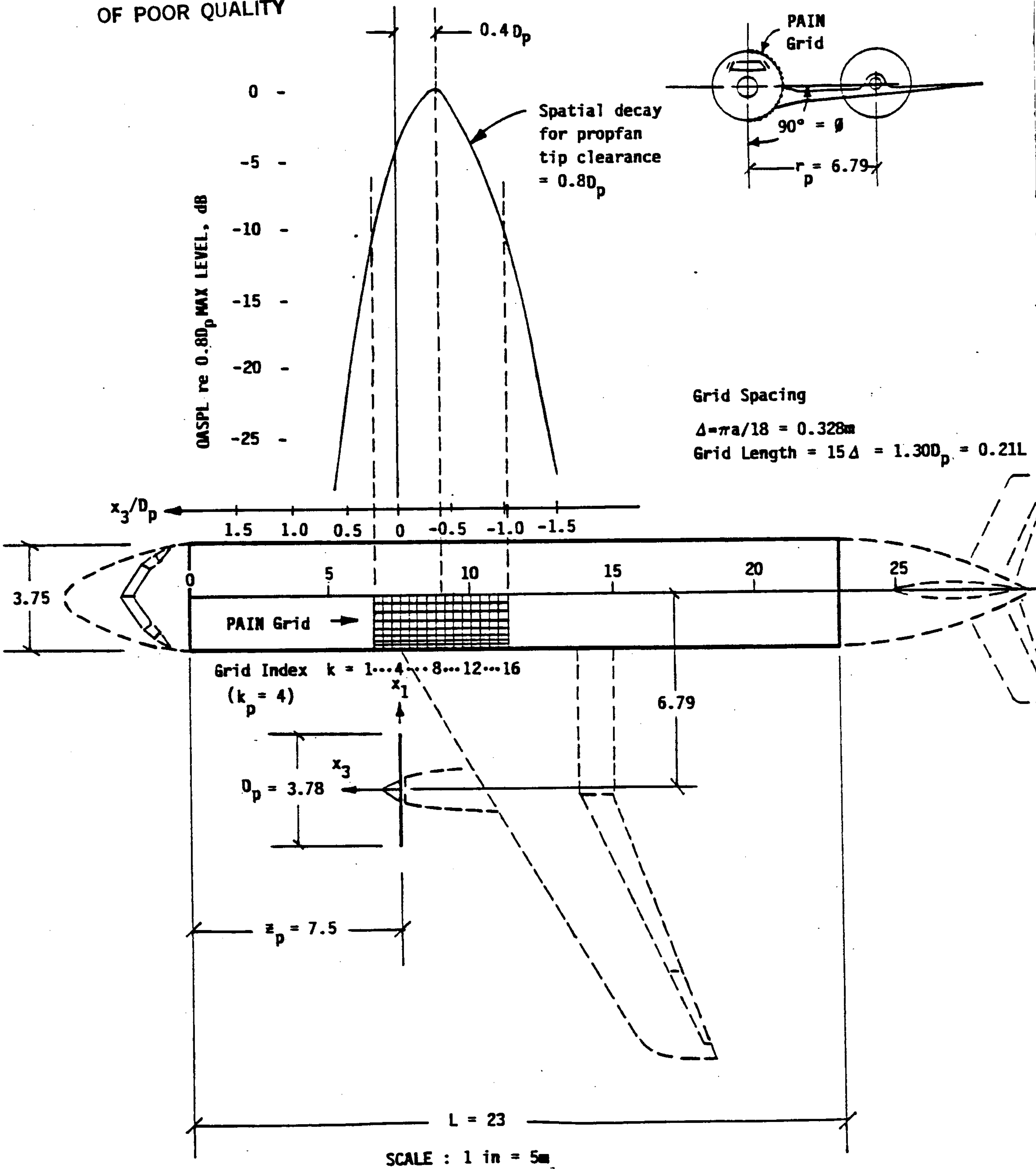

FIGURE 38. NARROW BODY AIRCRAFT - PROPFAN CONFIGURATION

their effects at the blade passage frequency and its harmonics. After the length L is determined, the remainder of the information will be fixed by the aircraft configuration. The location of the propeller, given by the radius r_p, angular position ϕ, and axially by z_p is to be specified. These parameters are exactly the same as defined in Figure 2.

The three aircraft shown have been chosen to illustrate the ranges of parameters which will likely confront the user. In most circumstances the propeller will be larger in diameter than the fuselage. This will almost always be true whenever there are only two engines (propellers), and will lead to a limitation on the allowed range of the propeller tip clearance. The PAIN software is designed to take the propeller noise signatures over a grid that covers a length of the fuselage equal to 15Δ, where Δ is given by $\pi a/18$, and a is the fuselage cylinder radius. For the business aircraft shown in Figure 36, the grid length is 0.24L or $0.82D_p$. For the small body aircraft of Figure 37, it is 0.23L ($0.82D_p$) and for the narrow body aircraft of Figure 38, the grid length is 0.21L ($1.30D_p$). The optimum is to have a long grid length, i.e., as a percentage of both L and D_p. Over the length of the grid, it is desirable to have a significant decay in the sound pressure levels (at each harmonic) to assure that most of the acoustic energy is being taken into account. The grid length is fixed by the radius of the fuselage, thus when the propeller diameter is significantly larger than the diameter of the fuselage, there is concern that the propeller noise field may not decay rapidly enough over the length of the grid. This concern is aggravated by the fact that the cylinder length to diameter ratio (L/D) of a typical fuselage (cylinder) is in the range between about 5.3 and 6.3, and thus the grid is never going to cover more than about 20-25% of the length of the fuselage cylinder. To top this off, the decay of the propeller field on the fuselage is highly dependent on the propeller tip clearance.

Consider the airplane in Figure 36. The diameter of the propeller is more than a meter larger than the diameter of the fuselage. The tip clearance is 0.165m or 0.06 D_p. The selected grid location, with the axial index k=8 lying in the propeller plane (i.e., $k=k_p$), puts the forward-most position on the grid at $x_3=7\Delta$ or 1.02m (0.38 D_p). The aft-most position is $x_3=-8\Delta$ or -1.18m (-0.44 D_p). Figure 39 shows that the overall sound level at the forward-most grid point ($k=1,\ell=1$) can be expected to be about 10 or 11 dB below that at the propeller plane. At the aft-most grid point ($k=16,\ell=1$), it can be expected to be 13 or 14 dB below the level at the propeller plane. But if the tip clearance is increased to 0.2 D_p these values would drop to only 4 dB and 6 dB respectively (see Figure 37). Thus if the tip clearance exceeds about $(0.2 \text{ to } 0.3)\cdot D_p$, the PAIN model probably should not be used. However this is not an unbendable rule. The spatial decay of the overall level as plotted versus tip clearance in Figure 39 is usually dominated by one harmonic (the blade passage frequency). The 2nd and higher harmonics will decay more rapidly. Figure 39 can be used as a guide to gain some insight into the likely nature of the computed propeller noise field. However, ultimately, the predictions made with the propeller noise program must be used to determine if sufficient spatial decay is present.

The axial location of the grid is to be selected such that the peak overall sound level occurs as near to the center of the grid as is possible. In the turbo-prop circumstance, since the tip clearance is limited to about 0.2 D_p to 0.3 D_p, the grid should be located with the axial index k_p set to 8 or 9. The entire grid must be located on the fuselage cylinder, thus there is a requirement that $\Delta\cdot(k_p-1)<z_p$.

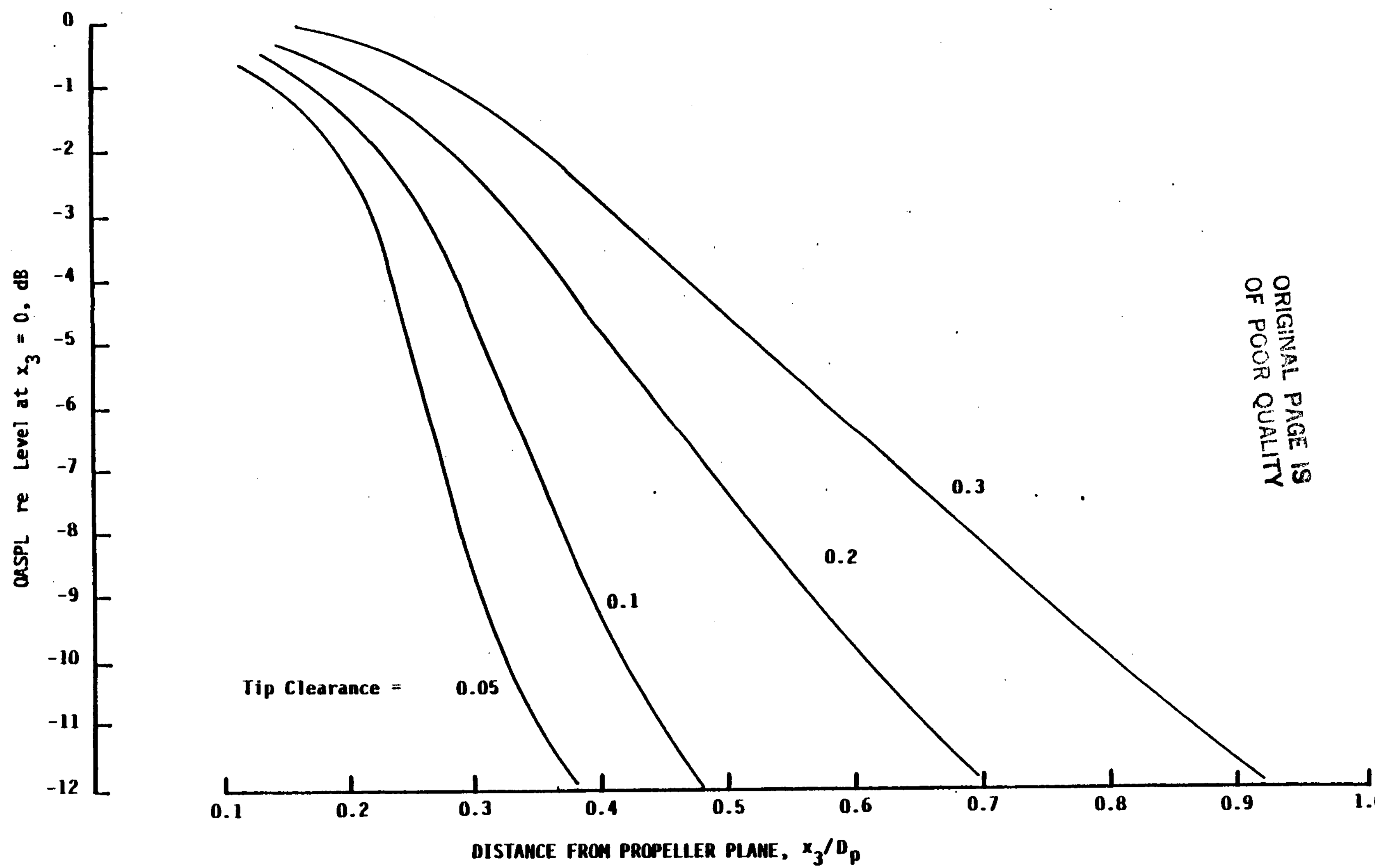

FIGURE 39. VARIATION OF OVERALL FREE FIELD PROPELLER LEVELS [11]

For instance, in Figure 36, k_p must be 8 or less. Since k_p = 8 (or 9) is optimum, the choice is 8 in this case. For the aircraft of Figure 37, k_p could be selected as high as 13 and the grid would still remain entirely on the cylinder. However again the optimum value is 8 or 9, so 8 is the selected value.

In a Propfan configuration, the tip clearance will be increased significantly because the exterior levels will be so intense. The tip clearance shown in Figure 38 is 0.8 D_p. At the flight Mach number M = 0.8, the peak overall sound pressure level will occur aft of the propeller plane. Reference 12 has been used to predict that the axial location of the peak level will be $x_3 = -0.4\ D_p$. Predictions are that the exterior levels for the Propfan configuration will decay more rapidly than for a turbo-prop. In the present circumstance, the decay is expected to exceed 10 dB at the extremes of the grid even though the tip clearance is quite large. In this particular case, in order to center the grid about the peak overall level (i.e., have the peak lie somewhere between k = 8 and k = 9), a value of $k_p = 4$ is selected.

The noise signatures (Fourier amplitudes and phases for each harmonic) are to be computed at the 160 grid points as given in Section 3 of Reference (2). That calculation completes the description of the exterior pressure field required by the PAIN program.

4.2 Modeling for Cabin and Fuselage Modes

The next step is to determine the modal properties of the fuselage (both the structural and the acoustic properties).

4.2.1 Cabin

The 2-dimensional (cabin cross-sectional) modal properties are computed with the program CYL2D. That program requires the floor angle θ_0 as an input. Figure 40 shows typical cabin cross sections such as might correspond to the three aircraft being studied here. In the cases of the small body and narrow body aircraft, the floors extend from sidewall to sidewall. The intersection of the floor surface (or its extension) with the sidewall skin defines the floor angle. CYL2D computes the mode shapes in 2-dimensions for a cylinder with floor partition having unit radius. Thus the cabin diameter is of no concern until the PAIN program utilizes the CYL2D output file.

Business aircraft such as that of Figures 36 and 40 typically have a rather small diameter and a recessed aisle. In the present case a floor angle of 50° is selected because 70% of the floor surface is at the level defined by $\theta_0=50^\circ$. Moreover, when the structural modes are computed, the cabin sidewall surface should match the cabin space. In the present case, the cabin floor lays over frames with webs extending downward to the shell. Thus it is desirable to model the shell-floor juncture as rigid at the floor line, i.e., to place the floor at 50°. Since the angles θ_0 appearing in the acoustics program CYL2D and the structural program MRP must match, 50° is the best overall compromise.

The headliners and baggage storage (shown in phantom in Figure 40) are ignored. Presently CYL2D cannot handle these details.

4.2.2 Fuselage

The next step is to prepare the input data for the program MRP. Table 13 contains the type of structural information that is

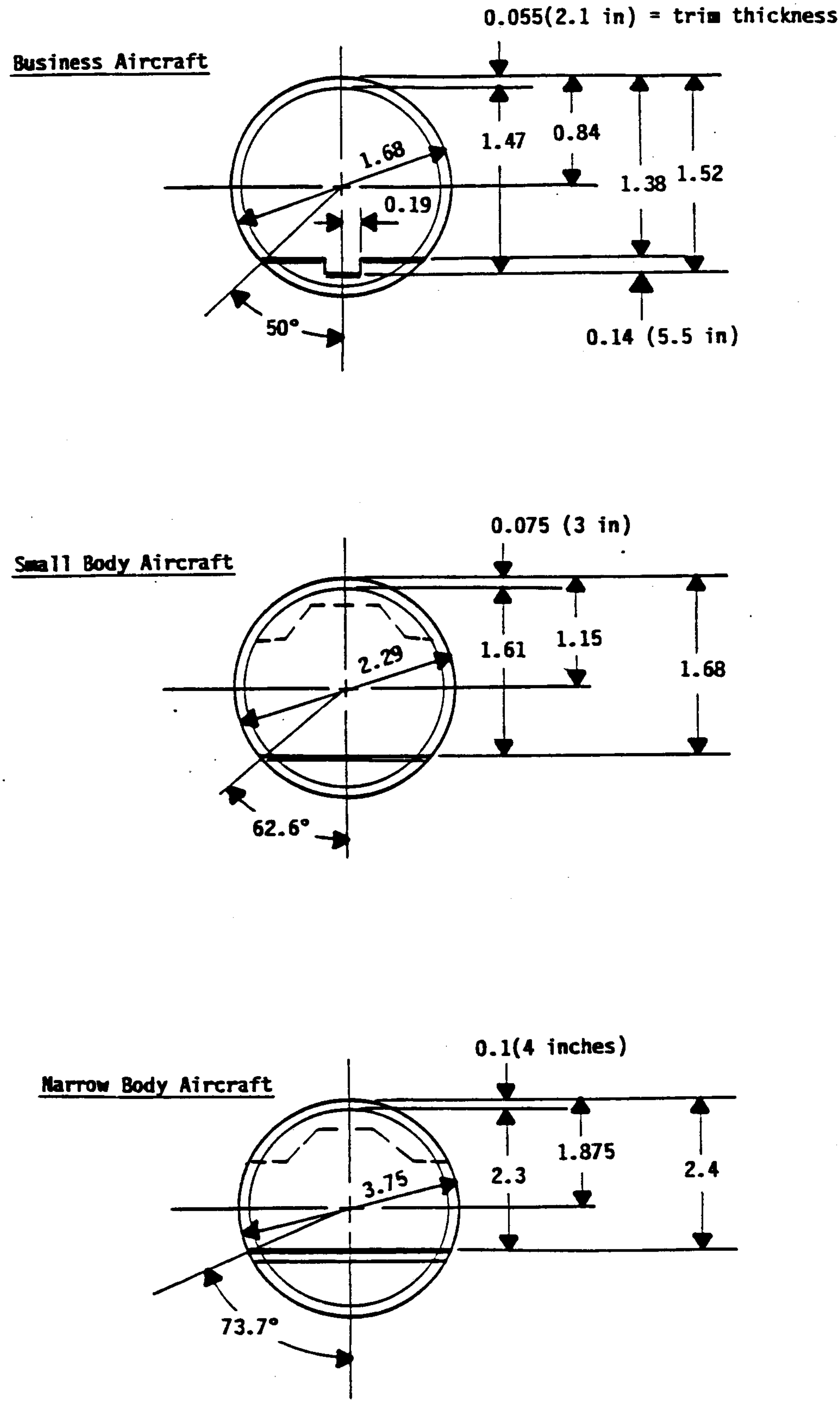

FIGURE 40. CABIN FLOOR ANGLES

Table 13. Selected Fuselage Characteristics

ITEM	TYPE: Business	Small body	Narrow body
Fuselage diameter, D	1.68m	2.29m	3.75m
Fuselage cylinder length, L	9.27m (L/D=5.4)	13m (L/D=5.7)	23m (L/D=6.1)
Cabin length, L_c	7.75m (L_c/D=4.6)	11.5m (L_c/D=5.0)	21m (L_c/D=5.6)
Cabin width	1.57m	2.14m	3.55m
Cabin height	1.45m (max, aisle)	1.61m	2.3m
Floor angle, θ_o	50.0^o	62.6^o	73.7^o
Skin thickness, range (assumed), t_s	0.81-1.27mm	0.81-1.27mm	1.02-3.05mm
Equivalent shell thickness, t_e	1.64mm	1.93mm	2.43mm
Surface density (skin+stiffeners), m	$4.54 kg/m^2$	$5.34 kg/m^2$	$6.73 kg/m^2$
Structure/cavity offset, d	0.0m	0.0m	0.0m
Frame spacing, l_f	0.38m	0.33m	0.51m
Stringer spacing, l_s	0.183m	0.13m	0.23m
Frame cross-sectional area, A_R	$8.89 x 10^{-5} m^2$	$9.4 x 10^{-5} m^2$	$1.76 x 10^{-4} m^2$
Frame moment of inertia re shell (skin) inner surface, I_f	$9.218 x 10^{-8} m^4$	$1.988 x 10^{-7} m^4$	$7.878 x 10^{-7} m^4$
Frame bending rigidity, $D_{R\theta}$	$1.756 x 10^4$ nt-m	$4.362 x 10^4$ nt-m	$1.118 x 10^5$ nt-m
Stringer cross-sectional area, A_s	$7.16 x 10^{-5} m^2$	$4.98 x 10^{-5} m^2$	$1.03 x 10^{-4} m^2$
Stringer moment of inertia, I_s	$6.85 x 10^{-9} m^4$	$3.397 x 10^{-9} m^4$	$4.036 x 10^{-8} m^4$
Stringer bending rigidity, D_{xs}	$2.712 x 10^3$ nt-m	$1.892 x 10^3$ nt-m	$1.271 x 10^4$ nt-m

Selected Fuselage Characteristics (Continued)

ITEM	TYPE: Business	Small body	Narrow body
Floor plate thickness, t_p	1.01mm	1.27mm	1.63mm
Floor surface density (including stiffeners), m_p	$4.18kg/m^2$	$5.29kg/m^2$	$7.83kg/m^2$
Floor surface density (including seating), m_p	$13.66kg/m^2$	$19.68kg/m^2$	$23.64kg/m^2$
Equivalent floor thickness, t_e^p	1.51mm	1.91mm	2.83mm
Transverse floor beams			
Spacing, l_y	0.38m	0.33m	0.51m
Cross-sectional area, A_y	$1.07x10^{-4}m^2$	$8.53x10^{-5}m^2$	$3.85x10^{-4}m^2$
Moment of inertia re lower surface of floor, I_y	$3.93x10^{-7}m^4$	$1.99x10^{-7}m^4$	$4.92x10^{-6}m^4$
Bending rigidity, D_{yp}	$7.48x10^4$nt-m	$4.362x10^4$nt-m	$6.98x10^5$nt-m
Longitudinal floor beams			
Spacing, l_x	0.43m	0.13m	0.23m
Cross-sectional area, A_x	$1.43x10^{-4}m^2$	$4.98x10^{-5}m^2$	$1.03x10^4m^2$
Moment of inertia re lower surface of floor, I_x	$9.33x10^{-7}m^4$	$3.397x10^{-9}m^4$	$4.036x10^{-8}m^4$
Bending rigidity, D_{xp}	$1.57x10^5$nt-m	$1.892x10^3$nt-m	$1.271x10^4$nt-m
Trim			
Insulation thickness, h_t	0.055m	0.075m	0.1m
Lining surface density, m_t	$1.61kg/m^2$	$1.61kg/m^2$	$1.61kg/m^2$
Material (fuselage)	2024-Aluminum Alloy	2024-Aluminum Alloy	2024-Aluminum Alloy
Elastic modulus, E	$7.24x10^{10}nt/m^2$	$7.24x10^{10}nt/m^2$	$7.24x10^{10}nt/m^2$
Density, ρ	$2.77x10^3kg/m^3$	$2.77x10^3kg/m^3$	$2.77x10^3kg/m^3$

needed. Typical values of section properties are given which allow comparisons between the smaller and larger aircraft. Structural details of fuselage and floor stiffening elements are required before the type of data in Table 13 can be generated. Stiffener properties, skin thicknesses, shell and floor surface densities, and seating arrangements are needed.

Note in the table that there will almost always be a variation in the fuselage skin thickness. Some value t_s must be chosen, and an average is recommended.

Usually the shell frame and stringer properties and their spacings l_f and l_s will be uniform. The stiffener cross-sectional areas A_R and A_s are used with the spacings to determine the equivalent shell thickness, i.e.,

$$t_e = t_s + A_R/l_f + A_s/l_s \quad .$$

The shell surface density (including skin and stringers) is then $m=\rho t_e$, where ρ is the mass density of the material (it is assumed that skin and stiffeners are of the same material).

The moments of inertia of the frames and stringers are to be computed about the inner surface of the skin. The values given in Table 13 are for the typical stiffeners shown in Figure 41. The shell bending rigidities are defined by

$$D_{R\theta} = EI_f/l_f \ ; \ D_{xs} = EI_s/l_s \quad .$$

The floor properties are similarly computed, however, there is usually going to be a greater degree of flexibility in the modeling of the floor because many of the floors are not free standing (do not run unsupported from sidewall to sidewall). In the business and small body aircraft, the floor is normally

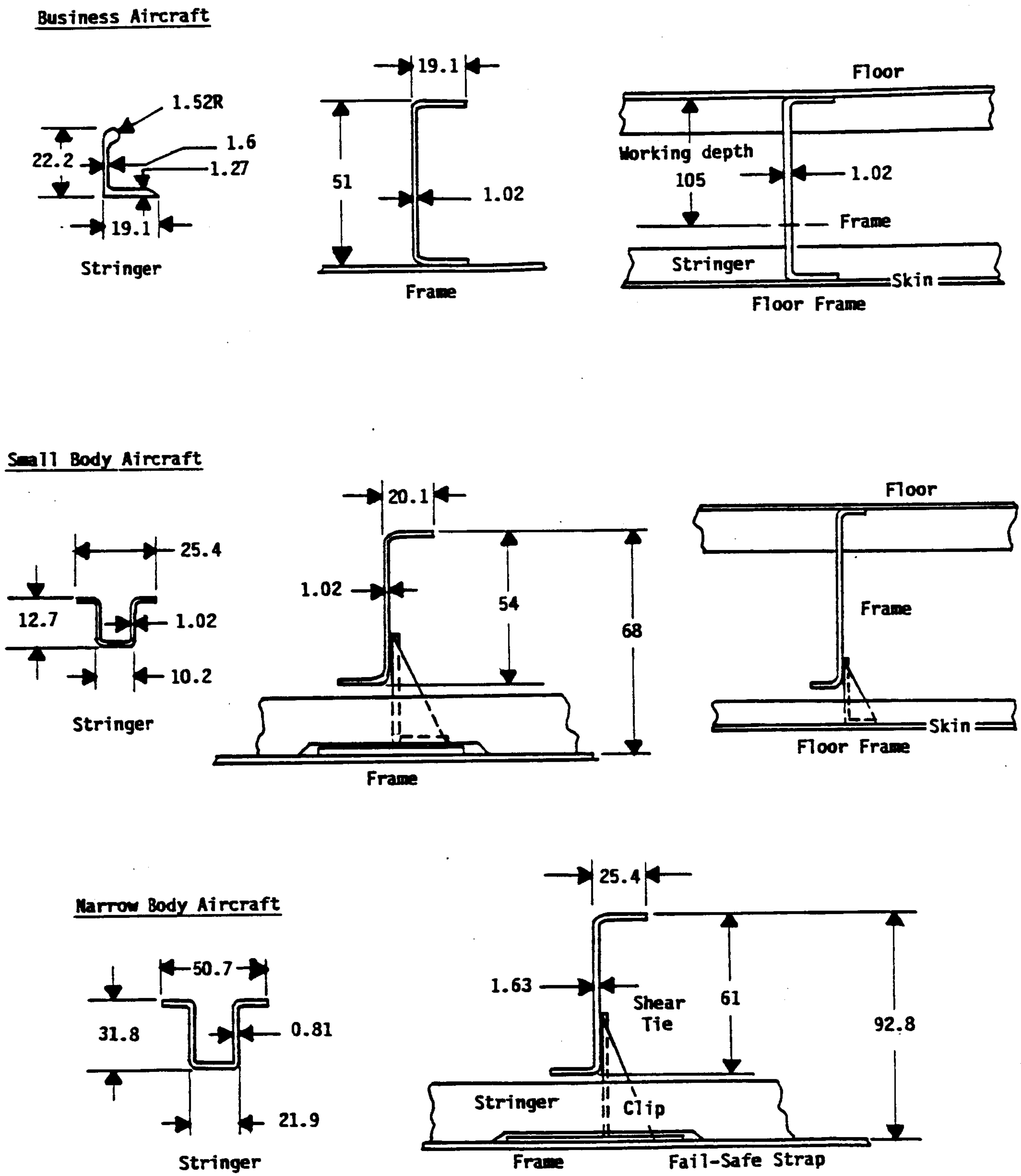

Dimensions in millimeters

FIGURE 41. TYPICAL AIRCRAFT CONSTRUCTION

built over webs formed by increasing the depth of the shell frames. In the case of the business (smallest) aircraft, the assumed properties of the transverse floor beams are based on the material depth beneath the aisle floor, that is, that which remains after material already assigned to the shell frame is excluded. In the present case, the floor frame depth is taken to be 0.105m (refer to Figure 40).

The transverse floor beams on the small body aircraft (which can be properly described as extensions of shell frames) should be assumed to have a working depth (below the floor) no greater than the height of the frame web above the shell skin required to yield the frame stiffness. Simply define the floor frame (transverse beam) such that its stiffness equals the shell frame stiffness. Once the floor stiffness gets that large, it should not matter that there may yet remain some uncertainty as to its actual working stiffness.

Generally properties of longitudinal floor beams should be determinable from drawings. For the small and narrow body aircraft here, they are simply taken to be roughly equivalent to the shell stringers. Intercostals should be accounted for as increased mass and stiffness (i.e., thickness) of the floor plate if necessary.

In actual case of narrow body aircraft, where the floor extends sidewall to sidewall, floor stiffeners (beams) should be identifiable from drawings. Table 13 contains some estimates of their section properties.

The business aircraft is complicated by the presence of the aisle. The longitudinal floor beams here are assumed to be the walls of the aisle (0.14m high) with thickness of 1.02mm and an average spacing of 0.43m. This leads to a very stiff floor (fore-to-aft).

The bending rigidities of the floor stiffeners are given by

$$D_{yp}=EI_y/l_y \; ; \; D_{xp}=EI_x/l_x \quad ,$$

and the equivalent floor thickness is

$$t_e^p = t_p+A_x/l_x+A_y/l_y \quad .$$

Program MRP will accept both the equivalent floor thickness and the floor surface mass per unit of area. The latter is

$$m = \rho t_e^p \quad ,$$

i.e., if there is no dead weight on the floor. The dead weight of seats must be added when seating is present since the seats are rigidly attached to the floor or to the supporting floor structure. The passenger load is assumed to be dynamically isolated.

On the business aircraft of Table 13, 11 seats have been assumed at 8.62 kg/seat (19 lb/seat). The distributed surface mass becomes 13.66 kg/m^2 (as opposed to 4.18 kg/m^2 without seats). In the case of the small body aircraft, 13 seat rows with 3 seats per row (19 lb/seat) yields a floor mass of 19.68 kg/m^2 (as opposed to 5.29 kg/m^2 without seats). For the narrow body aircraft, 23 seat rows with 6 seats/row increases the floor mass to 23.64 kg/m^2 (as opposed to 7.83 kg/m^2 without seats). The seating mass per unit of area is based on cabin floor area (length L_c) since this leads to the highest value of m_p. The important thing to note here is that the total dead weight of the loaded floor when seats are present may be 2 or 3 times the combined weight of the floor and its supporting structure. A reasonable estimate for seating loads should be included.

4.3 Modal Characteristics of Typical Airplanes

The aircraft selected for the present study represent significantly different scales in terms of size and stiffness of fuselages. The largest aircraft conforms to a narrow body, and it was selected because it is considered to be the largest turboprop airplane likely to be encountered by a user of the PAIN program. The two "small diameter" aircraft (small body and business) are typical short-haul or commuter configurations. The relative sizes of these airplanes can be judged quickly from Figures 36, 37, and 38, where they are drawn to the same scale.

Modal characteristics of each fuselage (cabin and structure) will determine the correct way to use the PAIN program. Modal spectra will determine the maximum number of interior propeller harmonics that can be computed and also the particular computation procedure required. The modal characteristics of larger aircraft impose more severe requirements for vigilance on the part of a user. Even so, it will be found that there are no debilitating restrictions even in the case of the largest aircraft considered herein.

4.3.1 Acoustic Modes

The PAIN program creates 400 acoustic modes for use in the interior noise calculations. These are constructed by combining the CYL2D output file (resonance frequencies and mode shapes of the twenty 2-dimensional modes ($i = 0$ to 19) of the cabin of unit radius) with twenty axial modes whose index q (that defines shapes and frequencies) ranges from 0 to 19 also. The resulting modal array (or file) is <u>not</u> complete.

Consider, for example, the computed acoustic modes for the cabin of the smallest (or business) aircraft (see Appendix C). The lowest resonance frequency (q = 1, i = 0) is predicted to be 22.1 Hz. The last mode in the list (q = 19, i = 19) is predicted to occur at about 665 Hz. The (q = 19, i = 0) mode (No. 184) occurs at 420.5 Hz. There are modes missing in the list (file) above this frequency. The first is the (q = 20, i = 0) mode at 442.6 Hz. Since modes of the type (q > 19, i = 0) do not appear, there are a number of modes missing in the range between 420.5 Hz and 665 Hz, but they are widely scattered. The (q = 19, i = 1) mode occurs at 436.1 Hz. Above this frequency, modes of the type (q > 19, i = 1) are missing. The (19, 2) mode occurs at 441.3 Hz and above this frequency modes of the type (q > 19, i = 2) are not included, and so on. Thus as one nears the bottom of the file (the higher frequencies), there are more and more missing modes.

PAIN uses all of the acoustic modes in the list (regardless of their resonance frequencies) to calculate the interior levels for a given propeller harmonic. Usually (and as has already been verified in the scale model studies) acoustic modes that are resonant close to the harmonic frequency will contribute most to the predicted interior level. As long as PAIN has data for modes near a given harmonic, it can predict the interior level using a (preferred) low frequency calculation procedure (that procedure was used in the scale model studies of Section 3). However, if the modal information for the cavity is not available (or incomplete), a high frequency calculation technique must be utilized. That procedure does not rely on the specific acoustic modal properties.

Consider then the business aircraft, and assume a blade passage frequency of say 102 to 107 Hz. Further suppose that results for the fifth harmonic will be sought. The highest frequency of concern will then be 535 Hz. The fourth harmonic could be as high as 428 Hz. It is seen that at least four harmonics can be computed with the low frequency procedure since the modal list is complete up to 442.6 Hz. The acoustic modal density is so great, that a missing mode or two (near the fifth harmonic) would not disallow use of the low frequency procedure for the fifth harmonic also. However knowledge of the missing data in that region would be useful. Remember that the calculation with the high frequency procedure is always output, so it is useful to obtain the low frequency result also whenever possible, even when the harmonic lies in a region where the modal file is incomplete.

Next consider the intermediate size fuselage (small body). The cabin has its lowest acoustic mode at 14.9 Hz; the last mode in the file is 486 Hz. The file is complete below 298.3 Hz. Thus if the blade passage frequency is in the range of 110 Hz or so, 3 harmonics can probably be predicted with the low frequency procedure. The fourth should be computed with that procedure also (although it will be an incomplete calculation), and the fifth would have to be done with the high frequency technique.

The cabin of the narrow body aircraft has its lowest acoustic mode at 8.2 Hz. The last mode in the file is at 297 Hz. The file is complete below 163.3 Hz. In the Propfan configuration with a blade passage frequency of say 165 Hz, only one harmonic can be computed with the low frequency procedure. If results for five harmonics are desired, the remaining four must be obtained with the high frequency procedure.

4.3.2 Structural Modes

The modal data file which is created with program MRP and then conditioned with MRPMOD is needed for two purposes: (1) for calculating the generalized (or modal) forces $\Psi_G(r,H)$ for the propeller noise excitation, and (2) for calculating the structure-interior coupling functions $\bar{f}'(n,r)$. (Note: r is the structural mode index, n is the acoustic mode index, and H is the propeller harmonic index.)

The structure-interior coupling functions are needed in the low frequency procedure. Calculations with that procedure are not possible if either the acoustic or the structural modal files do not extend beyond the harmonic frequency of concern. But PAIN can make an interior prediction even if the acoustic data file is exhausted. It can bypass the calculation of $\bar{f}'(n,r)$ by going to the high frequency procedure.

The modal forces, $\Psi_G(r,H)$, on the other hand, must always be computed, that is, for use in either the low or the high frequency procedure. Once a harmonic is selected, the corresponding modal forces (for all modes) must be computed. Although the entire file is utilized, it is important that the file extend beyond the frequency of the harmonic being calculated. This is required because structural modes resonant in a fairly wide region centered about the harmonic will (likely) contribute most to the interior levels. (This was found to be true in the scale-model predictions of Appendix B.)

<u>ANOPP Imposed Limitations</u>

The accuracy of the NASA ANOPP propeller noise prediction program (or any other comparable program) is suspect beyond the fourth or fifth harmonic. ANOPP should not be used to create input data for PAIN beyond the fourth or fifth propeller harmonic. This is not a critical deficiency. The highest exterior levels will be in the lowest few harmonics and the attenuation afforded by the structure will be lowest at the bottom end of the frequency spectrum also. This means that the capabilities of the PAIN program can be reasonably examined in terms of computing, say a maximum of five interior harmonics.

Program Changes to MRPMOD

The sizes of the fuselage cylinders of concern in Table 13 suggest that a software modification be made to enhance the potential utility and completeness of the structural modal file, i.e., to extend it to as high a frequency as is practical. To this end, before beginning any computations, the MRPMOD program is modified to accept an increased eigenvector output from the program MRP, i.e., 40 eigenvectors (20 symmetric and 20 antisymmetric) instead of thirty. A total of 440 structural modes can then be predicted with an allowable range of axial mode numbers M from 1 to 11. The number of axial half-waves M is limited to 11 because a maximum of 450 modes can be used by PAIN ($12 \cdot 40 = 480 > 450$). The structural program MRP itself need not be changed since it can be made to compute all of the modes required simply by specifying the maximum value of M and the number of eigenvectors desired. However, "Dimension" statements must be changed in MRPMOD to allow it accept the MRP output. Because of the increased size, the new output file from MRPMOD (that to be used by PAIN) must become a direct access instead of an indirect access permanent file. This requires some changes in the control statements for MRPMOD and PAIN (see Appendix A for more details).

Typical Results

The lowest structural mode of the fuselage cylinder of the business aircraft of Table 13 is predicted to occur at 39.6 Hz and is given in the "Structural Modes" list that is output by the PAIN program and which summarizes the MRPMOD output file

(Appendix C). The last mode in the file, i.e., the 400th mode in this case (since M is limited to 10 for the present) is predicted to occur at 2054 Hz. The corresponding results for the small body aircraft are 23.5 Hz and 1414 Hz and for the narrow body aircraft 13.1 Hz and 823 Hz respectively.

The predicted fundamental resonance frequencies here are considered reasonable. For instance, the narrow body fuselage cylinder is a large aeronautical structure by almost any measure (23m(75 ft) long by 3.75m(12.3 ft) in diameter) and it is quite stiff. A comparable structure once considered in noise studies was the payload bay door of the space shuttle orbiter vehicle (4.87m diameter by 18.3m long). Analyzed by elaborate finite element techniques, it was found to have a fundamental resonance frequency of 7.4 Hz (modeled as an incomplete cylinder (or sector) supported on its edges). Also the bottom structure of the shuttle vehicle (a stiffened curved panel) similarly analyzed had a fundamental resonance frequency of 9.6 Hz.

The question is now raised as to whether the structural modal files are complete over typical required frequency ranges. Aircraft in the turbo-prop configuration will typically have the fifth harmonic below about 550 Hz. In the Propfan configuration this upper frequency could become 825 Hz or more. The main question is whether a reliable prediction of modal forces can be made up to these frequencies.

The structural modal file is much more difficult to analyze in terms of determining its completeness. This is because the fuselage cylinder is so complicated. The modal behavior of a stiffened cylinder with floor partition is much more difficult to describe than a stiffened cylinder without floor (Ref. 1). As one examines the output of MRPMOD, it is found that for many modes of a given axial mode index M, the same shell indexes n_s will appear (n_s defines the number of full circumferential waves of a given component of the displacement series used to describe the shell circumferential mode shape). Also, the same indexes n_p (giving the number of transverse halfwaves of a given component of the displacement series used to describe the transverse floor mode shape) may appear as well. But each structural mode is unique. Each has its own set of generalized coordinates that ultimately define the particular mode shape. Each has its own generalized mass. Some of the modes are predominantly floor modes, others predominantly shell modes.

Business Aircraft

The modal file for the business aircraft (PAIN summary in Appendix C) shows that the maximum value of M (i.e., M=10) occurs the first time at the 40th mode (227.7 Hz). It therefore seems logical to assume that a mode with index M=11 will occur soon afterward and that somewhere in the range slightly above 227.7 Hz the file must become incomplete (since M=11 is excluded). Close examination, however, shows that the first M=10 mode is a floor mode. Almost all of the energy of the mode is in flexural motion of the floor. This can be recognized by examining the generalized mass. The shell flexure, w, contributes little to the total modal mass (about 2%). Since this mode will not respond well to the propeller excitation of the sidewall, it is somewhat an extraneous mode (even though listed) and a comparable mode with M=11 would be also.

The adequacy of the file (in the sense of completeness) is assured if when either M, n_s, or n_p reach their maximum values (in this case M=10, n_s=14, and n_p=5) the mode is a genuine shell mode or at least has some significant flexural energy in the shell. Going down the file, it is seen that the second time M=10 appears is at the 48th mode (250.5 Hz) where the shell flexural modal mass is but 0.2% of the total. M=10 occurs again at the 72nd mode (363.4 Hz) where the shell flexural modal mass has risen to about 24% of the total generalized mass. Somewhere slightly above this frequency, there will begin to be some modes of the type M=11 missing that should legitimately be in the file. Note that by the 147th mode (at 579.4 Hz), where the M=10 index once again appears, the shell modal mass is 89% of the total generalized mass.

There are 8 modes between the 72nd and 147th modes having M=10, all of which have significant percentages of their energy in shell flexure. There will be less than 8 missing modes of the type M=11 below 550 Hz (which is the maximum frequency of concern for the business aircraft). Within a band about 100 Hz wide centered at 550 Hz, there are 29 modes (Modes 124 through 152). There are four modes with M=10. Thus there will be less than four modes with M=11 missing over this range and fewer still with M=12 (perhaps none). It is clear that even though the file is incomplete, if the primary contributing modes to the interior noise are selected (by the program) out of those lying 50 Hz either side of the harmonic (assumed at 550 Hz), there is only a small chance that an M=11 mode will appear as one of the top five contributors and only a miniscule chance that it will be the dominant contributor. Thus, in this case, since n_s and n_p are well below their maximum values (i.e., in the range below 600 Hz or so), the modal file can be considered <u>sufficiently</u> complete.

This file can be made complete by including significant flexural (shell) modes of the type M=11 for frequencies below say 650 or 700 Hz. Its length can also be optimized if when M is increased to 11, the maximum values of n_s and n_p are reduced to 8 and 4 respectively. These values are chosen by examining the printed output of MRPMOD where (in the present case) the 5 terms used in the shell displacement series (i.e., the n_s's) and the 3 terms used in the floor displacement series (i.e., the n_p's) and which are passed to PAIN and used to construct the mode shape, lie below the maximums selected. The number of eigenvectors computed by MRP should remain at 40 if this is done.

<u>Small Body Aircraft</u>

Similar results are found for the small body aircraft. Scanning the M=10 modes leads to the following results. The first is the 18th mode (41.4 Hz) with shell flexural modal mass representing 0.04% of the total generalized mass. The second is No. 21 (42.5 Hz) and 0.9%. Then No. 40 (111.0 Hz) and 0.35%; No. 48 (118.1 Hz) and 5.1%; No. 80 (206.8 Hz) and 7.7%; No. 92 (225.6 Hz) and 13.7%; No. 124 (296.6 Hz) and 51.5%; No. 125 (298.3 Hz) and 82.4%; and so on. In these cases n_s is below its maximum of 14 (never exceeding n_s=8 passed to PAIN) and n_p is 5 or less (it reaches its allowed limit). Here it is clear that the M=11 modes should be in the file beginning at about 300 Hz.

To complete this file, the maximum value of M must be increased, but to no more than 15 (the maximum allowed). It is necessary to simultaneously reduce the number of eigenvectors computed by MRP (changing n_s or n_p is irrelevant). Thus 40 eigenvectors can be computed if M=11 is sufficient to complete the file (40·11=440<450), but only 36 if M=12 is required (36·12=432<450) and 34 if M=13 is needed (34·13=442), 32 if M=14 is necessary and 30 if M=15 must be used. The object is to assure that there are few (if any) missing shell modes of the highest M selected below about 650 to 700 Hz (i.e., if five harmonics are to be computed). All modes having the maximum selected value of M with more than

50% of their modal mass in shell flexure should lie 50 Hz or so above the frequency of the highest harmonic to be computed with PAIN.

Narrow Body Aircraft

The narrow body aircraft has its first M=10 mode at 35.2 Hz (mode No. 12). The fifth M=10 mode occurs at 159.9 Hz (mode No. 94) and is the first true M=10 shell mode (shell flexural modal mass=73% of total). Therefore the modal file begins to be incomplete at a frequency well below 550 Hz and very much below 825 Hz. In the case of the narrow body it is concluded that the maximum value M=15 may be required (reducing the number of eigenvectors computed by MRP to a total of 30).

The maximum frequency of a harmonic attempted with PAIN should not exceed the frequency where the highest M mode type has more than say 50% of its modal energy in the cylinder flexural response. Above that frequency, the structural modal file used by PAIN is <u>insufficiently</u> complete. This will probably limit PAIN to 3 harmonics (perhaps 4). While a computation can still be made that will yield an answer for the fourth harmonic (since the incomplete file extends out to 823 Hz), the result will be questionable.

Now as M is increased and the number of eigenvectors reduced, there will begin to be some modes of low order M missing from the file. For example, when the maximum value of M is used and only 30 eigenvectors can be computed, there will be 30 modes listed for each value of M. The 30th mode in the file for any given M will have the highest frequency of any mode of type M. Beyond that frequency there will be modes missing of that type M.

In the present narrow body case (where M is limited to 10) there are 40 eigenvectors or 40 modes listed for each value of M. Consider the M=1 modes. The 40th mode with M=1 occurs at 618.3 Hz and has a major circumferential component n_s=11 (11 full circumferential waves). Above 618.3 Hz there are modes missing of the type M=1. Had the number of eigenvectors been limited to 30, the last M=1 mode would have been at 432 Hz. To complete the M=1 modes out beyond the third harmonic (3x165=495 Hz), 36 eigenvectors are needed (the 36th M=1 mode occurs at 503 Hz). Thus the maximum value of M would be limited to 12. This might not be optimum however. It may be necessary to increase the maximum M and allow some modes of low order M to be missing. Each case will warrant an investigation.

4.4 Computation Times

The central processor unit (CPU) times for typical fuselages are given in Table 14. These are for the Control Data Corporation (CDC) CYBERNET Network Operating System (NOS) 176 service (essentially the computer speed is comparable to (but faster than) the CDC 6600 vintage computer). CPU time is a resultant of processing periods and is not clock time. CPU times will vary from computer to computer depending upon speed and program handling. It is a useful measure for comparing speed and costs from computer to computer and for estimating costs and practicality on a particular machine.

The most time consuming is the structural calculation. The program MRP runs all fuselages at about the same speed, regardless of the dimensions (or stiffnesses) concerned. For large numbers of modes, the run-times increase almost in direct proportion to the increase in the number of computed modes. For instance, calculation of a total of 300 symmetric and antisymmetric modes of the scale model fuselage required 1506 secs. When 400 modes

Table 14. Program Run-Times (Typical)

	Program	Calculation	CPU Time (Secs.)
Scale Model	CYL2D	Floor angle = 56.6°	119
	MRP	150 symmetric modes	795
		150 antisymmetric modes	711
	MRPMOD	300 structural modes	66
	PAIN	400 acoustic/300 structural(4Hlf/6Hhf)	249
Business	CYL2D	Floor angle = 50.0°	197
	MRP	200 symmetric modes	1087
		200 antisymmetric modes	1043
	MRPMOD	400 structural modes	91
	PAIN	Modal summary/400 acoustic/400 structural	82
		400 acoustic/400 structural(3Hlf/7Hhf)	340
Small Body	CYL2D	Floor angle = 62.6°	157
	MRP	200 symmetric modes	1049
		200 antisymmetric modes	965
	MRPMOD	400 structural modes	90
	PAIN	Modal summary/400 acoustic/400 structural	95
		400 acoustic/400 structural(3Hlf/2Hhf)	300
		400 acoustic/450 structural(3Hlf/2Hlf)	500
Narrow Body	CYL2D	Floor angle = 73.7°	70
	MRP	200 symmetric modes	1040
		200 antisymmetric modes	940
	MRPMOD	400 structural modes	91
	PAIN	Modal summary/400 acoustic/400 structural	106
		400 acoustic/400 structural(1Hlf/3Hhf)	300

were computed for each of the three aircraft fuselages, the average CPU time was 2041 secs. Thus 33% more modes required an average of 35% more computation time. Therefore it is anticipated that for a case where 450 modes are computed (the maximum number that PAIN will work with), about 2300 CPU seconds will be required.

A complete calculation with PAIN for the scale-model fuselage, utilizing 400 acoustic modes and 300 structural modes (where 10 interior harmonics (H) were calculated; 4 with the low frequency (lf) scheme and 6 with the high frequency (hf) procedure) required 249 secs.

Calculation of 10 interior harmonics for the typical business aircraft using 400 (instead of 300) structural modes required 340 secs. 82 seconds were needed to complete the calculation through the output of the modal summary. The remaining time was used in calculating the modal forces for the propeller noise field and the interior levels (3 harmonics were calculated with the (slower) low frequency procedure).

In the case of the small body aircraft, a maximum of 3 interior harmonics can be computed with the low frequency procedure. 5 interior harmonics (2 using the hf procedure) required approximately 300 secs.

There is a practical limit of 4 interior harmonics for the case of a narrow body aircraft (Propfan configuration). Only one can be obtained with the low frequency technique. The CPU time should be less than 300 secs.

In the extreme case, where say 5 interior harmonics are desired (3 to be calculated with the low frequency procedure), and where the number of structural modes is the allowed maximum of 450, the CPU time for PAIN is expected to be less than about 500 secs.

5.0 FLIGHT TEST COMPARISONS

Flight tests were performed on a trimmed and outfitted Merlin IVC aircraft (corporate version of the Fairchild Industries Swearingen Metroliner III turboprop commuter aircraft). The Merlin IVC is identical to the business aircraft shown in Figures 36 and 40 and the fuselage construction is basically as shown in Figure 41 and as detailed in Table 13.

5.1 Description of Aircraft

The Merlin IVC has twin Garrett TPE331 turboprop engines driving Dowty Rotol four-blade constant speed propellers. The propeller diameter is 2.69 m with a tip clearance of about 0.06 times the propeller diameter. The fuselage is an all metal cylindrical semi-monocoque, pressurized fail-safe structure of 2024 aluminum alloy having a diameter of 1.68 m.

The cabin of the aircraft used in the tests is shown in Figure 42. A bulkhead located at Station 126 separates the crew flight deck from the forward end of the cabin and the aft end of the cabin terminates at Station 437 where a bulkhead (with door) closes off the rear baggage compartment.

The interior of the cabin is trimmed with 0.05 m (2 inches) of PF-105 Fiberglas in mylar bags with a headliner of 3.2 mm (1/8 inch) thick heat-formable Klegecell with two glass face sheets of Tedlar. The trim surface mass is 1.95 kg/m^2 (0.4 lb/ft^2). A relatively small portion of the interior trim surface is covered with decorative Teak wood (less than 10%) and is not felt to warrant consideration in the modeling .

The aircraft tested has leather upholstered seating for eight passengers in the mid and aft sections of the cabin plus a

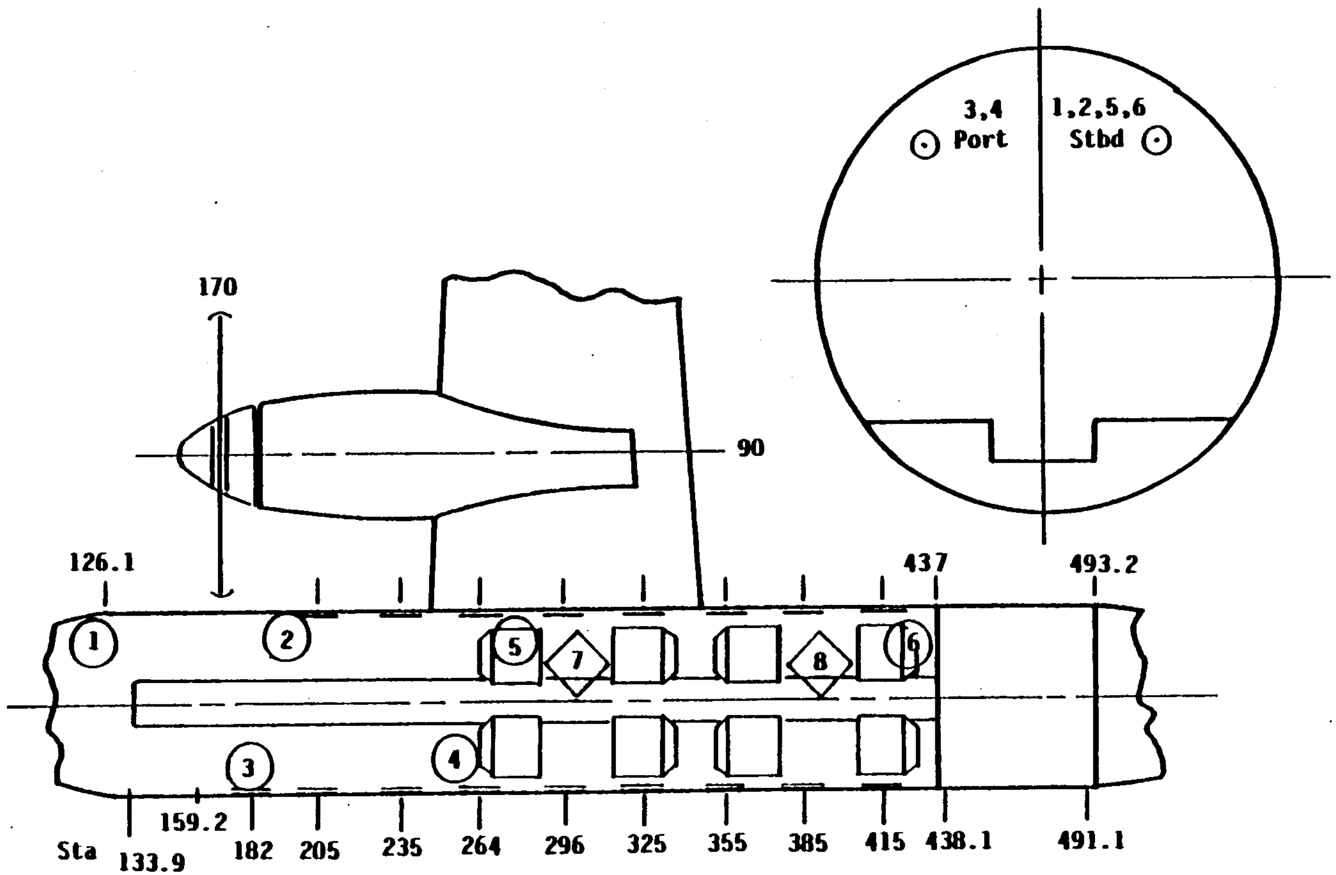

FIGURE 42. CABIN OF AIRCRAFT SHOWING SEATING AND MICROPHONE LOCATIONS

couch (sofa) of about 1 meter length located in the forward end of the cabin. In addition, food and beverage storage and preparation facilities are present in the forward end.

The seating structure dead weight on the floor spread over Stations 264-437 is about 12.2 kg/m^2. This same weight spread over the entire length of the cabin gives 6.8 kg/m^2. An average of these is 9.5 kg/m^2 which is assumed to be a representative distributed mass. The mass per unit of area of the floor used as an input to MRP is then 9.5 kg/m^2 plus the weight of the floor and supporting floor structure, i.e., about 4.2 kg/m^2 (Table 13) yielding a total of 13.7 kg/m^2. This number is very close to the result used in the studies of Section 4 (and Table 13) so the structural modal file for the business aircraft given in Appendix C is identical to that of the present test aircraft.

The surface area of cabin sidewall trim (floor-to-floor) is given by

$$A_t = 2\pi L_c(a-h_t)(1-\theta_o/180) \quad ,$$

where θ_o is the floor angle (50^o), a is the fuselage radius (0.84 m), L_c is the cabin length (7.89 m) and h_t is the trim insulation thickness (0.055 m). In the present case A_t is 28.1 m^2. All absorption in the cabin space is assumed on the sidewall. The forward and aft bulkheads are taken rigid and unabsorbing. This is a simplification because they do absorb and transmit sound. Also it was determined after the tests that the door to the baggage compartment had been inadvertently left open in flight.

The absorption by the seating and carpets is assumed to have negligible influence on the interior sound levels in the range between 100 and 550 Hz. This assumption can be justified by examining the relative absorption capabilities of the sidewall trim system versus that of the seating. For instance, at 500 Hz, the absorption of a typical upholstered seat would be limited to about 3 Sabins ($\alpha S=3$ ft^2 or 0.28 m^2). 8 seats plus the couch would give, say 27 Sabins, or an absorption of 2.5 m^2. The PAIN computed conductance ξ of the sidewall trim for a lightly damped trim panel, say $\eta_T=0.2$, at 500 Hz, is 0.017 and for a heavily damped trim panel, say $\eta_T=2$, it is 0.027 at 500 Hz. The absorption afforded by sidewall trim is therefore at a minimum

$$\alpha S = 8 \xi A_t = 3.8 \text{ m}^2 \quad ,$$

or approximately 41 Sabins. Now it is seen from these numbers that the seating could conceivably lead to a slight reduction in space-average interior levels. However, in the present case, the seating is located in the aft two-thirds of the cabin (except for the couch) and in that region, as will be shown in the flight test data, the sound pressure levels are significantly lower than in the forward third of the cabin. Thus the absorption in the forward third of the cabin is of more concern since total absorption is the product of mean square pressure times αS. In the forward third there is the couch (approximately 3 Sabins) plus carpeting (ignored) plus sidewall trim (approximately 41/3=13.7 Sabins). Thus seating should reduce interior levels by less than 1 dB (on the space average) although the actual reduction may be slightly more in the area where seating is located.

5.2 Test Program

The measurement program consisted of both ground and flight tests. The primary purpose of the ground tests was to obtain some minimal data outside the aircraft so that ANOPP predictions of the propeller noise field could be compared to measurements. No attempt was made to instrument the aircraft to allow in-flight measurements of the propeller field on the fuselage. This was an unavoidable deficiency in the flight tests due largely to the status of the aircraft and the limited time that the plane could be dedicated to the effort. Moreover, ANOPP is unable to predict the actual blocked pressure field on the skin anyway (it calculates free-field levels as previously noted), and therefore it seemed that for the present tests, some relative measure of comparisons on the ground would be sufficient. The quality of ANOPP free field predictions had already been established (such as through the scale-model comparisons presented in Section 3 of this report).

There were a number of different stationary ground tests that were performed while varying propeller speed, torque (pitch), with one prop or the other. However, comparisons between exterior measurements and exterior predictions were never attempted because the ANOPP program was unable to predict the propeller harmonics without significant air inflow velocity to the prop disk. Thus for all practical purposes, the only useful data were the interior measurements made in-flight during the test runs listed in Table 15.

The in-flight data obtained during Runs 2 and 8 were all from fixed microphone measurements. Sound pressure levels were recorded at head (ear) levels with six microphones (1 through 6) as shown in Figure 42. These measurement data cannot be used in the comparisons because space-average interior levels are required and the five microphones in the cabin (2 through 6) were not located to provide that particular measurement. The comparison data were taken in Runs 10, 11, and 12. In these three runs, the airspeed was varied (at the same flight altitude) and swept microphone data were taken at various

Table 15. Flight Tests

Run Number	Airspeed (KIAS)	Altitude (ft x 10^{-3})	% RPM* Port/Starboard	% Torque Port/Starboard	Cabin Pressure Differential (psi)	Air Temp. (°C)	Fuel Level (lbs)
2	192	17.5	97/97	56/56	6.9	-6	2000
8	210	12.0	97/97	60/60	2.9	7	1800
10	238	5.0	97/97	74/74	2.5	17	1700
11	216	5.0	97/97	57/57	2.5	17	1700
12	165	5.0	97/97	35/35	2.5	17	1700

* 97% = 1568 rpm

axial positions along the cabin. The objective was to be able to calculate the space average interior levels for five harmonics at each of the three flight conditions providing a data pool of 15 measurements for comparisons with PAIN predictions. In order to obtain the desired measurements, swept data were to be taken at a minimum of three axial stations. Two of the stations eventually selected are shown in Figure 42, i.e., locations 7 and 8 (in the aisles between the seats), where microphones 5 and 6 were swept by hand following the scheme shown in Figure 43.

During the flight tests, there were no swept measurements made in the forward third of the cabin. The presence of the couch and cabinetry in the forward end did not allow the flight personnel to follow the desired sweeping pattern and a decision was made by them to obtain swept data only at positions 7 and 8 and to retain fixed microphone data at positions 2, 3, and 4 as had been done in Runs 2 and 8. This decision necessitates the use of a rather cumbersome analytical approach to obtain the space-average levels in the cabin. The propeller noise peaks over the forward third of the cabin, and the highest interior levels occur in that region. Any errors made in estimating space-average sound pressure levels in the forward third of the cabin are strongly reflected in estimates of the total space-average levels.

5.2.1 Interior Measurements

To review, the data consist of two basic types of measurements: (1) fixed position microphone data at the head (or ear) level at up to five locations in the cabin (microphone 1 was in the crew flight deck area) and (2) swept microphone data at two fixed axial stations. In Run Nos. 2 and 8, all microphones were fixed at the head (ear) level. In Run Nos. 10, 11, and 12 microphones 2, 3, and 4 were fixed at the head (ear) level (in the same posi-

ORIGINAL PAGE IS
OF POOR QUALITY

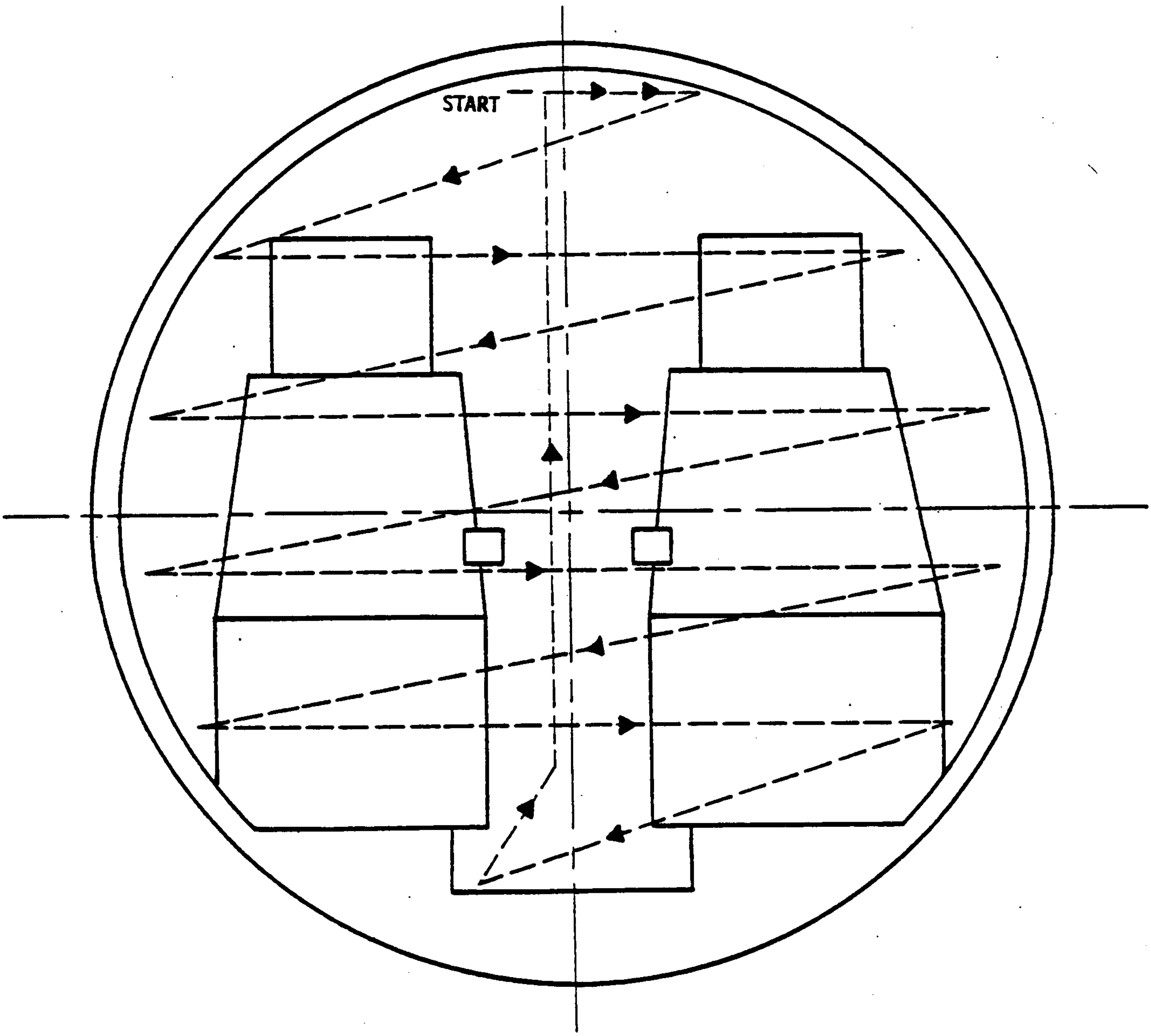

FIGURE 43. MICROPHONE SWEEP PATH FOR SPACE AVERAGE (ABOUT 15 SEC/CIRCUIT TRAVERSED TWICE)

tions as in Runs 2 and 8) and microphones 5 and 6 were swept at positions 7 and 8. In these latter tests, no fixed head (ear) level measurements were made with microphone 5 or 6.

The cabin can be divided into 3 subvolumes: Stations 126-230, 230-333, and 333-437. The swept microphone measurement taken at position 7 (with microphone 5) is considered to give the space average level in Subvolume 2 (230-333) and the swept measurement taken at position 8 (with microphone 6) is considered to give the same data for Subvolume 3 (333-437). Measurements made with microphones 2 and 3 (which lie in Subvolume 1 (126-230)) are averaged to determine an average head (ear) level μ_1^H for each harmonic. Also, measurements with head (ear) level microphones 4 and 5 which lie in Subvolume 2 in Run Nos. 2 and 8 are averaged to determine an average head (ear) level for each harmonic, i.e., μ_2^H.

In summary, let

μ_j^H=mean head (ear) level measurement for those microphones located in Subvolume j (harmonic H), i.e.,

$$\mu_j^H = 10\log\left\{(1/N)\sum_{i\epsilon j}^{N} 10^{SPL_i^H/10}\right\} ,$$

and also let

s_j^H=space average (swept) level measurement made in Subvolume j (harmonic H)

The available measurements are then as given below.

Microphone Locations and Usage

Subvolume, j	Run Nos.	Microphones, i	
		Head (ear)	Swept
1	2,8,10,11,12	2,3	-
2	2,8	4,5	-
2	10,11,12	4	5
3	2,8	6	-
3	10,11,12	-	6

Table 16 summarizes all of the pertinent interior flight measurements. Figure 44 shows one of the interior spectrum of the type from which the data in the table were taken. The table contains the measurements and also the calculated mean head (ear) levels where such a calculation is meaningful. Note that the highest levels in the aircraft occur in Subvolume 1 (which the propeller plane passes through) and thus the space-average interior level in the cabin will be dominated by the space-average level in the forward-most subvolume. Unfortunately, there is no direct way of determining a relationship between the measured (average) head (or ear) level and the space-average level so the latter must be estimated. Also note that there is a considerable decrease in sound levels from the forward to the aft subvolume. This makes an accurate estimation of the space-average level in the forward subvolume even more critical.

5.2.2 Space-Average Levels

The mean difference can be calculated between the mean head levels in Subvolumes 1 and 2 for Runs 2 and 8, i.e.,

$$\langle \mu_1^H - \mu_2^H \rangle_{2\&8} \quad .$$

For Runs 10, 11, and 12, there can also be calculated the mean difference

$$\langle \mu_1^H - s_2^H \rangle_{10,11\&12} \quad ,$$

Table 16. Interior Measurements

Run #2 V =192 kt, Alt.=17,500 ft

H	Head (Ear) Levels						
	SPL_2^H	SPL_3^H	SPL_4^H	SPL_5^H	μ_1^H	μ_2^H	SPL_6^H
1	102.2	102.4	95.5	103.8	102.3	101.4	98.4
2	99.0	100.0	98.2	84.8	99.5	95.4	87.5
3	94.2	95.6	80.5	82.0	94.9	81.3	82.0
4	81.5	76.3	67.0	65.8	79.6	66.4	66.7
5	69.0	76.3	69.0	68.2	74.0	68.6	63.0

Run #8 V =210 kt, Alt.=12,000 ft

H	Head (Ear) Levels						
	SPL_2^H	SPL_3^H	SPL_4^H	SPL_5^H	μ_1^H	μ_2^H	SPL_6^H
1	100.6	101.7	96.7	102.0	101.2	100.1	97.0
2	98.4	97.8	96.5	80.5	98.1	93.6	84.5
3	90.6	95.5	76.7	78.1	93.7	77.5	79.8
4	66.6	71.0	66.0	66.2	69.3	66.1	65.0
5	72.0	75.0	64.0	69.5	73.8	67.5	66.7

Run #10 V =238 kt, Alt.=5,000 ft

H	Head (Ear) Levels				Swept	
	SPL_2^H	SPL_3^H	μ_1^H	SPL_4^H	$s_2^H=SPL_7^H$	$s_3^H=SPL_8^H$
1	104.4	102.5	103.6	95.8	102.0	99.5
2	98.8	103.2	101.5	98.8	90.2	82.0
3	92.5	99.7	94.5	82.6	80.8	78.8
4	80.2	82.0	81.2	72.0	73.2	68.1
5	72.2	76.7	75.0	63.0	70.7	67.3

Table 16. Interior Measurements (Continued)

Run #11 V =216 kt, Alt.=5,000 ft

	Head (Ear) Levels				Swept	
H	SPL_2^H	SPL_3^H	μ_1^H	SPL_4^H	$s_2^H=SPL_7^H$	$s_3^H=SPL_8^H$
1	101.7	102.0	101.9	96.7	97.6	97.7
2	96.6	99.0	98.0	94.4	88.8	79.5
3	90.5	96.2	94.2	80.8	79.2	75.1
4	70.5	77.0	74.9	71.4	71.7	64.5
5	72.7	77.2	75.5	59.0	67.8	64.0

Run #12 V =165 kt, Alt.=5,000 ft

	Head (Ear) Levels				Swept	
H	SPL_2^H	SPL_3^H	μ_1^H	SPL_4^H	$s_2^H=SPL_7^H$	$s_3^H=SPL_8^H$
1	97.8	95.6	96.8	92.7	93.8	96.2
2	94.2	91.7	93.1	92.3	87.0	76.1
3	89.4	91.4	90.5	75.4	75.2	67.9
4	73.5	76.8	75.5	69.5	67.0	60.5
5	68.8	72.0	70.7	58.0	63.2	60.0

ORIGINAL PAGE IS
OF POOR QUALITY

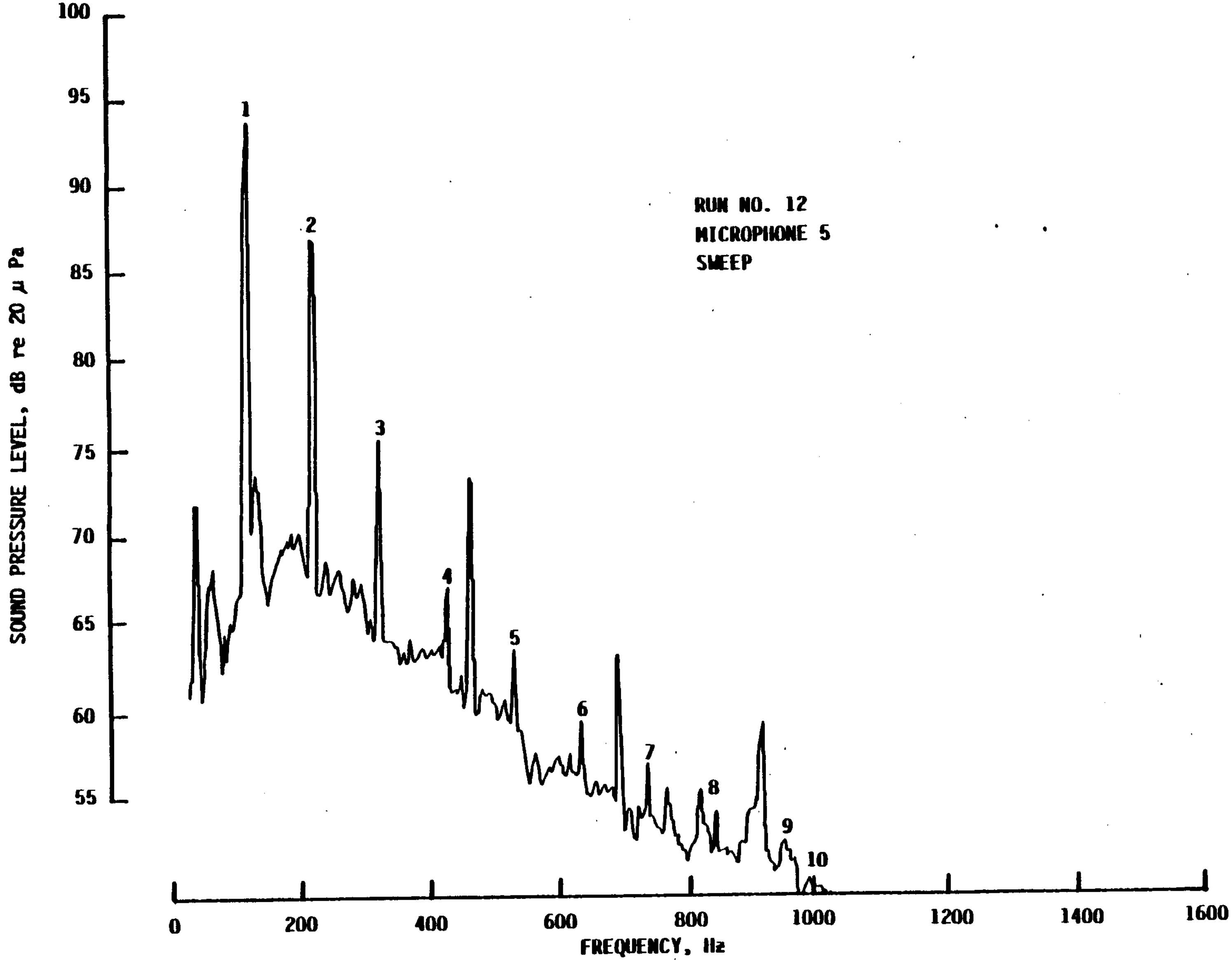

FIGURE 44. TYPICAL INTERIOR MEASUREMENT

where s_2^H is the space average level in Subvolume 2 (swept measurement with microphone 5). Table 17 shows the results of the calculations. There are a number of different things to be noted. First, all runs are for the same propeller speed (Table 15). From a frequency selection standpoint, this means that the propeller harmonics will sample the cabin modes in the same manner. However the exterior fields will be different from run to run thus from a spatial coupling standpoint, the sampling of interior modes will not be the same. Nevertheless, there is a certain consistency in the data, i.e., between the differences in head (ear) levels and the differences in head and space average levels for the two subvolumes. For instance, the third harmonics show the largest differences. On the average there are similar magnitudes of differences for all of the harmonics except for the fourth (and possibly the second). There is not much scatter except in the case of the fourth harmonics.

A standard hypothesis test is performed on the data on a harmonic-by-harmonic basis. Let μ_δ^H be the true mean difference (mean over Runs R and N) of the difference of the means in Subvolumes 1 and 2, i.e., for harmonic H:

$$\mu_\delta^H = (1/N \cdot R) \sum_r^R \sum_n^N \delta_{nr}^H = \langle \delta_{nr}^H \rangle_{N+R} \quad ,$$

where

$$\delta_{nr}^H = (\mu_1^H - \mu_2^H)_n - (\mu_1^H - s_2^H)_r \quad ,$$

and n is one from a large sample of runs (of total number N) where μ_2^H are the available measures of average sound pressure levels in Subvolume 2, and r is similarly from a large sample R where s_2^H are the available measures of average sound pressure levels in Subvolume 2. The hypothesis is that μ_δ^H is zero, i.e.,

$$H_o : \mu_\delta^H = 0.$$

Table 17. Differences Between Average Sound Levels in Forward and Middle Subvolumes

H	$\mu_1^H-\mu_2^H$ Run 2	Run 8	$<\mu_1^H-\mu_2^H>_{2\&8}$
1	0.9	1.1	1.0
2	4.1	4.5	4.3
3	13.6	16.2	14.9
4	13.2	3.2	8.2
5	5.4	6.3	5.9

H	$\mu_1^H-s_2^H$ Run 10	Run 11	Run 12	$<\mu_1^H-s_2^H>_{10,11,\&12}$
1	1.6	4.3	3.0	3.0
2	11.3	9.2	6.1	8.9
3	13.7	15.0	15.3	14.7
4	8.0	3.2	8.5	6.6
5	4.3	7.7	7.5	6.5

ORIGINAL PAGE IS OF POOR QUALITY

The estimator for μ_δ^H is

$$\bar{\delta}^H = (1/2\cdot 3)\left\{\sum_{n=2\&8}\ \sum_{r=10,11\&12} \delta_{nr}^H\right\}$$

$$= (1/6)(\delta_{2,10}^H + \delta_{2,11}^H + \delta_{2,12}^H + \delta_{8,10}^H + \delta_{8,11}^H + \delta_{8,12}^H) \quad ,$$

with sample standard deviation

$$s_\delta^H = \left\{(1/5)\cdot\sum_{n=2\&8}\ \sum_{r=10,11\&12} (\delta_{nr}^H - \bar{\delta}^H)^2\right\}^{\frac{1}{2}} \quad .$$

The acceptance region for the hypothesis at the α level of significance is given by

$$|\bar{\delta}^H| \leq s_\delta^H t_{5;\alpha/2}/\sqrt{6} \quad ,$$

where $t_{5;\alpha/2}$ is the Student t-distribution with n=5 degrees of freedom. The results are given in Table 18.

Table 18. Results of Hypothesis Tests

Hypothesis Test for Harmonic	Sample Statistics		Level of Significance α	Acceptance Region ($\pm$dB)	Accept?
	$\bar{\delta}^H$(dB)	s_δ^H(dB)			
1	-1.96	1.21	0.2	0.73	no
2	-4.57	2.35	0.2	1.42	no
3	0.23	1.61	0.2	0.97	yes
4	1.63	6.07	0.2	3.65	yes
5	-0.65	1.78	0.2	1.07	yes

Bias is indicated for harmonics 1 and 2, where the hypothesis is rejected. For the higher harmonics there is no proven bias.

Let $\bar{\mu}_\delta^1=\mu_\delta^1+2$ and $\bar{\mu}_\delta^2=\mu_\delta^2+4.5$. A new hypothesis test (for the first two harmonics) of the form

$$H_o:\bar{\mu}_\delta^H=0 \quad ,$$

does not indicate bias.

The space-average interior levels are calculated using the following interpretation of the results above and other assumptions:

1) Implications are that on the average, for Runs 10, 11, and 12:

$$s_2^1=\mu_2^1-2dB \qquad s_2^4=\mu_2^4$$
$$s_2^2=\mu_2^2-4.5dB \qquad s_2^5=\mu_2^5$$
$$s_2^3=\mu_2^3$$

2) The relationships assumed above between the average head (ear) levels and space-average levels in Subvolume 2 are reasonable for use in Subvolume 1 as well, i.e.,

$$s_1^1=\mu_1^1-2dB \qquad s_1^4=\mu_1^4$$
$$s_1^2=\mu_1^2-4.5dB \qquad s_1^5=\mu_1^5$$
$$s_1^3=\mu_1^3$$

3) The space-average levels in the cabin (for Runs 10, 11, and 12) can be estimated using the swept microphone data taken in Subvolumes 2 and 3 and the

average head (ear) level data from Subvolume 1 corrected for bias according to 2) above.

Note that the sample standard deviation in Table 18 lies in the narrow range between 1.2 and 2.4 dB for four of the five harmonics, but it is about 6 dB for the fourth harmonic. Although no bias adjustment is warranted for that harmonic, there is a high probability (1 chance out of 3) that the predicted space average in Subvolume 1 will be off by more than 6 dB, even if all of the assumptions above are accurate.

The space-average levels are computed from the measurement data with the following relations, where s_j^H is the space average sound pressure level in Subvolume j:

$$x_j^H = 10^{s_j^H/10} \quad ,$$

$$\bar{x}_H = (1/N)\sum_{j=1}^{N} x_j^H \quad ; \ N=3 \text{ subvolumes} \quad ,$$

$$s_H = \left\{ (1/m)\sum_{j=1}^{N} (x_j^H - \bar{x}_H)^2 \right\}^{\frac{1}{2}}_{m=N-1} .$$

Space-Average Level (Harmonic H)

$$\overline{SPL}_H = 10\log \bar{x}_H$$

(1-α)% Confidence Limits (on the space average)

$$SPL_H^{1-\alpha} = 10\log(\bar{x}_H + s_H t_{N-1;\alpha/2}/\sqrt{N}) \quad .$$

The calculated space-averages and the 95% and 99% confidence limits are given in Table 19.

Table 19. Measured Space Averages and Confidence Limits

Run No. 10

H	μ_1^H	Bias Correction	s_1^H	s_2^H	s_3^H	$\overline{SPL}_H$	SPL_H^{95} *	SPL_H^{99} *
1	103.6	-2	101.6	102.0	99.5	101.2	96.1-103.5	<105.3
2	101.5	-4.5	97.0	90.2	82.0	93.2	<99.3	<102.3
3	94.5	0	94.5	80.8	78.8	90.0	<96.9	<100.0
4	81.2	0	81.2	73.2	68.1	77.2	<83.5	<86.4
5	75.0	0	75.2	70.7	67.3	72.2	<77.2	<80.0

Run No. 11

H	μ_1^H	Bias Correction	s_1^H	s_2^H	s_3^H	$\overline{SPL}_H$	SPL_H^{95}	SPL_H^{99}
1	101.9	-2	99.9	97.6	97.7	98.5	91.7-101.1	<103.1
2	98.0	-4.5	93.5	88.8	79.5	90.1	<95.8	<98.6
3	94.2	0	94.2	79.2	75.1	89.6	<96.6	<99.8
4	74.9	0	74.9	71.7	64.5	72.1	<77.1	<79.9
5	75.5	0	75.5	67.8	64.0	71.7	<77.8	<80.7

Run No. 12

H	μ_1^H	Bias Correction	s_1^H	s_2^H	s_3^H	$\overline{SPL}_H$	SPL_H^{95}	SPL_H^{99}
1	96.8	-2	94.8	93.8	96.2	95.0	89.8-97.3	<99.2
2	93.1	-4.5	88.6	87.0	76.1	86.3	<91.5	<94.4
3	90.5	0	90.5	75.2	67.9	85.9	<92.9	<96.0
4	75.5	0	75.5	67.0	60.5	71.4	<77.9	<80.9
5	70.7	0	70.7	63.0	60.0	66.9	<72.9	<75.9

* Only the upper limit is defined for those cases with the "less than (<)" symbol

5.3 Computer Simulation of Flight Tests

As discussed in Section 4, the exterior field predictions made with the ANOPP program need to be examined to determine whether the PAIN grid is properly located and also to see if the pressure field decreases sufficiently over the length of the grid. For the present aircraft, a preliminary selection of the grid centering variable (i.e., centering relative to the maximum predicted sound pressure level on the exterior of the fuselage) is $k_p=8$. Figure 36 illustrates the selection.

5.3.1 ANOPP Prediction Methodology

The ANOPP program can predict propeller tones using various methods and the degree of complexity of the calculations will impact the user. Two methods of concern that can be used to predict the free field propeller noise in-flight are the so-called Method 1 or full blade formulation in which only 40 of the pressure signatures (out of 160 required) can be computed at any one time, and the Method 3 or compact chord approximation (line source model) in which all 160 signatures can be computed simultaneously.

Run No. 2 was selected for comparing the full blade and compact chord models, with the hope being to use the simpler Method 3 on the three flight comparison runs 10, 11, and 12. Figures 45 and 46 illustrate the differences in the results of the calculations. Figure 45 gives the sound pressure levels predicted along the line $\ell=1$ (Figure 3) that were computed using both methods (the Method 1 or full blade prediction is considered the most accurate prediction possible). It is seen that the amplitudes forward of and also near to the propeller plane compare quite well for all harmonics. The full blade predictions exceed the line source predictions aft of the propeller plane, usually by 2 to 5 dB after each has rolled off about 10 dB below the peak

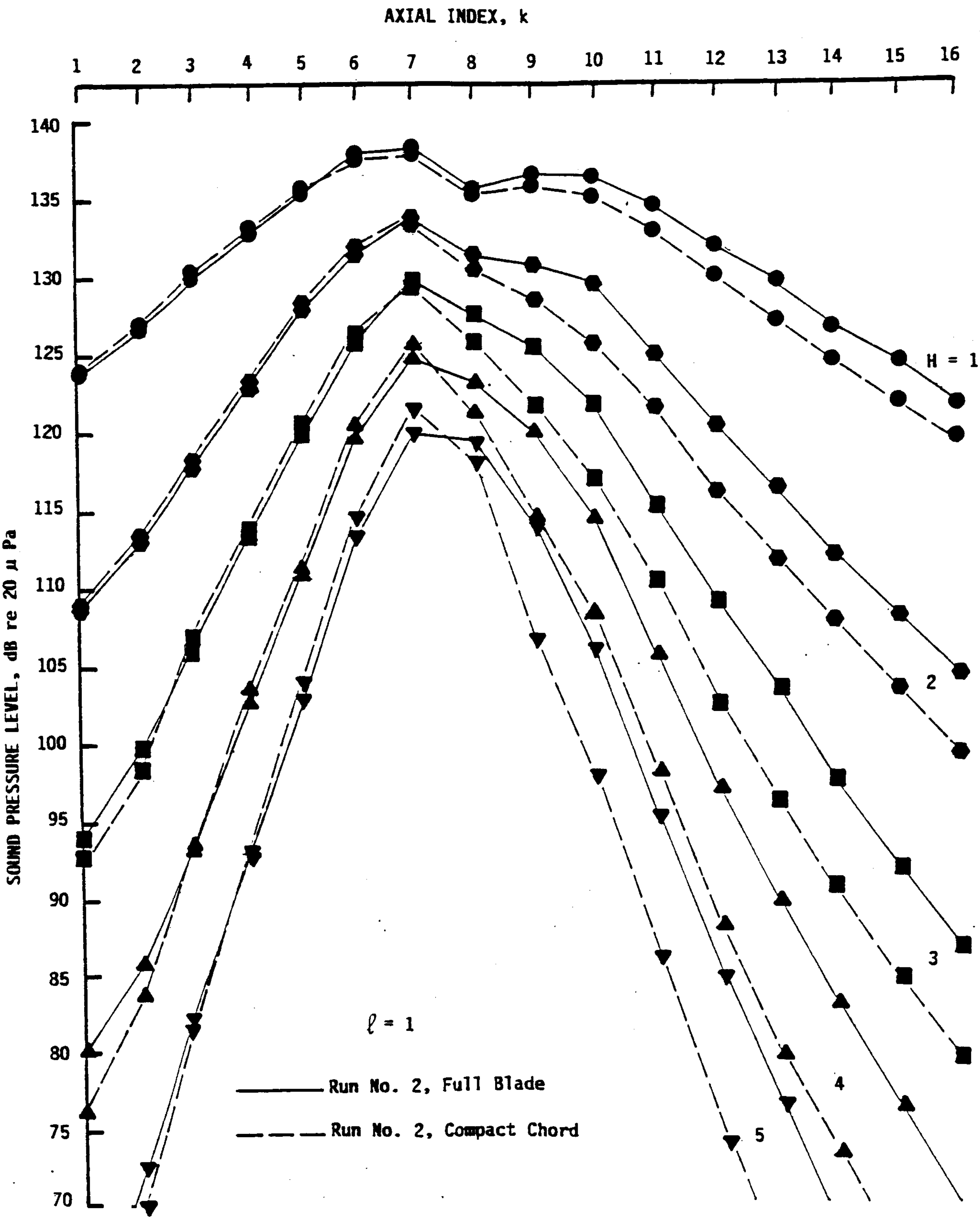

FIGURE 45. AMPLITUDE COMPARISON, FULL BLADE VS. COMPACT CHORD FORMULATIONS

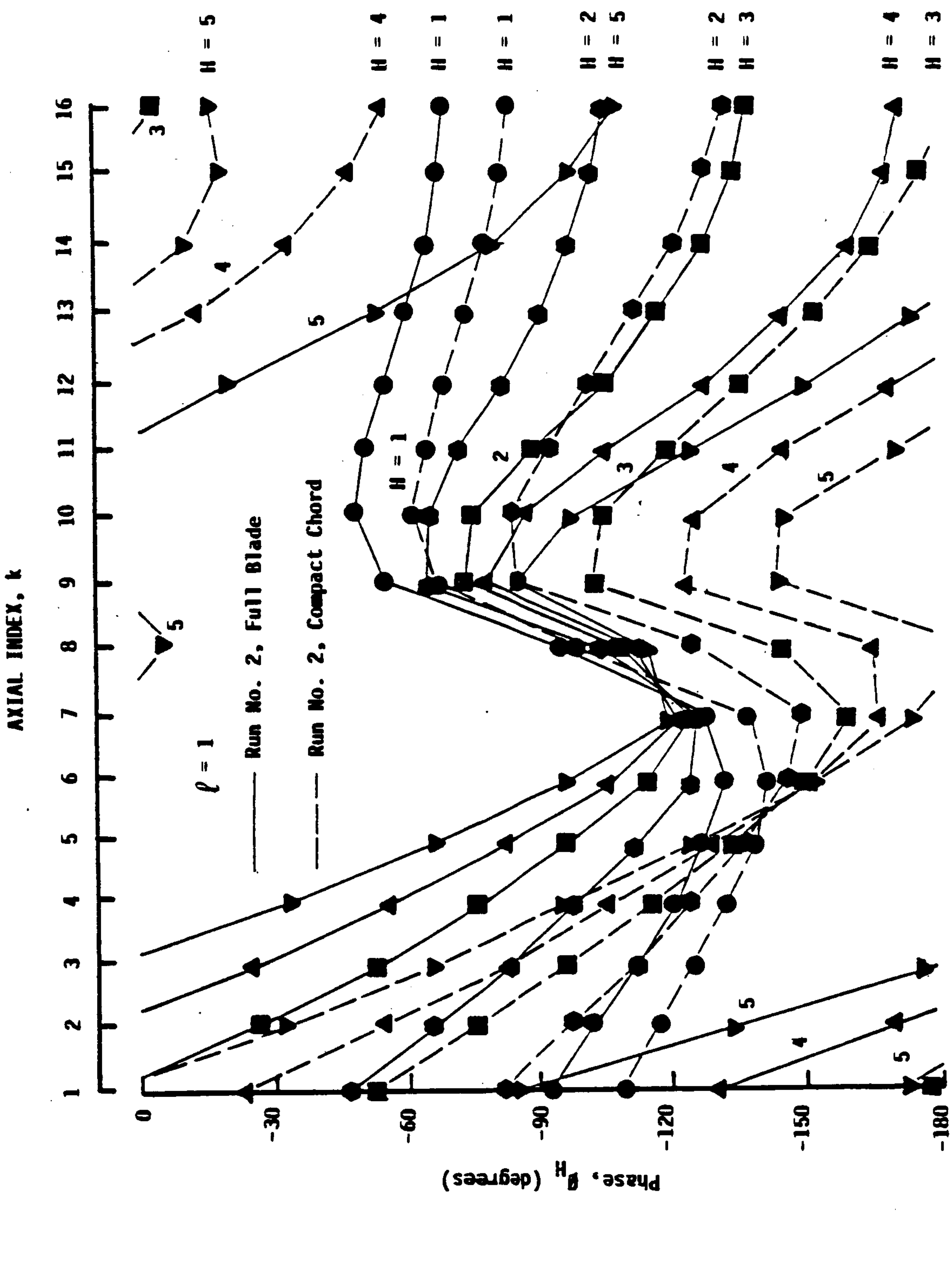

FIGURE 46. PHASE COMPARISON

levels. Certainly in the case examined most of the acoustic energy incident on the fuselage is within the grid area. The levels of the first harmonic decrease more than 12 dB from k=7 to the extremes of the grid and much larger roll-offs are predicted for the higher harmonics. The ANOPP predicted roll-off of the over-all sound level is quite consistent with the empirical prediction made using Figure 39 as discussed in Section 4.1.

Figure 46 shows the phase calculations (ℓ=1) for the various harmonics as predicted by ANOPP using the two methods. There appears to be very little similarity. But the PAIN program is concerned not with phase point-by-point on the grid, but with phase difference point-to-point. Phase differences can be compared by adjusting the phase predictions to their respective means and then by overlaying them as done in Figure 47, where it is observed that the phase information compares quite well. On the basis of these comparisons, it was decided that the ANOPP Method 3 was sufficiently accurate. Later to verify the correctness of this decision, the Run 2 propeller noise predictions (both methods) were used as an input to the PAIN program and the interior levels predicted in the Merlin IVC aircraft were compared. This was done for blade downsweep only. The differences in predicted interior levels were such that the full blade model resulted in very slightly higher interior levels. The results for the first harmonics differed by 1.05 dB; for the second: 1.46 dB; the third: 0.05 dB; the fourth: 2.04 dB; the fifth: 1.84 dB.

5.3.2 Predicted Exterior Levels

Tables 20, 21, and 22 give the ANOPP predicted free field flight levels along the grid line ℓ=1. The data are also given in Figures 48-53. It should be recalled that the free field amplitudes are increased according to Eq. (43) of Ref-

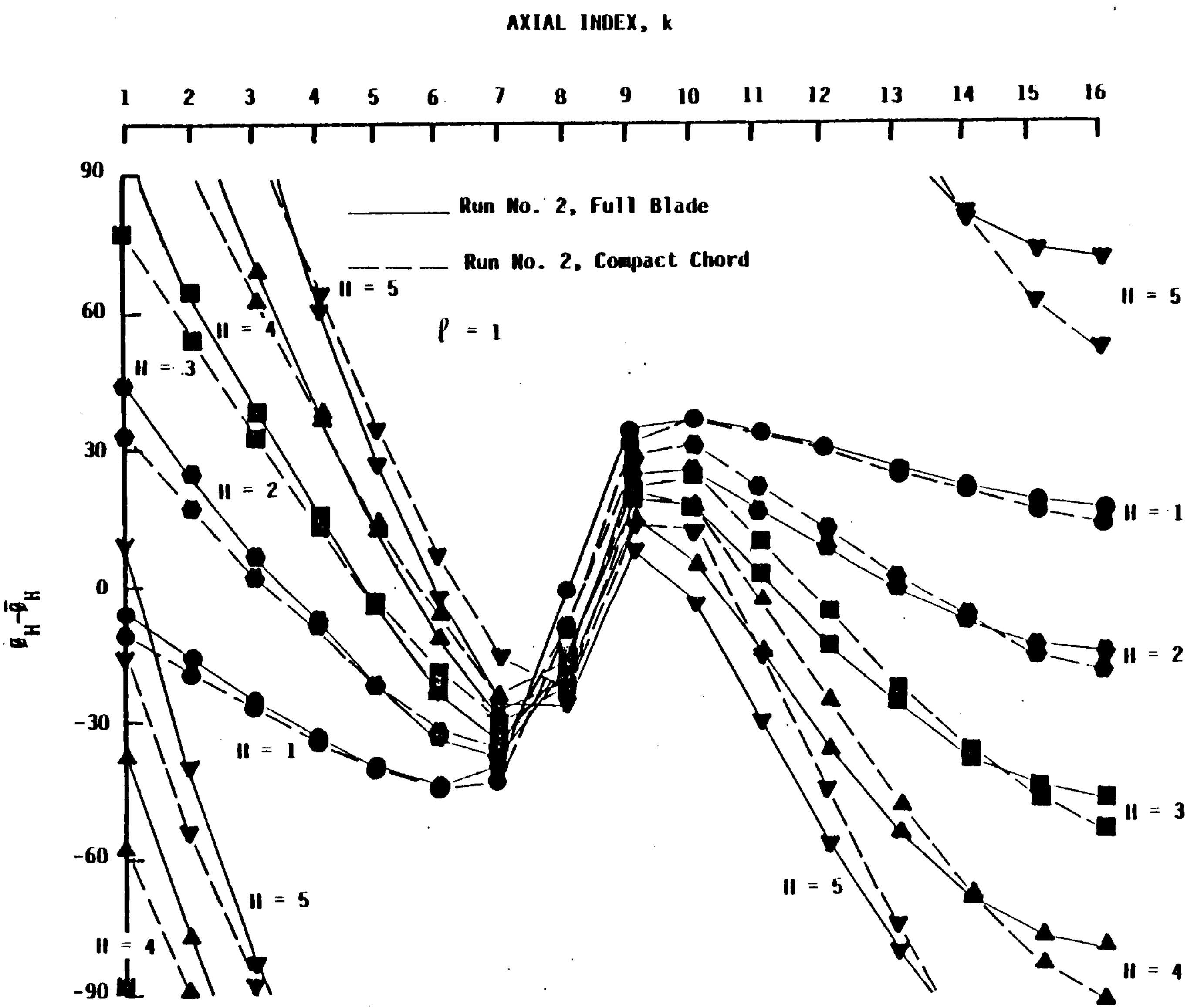

FIGURE 47. PHASE COMPARISON WHEN ADJUSTED TO MEANS $\bar{\phi}_H$

Table 20. Exterior Levels in Flight Run No. 10
(ANOPP Compact Chord, free field, $\ell = 1$)

Harmonic H	Sound Pressure Level, dB re 20 μPa k=1	2	3	4	5	6	7	8
1	122.4	125.4	128.4	131.4	134.1	136.1	136.3	133.5
2	107.4	112.3	117.3	122.3	127.1	131.2	133.0	129.2
3	92.2	98.8	105.7	112.7	119.6	125.8	129.3	125.3
4	77.0	85.2	93.9	102.9	112.0	120.2	125.5	121.7
5	61.7	71.7	82.1	93.0	104.1	114.5	121.6	118.4
	Phase, ϕ_H (degrees)							
1	-91.7	-102.1	-111.9	-120.9	-129.0	-135.1	-134.3	-103.7
2	-52.3	-72.6	-91.2	-108.2	-124.9	-137.7	-146.7	-132.2
3	-11.7	-42.2	-69.3	-94.5	-117.3	-138.3	-155.7	-156.4
4	29.9	-11.0	-47.2	-79.7	-109.5	-137.4	-162.7	-177.4
5	71.9	20.9	-24.0	-64.1	-101.0	-135.6	-168.3	164.2

Harmonic H	Sound Pressure Level, dB re 20 μPa k=9	10	11	12	13	14	15	16
1	133.4	132.3	130.0	127.4	124.7	122.1	119.5	117.0
2	125.9	122.9	118.7	114.1	109.6	105.2	101.1	97.2
3	118.2	113.2	106.9	100.5	94.3	88.6	83.1	77.8
4	110.4	102.9	94.7	86.5	79.0	71.9	65.2	58.6
5	102.8	91.3	81.3	71.8	63.3	55.3	47.4	39.5
	Phase, ϕ_H (degrees)							
1	-70.7	-67.0	-70.4	-75.6	-80.9	-85.8	-90.0	-93.2
2	-97.2	-96.1	-105.9	-117.8	-129.2	-138.0	-146.4	-151.3
3	-123.8	-123.7	-140.0	-159.6	-177.9	167.5	157.2	151.3
4	-154.2	-151.3	-174.1	157.7	132.1	112.9	100.5	94.1
5	167.0	178.4	150.5	112.3	79.3	56.5	43.0	37.5

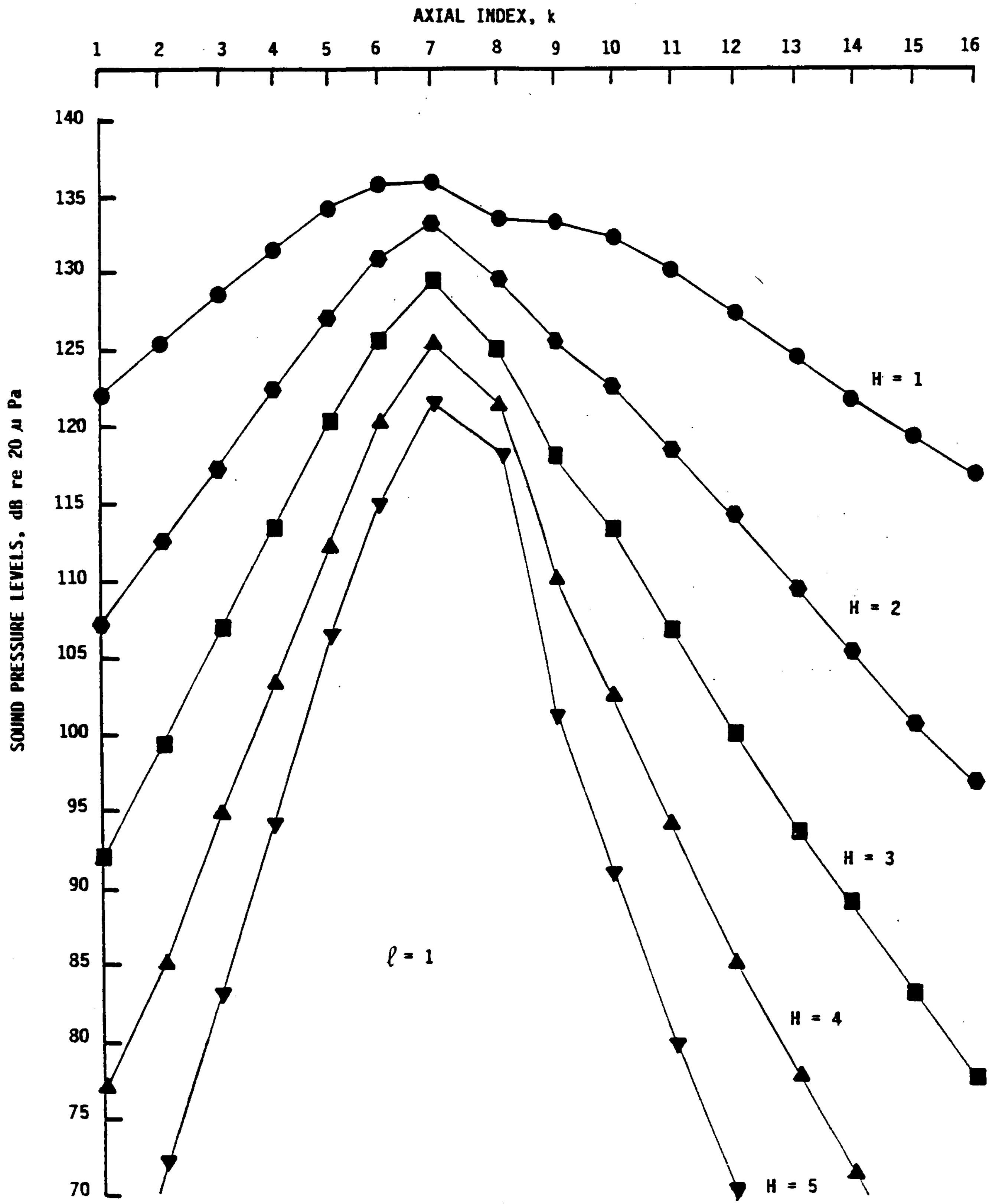

FIGURE 48. EXTERIOR LEVELS (FREE FIELD), FLIGHT RUN NO. 10

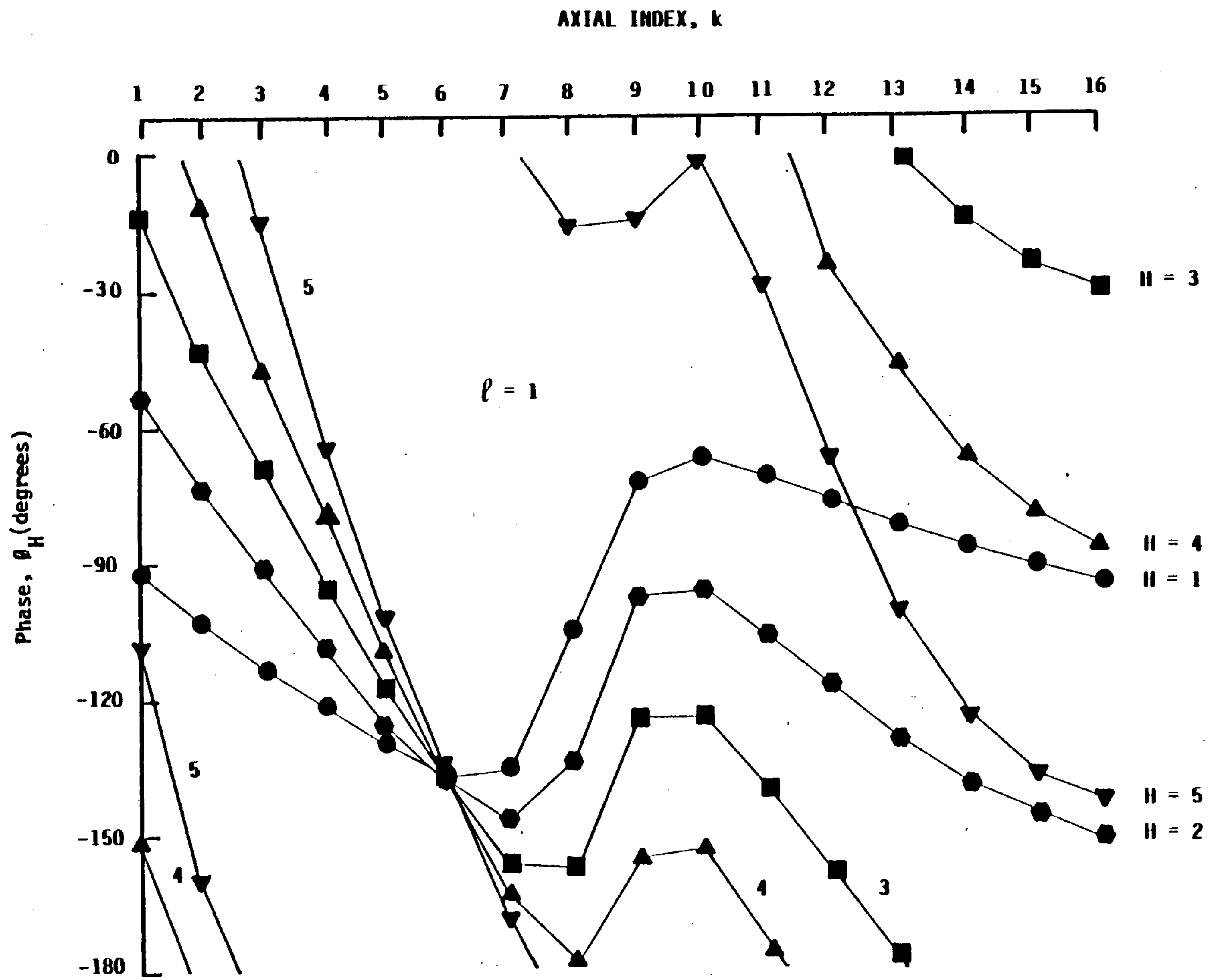

FIGURE 49. PHASE (FREE FIELD), FLIGHT RUN NO. 10

Table 21. Exterior Levels in Flight Run No. 11
(ANOPP Compact Chord, free field, $\ell=1$)

Harmonic H	Sound Pressure Level, dB re 20 μPa k=1	2	3	4	5	6	7	8
1	121.0	124.0	127.0	129.9	132.6	134.6	134.7	131.5
2	105.9	110.8	115.8	120.8	125.6	129.6	131.4	127.4
3	90.5	97.1	104.0	111.1	118.1	124.2	127.7	123.7
4	75.1	83.4	92.1	101.2	110.3	118.6	123.9	120.3
5	59.7	69.6	80.1	91.2	102.4	112.8	119.9	117.1
	Phase, ϕ_H (degrees)							
1	-100.7	-110.1	-118.8	-126.9	-134.0	-139.3	-138.2	-107.4
2	-67.8	-85.9	-102.4	-117.5	-131.3	-143.5	-151.4	-137.8
3	-33.8	-60.8	-85.0	-106.9	-127.0	-145.5	-161.0	-162.8
4	1.3	-34.9	-66.8	-95.3	-121.5	-146.1	-168.6	176.3
5	36.8	-8.1	-47.7	-82.9	-115.2	-145.7	-174.9	158.3

Harmonic H	Sound Pressure Level, dB re 20 μPa k=9	10	11	12	13	14	15	16
1	131.3	130.4	128.2	125.6	122.9	120.2	117.6	115.6
2	123.5	120.6	116.4	111.8	107.3	102.9	98.8	94.9
3	115.4	110.3	104.1	97.6	91.5	85.7	80.3	75.1
4	107.4	99.0	90.9	82.7	75.3	68.4	61.9	55.4
5	100.8	85.3	75.4	66.3	58.6	51.1	43.6	36.0
	Phase, ϕ_H (degrees)							
1	-70.1	-64.5	-67.1	-71.6	-76.5	-81.0	-84.9	-87.9
2	-97.7	-92.7	-100.6	-111.4	-122.1	-131.4	-138.5	-143.2
3	-127.0	-119.5	-132.8	-150.9	-168.4	177.2	167.3	161.8
4	-163.8	-148.0	-165.5	167.8	142.4	123.4	111.6	106.2
5	148.7	172.4	156.4	118.8	86.2	65.2	53.9	50.4

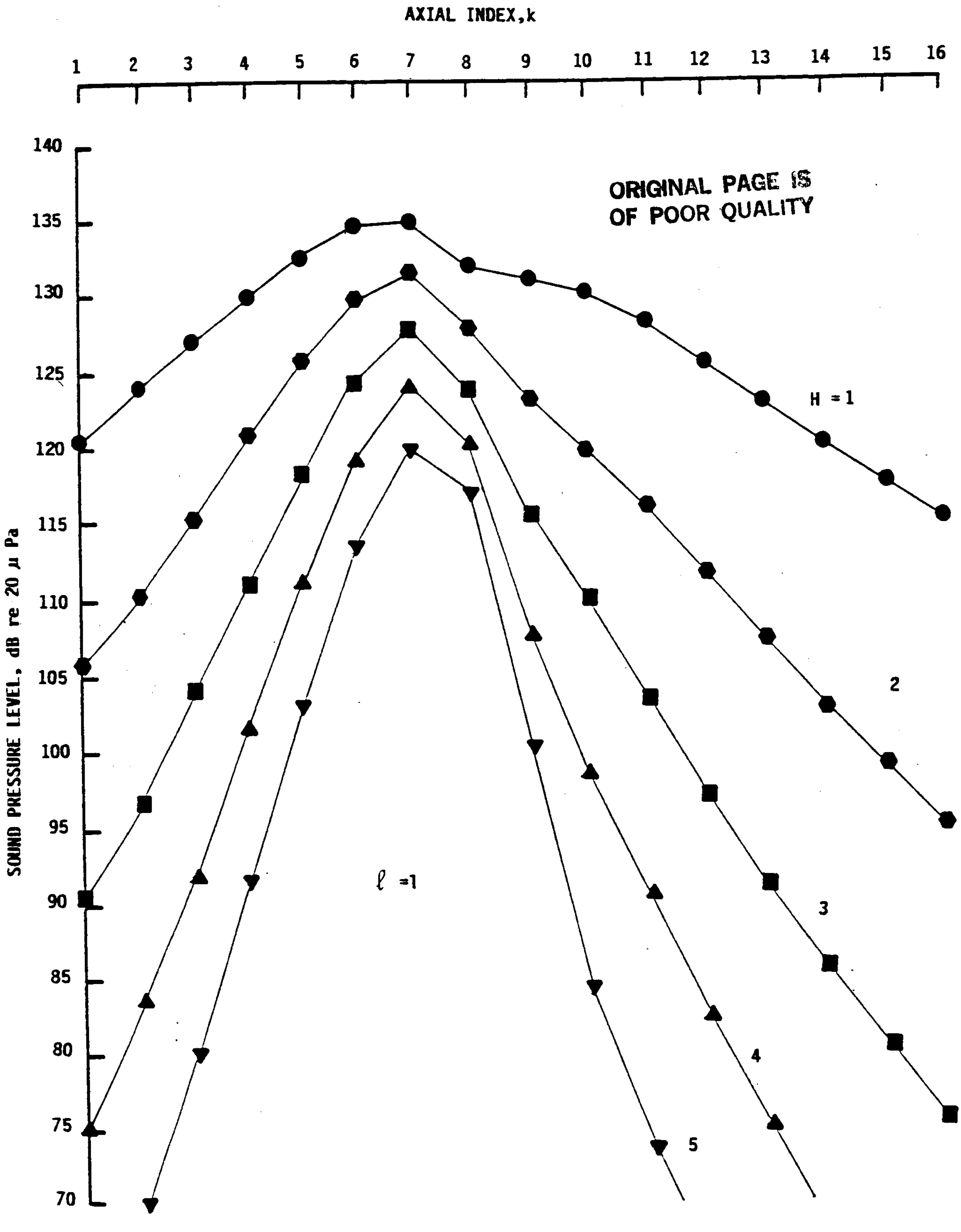

FIGURE 50. EXTERIOR LEVELS (FREE FIELD), FLIGHT RUN NO. 11

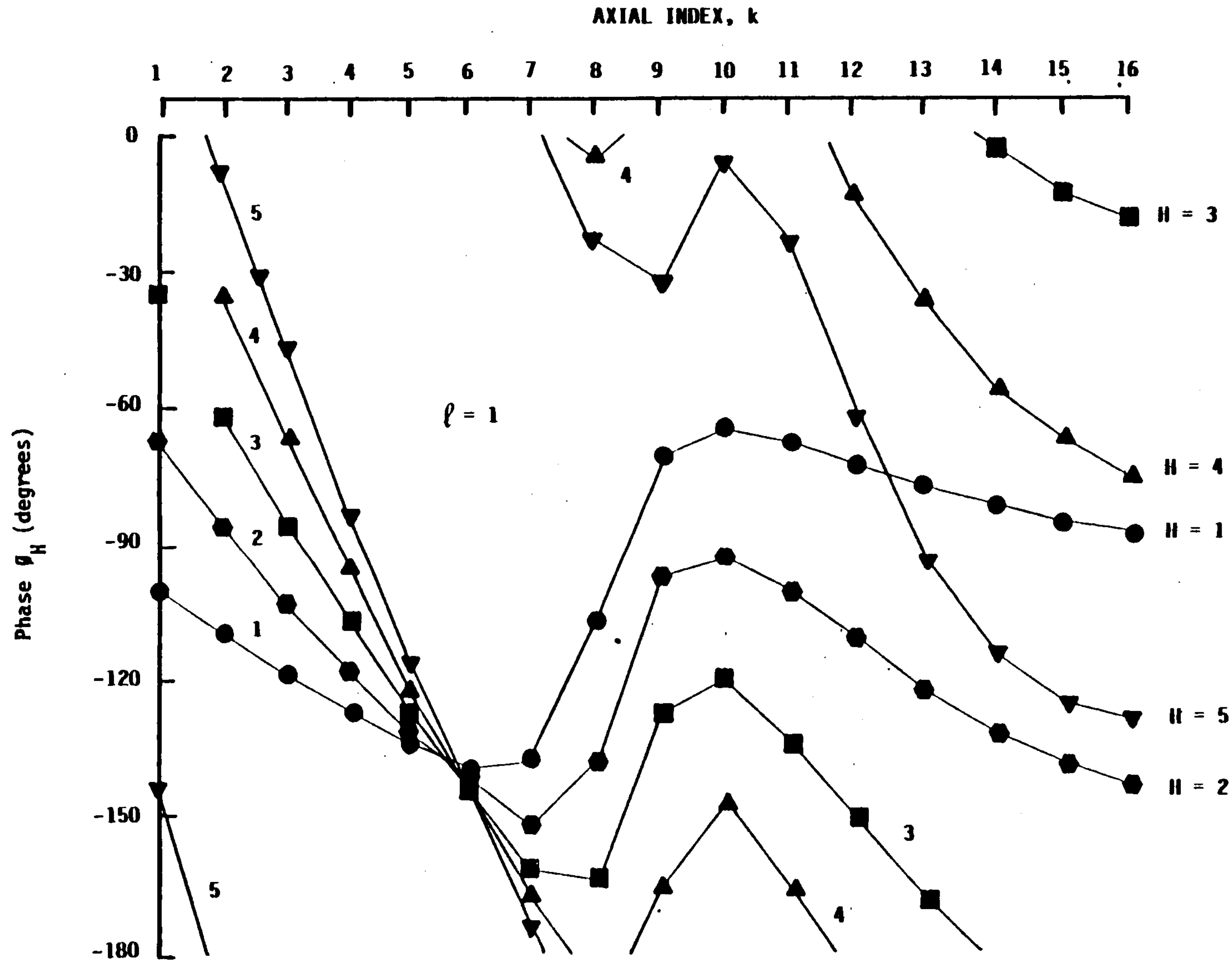

FIGURE 51. PHASE (FREE FIELD), FLIGHT RUN NO. 11

Table 22. Exterior Levels in Flight Run No. 12
(ANOPP Compact Chord, free field, $\ell=1$)

Harmonic H	Sound Pressure Level, dB re 20 μPa k=1	2	3	4	5	6	7	8
1	118.2	121.1	124.1	126.9	129.5	131.3	131.3	127.3
2	102.7	107.6	112.6	117.6	122.3	126.3	128.1	123.8
3	87.0	93.6	100.6	107.7	114.6	120.8	124.4	120.8
4	71.1	79.5	88.4	97.6	106.7	115.0	120.5	118.0
5	55.2	65.3	76.1	87.4	98.7	109.2	116.6	115.1
	Phase, ϕ_H (degrees)							
1	-120.7	-127.8	-134.3	-140.2	-145.4	-148.9	-147.2	-118.5
2	-101.3	-114.9	-127.1	-138.2	-148.2	-156.9	-162.6	-153.6
3	-80.8	-100.9	-118.6	-134.5	-148.9	-162.2	-173.8	-178.9
4	-59.2	-86.0	-109.1	-129.5	-148.3	-165.9	177.3	161.6
5	-36.7	-70.3	-98.9	-123.8	-146.8	-168.6	169.8	145.6

Harmonic H	Sound Pressure Level, dB re 20 μPa k=9	10	11	12	13	14	15	16
1	126.5	126.0	124.1	121.6	118.9	116.2	113.6	111.1
2	117.4	114.8	110.9	106.3	101.8	97.4	93.4	89.5
3	109.1	102.1	96.2	89.8	83.8	78.3	73.2	68.4
4	104.4	87.8	77.1	70.3	64.9	59.5	53.8	48.0
5	102.0	86.1	72.6	61.6	52.4	44.3	36.7	29.2
	Phase ϕ_H (degrees)							
1	-70.5	-60.3	-60.6	-63.7	-67.4	-71.0	-74.2	-76.7
2	-105.6	-88.0	-90.9	-98.9	-108.0	-116.3	-122.7	-126.7
3	-153.4	-120.8	-123.2	-137.5	-153.9	-167.6	-176.4	179.8
4	152.6	164.4	174.7	156.8	137.3	125.5	120.4	120.8
5	114.9	78.4	50.9	41.7	42.8	46.4	51.5	59.3

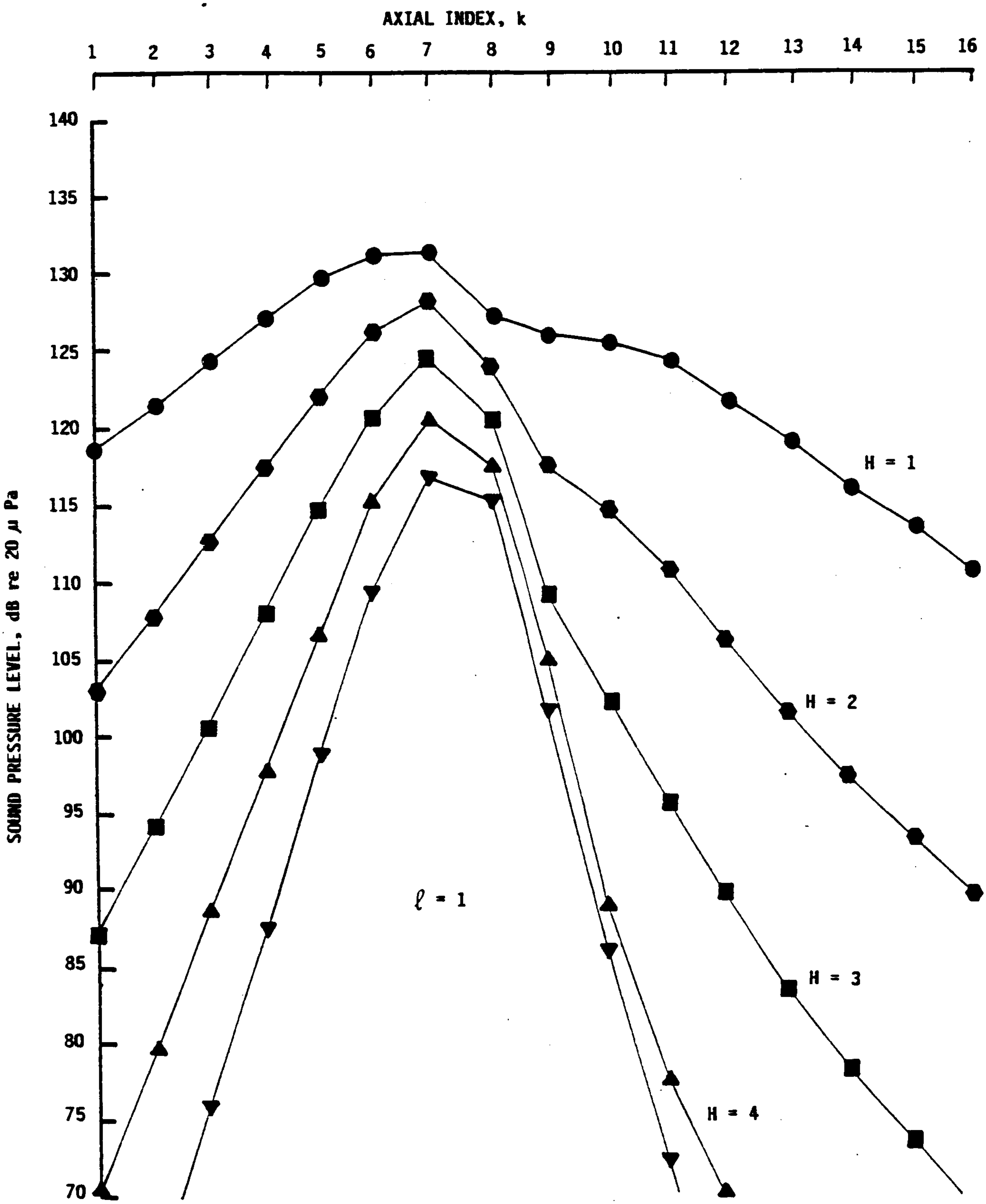

FIGURE 52. EXTERIOR LEVELS (FREE FIELD), FLIGHT RUN NO. 12

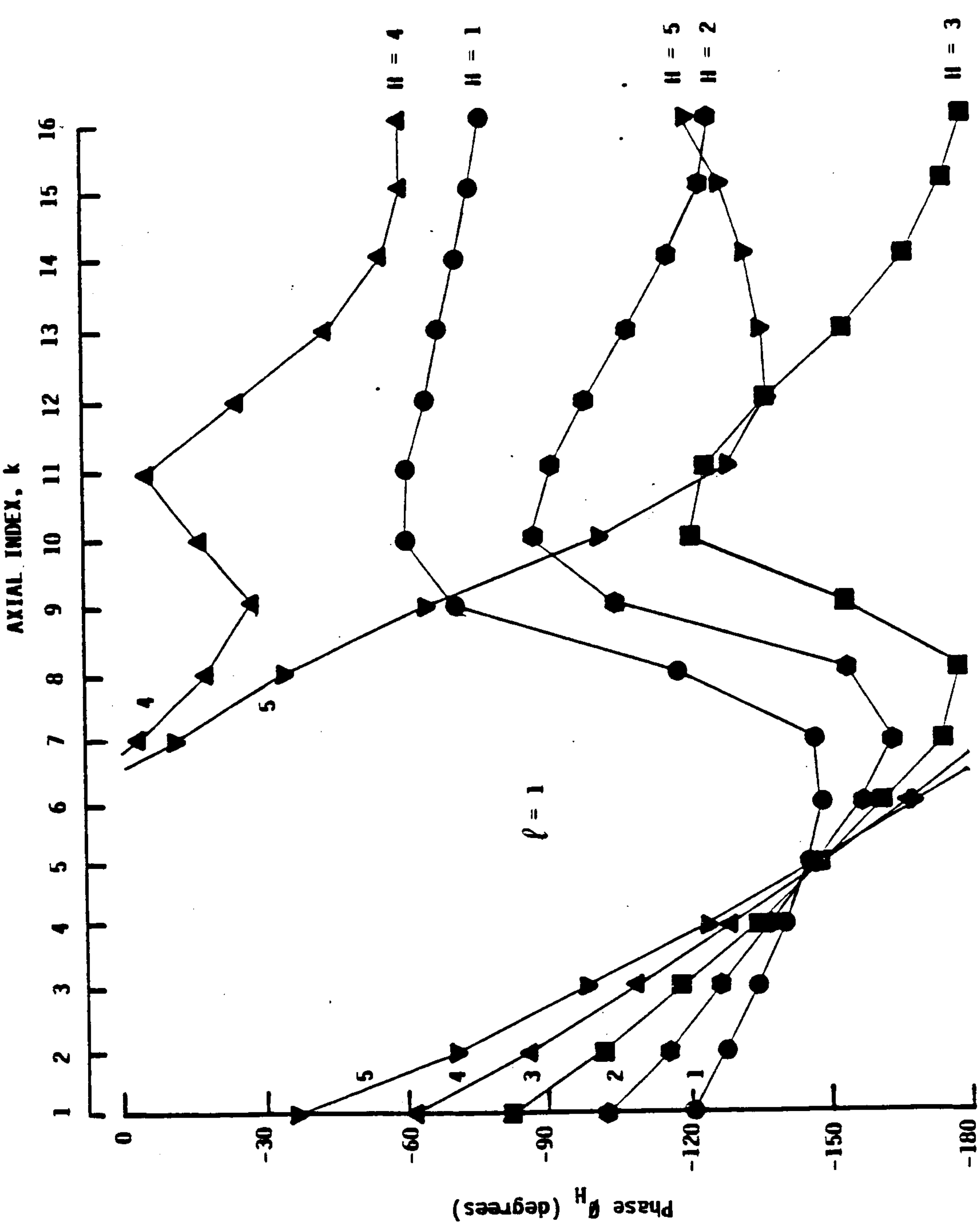

FIGURE 53. PHASE (FREE FIELD), FLIGHT RUN NO. 12

erence 1 to account for the blocking by the fuselage surface. For consistency with the scale model test results, a maximum increase of 4 dB is allowed, i.e., the right hand side of Eq. (43) is multiplied by a factor 0.8.

The scale-model tests showed that the reflection effects dissipate faster than the PAIN model predicts, so the computer generated field may be "stronger" than the actual field. No changes are proposed in propeller data input, however, until ANOPP calculated blocked pressures are available.

5.3.3 Fuselage and Cabin Modeling

The fuselage modeling is exactly as detailed in Section 4.2.2. The structural modal file (identical to that in Appendix C) is created using the input data specified for the business aircraft as given in Table 13.

The cabin modeling is also basically identical. The floor angle is taken as 50°. The acoustic modal file such as shown in Appendix C (that output by PAIN) is created once the cabin length is specified. Results given in Appendix C were for a cabin length of 7.75 m. In the present case, the length is 7.89 m. Also the trim panel surface mass is different (1.95 kg/m^2 as noted in Section 5.1).

Both of the input files (to PAIN) are complete, or sufficiently complete to allow use of the low frequency calculation procedure for all 5 harmonics.

5.3.4 PAIN Input and Output Data

Input data for the PAIN program consist of the output files from MRPMOD and CYL2D plus its own exclusive data. These data are the same type as was used for PAIN input in the scale model tests. Table 6 should be consulted to review the requirements.

Damping

The structural loss factors of the bare (or untrimmed) fuselage are taken as $2/f_r$ where f_r is the resonance frequency. PAIN will calculate trimmed fuselage "loss factors" necessary for the transmission predictions, i.e., η_r' and η_r'' .

The acoustic loss factors are input as zero so that PAIN will calculate the sidewall conductance and then the loss factors.

The trim panel loss factor η_T is set to 2.0 to force PAIN to calculate (what is believed to be) the most accurate transmission coefficient. Figure 54 shows the effects of changing η_T. The predicted interior levels will not be affected nearly as much as these curves might imply because a resonance controlled trim will also more readily absorb sound from the cabin space. For instance in Run 10, reducing η_T from 2.0 to 0.2 increases the predicted space average level by only 2.75 dB for the first harmonic (104.5 Hz). It actually decreases it by 0.48 dB for the second harmonic (209.1 Hz) and increases it by only 1.95 dB for the third harmonic (313.6 Hz). An increase of 4.58 dB is predicted for the fourth harmonic (418.1 Hz) and 3.73 dB for the fifth harmonic (522.7 Hz). The above differences (quoted for blade downsweep) show that the trim effects are not simply describable in terms of a transmission coefficient (or transmission loss), but only within the context of the PAIN analytical model. Until future superior developments replace the present trim model, it is recommended that η_T be arbitrarily set at 2 to create a trim model valid in the frequency range from about 50 to perhaps 1000 Hz. Reference 6 may be consulted for review of the trim model.

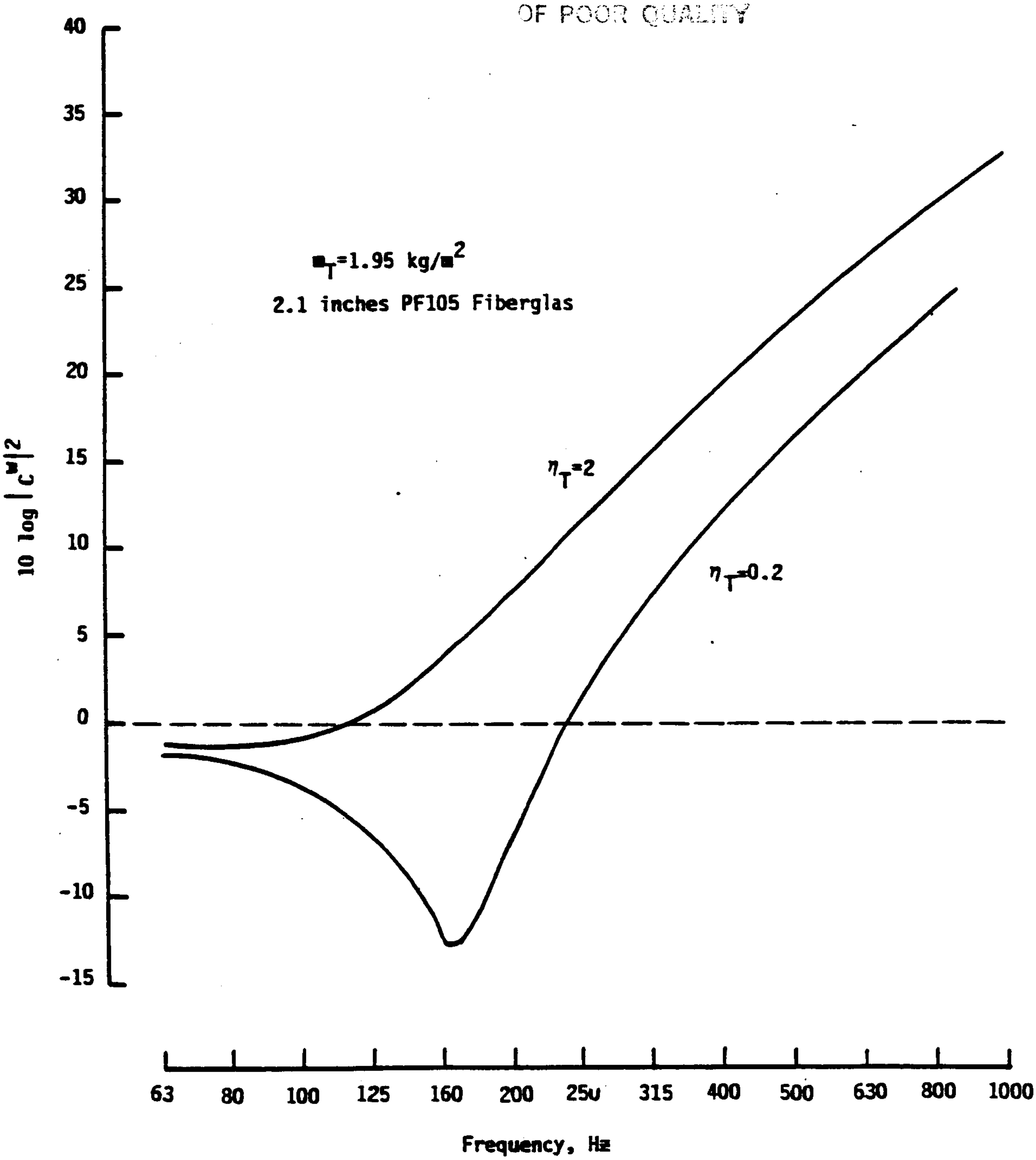

FIGURE 54. EFFECT OF VARYING LOSS FACTOR, η_T ON TRIM FACTOR $\tau_t = |C^w|^2$

Propeller

The propeller is located as before by the variables r_p, z_p, and ϕ (Figure 36). As can be seen in the figure r_p is 2.35 m, z_p is 1.12 m, and ϕ is 75° (recall that the PAIN input requirement for ϕ is to the nearest 5° increment). In the present case, the number of blades B is 4 and the propeller rotation speed N is 1568 rpm. The blade sweep variable is +1 (downsweep) or -1 (upsweep). PAIN must be run twice since there are two propellers rotating in the same direction and the interior levels predicted for blade downsweep and upsweep must be added (on a power basis) to obtain the predicted levels in-flight.

Pressurization

The effects of pressurization are accounted for (in PAIN) through adjustment of the exterior and interior air densities and sound speeds. The flight status is determined by the exterior and cabin temperatures and the cabin pressure. The correct exterior sound speed is 341.6 m/s. This is based on on temperature of 17°C (Table 15) which is higher than the standard at 5000 ft. The ANOPP exterior sound speed was taken as 334.1 m/s which is nearer that of standard temperature. This was an error in the ANOPP input, but a difference of only slightly over 2% less than the true sound speed is not significant. The PAIN input duplicates the ANOPP input of 334.1 m/s with an exterior density of 1.1012 kg/m^2. The interior sound speed is 343 m/s with a density of 1.204 kg/m^2. This latter value is based on an ICAO standard pressure altitude (12.243 psia at 5000 ft plus a 2.5 psi differential) and 68°F in the cabin. Had comparisons been attempted at higher altitudes, greater care would have had to have been taken in duplicating flight exterior conditions. However here the errors incurred in predicting exterior prop noise are not considered to be sufficiently great to force a re-run of ANOPP for the three runs 10, 11 and 12. Estimates are that much less than a one decibel change in exterior levels would result if re-run.

Input and Output Data

Formatted input data for Programs MRP, MRPMOD and PAIN are given in Appendix D (Run 10 only). Also given in the same Appendix are the propeller blocked field data output by PAIN (Run 10) and the interior predictions for that run. In the interest of brevity, similar input and output data for Runs 11 and 12 are not shown.

5.4 Comparisons to Flight Test Results

The fundamental flight test comparisons are summarized in Tables 23 and 24 and in Figures 55, 56 and 57. The following is a brief description of the findings:

1) Predictions for four of the five harmonics fall within the 99% confidence limits of the measurements (for all three runs (10, 11 and 12)).

2) Predictions for 4 out of 5 harmonics also fall within the narrower 95% confidence limits for Run 10, and in Runs 11 and 12, 3 out of 5 predictions fall within the 95% confidence limits and predictions for the 2nd harmonics fall outside by 1.3 and 1.4 dB respectively.

3) In each run, the prediction for the fourth harmonic yields the major discrepancy.

4) The sample mean error between predicted (downsweep plus upsweep) and the measured space average level is +4.3 dB across all harmonics and runs (15 datum; predictions exceeding measurements) with a standard

Table 23. Predicted Versus Measured Space Average Sound Pressure Levels in Flight

Run No.	Harmonic H	Freq. (Hz)	$\overline{SPL}_H$ (dB) Predicted Downsweep	Predicted Upsweep	Predicted Both	Measured	Prediction-Measurement Δ_1
10	1	104.5	99.9	99.9	102.9	101.2 (102.0)	1.7 (0.9)
	2	209.1	96.6	95.5	99.1	93.2 (97.1)	5.9 (2.0)
	3	313.6	88.1	89.4	91.8	89.9	1.9
	4	418.1	83.9	83.5	86.7	77.2	9.5
	5	522.7	71.0	69.2	73.2	72.2	1.0
11	1	104.5	97.9	97.8	100.9	98.5 (99.6)	2.4 (1.3)
	2	209.1	94.6	93.5	97.1	90.1 (93.8)	7.0 (3.3)
	3	313.6	86.6	87.8	90.3	89.6	0.7
	4	418.1	82.2	81.8	85.0	72.1	12.9
	5	522.7	69.3	67.6	71.5	71.7	-0.2
12	1	104.5	93.4	93.3	96.4	95.0 (95.8)	1.4 (0.6)
	2	209.1	90.4	89.4	92.9	86.3 (89.3)	6.6 (3.6)
	3	313.6	83.9	84.7	87.3	85.9	1.4
	4	418.1	78.9	78.6	81.8	71.4	10.4
	5	522.7	66.1	64.7	68.5	66.9	1.6

Table 24. Sample Statistics and Acceptance Regions for Interior Sound Levels (Table 23)

Hypothesis Test on	Sample Statistics $\overline{\Delta}$(dB)	Sample Statistics s(dB)	Level of Significance α	Acceptance Region (±dB)	Accept?
All 15 datum (3 runs x 5 harmonics)	4.28	4.12	0.2	1.43	no
			0.05	2.28	no
12 datum (H=4 excluded)	2.62	2.43	0.2	0.96	no
			0.05	1.54	no
Run #10 (5 harmonics)	4.00	3.62	0.2	2.48	no
			0.05	4.49	yes
Run #11 (5 harmonics)	4.56	5.42	0.2	3.71	no
			0.05	6.72	yes
Run #12 (5 harmonics)	4.28	4.08	0.2	2.80	no
			0.05	5.07	yes
H=1 (10, 11 and 12)	1.83	0.51	0.2	0.56	no
			0.05	1.26	no
H=2 (10, 11 and 12)	6.5	0.56	0.2	0.61	no
			0.05	1.39	no
H=3 (10, 11 and 12)	1.33	0.60	0.2	0.65	no
			0.05	1.49	yes
H=4 (10, 11 and 12)	10.93	1.76	0.2	1.92	no
			0.05	4.37	no
H=5 (10, 11 and 12)	0.80	0.92	0.2	1.00	yes
			0.05	2.28	yes

ORIGINAL PAGE IS
OF POOR QUALITY

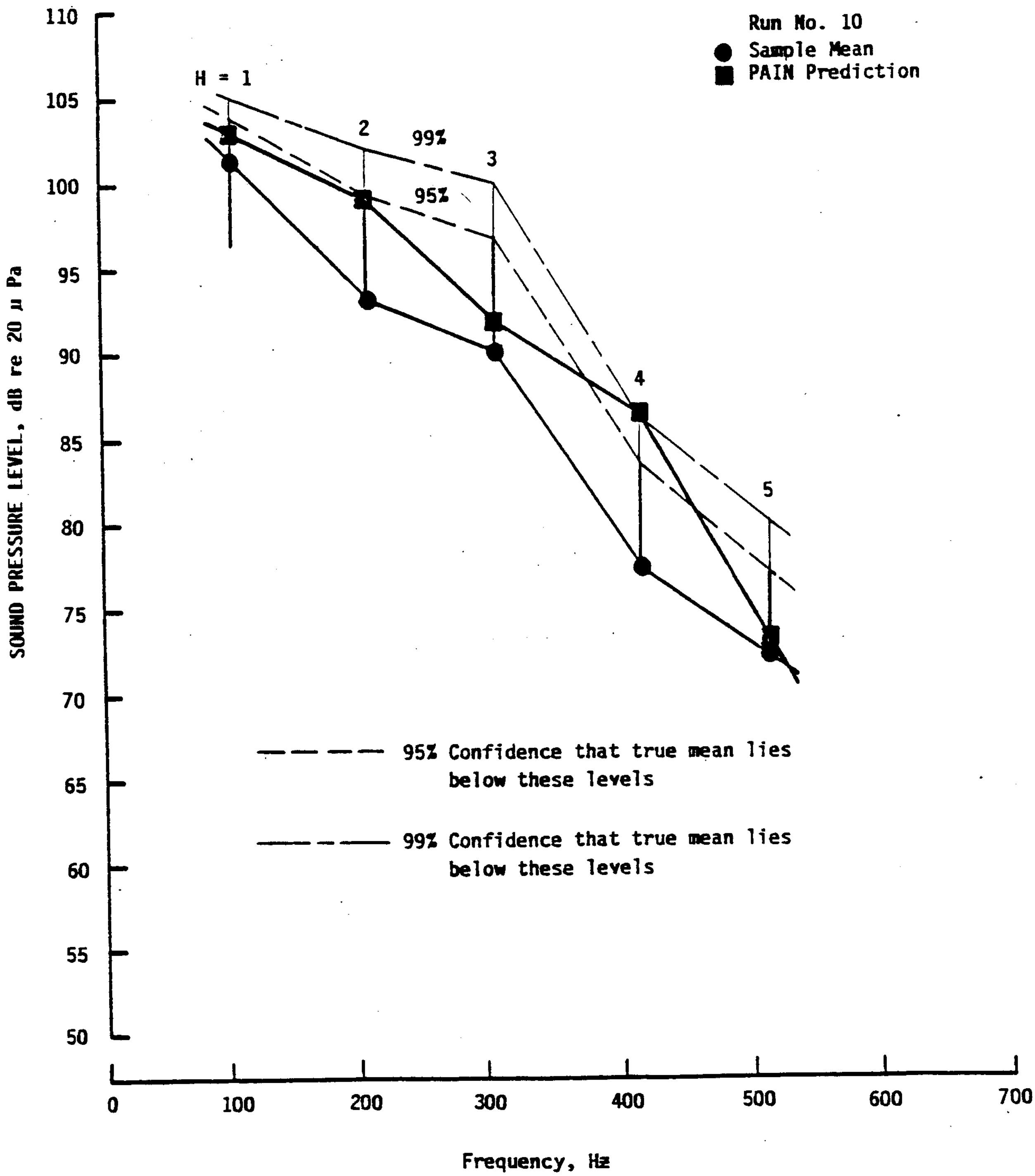

FIGURE 55. SPACE-AVERAGE SOUND LEVELS INSIDE AIRCRAFT @ 238 KIAS (ALTITUDE=5000ft)

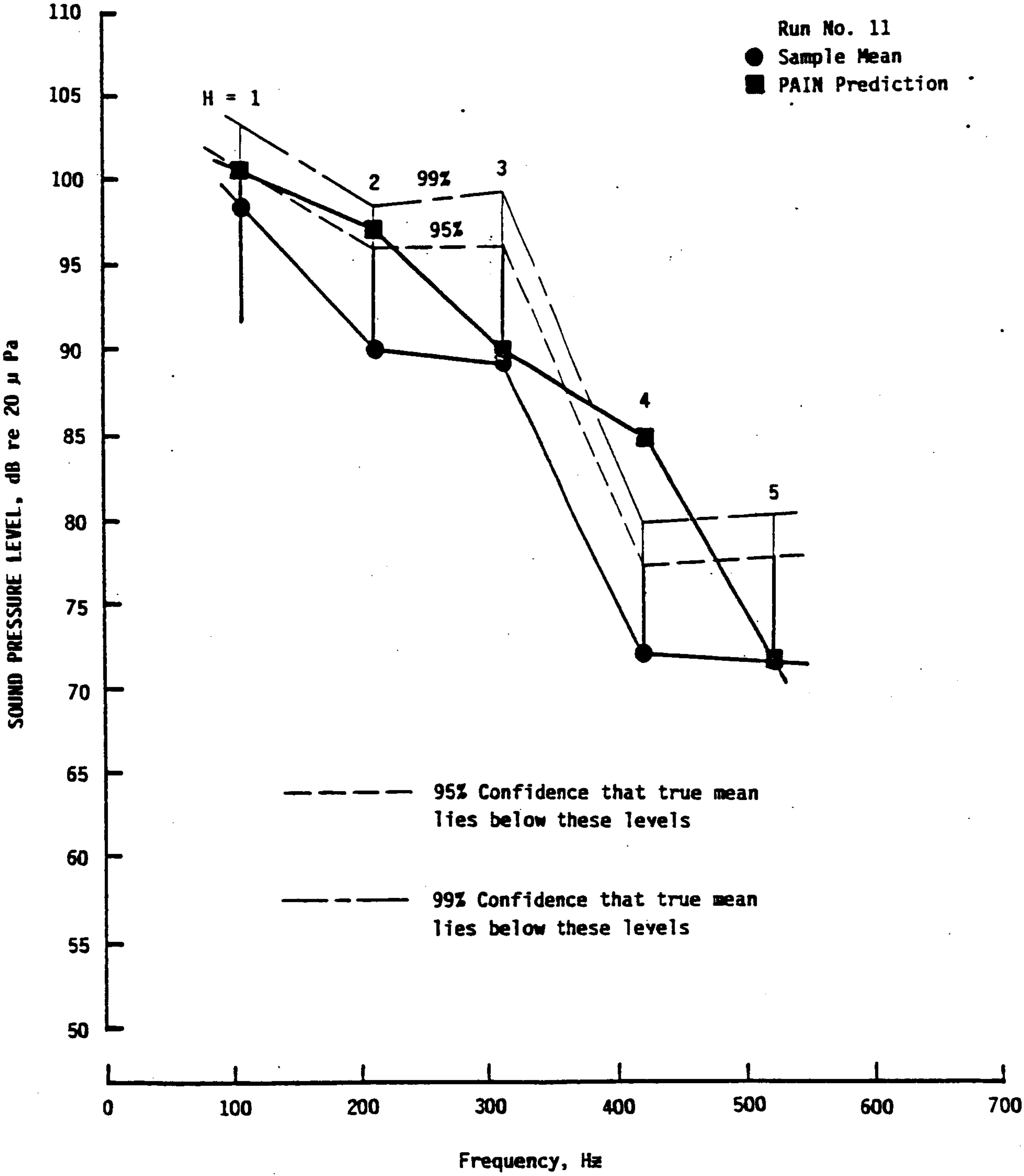

FIGURE 56. SPACE-AVERAGE SOUND LEVELS INSIDE AIRCRAFT @ 216 KIAS (ALTITUDE=5000ft.)

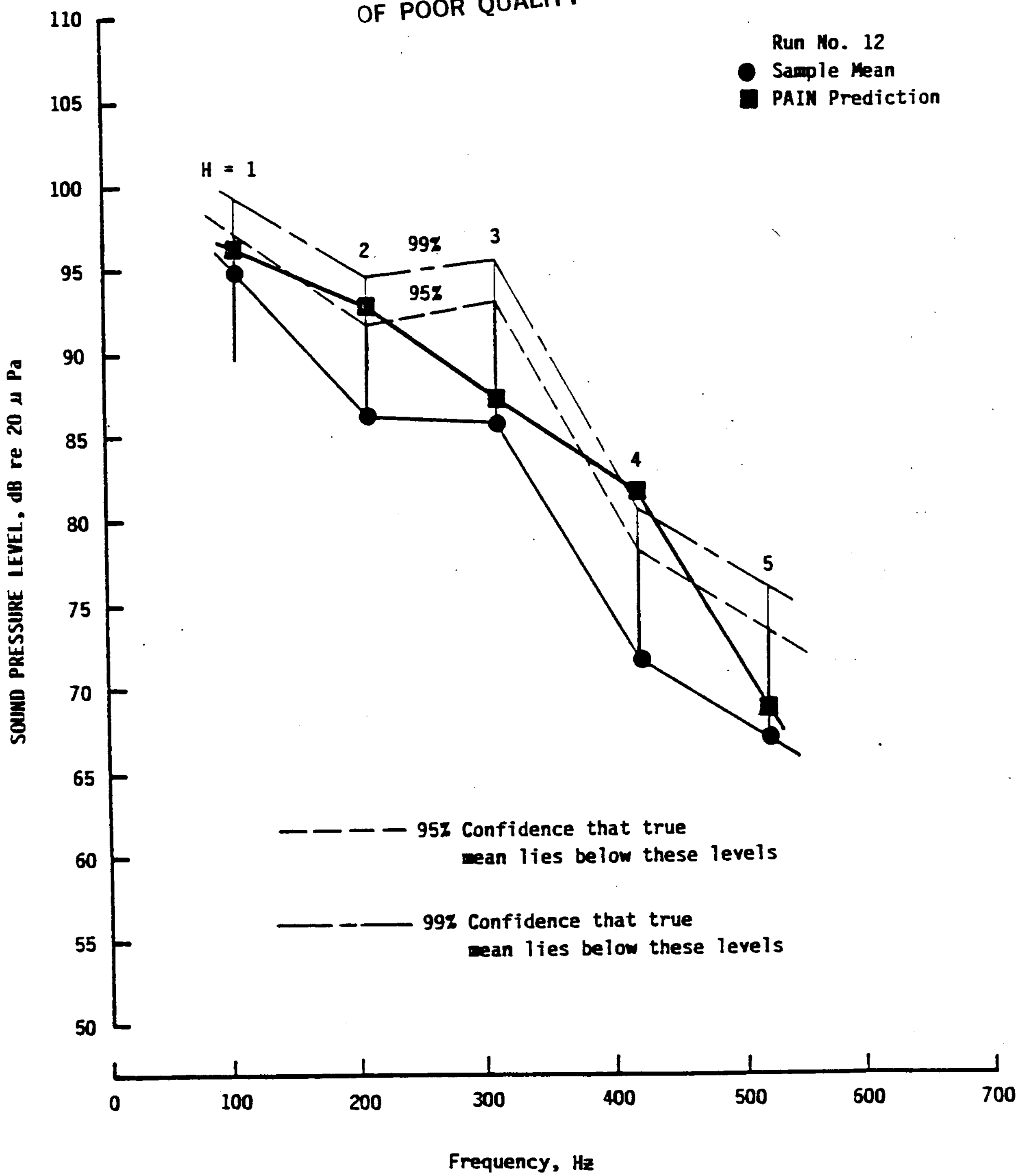

FIGURE 57. SPACE-AVERAGE SOUND LEVELS INSIDE AIRCRAFT @ 165KIAS (ALTITUDE=5000ft)

deviation of 4.1 dB (Table 24).

5) Excluding the results for the fourth harmonic (i.e., using 12 datum), the mean error is 2.6 dB with a standard deviation of 2.4 dB.

6) In both cases 4) and 5) above, a standard hypothesis test clearly (but not surprisingly) shows a bias present in predictions.

7) Examined run-by-run, the sample mean errors ranged between 4.0 and 4.6 dB and the sample standard deviations between 3.6 and 5.4 dB. At a sufficiently low level of significance, none of the three runs can be shown to be biased, but actually this is due to the large discrepancies between the predictions and measurements for the fourth harmonics.

8) Examined harmonic-by-harmonic, the sample mean errors ranged between 0.8 and 6.5 dB, but ballooned to 10.9 dB for harmonic 4. In all except the case of the third harmonics bias is present. Of great significance however is the low level of random error as exhibited by a standard deviation of less than 1 dB for four of five harmonics and only 1.8 dB for the fourth harmonic.

It should be noted that bias adjustments were previously made to the raw data to obtain estimates for the space average levels in the forward subvolume. Had those adjustments not been made, i.e., if the head level measurements had been taken as representative random samples and the average level taken as the space average in the forward subvolume for the first two harmonics, the errors would have been smaller (see the numbers in the parentheses in Table 23 and also refer to Figure 58). The sample mean error between predictions and measurements across all 15 datum would

ORIGINAL PAGE IS
OF POOR QUALITY

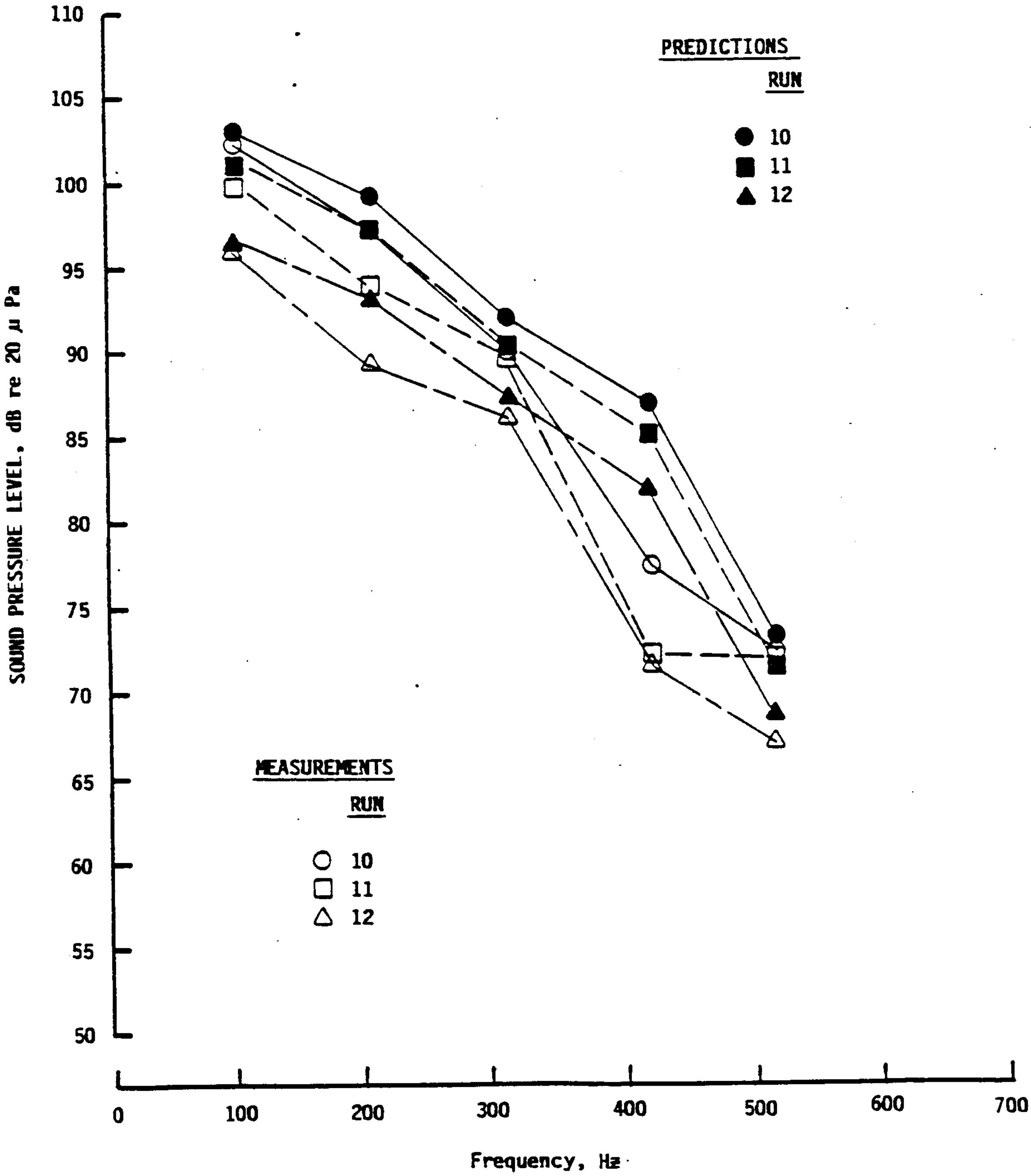

FIGURE 58. COMPARISON OF PREDICTIONS AND MEASUREMENTS WITHOUT ASSUMED BIAS CORRECTIONS.

be reduced to 3.4 dB with a standard deviation of 4.1 dB. By excluding the fourth harmonics these become 1.5 dB and 1.1 dB respectively. As before bias is indicated. Now however the mean errors (averaged across the three runs) for the 1st and 2nd harmonics are only 0.9 and 3.0 dB respectively with standard deviations of 0.35 dB and 0.85 dB. What these mean to the eventual user of the PAIN program is a matter to be discussed in the concluding section.

Next consider the accuracy of the predictions made with the "high frequency formulation". As previously stated, these calculations are always output by PAIN. Thus there are comparitive predictions for all harmonics where results from the low frequency technique are available. At sufficiently low frequencies predictions made with the high frequency procedure may be spurious and if so, they should be ignored. Use of the low frequency procedure is preferred whenever possible. However, as noted in Section 4.0, for large fuselages, the high frequency procedure will have to be used above the first few harmonics.

The results for the present flight tests are shown in Table 25. Predictions for the first harmonics are spurious and are discarded. The mean error for the twelve remaining datum (2nd through 5th harmonics) is -1.43 dB with a fairly large standard deviation of 6.26 dB. At the α=0.05 and 0.2 levels of significance, a zero bias hypothesis test yields acceptance regions of $\pm$3.97 and $\pm$2.46 dB. Since the mean error falls within either of these bounds, the hypothesis is accepted.

Reviewing the results, it can be seen that the low frequency formulation tends to over-predict, while the high frequency formulation does not. Nevertheless the latter predictions are to be considered strictly supplementary in any instance where predictions can be obtained with the low frequency procedure.

Table 25. Predictions with High Frequency Formulation

Run No.	Harmonic H	Freq. (Hz)	$\overline{SPL}_H$ (dB) Downsweep	Upsweep	Both	Measurement (Table 23)
10	1	104.5	117.6	118.2	(Spurious)	101.2(102.0)
	2	209.1	96.9	98.5	100.7	93.2(97.1)
	3	313.6	84.9	83.7	87.4	89.9
	4	418.1	70.8	69.4	73.2	77.2
	5	522.7	62.6	60.1	64.5	72.2
11	1	104.5	115.5	116.1	(Spurious)	98.5(99.6)
	2	209.1	95.0	96.6	98.9	90.1(93.8)
	3	313.6	83.1	82.1	85.6	89.6
	4	418.1	68.9	67.4	71.2	72.1
	5	522.7	61.0	58.7	63.0	71.7
12	1	104.5	111.0	111.5	(Spurious)	95.0(95.8)
	2	209.6	91.1	92.5	94.9	86.3(89.3)
	3	313.6	79.4	78.7	82.1	85.9
	4	418.1	65.3	64.0	67.7	71.4
	5	527.7	57.9	56.1	60.1	66.9

5.5 Understanding Sidewall Transmission

Appendix D contains a copy of the predictions for Run 10 (the case of blade downsweep). There are a number of interesting things about the results that lend to an understanding of the physics involved in the transmission of propeller tones. For instance, the top five contributing modal pairs are all of the following type: 1) either the acoustic and structural modes are both resonance controlled (or nearly so), or 2) a resonant or nearly resonant acoustic mode is coupled to a nonresonant structural mode (exceptions mainly confined to the 1st harmonic). In no case, however, is there a single dominating pair of modes. In fact, the five highest contributing pairs are responsible for only 47.9% of the acoustic energy in the cabin at the 1st harmonic. This value rises to 59.3% and 58.0% for the 2nd and 3rd harmonics, but then falls to only 24.9% and 28.1% for the 4th and 5th harmonics. Thus the propeller tones are being transmitted by a rather large number of modal pairs. The impracticality of the idea of moving modes around in frequency or changing the wavenumber coupling to affect noise reduction is evident. However this "modal insensitivity" is no doubt part of the reason that the predictions are as good as they are. Furthermore, the results make clear that improved sidewall treatment will remain the one particular topic of greatest need if further reductions in cabin levels (arising from sidewall transmission) are to be achieved in these types of airplanes.

6.0 FINDINGS AND CONCLUSIONS

The comparisons in this report have led to a number of findings, the most important of which are reviewed below:

1) In the case of the scale-model tests, the PAIN program made unbiased predictions. The standard deviation of the errors was about 4 dB (case of "a heavily damped trim panel" after excluding the extraneous low frequency datum).

2) In case of the flight tests, the predictions with the preferred "low frequency formulation" showed a bias (on the high side) of between 2.6 and 4.3 dB and the standard deviation of the errors ranged between 2.4 and 4.1 dB. Predictions made with the "high frequency formulation" showed no bias but had a high random error as exhibited by a standard deviation of 6.3 dB.

3) Predictions made for given harmonics at different flight conditions were found to be biased but the level of random error was extremely low as exhibited by the small standard deviations, indicating that changes occurring in interior levels caused by flight reconfiguration are being predicted by the model.

All of the above findings are based on increasing by 4 dB, the ANOPP free-field predictions of the pressure amplitudes to account for fuselage surface reflections (rather than 6 dB as originally programmed in the model). Scale-model blocked pressure measurements imply that surface reflection effects dissipate faster (as one moves away from the propeller plane) than the PAIN model admits. Thus the computer generated blocked pressure field may be "stronger" than it should be. This may be offset somewhat by the use of the so-called ANOPP method 3 predictions which lead to a "weaker" exterior field than would be predicted using ANOPP Method 1. Ultimately, the blocked pressure predictions by ANOPP are needed to resolve the difficulties, because regardless of the amplitude uncertainties, there are virtually no data available to allow comparisons of phase differences between the free and blocked fields. The PAIN program presently uses the free field phase data (without modification). Future changes in predictions that might be realized when the bona fide blocked field is used are unknown.

6.1 Use of the PAIN Program

PAIN predictions made using ANOPP Method 3 propeller data should be adjusted downward by 3 or 4 dB. The resulting numbers should be considered the basic estimates of the space-average levels in the cabin. Keeping in mind that random errors are going to be present, a one-sigma band of about 3.5 dB about the adjusted computer predictions will then give estimates of levels within which about 2 out of 3 of the flight measurement data should fall. Approximately 1 out of 3 should fall outside the band (hopefully by not much). As time passes and more flight comparison data are made available, this technique may need to be revised.

Calculations made using the high frequency formulation should be carefully scrutinized. Although no bias was indicated by the hypothesis test on the four harmonics 2 through 5, it is pretty obvious from Table 25 that for harmonics 3 through 5, there is a bias (an under-prediction) of more than 4.5 dB. This is probably caused by not including enough modes in the summation in Eq. (16) of Reference 1. Future validation work should confirm this.

6.2 PAIN Validation Status

The propeller tone prediction capability of the PAIN program has been validated to the extent that, at the conclusion of the present study, no significant changes to the PAIN program have been shown to be warranted. It is felt that the present model is "hamstrung" to a certain extent by the need for ANOPP prediction capability of the actual blocked pressure field on the fuselage. Eventually, given this information, the PAIN program can be modified to include effects such as synchrophasing. In order to perform such calculations, the PAIN grid will need to be extended to cover the entire periphery of the fuselage. The length of the grid should be extended at that time to allow predictions to be made for cases having high tip clearance to propeller diameter ratios. Some consideration should be given to reducing the grid spacing at the same time.

The cabin trim model is simple yet somewhat sophisticated. Stiffness of the trim panel is not taken into account nor are details regarding trim installation included. However, the model has been found to be essentially adequate over the limited frequency range from, say, about 50 to 1000 Hz. Above this range, sound isolation will be over-predicted because skin-to-trim vibration transmission will lead to increased internal radiation.

Noise Reduction

The PAIN program has noise reduction prediction capability. However, the quality of the predictions has not been fully investigated. Studies undertaken in Appendix E of Ref. (1) were extremely limited. The poor results shown in that work are, however, expected to be typical for frequencies where the cavity modes are driven in the stiffness controlled region and where the trim transmission is dominated by the mechanical vibration path (see Section 2.8 of Ref. 6 and Eq. A.22 of Ref. 1).

It is felt that the noise reduction calculation option in PAIN should be removed (perhaps made into a separate program) so that the propeller prediction capability is allowed to stand alone (at least until the extreme limitations on the use of the noise reduction section of the program are clearly defined; for instance, the use of incomplete modal files must be avoided).

REFERENCES

1. Pope, L.D., Wilby, E.G. and Wilby, J.F., "Propeller Aircraft Interior Noise Model," NASA CR-3813, 1984.
2. Wilby, E.G. and Pope, L.D., "Propeller Aircraft Interior Noise Model, Users' Manual For Computer Program," NASA CR-172425, 1984.
3. Pope, L.D. and Wilby, J.F., "Band-limited Power Flow into Enclosures, I," J. Acoust. Soc. Am., 62, 4, 906-911 (1977).
4. Pope, L.D. and Wilby, J.F., "Band-limited Power Flow into Enclosures, II," J. Acoust. Soc. Am., 67, 3, 823-826 (1980).
5. Pope, L.D., Rennison, D.C., Willis, C.M. and Mayes, W.H., "Development and Validation of Preliminary Analytical Models for Aircraft Noise Prediction," J. Sound and Vib., 82, 4, 541-575 (1982).
6. Pope, L.D., Wilby, E.G., Willis, C.M. and Mayes, W.H., "Aircraft Interior Noise Models: Sidewall Trim, Stiffened Structures, and Cabin Acoustics with Floor Partition," J. Sound and Vib., 89, 3, 371-417 (1983).
7. Martin, R.M. and Farassat, F., "Users' Manual for a Computer Program to Calculate Discrete Frequency Noise of Conventional and Advanced Propellers," NASA TM 83135, 1981.
8. Zorumski, W.E., "Aircraft Noise Prediction Program Theoretical Manual," NASA TM 83199, 1981.
9. Magliozzi, B., "Acoustic Pressures on a Prop-fan Aircraft Fuselage Surface," J. Aircraft, 19, 2, 104-111 (1980).
10. Bendat, J.S. and Piersol, A.G., Random Data: Analysis and Measurement Procedures, Wiley-Interscience, New York, 1971.
11. "Prediction Procedure for Near Field and Far Field Propeller Noise," Soc. Auto. Engr. Aerospace Information Report 1407, May 1977.
12. Anon., "Prop-fan and Gearbox Near Field Noise Predictions," United Technologies/Hamilton Standard Report SP15A77, Rev. A, February 1978.

Appendix A

- Analytical Modification of PAIN
- Program Changes
- Control Card Changes

Analytical Modification of PAIN

The basic results of the analyses presented in Refs. (1) and (6) inadvertently lead to errors in the calculation of the fuselage loss factor η_r', i.e., application of the results directly to the fuselage of Figure 1, without modification, leads to a calculation of η_r' for a case where trim is installed not only on the cabin sidewall but also the floor. Also there is a failure to properly take into account the fact that significant modal energy of lower order structural modes can be in axial and circumferential stretching motion of the skin (non-bending).

Consider Fig. 1 of Ref. (6) and refer to Eqs. (1a), (2a), and (3)-(6) of that paper. Note that if trim is not installed over a portion of the surface area (such as the floor), for that portion

$$C_p = 1 \; ; \quad C^p = 0.$$
$$C^w = 1 \; ; \quad C_w = 0.$$

Let X be the set of all points lying on the structure surface covered with trim, and let Ω be the entire surface area (all points). Eqs. (1a) and (2a) of the paper can be written as

$$\int_{\bar{x}'\in\Omega}(\delta(\bar{x}'-\bar{x})+C_w G(\bar{x}/\bar{x}';\omega))w_1(\bar{x}')d\bar{x}' = \int_{\bar{x}'\in\Omega} G(\bar{x}/\bar{x}';\omega)(p^o(\bar{x}')-C_p p_2^i(\bar{x}'))d\bar{x}' \tag{1a}$$

and

$$\int_{\bar{x}\in\Omega}(\delta(\bar{x}-\bar{x}')+\rho\omega^2 C^p G_p(\bar{x}/\bar{x}';\omega))p_2^i(\bar{x})d\bar{x} = -\rho\omega^2 C^w\int_{\bar{x}\in\Omega} G_p(\bar{x}/\bar{x}';\omega)w_1(\bar{x})d\bar{x} \; . \tag{2a}$$

In the present circumstances, C_w and C^p are replaced by

$$C_w H(\bar{x}/X), \qquad C^p H(\bar{x}/X),$$

where

$$H(\bar{x}/X) = \begin{cases} 1 ; & \bar{x} \in X \\ 0 ; & \bar{x} \notin X \end{cases} .$$

Note that since C_p and C^w are nonzero, no change in the manner that they are handled in the analysis is required. The fact that these terms are discontinuous at the boundaries of the trim covered areas is of no consequence.

Substitution for C_w and C^p in Eqs. (1a) and (2a) gives

$$\int_\Omega (\delta(\bar{x}'-\bar{x})+C_w H(\bar{x}'/X)G(\bar{x}/\bar{x}';\omega))w_1(\bar{x}')d\bar{x}' = \int_\Omega G(\bar{x}/\bar{x}';\omega)(p^o(\bar{x}')-C_p p_2^i(\bar{x}'))d\bar{x}' \quad (1a)$$

and

$$\int_\Omega (\delta(\bar{x}-\bar{x}')+\rho\omega^2 C^p H(\bar{x}/X)G_p(\bar{x}/\bar{x}';\omega))p_2^i(\bar{x})d\bar{x} = -\rho\omega^2 C^w \int_\Omega G_p(\bar{x}/\bar{x}';\omega)w_1(\bar{x})d\bar{x} . \quad (2a)$$

Consider the left hand side of Eq. (1a). Let

$$w_1(\bar{x}) = \sum_s \xi_s \psi^s(\bar{x}).$$

Then

$$\int_\Omega (\delta(\bar{x}'-\bar{x})+C_w H(\bar{x}'/X)G(\bar{x}/\bar{x}';\omega)) \sum_s \xi_s \psi^s(\bar{x}')d\bar{x}'$$

$$= \sum_s \xi_s \left(\psi^s(\bar{x}) + \int_\Omega C_w H(\bar{x}'/X)\psi^s(\bar{x}')G(\bar{x}/\bar{x}';\omega)\,d\bar{x}'\right)$$

$$= \sum_s \xi_s \left(\psi^s(\bar{x}) + \int_X C_w \psi^s(\bar{x}')G(\bar{x}/\bar{x}';\omega)\,d\bar{x}'\right).$$

Now

$$G(\bar{x}/\bar{x}';\omega) = \sum_n \frac{\psi^n(\bar{x})\psi^n(\bar{x}')}{M_n Y_n(\omega)} .$$

Thus the left-hand side of (1a) becomes

$$= \sum_s \xi_s \left(\psi^s(\bar{x}) + C_w \int_X \sum_n \frac{\psi^n(\bar{x})\psi^n(\bar{x}')}{M_n Y_n(\omega)} \psi^s(\bar{x}')\,d\bar{x}'\right)$$

$$= \sum_s \xi_s \left(\psi^s(\bar{x}) + (C_w/m) \sum_n \frac{\psi^n(\bar{x})}{M_n Y_n(\omega)} \int_X m\psi^n(\bar{x}')\psi^s(\bar{x}')\,dx'\right) .$$

Now

$$\int_\Omega m\psi^n(\bar{x}')\psi^s(\bar{x}')\,dx' = \begin{cases} M_s & ; \ n=s \\ 0 & ; \ n\neq s \end{cases} .$$

In the referenced paper, it was an oversight that $\int_X$ above was evaluated as $\int_\Omega$. Note if $X = \Omega$,

$$\sum_n (\psi^n(\bar{x})/M_n Y_n(\omega)) \int_X m\psi^n(\bar{x}')\psi^s(\bar{x}')d\bar{x}'$$
$$= \psi^s(\bar{x})M_s/M_s Y_s(\omega) \quad = \quad \psi^s(\bar{x})/Y_s(\omega) \;.$$

This yields for the left-hand side

$$\sum_s (1+(C_w/mY_s(\omega)))\xi_s \psi^s(\bar{x}),$$

which is the result in the paper.

It can be seen that the actual result should have been

$$\sum_s (1+(C_w/mM_s Y_s)\int_X m\psi^{s^2}(\bar{x}')d\bar{x}')\xi_s\psi^s(\bar{x})$$
$$+\sum_{s}\xi_s \sum_{\substack{n \\ (s\neq n)}} (C_w\psi^n(\bar{x})/mM_n Y_n)\int_X m\psi^s(\bar{x}')\psi^n(\bar{x}')d\bar{x}' \;.$$

Let

$$\int_X m\psi^s(\bar{x}')\psi^n(\bar{x}')d\bar{x}' = \begin{cases} M_s^X & ; \quad n = s \\ \epsilon_{ns}M_s^X & ; \quad n \neq s \;. \end{cases}$$

The above becomes

$$\sum_s (1+C_W M_s^X/mM_sY_s)\xi_s\psi^s(\bar{x}) + \sum_{\substack{s \\ (s\neq n)}}\sum_n \xi_s\psi^n(\bar{x})\,C_W\epsilon_{ns}M_s^X/mM_nY_n \quad .$$

The last term (double sum) can be understood as coupling of the structural modes introduced by the trim installation.

It is reasonable to expect that for all significantly transmitting modes (i.e., those that are largely shell as opposed to totally floor modes), that

$$|\epsilon_{ns}| < 1$$

and that for those modes

$$\frac{1}{N_n}\sum_n^{N_n}\epsilon_{ns} \ll 1.$$

Assuming this is so is equivalent to assuming that the double sum can be neglected, i.e., that damping of structural modes through intermodal coupling is insignificant because energy flowing out of one mode to another will be replaced by energy flow into the mode via yet a third mode. This assumption reduces the left hand side of (1a) to

$$\sum_s (1+(C_W/\bar{m}_sY_s(\omega)))\xi_s\psi^s(\bar{x}) \quad ,$$

where

$$\bar{m}_s = mM_s/M_s^X \quad .$$

Continuing, reconsider (1a) which leads to Eq. (6) of the reference. In the present circumstance (6) becomes

$$-Y_r(1+(C_w/\bar{m}_r Y_r))M_r\xi_r + \Gamma^r_{p_r} - C_p\Gamma^{r_i}_{p_2} = -\Gamma^r_{p_{b1}} \quad .$$

Thus no significant algebraic changes appear.

Now consider Eq. (2a). $w_1(\bar{x})$ is replaced by the modal sum, (2a) is multiplied through by $\psi^r(\bar{x}')$ and integrated to obtain:

$$\int_\Omega \psi^r(\bar{x}')\int_\Omega (\delta(\bar{x}-\bar{x}')+\rho\omega^2 C^p H(\bar{x}/X)G_p(\bar{x}/\bar{x}';\omega))p_2^i(\bar{x})\,d\bar{x}d\bar{x}' = -\rho\omega^2 C^w \sum_s I^{rs}\xi_s \quad .$$

This reduces to

$$\Gamma^{r_i}_{p_2} + \rho\omega^2 C^p \int_\Omega\int_X \psi^r(\bar{x}')G_p(\bar{x}/\bar{x}';\omega)p_2^i(\bar{x})\,d\bar{x}d\bar{x}' = -\rho\omega^2 C^w \sum_s I^{rs}\xi_s \quad .$$

Following the analysis in the reference, the above can be shown to lead to a modification of Eq. (10) of the paper, i.e.,

$$b_{rn} = \frac{C_p C^p \rho\omega^2 \epsilon_n A f'(n,r)}{V(\bar{\lambda}_n^2 - k^2)} \int_X \phi_n^2(\bar{x})\,d\bar{x} \quad .$$

Other than this, there are no changes.

It follows, that as a final conclusion, the "structural" loss factor η'_r should be given by the result

$$(\eta'_r)^2 = |C_w|^2/\bar{m}_r^2\omega_r^4 - 2C_w^I\eta_r/\bar{m}_r\omega_r^2 + \eta_r^2 \quad .$$

(Note that the new variable $\bar{m}_r$ is used only within the context of the calculation of η'_r).

A question might now be asked as to whether the trim coverage is correct as related to the prediction of transmission through the trim. The answer is "yes", because the presence of trim on the sidewall and its absence on the floor is accounted for in Eq. (52) of the PAIN model (Ref. 1). Note that the trim transmission coefficient $\tau_t (= |C^w|^2)$ multiplies only one of the two terms in the braces of Eq. (52). A bar is placed over the f, in $\bar{f}'(n,r)$ to distinguish it from the term f'(n,r) (no bar over f) with purpose being to limit trim to sidewall and exclude it from the floor.

Program Changes

All required programming changes to PAIN and its subroutines, or to auxiliary programs, are specified below.

Program PAIN

1) Changes required to calculate the modified result for η_r' as found in this appendix, letting

$$M_s^X = \text{GMASS(IR,2)} \;;\; M_s = \text{GMASS(IR,1)} :$$

Subroutine ETASTR

Line 47 to become

```
CWI=AIMAG(CW)*GMASS(IR,2)/GMASS(IR,1)
```

Line 50 to become

```
CWMOD2=REAL(CMOD2)*(GMASS(IR,2)/GMASS(IR,1))**2
```

2) Changes required in the calculations of $f'(n,r)$ and $\bar{f}'(n,r)$ of Eq. (52) of Ref. (1) related to misinterpretation of sign convention used in the program MRP:

Subroutines TONE and NRED

Line 107 of TONE and Line 79 of NRED to become

```
FNR2=(FQM(IQ,M)*(FINS(N1,IR)-FINP(N1,IR)))**2
```

Line 111 of TONE to become

```
FNR2=(FQM(IQ,M)*(FINS(N1,IR)*SQRT(TAUH)-FINP(N1,
IR)))**2
```

Line 83 of NRED to become

```
FNR2=(FQM(IQ,M)*(FINS(N1,IR)*SQRT(TAU)-FINP(N1,
IR)))**2
```

3) Changes required to limit blocked pressure amplitudes of propeller field to a 4 dB increase over free field levels:

ORIGINAL PAGE IS
OF POOR QUALITY

Subroutine PROP

Line 49 to become

```
REFL=(10.0**(0.3-0.000224*EXP(0.08*GAMA)))*0.8
```

4) Changes to prevent printing truncation of large values of generalized masses for narrow body fuselages:

Program PAIN

Line 379 to become

```
6005 FORMAT (T10,I3,F8.2,1X,A5,F9.5,I4,I3,
F7.4,I4,F7.4,F9.2,F8.3,F8.3
```

5) Changes to allow propeller input data to be of the form of that for blade downsweep only:

Program PAIN

Following the Comment Card "C...Propeller Data", add

```
C   INPUT DATA CREATED WITH ANOPP TO BE BLADE
    DOWNSWEEP ONLY
C   PAIN WILL CREATE DOWNSWEEP OR UPSWEEP USING
    ANOPP DOWNSWEEP
```

Subroutine PROP

Line 54 to become

```
DELPH=2.0*B*IH*ALPHAL(L)
```

Following Line 63:"24 CONTINUE", insert 12 Cards

```
IF(ROTN.EQ.+1.0) GO TO 30
DO 29 IH=1,NHARM
DO 29 K=1,NK
DO 29 L=1,10
LU=L+9
LB=11-L
PX=PMH(K,LU,IH)
PY=PMH(K,LB,IH)
PMH(K,LU,IH)=PY
```

```
      PMH(K,LB,IH)=PX
   29 CONTINUE
   30 CONTINUE
```


Program MRPMOD

1) Changes to allow acceptance of increased eigen-vector output by MRP (40 instead of 30 eigen-vectors)

Line 13 to become

```
C...MTOTAL=HIGHEST VALUE OF M CONSIDERED (MAX 15)
```

Lines 15 and 16 to become

```
C...FOR EACH VALUE OF M (MAX NMODES=20)
C...NMOD=2*NMODES (MAX NMOD=40)
```

Lines 64 through 67

```
DIMENSION STYPE(2),TYPE(2,5),FREQ(40),TYPNM(2),
NMODE(40),
1  DMAX(40),COORDS(41),COORDP(41),DISPS(41,3,40),
   TMODE(40,5),
2  DISPP(41,3,40),GENM(6,40),GENMAS(40),DUMMY(700),
   NA(700),
3  TITLE(16),NORD(700)
```

Lines 68 through 70

```
DIMENSION EVALS(72),MVALS(40,15),NVALS(40,15),
EVECS(40,15),
1  MVALP(40,10),NVALP(40,10),EVECP(40,10),MVLS(40,
   15),NVLS(40,15),
2  EVCS(40,15),MVLP(40,10),NVLP(40,10),EVCP(40,
   10),TYPP(40)
```

Lines 72 through 74

```
DIMENSION FR(40,15),TYP(40,15),GMASS(40,3,15),
MVS(40,5,15),
1  NVS(40,5,15),EVS(40,5,15),MVP(40,3,15),NVP(40,
   3,15),EVP(40,3,15),
2  DIS(40,41,15),KTL(2)
```

Control Card Changes

1) Control cards for MRPMOD showing required DEFINE statement needed to create direct access permanent file.

```
/JOB
PAIN,T400,P1.
/USER
/CHARGE
ROUTE,OUTPUT,DC=PR,UN=*,ST=**,FID=POPE,DEF.
DEFINE,TAPE9=STR50. ←————————
GET,MRPMOD4.
ATTACH,TAPE7=MRPSM4.
ATTACH,TAPE8=MRPAM4.
GET,MRPMODC.
COPYBF,MRPMODC,LGO.
LDSET(PRESET=ZERO)
LGO,PL=50000.
GOTO,SUMMARY.
EXIT.
SUMMARY.
DAYFILE.
/NOSEQ
/EOR
/READ,MRPMOD4
/EOF
```

2) PAIN control cards (modified program PAINM) showing use of structural modal file as direct access type.

```
/JOB
PAIN,T400,P1.
/USER
/CHARGE
ROUTE,OUTPUT,DC=PR,UN=*,ST=**,FID=POPE,DEF.
GET,PAINMD4.
GET,TAPE11=CYL50.
ATTACH,TAPE9=STR50.←——Direct access file to local file
GET,PAINMC.
COPYBF,PAINMC,LGO.
LDSET(PRESET=ZERO)
LGO,PL=50000.
GOTO,SUMMARY.
EXIT.
SUMMARY.
DAYFILE.
/NOSEQ
/EOR
/READ,PAINMD4
/EOF
```

3) CYL2D control card change required to access the International Mathematical and Statistical Library (IMSL) subroutines.

Instead of

```
ATTACH, IMSL/UN=LIBRARY.
```

Use

```
BEGIN, IMSL4, IMSLCCL.
```

Appendix B

SCALE MODEL PREDICTIONS

- Structural modes list (partial)
- Acoustic modes list (partial)
- Modal distributions

In sequence for the 3000, 4000 and 5000 rpm runs:

- Propeller noise data (1st 3 harmonics)
- Interior predictions
- Highest modal contributors to interior levels

NASA LANGLEY SCALE MODEL FUSELAGE WITH FLOOR
STIFFENED 0.032 IN CYLINDER, STIFFENED FLOOR AT 56.6 DEGREES, RIGID JUNCTION
CAVITY 72 IN LONG, STRUCTURE 71 IN LONG
TRIM PANEL, FIBERGLAS TYPE PF105 2.0 IN THICK + LINING = 1.46 KG/M2

STRUCTURAL MODES

MODE NO	FREQ (HZ)	MODE TYPE	LOSS FACTOR	SHELL M	SHELL NS	SHELL CMNS	PLATE NP	PLATE CMNP	GENERALIZED MASS (KG) TOTAL	SHELL W	PLATE W	JREVB
1	188.52	SYMM	.08121	1	2	-.0664	0	.4150	1.1392	.0283	1.1028	3.6795E-05
2	208.24	SYMM	.17692	1	2	-.0769	1	1.4237	1.1267	.0567	1.0597	6.1851E-05
3	217.88	SYMM	.01241	2	4	.0127	0	.4454	1.0627	.0014	1.0610	1.1528E-06
4	231.01	SYMM	.02564	2	4	.0433	1	1.0843	1.0546	.0144	1.0392	2.1092E-06
5	293.25	SYMM	.00636	3	4	.0082	0	.4652	1.0556	.0005	1.0550	1.7030E-07
6	301.93	SYMM	.29157	1	2	.6043	2	.3421	3.3565	2.3293	.4748	5.0894E-03
7	303.67	SYMM	.00778	3	4	.0306	1	1.0024	1.0404	.0087	1.0313	6.7549E-07
8	318.73	ANTI	.19834	1	2	-.6979	1	-.7181	5.3369	2.8739	1.5659	7.1061E-03
9	346.71	ANTI	.19988	1	3	.6576	2	-.3743	3.0768	2.3838	.3003	4.5098E-03
10	434.31	SYMM	.00501	4	4	.0057	0	.4768	1.0529	.0002	1.0526	1.2207E-07
11	441.78	SYMM	.00522	4	5	-.0256	1	.9644	1.0333	.0063	1.0268	1.9736E-06
12	470.53	ANTI	.03837	2	3	.4241	2	-.4820	2.2756	.8281	1.3435	1.0370E-03
13	502.23	SYMM	.05983	1	1	-.7676	2	.6667	6.3152	2.7696	.7642	2.9842E-03
14	528.78	ANTI	.06963	1	4	-.6679	1	1.1293	3.7192	2.7054	.2363	2.6837E-03
15	555.05	SYMM	.06727	1	4	.6155	3	-.2605	3.0269	2.5538	.1810	2.1738E-03
16	558.43	ANTI	.02146	2	3	.3094	1	1.0023	1.6577	.4811	1.1060	4.3450E-04
17	560.65	ANTI	.02120	1	1	-.2583	3	.5509	2.0101	.5447	1.1155	4.8758E-04
18	572.86	ANTI	.00480	3	3	-.0855	1	.5589	1.2298	.0426	1.1825	3.5093E-05
19	591.88	SYMM	.05297	2	3	.4256	2	.0683	1.7403	1.5269	.0020	1.1752E-03
20	607.50	ANTI	.04502	2	4	.4427	2	.8437	2.8873	1.7891	.8836	1.3539E-03
21	626.01	ANTI	.02170	3	3	-.2932	2	1.5886	1.9538	.6668	1.2366	4.5180E-04
22	632.02	ANTI	.01723	1	1	.2243	2	.6404	1.9975	.5134	1.0730	3.5039E-04
23	636.15	SYMM	.00321	5	4	.0046	0	.4804	1.0520	.0002	1.0518	1.1076E-07
24	641.20	SYMM	.00342	5	5	-.0255	1	.9537	1.0324	.0059	1.0263	3.2791E-06
25	648.70	SYMM	.05034	2	4	.5414	3	-.3184	3.1224	2.2294	.5807	1.4396E-03
26	663.30	ANTI	.00356	4	3	-.0361	1	.6017	1.1704	.0100	1.1594	6.1425E-06
27	716.23	ANTI	.00834	4	4	.1159	2	1.1220	1.3351	.1683	1.1588	8.6624E-05
28	717.33	ANTI	.03011	2	2	-.4201	2	.5542	2.3212	1.1188	.9886	6.1250E-04
29	738.44	ANTI	.03796	1	4	-.5923	2	.8151	3.6328	1.8533	.9385	9.4360E-04
30	761.91	SYMM	.05403	3	4	-.6395	3	.3173	2.9099	2.4133	.3165	1.1383E-03
31	779.76	ANTI	.05189	3	3	-.6081	2	-.2540	2.5922	2.1303	.2651	9.9209E-04
32	811.04	ANTI	.04724	2	4	.4486	2	-.3399	2.1064	1.6951	.2040	7.2187E-04
33	811.63	ANTI	.00273	5	3	-.0250	1	.6102	1.1595	.0058	1.1533	2.4197E-06
34	837.12	SYMM	.03663	1	5	.3014	3	.3333	1.2480	.8936	.2669	3.4380E-04
35	855.38	ANTI	.00732	5	4	.1009	2	1.0652	1.2819	.1286	1.1490	4.7712E-05
36	873.18	ANTI	.05285	3	4	.6547	2	-.4662	3.8691	2.7859	.8762	1.0208E-03
37	873.45	ANTI	.00602	1	5	.2484	3	-.8595	11.2177	.2991	.7172	1.1083E-04
38	884.04	SYMM	.03902	2	5	-.3936	3	-.3903	1.4751	1.0801	.3057	3.7703E-04
39	885.33	SYMM	.04968	3	3	.5217	3	.5075	4.3337	2.8015	1.2407	9.8392E-04
40	892.97	SYMM	.00251	6	4	.0052	0	.4713	1.0521	.0002	1.0518	8.0586E-08
41	896.04	SYMM	.00237	6	5	-.0308	1	.9806	1.0412	.0083	1.0327	2.7028E-06
42	919.55	SYMM	.05680	4	4	.7937	3	-.5543	4.4953	3.3426	.9622	1.0927E-03
43	922.74	ANTI	.05781	1	5	-.9083	3	.3487	5.5922	3.7474	.4295	1.2483E-03
44	972.25	ANTI	.05232	4	3	.4278	3	.0474	1.8224	1.7180	.0014	5.1547E-04
45	980.22	SYMM	.05337	3	5	.5892	3	.4766	2.7194	2.3432	.1992	6.7532E-04
46	987.77	SYMM	.03423	2	1	-.5035	2	.5979	3.5090	1.7442	1.2347	4.8596E-04

ORIGINAL PAGE IS
OF POOR QUALITY

NASA LANGLEY SCALE MODEL FUSELAGE WITH FLOOR
STIFFENED 0.032 IN CYLINDER, STIFFENED FLOOR AT 56.6 DEGREES, RIGID JUNCTION
CAVITY 72 IN LONG, STRUCTURE 71 IN LONG
TRIM PANEL. FIBERGLAS TYPE PF105 2.0 IN THICK + LINING = 1.46 KG/M2

ACOUSTIC MODES

MODE NO	FREQ (HZ)	MODE TYPE	Q	I	LOSS FACTOR	EPSILON
1	.00	SYMM	0	0	0.00000	1.0065E+00
2	93.78	SYMM	1	0	.05503	2.0131E+00
3	187.55	SYMM	2	0	.05754	2.0131E+00
4	195.87	ANTI	0	1	.08249	2.5242E+00
5	217.16	ANTI	1	1	.06720	5.0484E+00
6	236.96	SYMM	0	2	.68589	3.6028E+00
7	254.84	SYMM	1	2	.59372	7.2056E+00
8	271.18	ANTI	2	1	.62861	5.0484E+00
9	281.33	SYMM	3	0	.07028	2.0131E+00
10	302.20	SYMM	2	2	.07907	7.2056E+00
11	342.80	ANTI	3	1	.07342	5.0484E+00
12	346.24	ANTI	0	3	.07789	3.8375E+00
13	358.71	ANTI	1	3	.03124	7.6750E+00
14	367.83	SYMM	3	2	.02288	7.2056E+00
15	369.93	SYMM	0	4	.02796	3.6095E+00
16	375.11	SYMM	4	0	.01706	2.0131E+00
17	381.64	SYMM	1	4	.02674	7.2191E+00
18	393.77	ANTI	2	3	.02592	7.6750E+00
19	414.76	SYMM	2	4	.02264	7.2191E+00
20	423.17	ANTI	4	1	.02059	5.0484E+00
21	433.82	SYMM	0	5	.01932	5.2461E+00
22	443.60	SYMM	4	2	.01573	7.2056E+00
23	443.84	SYMM	1	5	.01880	1.0492E+01
24	446.13	ANTI	3	3	.02020	7.6750E+00
25	464.76	SYMM	3	4	.01388	7.2191E+00
26	468.89	SYMM	5	0	.00838	2.0131E+00
27	472.63	SYMM	2	5	.01276	1.0492E+01
28	498.35	ANTI	0	6	.01503	4.7876E+00
29	507.10	ANTI	1	6	.01470	9.5752E+00
30	508.15	ANTI	5	1	.01098	5.0484E+00
31	510.19	SYMM	0	7	.00975	5.1492E+00
32	510.48	ANTI	4	3	.01187	7.6750E+00
33	517.06	SYMM	3	5	.01066	1.0492E+01
34	518.74	SYMM	1	7	.00961	1.0298E+01
35	525.36	SYMM	5	2	.00862	7.2056E+00
36	526.84	SYMM	4	4	.01080	7.2191E+00
37	532.47	ANTI	2	6	.01333	9.5752E+00
38	543.57	SYMM	2	7	.00875	1.0298E+01
39	562.66	SYMM	6	0	.00541	2.0131E+00
40	570.22	ANTI	0	8	.00770	5.0723E+00
41	572.28	ANTI	3	6	.01069	9.5752E+00
42	573.50	SYMM	4	5	.00804	1.0492E+01
43	577.89	ANTI	1	8	.00764	1.0145E+01
44	582.62	SYMM	3	7	.00707	1.0298E+01
45	582.87	ANTI	5	3	.00844	7.6750E+00
46	590.91	SYMM	0	9	.00990	7.1459E+00
47	595.78	ANTI	6	1	.00741	5.0484E+00
48	597.25	SYMM	5	4	.00779	7.2191E+00
[illegible]	[illegible]	[illegible]	[illegible]	[illegible]	[illegible]	[illegible]

C-3

ORIGINAL PAGE IS
OF POOR QUALITY

NASA LANGLEY SCALE MODEL FUSELAGE WITH FLOOR
STIFFENED 0.032 IN CYLINDER, STIFFENED FLOOR AT 56.6 DEGREES, RIGID JUNCTION
CAVITY 72 IN LONG, STRUCTURE 71 IN LONG
TRIM PANEL. FIBERGLAS TYPE PF105 2.0 IN THICK + LINING = 1.46 KG/M2

MODAL INFORMATION

FREQUENCY (HZ)	STRUCTURE NO OF MODES IN BAND	STRUCTURE FIRST MODE IN BAND	CAVITY NO OF MODES IN BAND	CAVITY FIRST MODE IN BAND
	0		1	
50.0	0	0	0	0
63.0	0	0	0	0
80.0	0	0	0	0
100.0	0	0	1	2
125.0	0	0	0	0
160.0	0	0	0	0
200.0	3	1	3	3
250.0	1	4	3	6
315.0	5	5	4	9
400.0	2	10	12	13
500.0	6	12	14	25
630.0	9	18	37	39
800.0	14	27	64	76
1000.0	18	41	67	140
1250.0	41	59	75	207
1600.0	69	100	86	282
2000.0	36	169	33	368
2500.0	40	205	0	0
3150.0	26	245	0	0
4000.0	19	271	0	0
5000.0	9	290	0	0

ORIGINAL PAGE IS
OF POOR QUALITY

NASA LANGLEY SCALE MODEL FUSELAGE WITH FLOOR
STIFFENED 0.032 IN CYLINDER, STIFFENED FLOOR AT 56.6 DEGREES, RIGID JUNCTION
CAVITY 72 IN LONG, STRUCTURE 71 IN LONG
TRIM PANEL, FIBERGLAS TYPE PF105 2.0 IN THICK + LINING = 1.46 KG/M2

TRIM PANEL MASS/UNIT AREA = 1.4560 KG/M2
INSULATION THICKNESS = .05080 M
TRIM PANEL AREA = 3.57250 M*2
TRIM PANEL LOSS FACTOR = .130000
END CAP INSULATION THICKNESS = .01270 M
END CAP TRIM PANEL MASS/UNIT AREA = 0.0000 KG/M2
END CAP TRIM AREA = .67440 M*2
END CAP TRIM PANEL LOSS FACTOR = 1.000000

BAND AVERAGE

FREQUENCY HZ	TRIM FACTOR DB	LOSS FACTOR ETA R*	ADMITTANCE REAL	ADMITTANCE IMAG	ENDCAP REAL	ADMITTANCE IMAG
50.0	-.860	[illegible]	.73537E-01	.19551E+00	.31166E-03	-.17163E-01
63.0	-1.184	[illegible]	.52484E-01	.15210E+00	.31912E-03	-.18932E-01
80.0	-1.698	[illegible]	.37105E-01	.11099E+00	.31402E-03	-.21279E-01
100.0	-2.482	[illegible]	.26997E-01	.74532E-01	.22239E-03	-.24274E-01
125.0	-4.095	[illegible]	.22010E-01	.32660E-01	.51942E-03	-.29825E-01
160.0	-7.871	[illegible]	.25219E-01	-.27577E-01	.12106E-02	-.38065E-01
200.0	-17.316	.090182	.56526E-01	-.16340E+00	.35326E-03	-.50001E-01
250.0	-4.860	.025640	.66012E+00	.43192E-01	.30656E-02	-.63481E-01
315.0	2.701	.140783	.96060E-01	.23693E+00	.44587E-02	-.80829E-01
400.0	8.455	.005113	.31752E-01	.13697E+00	.28412E-02	-.10749E+00
500.0	12.475	.046292	.19616E-01	.96549E-01	.15785E-02	-.13564E+00
630.0	16.209	.022471	.14392E-01	.71735E-01	.12720E-02	-.17512E+00
800.0	19.992	.030452	.11656E-01	.54583E-01	.11206E-01	-.24023E+00
1000.0	23.229	.038648	.95801E-02	.43536E-01	.28631E-01	-.32123E+00
1250.0	27.827	.033388	.74347E-02	.35532E-01	.73771E-01	-.43522E+00
1600.0	33.918	.029042	.50542E-02	.28074E-01	.13507E+01	-.27651E+00
2000.0	39.134	.015655	.36905E-02	.22382E-01	.31970E+00	-.74743E+00
2500.0	43.725	.013037	.27730E-02	.17840E-01	.66590E+00	-.90756E+00
3150.0	48.095	.012491	.21165E-02	.14140E-01	.10782E+01	-.77303E+00
4000.0	52.158	.010201	.16101E-02	.11127E-01	.12401E+01	-.53681E+00
5000.0	56.197	.008462	.12552E-02	.88941E-02	.12496E+01	-.25157E+00

PROPELLER, 0.76 M DIAMETER, 3 BLADES, 3000 RPM, 0.076 M CLEARANCE

PROPELLER DATA
NUMBER OF BLADES = 3.
PROPELLER RPM = 3000.0
BLADE PASSAGE FREQUENCY (HZ) = 150.0
DISTANCE OF PROPELLER C/L FROM FUSELAGE C/L (M) = .9652
ANGLE BETWEEN VERTICAL AND LINE FROM PROP TO FUSELAGE C/L (DEGREES) = 90.00
DISTANCE OF PROPELLER PLANE FROM FORWARD END OF FUSELAGE (M) = .6620

PROPELLER HARMONIC 1 AT 150.0 HZ

CIRCUM. LOCATION L THETA	AXIAL LOCATION K= 1 Z= .041	2 .130	3 .219	4 .307	5 .396	6 .485	7 .573	8 .662	9 .751	10 .839	11 .928	12 1.017	13 1.105	14 1.194	15 1.283	16 1.371
	PRESSURE AMPLITUDE, DB RE 20 MICRO PA															
19 180.00	85.5	86.9	88.0	89.1	89.8	90.3	90.7	90.9	91.0	90.9	90.6	90.1	89.4	88.5	87.4	86.2
18 170.00	86.4	88.1	89.3	90.5	91.3	91.8	92.1	92.2	92.3	92.2	91.9	91.2	90.3	89.3	87.9	86.5
17 160.00	87.6	89.5	91.1	92.5	93.5	94.0	94.1	94.1	94.1	94.0	93.6	92.7	91.5	90.2	88.5	86.8
16 150.00	88.7	91.1	93.0	94.9	96.1	96.7	96.7	96.5	96.5	96.4	95.8	94.6	93.0	91.3	89.2	87.0
15 140.00	90.3	93.3	95.8	98.3	100.1	101.0	100.8	100.3	100.4	100.4	99.4	97.7	95.3	93.0	90.2	87.5
14 130.00	92.7	96.4	99.6	102.8	105.4	106.8	106.5	105.4	105.8	105.9	104.4	101.9	98.7	95.7	92.3	89.0
13 120.00	93.9	98.3	102.2	106.3	110.0	112.3	112.2	110.1	111.5	111.3	108.8	105.2	101.1	97.3	93.2	89.3
12 110.00	94.2	99.1	103.6	108.7	113.5	117.2	118.0	114.5	117.2	116.0	112.1	107.4	102.4	98.0	93.3	88.9
11 100.00	93.9	99.3	104.3	110.0	115.7	120.8	123.3	118.2	122.4	119.5	114.3	108.6	102.9	98.0	92.9	88.1
10 90.00	93.8	99.3	104.4	110.2	116.1	121.4	124.3	118.9	123.4	120.1	114.6	108.8	103.0	98.0	92.8	88.0
9 80.00	93.9	99.3	104.3	110.0	115.7	120.8	123.3	118.2	122.4	119.5	114.3	108.6	102.9	98.0	92.9	88.1
8 70.00	94.2	99.1	103.6	108.7	113.5	117.2	118.0	114.5	117.2	116.0	112.1	107.4	102.4	98.0	93.3	88.9
7 60.00	93.9	98.3	102.2	106.3	110.0	112.3	112.2	110.1	111.5	111.3	108.8	105.2	101.1	97.3	93.2	89.3
6 50.00	92.7	96.4	99.6	102.8	105.4	106.8	106.5	105.4	105.8	105.9	104.4	101.9	98.7	95.7	92.3	89.0
5 40.00	90.3	93.3	95.8	98.3	100.1	101.0	100.8	100.3	100.4	100.4	99.4	97.7	95.3	93.0	90.2	87.5
4 30.00	88.7	91.1	93.0	94.9	96.1	96.7	96.7	96.5	96.5	96.4	95.8	94.6	93.0	91.3	89.2	87.0
3 20.00	87.6	89.5	91.1	92.5	93.5	94.0	94.1	94.1	94.1	94.0	93.6	92.7	91.5	90.2	88.5	86.8
2 10.00	86.4	88.1	89.3	90.5	91.3	91.8	92.1	92.2	92.3	92.2	91.9	91.2	90.3	89.3	87.9	86.5
1 0.00	85.5	86.9	88.0	89.1	89.8	90.3	90.7	90.9	91.0	90.9	90.6	90.1	89.4	88.5	87.4	86.2
	PHASE (DEGREES)															
19 180.00	172.1	170.9	170.8	172.3	175.6	-179.1	-172.1	-164.0	-155.7	-148.2	-141.9	-136.8	-132.6	-129.2	-125.8	-122.3
18 170.00	159.5	158.0	157.8	159.2	162.7	168.6	177.0	-173.1	-163.0	-154.2	-147.3	-142.1	-138.0	-135.1	-132.1	-129.1
17 160.00	146.2	144.4	143.9	145.1	148.5	155.0	165.1	177.9	-169.1	-158.4	-150.8	-145.7	-142.2	-139.8	-137.6	-135.3
16 150.00	137.2	135.0	134.2	134.8	137.9	144.6	156.5	173.5	-169.2	-156.3	-148.3	-143.8	-141.2	-139.7	-138.3	-136.9
15 140.00	132.2	129.7	128.5	128.4	130.7	137.0	150.5	173.1	-163.5	-148.6	-141.1	-137.7	-136.2	-135.7	-135.4	-134.9
14 130.00	132.2	129.5	127.8	127.1	128.3	133.4	147.4	177.7	-150.6	-135.1	-129.2	-127.2	-126.9	-127.4	-128.0	-128.5
13 120.00	141.1	138.2	136.2	134.8	134.8	137.9	150.3	-168.6	-125.9	-112.6	-109.1	-108.8	-109.7	-111.0	-112.4	-113.7
12 110.00	156.6	153.6	151.3	149.4	148.4	149.5	158.4	-148.2	-95.6	-86.9	-85.8	-86.7	-88.3	-90.1	-92.1	-93.9
11 100.00	179.0	175.9	173.5	171.4	169.8	169.5	174.3	-120.4	-62.4	-58.0	-58.5	-60.1	-62.2	-64.2	-66.6	-68.7
10 90.00	-148.1	-151.2	-153.6	-155.8	-157.4	-158.0	-153.9	-86.1	-27.6	-24.1	-24.8	-26.5	-28.7	-30.8	-33.1	-35.3
9 80.00	-116.5	-119.6	-122.0	-124.2	-125.8	-126.1	-121.2	-55.9	2.1	6.4	6.0	4.4	2.3	.2	-2.1	-4.2
8 70.00	-85.7	-88.8	-91.1	-93.0	-93.9	-92.9	-84.0	-30.6	22.0	30.7	31.9	31.0	29.3	27.5	25.5	23.7
7 60.00	-64.0	-67.0	-69.0	-70.4	-70.4	-67.3	-54.9	-13.7	28.9	42.2	45.7	46.0	45.1	43.9	42.4	41.2
6 50.00	-50.5	-53.2	-54.9	-55.6	-54.4	-49.3	-35.3	-5.0	26.7	42.2	48.1	50.1	50.3	49.9	49.3	48.8
5 40.00	-39.7	-42.2	-43.4	-43.4	-41.2	-34.9	-21.4	1.2	24.7	39.5	47.0	50.5	51.9	52.5	52.8	53.2
4 30.00	-32.4	-34.5	-35.4	-34.7	-31.7	-25.0	-13.0	3.9	21.3	34.2	42.1	45.7	49.3	50.8	52.1	53.5
3 20.00	-27.3	-29.1	-29.5	-28.4	-24.9	-18.4	-8.4	4.5	17.5	28.2	35.8	40.9	44.4	46.7	49.0	51.2
2 10.00	-22.3	-23.8	-24.0	-22.5	-19.1	-13.2	-6.8	5.1	15.2	[illegible]	[illegible]	[illegible]	[illegible]	[illegible]	[illegible]	[illegible]

PROPELLER, 0.76 M DIAMETER, 3 BLADES, 3000 RPM, 0.076 M CLEARANCE

ORIGINAL PAGE IS OF POOR QUALITY

PROPELLER DATA
NUMBER OF BLADES = 3.
PROPELLER RPM = 3000.0
BLADE PASSAGE FREQUENCY (HZ) = 150.0
DISTANCE OF PROPELLER C/L FROM FUSELAGE C/L (M) = .9652
ANGLE BETWEEN VERTICAL AND LINE FROM PROP TO FUSELAGE C/L (DEGREES) = 90.00
DISTANCE OF PROPELLER PLANE FROM FORWARD END OF FUSELAGE (M) = .6620

PROPELLER HARMONIC 2 AT 300.0 HZ

CIRCUM. LOCATION		AXIAL LOCATION															
L	THETA	K= 1	2	3	4	5	6	7	8	9	10	11	12	13	14	15	16
		Z= .041	.130	.219	.307	.396	.485	.573	.662	.751	.839	.928	1.017	1.105	1.194	1.283	1.371
		PRESSURE AMPLITUDE, DB RE 20 MICRO PA															
19	180.00	59.6	62.0	63.9	65.8	67.3	68.2	68.8	68.9	68.8	68.2	67.4	66.1	64.5	62.9	60.8	58.6
18	170.00	60.1	63.0	65.2	67.4	69.1	70.2	70.7	70.8	70.5	69.8	68.7	67.1	65.2	63.2	60.8	58.2
17	160.00	60.8	64.2	67.0	69.7	71.8	73.1	73.6	73.5	73.0	72.1	70.7	68.7	66.2	63.7	60.7	57.7
16	150.00	61.4	65.6	69.1	72.6	75.3	77.0	77.5	77.1	76.5	75.4	73.5	70.8	67.5	64.3	60.6	56.8
15	140.00	62.2	67.4	71.9	76.6	80.4	82.8	83.5	82.8	82.0	80.7	78.1	74.4	69.9	65.6	60.8	56.1
14	130.00	63.8	70.1	75.6	81.6	86.8	90.3	91.3	90.1	89.5	88.0	84.3	79.2	73.3	67.9	61.9	56.3
13	120.00	63.8	71.2	78.0	85.5	92.4	97.8	99.8	97.7	97.7	95.4	89.9	82.9	75.4	68.8	61.6	54.9
12	110.00	62.7	71.1	78.9	87.9	96.7	104.2	108.1	104.9	106.0	101.7	94.0	85.2	76.3	68.5	60.3	52.7
11	100.00	61.1	70.2	78.8	89.0	99.2	108.8	115.2	111.1	113.1	106.2	96.5	86.2	76.1	67.5	58.5	50.4
10	90.00	60.7	70.0	78.8	89.1	99.6	109.5	116.6	112.3	114.5	106.9	96.8	86.3	76.0	67.3	58.2	49.9
9	80.00	61.1	70.2	78.8	89.0	99.2	108.8	115.2	111.1	113.1	106.2	96.5	86.2	76.1	67.5	58.5	50.4
8	70.00	62.7	71.1	78.9	87.9	96.7	104.2	108.1	104.9	106.0	101.7	94.0	85.2	76.3	68.5	60.3	52.7
7	60.00	63.8	71.2	78.0	85.5	92.4	97.8	99.8	97.7	97.7	95.4	89.9	82.9	75.4	68.8	61.6	54.9
6	50.00	63.8	70.1	75.6	81.6	86.8	90.3	91.3	90.1	89.5	88.0	84.3	79.2	73.3	67.9	61.9	56.3
5	40.00	62.2	67.4	71.9	76.6	80.4	82.8	83.5	82.8	82.0	80.7	78.1	74.4	69.9	65.6	60.8	56.1
4	30.00	61.4	65.6	69.1	72.6	75.3	77.0	77.5	77.1	76.5	75.4	73.5	70.8	67.5	64.3	60.6	56.8
3	20.00	60.8	64.2	67.0	69.7	71.8	73.1	73.6	73.5	73.0	72.1	70.7	68.7	66.2	63.7	60.7	57.7
2	10.00	60.1	63.0	65.2	67.4	69.1	70.2	70.7	70.8	70.5	69.8	68.7	67.1	65.2	63.2	60.8	58.2
1	0.00	59.6	62.0	63.9	65.8	67.3	68.2	68.8	68.9	68.8	68.2	67.4	66.1	64.5	62.9	60.8	58.6
		PHASE (DEGREES)															
19	180.00	103.7	98.3	95.1	93.3	93.7	96.5	101.4	108.1	115.5	122.9	129.5	135.4	140.9	145.7	151.6	158.0
18	170.00	82.5	77.2	74.1	72.5	73.3	76.6	82.8	91.3	100.7	109.4	116.6	122.3	127.2	131.3	136.2	141.8
17	160.00	60.7	55.7	52.7	51.2	52.2	56.3	64.2	75.5	88.2	99.1	106.9	112.1	115.9	118.7	122.1	126.4
16	150.00	47.9	43.0	40.2	38.7	39.7	44.1	53.8	69.3	86.9	100.6	108.7	112.9	115.0	116.2	117.8	120.2
15	140.00	42.8	38.2	35.4	33.7	34.3	38.6	49.6	70.7	95.5	111.6	119.1	121.7	122.1	121.7	121.4	121.9
14	130.00	47.3	42.9	40.1	38.1	37.9	41.2	52.6	81.2	115.6	132.4	137.9	138.8	137.7	136.0	134.1	132.9
13	120.00	69.2	65.0	62.0	59.6	58.5	60.1	70.1	108.8	155.6	169.4	172.1	171.2	169.0	166.4	163.3	160.8
12	110.00	103.1	98.9	95.9	93.1	91.2	91.2	97.9	147.9	-154.4	-146.0	-145.9	-147.9	-150.8	-153.9	-157.5	-160.8
11	100.00	149.7	145.6	142.5	139.5	137.2	135.9	139.2	-159.7	-96.5	-92.9	-94.3	-97.0	-100.3	-103.5	-107.4	-111.2
10	90.00	-144.2	-148.3	-151.4	-154.4	-156.8	-158.3	-155.7	-92.1	-28.5	-25.8	-27.4	-30.2	-33.5	-36.8	-40.7	-44.5
9	80.00	-91.4	-85.5	-88.6	-91.5	-93.9	-95.2	-91.9	-30.7	32.5	36.0	34.6	31.9	28.7	25.4	21.5	17.8
8	70.00	-21.7	-25.9	-28.9	-31.7	-33.6	-33.6	-26.8	23.2	80.8	89.2	89.4	87.4	84.4	81.4	77.7	74.4
7	60.00	18.9	14.6	11.7	9.3	8.2	9.8	19.8	58.4	105.3	119.1	121.7	120.9	118.7	116.0	113.0	110.5
6	50.00	41.9	37.5	34.6	32.6	32.5	35.8	47.2	75.7	110.2	126.9	132.4	133.3	132.2	130.5	128.6	127.5
5	40.00	59.1	54.5	51.6	50.0	50.6	54.8	65.8	86.9	111.7	127.9	135.3	138.0	138.3	138.0	137.6	139.2
4	30.00	68.8	63.9	61.0	59.6	60.6	65.0	74.7	90.2	107.8	121.5	129.6	133.8	135.9	137.1	138.7	141.1
3	20.00	73.9	68.8	65.8	64.4	65.4	69.5	77.3	88.7	101.3	112.2	120.1	125.3	129.0	131.9	135.3	139.5
2	10.00	78.9	73.6	70.5	68.9	69.7	73.1	79.3	87.7	97.1	105.8	113.0	118.8	123.6	127.7	132.7	138.3
1	0.00	76.8	71.4	69.2	66.4	66.8	69.6	74.5	81.2	88.6	96.0	102.6	108.5	114.0	118.9	124.7	131.1

PROPELLER, 0.76 M DIAMETER, 3 BLADES, 3000 RPM, 0.076 M CLEARANCE

PROPELLER DATA
NUMBER OF BLADES = 3.
PROPELLER RPM = 3000.0
BLADE PASSAGE FREQUENCY (HZ) = 150.0
DISTANCE OF PROPELLER C/L FROM FUSELAGE C/L (M) = .9652
ANGLE BETWEEN VERTICAL AND LINE FROM PROP TO FUSELAGE C/L (DEGREES) = 90.00
DISTANCE OF PROPELLER PLANE FROM FORWARD END OF FUSELAGE (M) = .6620

PROPELLER HARMONIC 3 AT 450.0 HZ

CIRCUM. LOCATION		AXIAL LOCATION															
L	THETA	K= 1 Z= .041	2 .130	3 .219	4 .307	5 .396	6 .485	7 .573	8 .662	9 .751	10 .839	11 .928	12 1.017	13 1.105	14 1.194	15 1.283	16 1.371
		PRESSURE AMPLITUDE, DB RE 20 MICRO PA															
19	180.00	33.9	37.3	40.1	42.8	44.9	46.3	47.1	47.2	46.8	45.8	44.3	42.4	40.0	37.6	34.7	31.6
18	170.00	34.0	38.0	41.3	44.4	47.0	48.7	49.5	49.5	48.8	47.5	45.6	43.2	40.3	37.5	34.0	30.5
17	160.00	34.2	39.0	43.0	47.0	50.2	52.3	53.2	53.0	52.0	50.3	47.9	44.7	41.0	37.3	33.1	28.8
16	150.00	34.1	40.1	45.1	50.3	54.5	57.4	58.5	58.1	56.7	54.5	51.3	47.1	42.1	37.4	32.0	26.7
15	140.00	34.3	41.6	48.0	54.8	60.6	64.7	66.3	65.6	63.9	61.3	57.0	51.2	44.5	38.2	31.3	24.7
14	130.00	34.8	43.7	51.7	60.4	68.1	73.9	76.4	75.2	73.5	70.4	64.4	56.6	48.0	40.1	31.6	23.6
13	120.00	33.2	43.9	53.7	64.6	74.9	83.3	87.4	85.6	84.3	79.7	71.2	60.9	50.1	40.6	30.6	21.6
12	110.00	30.4	42.7	54.0	67.0	79.8	91.2	98.2	95.6	95.0	87.5	76.0	63.2	50.3	39.4	28.1	18.2
11	100.00	28.6	41.2	53.3	67.8	82.5	96.6	107.2	104.3	103.9	92.8	78.6	63.7	49.1	36.6	23.1	10.5
10	90.00	27.9	40.8	53.2	67.8	82.9	97.5	108.8	105.9	105.5	93.7	79.0	63.8	49.2	36.8	24.0	12.6
9	80.00	28.6	41.2	53.3	67.8	82.5	96.6	107.2	104.3	103.9	92.8	78.6	63.7	49.1	36.6	23.1	10.5
8	70.00	30.4	42.7	54.0	67.0	79.8	91.2	98.2	95.6	95.0	87.5	76.0	63.2	50.3	39.4	28.1	18.2
7	60.00	33.2	43.9	53.7	64.6	74.9	83.3	87.4	85.6	84.3	79.7	71.2	60.9	50.1	40.6	30.6	21.6
6	50.00	34.8	43.7	51.7	60.4	68.1	73.9	76.4	75.2	73.5	70.4	64.4	56.6	48.0	40.1	31.6	23.6
5	40.00	34.3	41.6	48.0	54.8	60.6	64.7	66.3	65.6	63.9	61.3	57.0	51.2	44.5	38.2	31.3	24.7
4	30.00	34.1	40.1	45.1	50.3	54.5	57.4	58.5	58.1	56.7	54.5	51.3	47.1	42.1	37.4	32.0	26.7
3	20.00	34.2	39.0	43.0	47.0	50.2	52.3	53.2	53.0	52.0	50.3	47.9	44.7	41.0	37.3	33.1	28.8
2	10.00	34.0	38.0	41.3	44.4	47.0	48.7	49.5	49.5	48.8	47.5	45.6	43.2	40.3	37.5	34.0	30.5
1	0.00	33.9	37.3	40.1	42.8	44.9	46.3	47.1	47.2	46.8	45.8	44.3	42.4	40.0	37.6	34.7	31.6
		PHASE (DEGREES)															
19	180.00	35.4	25.4	18.8	13.7	11.4	11.7	14.6	19.8	26.5	33.6	40.6	47.4	54.3	61.0	69.5	79.3
18	170.00	4.4	-4.7	-10.7	-15.0	-16.7	-15.5	-11.2	-4.3	4.2	12.8	20.2	26.5	32.4	38.0	45.3	54.2
17	160.00	-26.7	-34.6	-39.7	-43.1	-44.0	-41.8	-35.9	-26.1	-14.2	-3.4	4.6	9.9	14.0	17.5	22.6	29.7
16	150.00	-43.7	-50.3	-54.5	-57.3	-57.8	-55.0	-47.3	-33.5	-16.2	-2.0	6.3	10.1	11.7	12.8	15.0	19.5
15	140.00	-48.9	-54.3	-57.9	-60.4	-60.9	-58.2	-49.3	-30.1	-4.9	12.4	19.9	22.0	21.6	20.6	20.2	22.0
14	130.00	-40.0	-44.5	-47.6	-50.2	-51.2	-49.3	-40.1	-14.0	21.9	39.9	45.3	45.5	43.7	41.5	39.6	39.9
13	120.00	-4.7	-8.9	-12.0	-14.9	-16.8	-16.3	-8.5	27.0	76.7	91.0	93.1	91.4	88.3	85.0	81.7	80.2
12	110.00	52.3	45.7	41.5	37.7	34.8	33.6	38.7	84.6	146.3	154.4	153.6	150.4	145.7	140.4	133.1	125.4
11	100.00	126.3	118.6	113.4	108.8	105.2	102.9	104.8	161.4	-130.9	-128.0	-130.4	-134.1	-138.9	-144.4	-153.7	-170.3
10	90.00	-146.1	-147.1	-149.4	-152.6	-155.8	-158.1	-156.7	-97.7	-29.6	-27.6	-30.0	-33.4	-36.8	-39.0	-39.0	-33.5
9	80.00	-40.3	-48.0	-53.2	-57.8	-61.4	-63.7	-61.8	-5.2	62.5	65.4	63.0	59.3	54.5	49.0	39.7	23.1
8	70.00	45.2	38.6	34.3	30.5	27.7	26.5	31.5	77.5	139.1	147.3	146.5	143.2	138.5	133.2	126.0	118.2
7	60.00	99.8	95.7	92.5	89.6	87.7	88.2	96.1	131.5	-178.8	-164.4	-162.4	-164.0	-167.2	-170.5	-173.9	-175.3
6	50.00	131.8	127.4	124.2	121.7	120.6	122.6	131.8	157.9	-166.2	-148.3	-142.9	-142.6	-144.5	-146.7	-148.6	-148.3
5	40.00	155.5	150.1	146.5	144.0	143.5	146.2	155.1	174.3	-160.5	-143.3	-135.7	-133.6	-134.0	-135.1	-135.4	-133.6
4	30.00	167.6	161.0	156.8	154.0	153.6	156.4	164.0	177.8	-164.9	-150.7	-142.4	-138.6	-136.9	-135.9	-133.7	-129.2
3	20.00	173.0	165.1	160.1	156.6	155.7	157.9	163.8	173.6	-174.5	-163.6	-155.7	-150.3	-146.3	-142.7	-137.6	-130.6
2	10.00	179.1	169.9	163.9	159.6	158.0	159.2	163.4	170.4	178.9	-172.6	-165.2	-158.8	-152.9	-147.3	-140.0	-131.1
1	0.00	175.0	165.1	158.6	153.6	151.0	151.3	156.3	159.5	166.1	173.2	-179.8	-173.0	-166.0	-159.4	[illegible]	[illegible]

NASA LANGLEY SCALE MODEL FUSELAGE WITH FLOOR
STIFFENED 0.032 IN CYLINDER, STIFFENED FLOOR AT 56.6 DEGREES, RIGID JUNCTION
CAVITY 72 IN LONG, STRUCTURE 71 IN LONG
TRIM PANEL. FIBERGLAS TYPE PF105 2.0 IN THICK + LINING = 1.46 KG/M2

PROPELLER, 0.76 M DIAMETER, 3 BLADES, 3000 RPM, 0.076 M CLEARANCE

TONE TRANSMISSION AT FREQUENCIES AT OR ABOVE 1250.0 HZ IS WITH HIGH FREQUENCY FORMULATION

TONE TRANSMISSION FOR PROPELLER HARMONICS

HARMONIC NO	HARMONIC FREQ	INTERIOR MEAN SQ. PRESSURE PA**2	INTERIOR MEAN SQ. PRESSURE DB RE 20 MICRO PA
1	150.0	8.5311E-04	63.29
2	300.0	1.6590E-03	66.18
3	450.0	3.5909E-04	59.53
4	600.0	1.7311E-05	46.36
5	750.0	6.1699E-07	31.88
6	900.0	2.1353E-07	27.27
7	1050.0	1.4964E-07	25.73
8	1200.0	1.3519E-07	25.29
9	1350.0	2.3912E-09	7.77
10	1500.0	4.3747E-11	-9.61

```
+ ACOUSTIC MODES:                                           +
+ Q = NO. OF AXIAL HALF-WAVES                               +
+ I = ASSIGNED ORDER OF 2-DIMENSIONAL MODAL PATTERN         +
+     IN CYLINDER CROSS-SECTION                             +
+                                                           +
+ STRUCTURAL MODES:                                         +
+ M = NO. OF AXIAL HALF-WAVES                               +
+ N = NO. OF CIRCUMFERENTIAL WAVES AROUND FUSELAGE FOR      +
+     LARGEST SHELL GEN. COORDINATES FOR THIS MODE          +
+++++++++++++++++++++++++++++++++++++++++++++++++++++++++++++
```

TONE TRANSMISSION FOR FREQUENCY 150.0 HZ, HARMONIC NO. 1

ACOUSTIC NO	ACOUSTIC FREQ	MODE Q	MODE I	STRUCTURAL NO	STRUCTURAL FREQ	MODE M	MODE N	ETA R#	M.S.PRESSURE (PA**2)
2	93.8	1	0	25	648.7	2	4	.00000	2.7523E-05
3	187.6	2	0	6	301.9	1	2	.00000	3.6774E-05
2	93.8	1	0	4	231.0	2	4	.00025	6.5000E-05
3	187.6	2	0	2	208.2	1	2	.00704	2.1515E-04
3	187.6	2	0	1	188.5	1	2	.10790	2.6273E-04

TOTAL = 63.29 DB 8.5311E-04

TONE TRANSMISSION FOR FREQUENCY 300.0 HZ, HARMONIC NO. 2

ACOUSTIC NO	ACOUSTIC FREQ	MODE Q	MODE I	STRUCTURAL NO	STRUCTURAL FREQ	MODE M	MODE N	ETA R#	M.S.PRESSURE (PA**2)
16	375.1	4	0	7	303.7	3	4	.00043	1.1221E-04
10	302.2	2	2	2	208.2	1	2	.00156	1.1944E-04
3	187.6	2	0	7	303.7	3	4	.00043	1.5914E-04
10	302.2	2	2	7	303.7	3	4	.15476	3.4573E-04
10	302.2	2	2	6	301.9	1	2	.01324	4.1730E-04

TOTAL = 66.18 DB 1.6590E-03

TONE TRANSMISSION FOR FREQUENCY 450.0 HZ, HARMONIC NO. 3

ACOUSTIC NO	ACOUSTIC FREQ	MODE Q	MODE I	STRUCTURAL NO	STRUCTURAL FREQ	MODE M	MODE N	ETA R#	M.S.PRESSURE (PA**2)
23	443.8	1	5	11	441.8	4	5	.00738	5.5951E-06
23	443.8	1	5	19	591.9	2	3	.00034	5.6903E-06
26	468.9	5	0	11	441.8	4	5	.00128	1.2673E-05
25	464.8	3	4	11	441.8	4	5	.00489	3.5622E-05
24	446.1	3	3	12	470.5	2	3	.00586	2.6455E-04

TOTAL = 59.53 DB 3.5909E-04

TONE TRANSMISSION FOR FREQUENCY 600.0 HZ, HARMONIC NO. 4

ACOUSTIC NO	ACOUSTIC FREQ	MODE Q	MODE I	STRUCTURAL NO	STRUCTURAL FREQ	MODE M	MODE N	ETA R#	M.S.PRESSURE (PA**2)

ORIGINAL PAGE IS OF POOR QUALITY

PROPELLER, 0.76 M DIAMETER, 3 BLADES, 4000 RPM, 0.076 M CLEARANCE

PROPELLER DATA
NUMBER OF BLADES = 3.
PROPELLER RPM = 4000.0
BLADE PASSAGE FREQUENCY (HZ) = 200.0
DISTANCE OF PROPELLER C/L FROM FUSELAGE C/L (M) = .9652
ANGLE BETWEEN VERTICAL AND LINE FROM PROP TO FUSELAGE C/L (DEGREES) = 90.00
DISTANCE OF PROPELLER PLANE FROM FORWARD END OF FUSELAGE (M) = .6620

PROPELLER HARMONIC 1 AT 200.0 HZ

PRESSURE AMPLITUDE, DB RE 20 MICRO PA

CIRCUM. LOCATION L	THETA	K= 1	2	3	4	5	6	7	8	9	10	11	12	13	14	15	16
	Z=	.041	.130	.219	.307	.396	.485	.573	.662	.751	.839	.928	1.017	1.105	1.194	1.283	1.371
19	180.00	94.6	95.9	97.0	98.0	98.9	99.6	100.3	100.9	101.4	101.7	101.7	101.4	100.9	100.2	99.3	98.3
18	170.00	95.4	96.8	98.0	99.1	100.0	100.8	101.4	101.9	102.4	102.6	102.6	102.2	101.5	100.7	99.6	98.4
17	160.00	96.3	98.1	99.5	100.8	101.7	102.4	102.9	103.4	103.8	104.0	103.8	103.2	102.3	101.3	99.9	98.4
16	150.00	97.2	99.4	101.1	102.7	103.9	104.6	104.8	105.1	105.5	105.7	105.3	104.5	103.2	101.8	100.1	98.3
15	140.00	98.6	101.3	103.6	105.8	107.4	108.3	108.3	108.3	108.7	108.8	108.2	106.8	104.9	103.0	100.7	98.5
14	130.00	100.8	104.1	107.0	109.9	112.2	113.5	113.3	112.7	113.3	113.5	112.3	110.2	107.6	105.1	102.3	99.5
13	120.00	101.8	105.7	109.3	113.1	116.4	118.6	118.4	116.8	118.1	118.0	115.8	112.7	109.2	106.1	102.7	99.5
12	110.00	101.9	106.4	110.5	115.2	119.6	123.1	123.8	120.6	123.2	122.2	118.7	114.4	110.1	106.3	102.3	98.7
11	100.00	101.5	106.4	111.0	116.4	121.7	126.5	128.8	124.0	128.0	125.3	120.5	115.3	110.3	106.0	101.6	97.7
10	90.00	101.4	106.4	111.1	116.6	122.1	127.1	129.7	124.7	129.0	125.9	120.8	115.5	110.3	106.0	101.5	97.5
9	80.00	101.5	106.4	111.0	116.4	121.7	126.5	128.8	124.0	128.0	125.3	120.5	115.3	110.3	106.0	101.6	97.7
8	70.00	101.9	106.4	110.5	115.2	119.6	123.1	123.8	120.6	123.2	122.2	118.7	114.4	110.1	106.3	102.3	98.7
7	60.00	101.8	105.7	109.3	113.1	116.4	118.6	118.4	116.8	118.1	118.0	115.8	112.7	109.2	106.1	102.7	99.5
6	50.00	100.8	104.1	107.0	109.9	112.2	113.5	113.3	112.7	113.3	113.5	112.3	110.2	107.6	105.1	102.3	99.5
5	40.00	98.6	101.3	103.6	105.8	107.4	108.3	108.3	108.3	108.7	108.8	108.2	106.8	104.9	103.0	100.7	98.5
4	30.00	97.2	99.4	101.1	102.7	103.9	104.6	104.8	105.1	105.5	105.7	105.3	104.5	103.2	101.8	100.1	98.3
3	20.00	96.3	98.1	99.5	100.8	101.7	102.4	102.9	103.4	103.8	104.0	103.8	103.2	102.3	101.3	99.9	98.4
2	10.00	95.4	96.8	98.0	99.1	100.0	100.8	101.4	101.9	102.4	102.6	102.6	102.2	101.5	100.7	99.6	98.4
1	0.00	94.6	95.9	97.0	98.0	98.9	99.6	100.3	100.9	101.4	101.7	101.7	101.4	100.9	100.2	99.3	98.3

PHASE (DEGREES)

L	THETA	1	2	3	4	5	6	7	8	9	10	11	12	13	14	15	16
19	180.00	-153.5	-156.2	-157.2	-156.3	-153.3	-148.3	-141.8	-134.5	-127.3	-120.5	-114.3	-108.5	-102.8	-97.7	-91.6	-85.1
18	170.00	-170.6	-173.8	-175.0	-174.4	-171.3	-165.6	-157.7	-148.8	-140.1	-132.3	-125.6	-119.7	-114.1	-109.1	-103.2	-96.9
17	160.00	171.2	167.5	165.7	165.8	168.8	175.1	-175.3	-163.7	-152.6	-143.3	-136.1	-130.2	-124.9	-120.3	-114.8	-108.9
16	150.00	157.8	153.4	151.0	150.4	152.8	159.4	171.0	-173.6	-158.9	-147.8	-140.2	-134.7	-130.2	-126.2	-121.5	-116.2
15	140.00	149.1	144.2	141.3	139.8	141.2	147.2	160.6	-178.7	-158.6	-145.6	-138.3	-133.8	-130.4	-127.5	-123.7	-119.2
14	130.00	146.0	140.9	137.5	135.2	135.4	140.0	154.0	-177.7	-149.8	-135.7	-129.7	-126.9	-125.0	-123.2	-120.6	-117.0
13	120.00	152.5	147.2	143.4	140.4	139.3	141.8	154.3	-166.4	-127.5	-114.8	-111.3	-110.5	-110.3	-109.8	-108.4	-105.8
12	110.00	166.3	160.9	157.0	153.6	151.6	152.0	160.7	-147.4	-97.6	-89.2	-88.2	-89.0	-90.1	-90.6	-90.2	-88.4
11	100.00	-172.3	-177.7	170.4	174.8	172.2	171.1	175.7	-120.3	-64.1	-60.1	-60.9	-62.7	-64.5	-65.6	-65.8	-64.7
10	90.00	-139.5	-144.9	-148.9	-152.5	-155.2	-156.4	-152.7	-86.1	-29.3	-26.1	-27.2	-29.1	-31.0	-32.2	-32.6	-31.6
9	80.00	-107.8	-113.2	-117.2	-120.7	-123.4	-124.4	-119.9	-55.8	.4	4.4	3.5	1.8	.0	-1.1	-1.4	-.2
8	70.00	-76.0	-81.4	-85.4	-88.7	-90.8	-90.4	-81.7	-29.8	20.0	28.5	29.4	28.6	27.5	27.1	27.4	29.2
7	60.00	-52.6	-58.0	-61.7	-64.7	-65.8	-63.3	-50.9	-11.6	27.4	40.1	43.6	44.4	44.6	45.1	46.5	49.0
6	50.00	-36.7	-41.8	-45.3	-47.5	-47.3	-42.7	-28.7	-.4	27.5	41.6	47.6	50.4	52.3	54.1	56.7	60.3
5	40.00	-22.8	-27.6	-30.6	-32.1	-30.7	-24.6	-11.3	9.5	29.6	42.5	49.9	54.3	57.7	60.6	64.4	69.0
4	30.00	-11.8	-16.1	-18.5	-19.1	-16.8	-10.2	1.4	16.8	31.6	42.7	50.3	55.7	60.3	64.2	68.9	74.3
3	20.00	-2.2	-5.9	-7.7	-7.6	-4.7	1.7	11.3	22.9	34.0	43.3	50.5	56.4	61.7	66.3	71.7	77.7
2	10.00	7.6	4.5	3.2	3.8	6.9	12.6	20.5	29.4	38.1	45.9	52.6	58.5	64.1	69.1	75.6	81.3
1	0.00	13.0	10.3	9.4	10.3	13.2	18.3	24.8	32.1	39.3	46.1	52.2	58.0	63.7	68.8	74.9	81.4

ORIGINAL PAGE IS
OF POOR QUALITY

PROPELLER, 0.76 M DIAMETER, 3 BLADES, 4000 RPM, 0.076 M CLEARANCE

PROPELLER DATA
NUMBER OF BLADES = 3.
PROPELLER RPM = 4000.0
BLADE PASSAGE FREQUENCY (HZ) = 200.0
DISTANCE OF PROPELLER C/L FROM FUSELAGE C/L (M) = .9652
ANGLE BETWEEN VERTICAL AND LINE FROM PROP TO FUSELAGE C/L (DEGREES) = 90.00
DISTANCE OF PROPELLER PLANE FROM FORWARD END OF FUSELAGE (M) = .6620

PROPELLER HARMONIC 2 AT 400.0 HZ

AXIAL LOCATION

PRESSURE AMPLITUDE, DB RE 20 MICRO PA

CIRCUM. LOCATION L	THETA	K= 1 Z= .041	2 .130	3 .219	4 .307	5 .396	6 .465	7 .573	8 .662	9 .751	10 .839	11 .928	12 1.017	13 1.105	14 1.194	15 1.283	16 1.371
19	180.00	75.5	77.6	79.3	81.0	82.5	83.7	84.6	85.3	85.6	85.6	85.1	84.3	83.1	81.8	80.0	78.1
18	170.00	75.7	78.2	80.1	82.1	83.6	84.9	85.8	86.4	86.6	86.5	85.9	84.8	83.4	81.8	79.8	77.6
17	160.00	75.9	78.6	81.2	83.5	85.3	86.6	87.5	88.0	88.1	87.8	86.9	85.5	83.6	81.7	79.3	76.7
16	150.00	75.9	79.4	82.3	85.2	87.5	89.1	89.8	90.1	90.0	89.4	88.2	86.3	83.8	81.4	78.4	75.4
15	140.00	76.1	80.5	84.2	88.1	91.3	93.3	94.1	93.9	93.6	92.7	90.8	88.0	84.7	81.5	77.8	74.1
14	130.00	77.0	82.3	86.9	92.0	96.4	99.4	100.3	99.6	99.1	97.9	95.0	90.9	86.5	82.4	77.8	73.5
13	120.00	76.3	82.6	88.4	94.9	100.9	105.7	107.4	105.6	105.6	103.6	98.9	93.1	87.0	81.8	76.4	71.3
12	110.00	74.6	81.8	88.6	96.5	104.4	111.3	114.7	111.7	112.7	108.9	102.0	94.3	86.7	80.5	74.1	68.3
11	100.00	72.6	80.5	88.1	97.2	106.5	115.4	121.3	117.3	119.3	112.9	103.9	94.7	85.9	78.8	71.7	65.4
10	90.00	72.2	80.2	87.9	97.2	106.8	116.1	122.6	118.4	120.5	113.5	104.2	94.7	85.7	78.5	71.2	64.9
9	80.00	72.6	80.5	88.1	97.2	106.5	115.4	121.3	117.3	119.3	112.9	103.9	94.7	85.9	78.8	71.7	65.4
8	70.00	74.6	81.8	88.6	96.5	104.4	111.3	114.7	111.7	112.7	108.9	102.0	94.3	86.7	80.5	74.1	68.3
7	60.00	76.3	82.6	88.4	94.9	100.9	105.7	107.4	105.6	105.6	103.6	98.9	93.1	87.0	81.8	76.4	71.3
6	50.00	77.0	82.3	86.9	92.0	96.4	99.4	100.3	99.6	99.1	97.9	95.0	90.9	86.5	82.4	77.8	73.5
5	40.00	76.1	80.5	84.2	88.1	91.3	93.3	94.1	93.9	93.6	92.7	90.8	88.0	84.7	81.5	77.8	74.1
4	30.00	75.9	79.4	82.3	85.2	87.5	89.1	89.8	90.1	90.0	89.4	88.2	86.3	83.8	81.4	78.4	75.4
3	20.00	75.9	78.8	81.2	83.5	85.3	86.6	87.5	88.0	88.1	87.8	86.9	85.5	83.6	81.7	79.3	76.7
2	10.00	75.7	78.2	80.1	82.1	83.6	84.9	85.8	86.4	86.6	86.5	85.9	84.8	83.4	81.8	79.8	77.6
1	0.00	75.5	77.6	79.3	81.0	82.5	83.7	84.6	85.3	85.6	85.6	85.1	84.3	83.1	81.8	80.0	78.1

PHASE (DEGREES)

L	THETA	1	2	3	4	5	6	7	8	9	10	11	12	13	14	15	16
19	180.00	179.0	168.6	161.6	156.6	154.7	155.7	159.4	164.9	171.6	178.9	-173.2	-164.6	-155.0	-145.5	-133.5	-120.2
18	170.00	148.1	137.2	129.9	124.6	122.8	124.4	129.2	136.2	144.2	152.5	160.9	169.6	179.1	-171.6	-159.8	-146.5
17	160.00	115.5	104.2	96.5	90.8	88.9	91.0	97.3	106.7	117.0	126.8	135.5	144.0	153.0	161.8	173.1	-174.0
16	150.00	92.3	80.7	72.8	66.8	64.6	67.0	75.0	87.9	101.9	113.5	122.3	129.9	137.6	145.3	155.6	167.7
15	140.00	78.2	66.7	58.8	52.7	50.1	52.4	61.9	79.9	99.7	113.3	121.4	127.0	132.5	138.5	147.1	158.0
14	130.00	75.4	64.2	56.6	50.5	47.5	49.1	59.3	84.5	113.5	128.4	134.2	136.9	139.5	143.2	149.7	159.0
13	120.00	91.2	80.7	73.5	67.6	64.2	64.4	73.5	109.2	151.5	164.5	166.8	166.3	165.9	167.0	171.0	178.3
12	110.00	121.1	111.3	104.5	98.9	95.1	93.8	99.9	147.4	-157.9	-150.1	-150.8	-153.3	-155.8	-156.6	-154.8	-149.2
11	100.00	165.4	156.1	149.7	144.2	140.2	137.8	140.4	-160.4	-99.1	-96.3	-98.7	-102.3	-105.8	-107.8	-107.4	-103.2
10	90.00	-128.9	-138.1	-144.4	-149.8	-153.9	-156.5	-154.5	-92.8	-31.0	-29.1	-31.7	-35.5	-39.1	-41.2	-41.0	-37.1
9	80.00	-65.7	-75.0	-81.4	-86.8	-90.9	-93.3	-90.7	-31.5	-29.8	32.6	30.2	26.6	23.1	21.1	21.6	25.8
8	70.00	-3.7	-13.5	-20.2	-25.9	-29.7	-30.9	-24.9	22.7	77.4	85.1	84.5	81.9	79.4	78.6	80.5	86.0
7	60.00	40.9	30.4	23.2	17.3	13.9	14.1	23.2	58.9	101.2	114.2	116.5	116.0	115.6	116.7	120.7	128.0
6	50.00	69.9	58.8	51.1	45.1	42.1	43.7	53.9	79.1	108.0	123.0	128.8	131.4	134.1	137.8	144.3	153.6
5	40.00	94.5	83.0	75.1	69.0	66.4	68.7	78.2	96.1	115.9	129.6	137.6	143.2	148.7	154.8	163.4	174.3
4	30.00	113.2	101.6	93.7	87.7	85.5	87.9	95.9	108.8	122.8	134.4	143.2	150.8	158.5	166.2	176.5	-171.4
3	20.00	128.7	117.3	109.6	104.0	102.0	104.2	110.5	119.8	130.2	139.9	148.7	157.2	166.1	175.0	-173.7	-160.9
2	10.00	144.6	133.7	126.4	121.1	119.2	120.8	125.6	132.6	140.7	148.9	157.3	166.0	175.5	-175.1	-163.3	-150.1

PROPELLER, 0.76 M DIAMETER, 3 BLADES, 4000 RPM, 0.076 M CLEARANCE

PROPELLER DATA
NUMBER OF BLADES = 3.
PROPELLER RPM = 4000.0
BLADE PASSAGE FREQUENCY (HZ) = 200.0
DISTANCE OF PROPELLER C/L FROM FUSELAGE C/L (M) = .9652
ANGLE BETWEEN VERTICAL AND LINE FROM PROP TO FUSELAGE C/L (DEGREES) = 90.00
DISTANCE OF PROPELLER PLANE FROM FORWARD END OF FUSELAGE (M) = .6620

PROPELLER HARMONIC 3 AT 600.0 HZ

PRESSURE AMPLITUDE, DB RE 20 MICRO PA

CIRCUM. LOCATION L	THETA	K= 1 Z= .041	2 .130	3 .219	4 .307	5 .396	6 .465	7 .573	8 .662	9 .751	10 .839	11 .928	12 1.017	13 1.105	14 1.194	15 1.283	16 1.371
19	180.00	57.2	60.1	62.5	64.8	66.8	68.3	69.5	70.1	70.3	69.9	69.0	67.6	65.7	63.7	61.0	58.2
18	170.00	56.9	60.2	62.9	65.6	67.8	69.5	70.6	71.2	71.3	70.7	69.6	67.9	65.6	63.3	60.3	57.1
17	160.00	56.3	60.2	63.5	66.7	69.4	71.3	72.4	72.9	72.7	71.9	70.3	68.1	65.3	62.5	59.0	55.3
16	150.00	55.2	60.0	64.0	68.1	71.5	73.9	75.1	75.2	74.7	73.4	71.3	68.3	64.8	61.3	57.1	52.9
15	140.00	54.2	60.1	65.2	70.6	75.2	78.5	79.9	79.7	78.7	76.8	73.6	69.5	64.8	60.3	55.2	50.1
14	130.00	53.6	60.7	67.1	74.1	80.5	85.3	87.4	86.6	85.0	82.4	77.7	71.8	65.5	59.9	53.8	47.9
13	120.00	51.0	59.5	67.4	76.6	85.4	92.6	96.2	94.6	93.2	89.2	82.0	73.5	65.0	57.9	50.5	43.7
12	110.00	47.5	57.2	66.5	77.7	89.1	99.3	105.6	103.2	102.4	95.7	85.4	74.2	63.5	54.9	46.3	38.5
11	100.00	44.2	54.7	65.0	77.8	91.1	104.1	113.8	110.9	110.6	100.4	87.3	73.9	61.4	51.4	41.5	32.7
10	90.00	43.1	54.0	64.7	77.7	91.4	104.9	115.4	112.4	112.1	101.1	87.5	73.9	61.1	51.0	41.2	32.8
9	80.00	44.2	54.7	65.0	77.8	91.1	104.1	113.8	110.9	110.6	100.4	87.3	73.9	61.4	51.4	41.5	32.7
8	70.00	47.5	57.2	66.5	77.7	89.1	99.3	105.6	103.2	102.4	95.7	85.4	74.2	63.5	54.9	46.3	38.5
7	60.00	51.0	59.5	67.4	76.6	85.4	92.6	96.2	94.6	93.2	89.2	82.0	73.5	65.0	57.9	50.5	43.7
6	50.00	53.6	60.7	67.1	74.1	80.5	85.3	87.4	86.6	85.0	82.4	77.7	71.8	65.5	59.9	53.8	47.9
5	40.00	54.2	60.1	65.2	70.6	75.2	78.5	79.9	79.7	78.7	76.8	73.6	69.5	64.8	60.3	55.2	50.1
4	30.00	55.2	60.0	64.0	68.1	71.5	73.9	75.1	75.2	74.7	73.4	71.3	68.3	64.8	61.3	57.1	52.9
3	20.00	56.3	60.2	63.5	66.7	69.4	71.3	72.4	72.9	72.7	71.9	70.3	68.1	65.3	62.5	59.0	55.3
2	10.00	56.9	60.2	62.9	65.6	67.8	69.5	70.6	71.2	71.3	70.7	69.6	67.9	65.6	63.3	60.3	57.1
1	0.00	57.2	60.1	62.5	64.8	66.8	68.3	69.5	70.1	70.3	69.9	69.0	67.6	65.7	63.7	61.0	58.2

PHASE (DEGREES)

CIRCUM. LOCATION L	THETA	1	2	3	4	5	6	7	8	9	10	11	12	13	14	15	16
19	180.00	154.3	135.4	121.8	110.2	102.9	99.6	100.2	103.9	110.1	118.2	128.0	139.6	153.3	167.3	-174.7	-154.4
18	170.00	109.4	90.0	76.0	64.1	56.8	54.0	55.5	60.6	68.0	77.0	87.3	99.1	112.7	126.6	144.4	164.6
17	160.00	61.8	41.9	27.7	15.7	8.5	6.2	9.1	16.3	26.0	36.3	46.9	58.3	71.2	84.6	101.9	121.8
16	150.00	27.9	8.2	-5.8	-17.5	-24.4	-26.0	-21.5	-11.1	2.0	14.0	24.2	34.2	45.4	57.4	73.6	92.6
15	140.00	7.6	-11.3	-24.5	-35.3	-41.6	-42.7	-36.5	-21.4	-2.4	11.7	20.4	27.2	35.2	44.7	58.8	76.5
14	130.00	4.2	-13.4	-25.3	-34.9	-40.5	-41.4	-34.2	-12.1	17.1	32.7	38.0	40.3	43.8	49.8	60.7	76.3
13	120.00	29.5	13.4	2.9	-5.4	-10.6	-12.1	-5.5	26.6	71.0	84.3	85.3	83.2	81.9	83.6	90.5	102.7
12	110.00	76.8	61.6	52.0	44.4	39.2	36.5	40.5	83.7	142.0	149.2	147.0	142.4	137.9	136.1	138.6	147.0
11	100.00	143.6	130.3	121.5	114.2	108.8	105.1	106.1	160.4	-134.2	-132.4	-136.3	-141.7	-147.5	-151.3	-151.3	-144.4
10	90.00	-121.6	-133.1	-140.6	-147.1	-152.2	-155.9	-155.6	-98.8	-32.8	-31.9	-35.8	-41.0	-46.1	-48.7	-46.6	-37.3
9	80.00	-23.0	-36.4	-45.1	-52.4	-57.8	-61.5	-60.6	-6.2	59.2	61.0	57.1	51.7	45.9	42.1	42.1	49.0
8	70.00	69.7	54.5	44.9	37.3	32.1	29.4	33.3	76.6	134.8	142.1	139.9	135.3	130.8	128.9	131.5	139.9
7	60.00	134.0	117.9	107.4	99.1	94.0	92.4	99.0	131.1	175.5	-171.2	-170.2	-172.3	-173.6	-171.8	-165.0	-152.8
6	50.00	176.0	158.4	146.5	136.9	131.3	130.5	137.7	159.7	-171.0	-155.4	-150.1	-147.8	-144.4	-138.4	-127.4	-111.9
5	40.00	-148.0	-166.9	179.9	169.1	162.8	161.7	167.9	-177.0	-158.0	-143.9	-135.2	-126.4	-120.4	-110.9	-96.8	-79.1
4	30.00	-120.8	-140.5	-154.5	-166.1	-173.1	-174.7	-170.1	-159.8	-146.7	-134.7	-124.4	-114.5	-103.2	-91.3	-75.1	-56.0
3	20.00	-98.5	-118.3	-132.6	-144.5	-151.8	-154.0	-151.1	-143.9	-134.3	-124.0	-113.4	-102.0	-89.0	-75.7	-58.4	-38.5
2	10.00	-75.9	-95.3	-109.4	-121.2	-128.6	-131.4	-129.9	-124.8	-117.3	-108.3	-98.0	-86.3	-72.7	-58.8	-41.0	-20.7
1	0.00	-66.1	-84.9	-98.5	-110.1	-117.5	-120.7	-120.2	-116.4	-110.3	-102.2	-92.4	-80.7	-67.1	-53.0	-35.1	-14.7

NASA LANGLEY SCALE MODEL FUSELAGE WITH FLOOR
STIFFENED 0.032 IN CYLINDER, STIFFENED FLOOR AT 56.6 DEGREES, RIGID JUNCTION
CAVITY 72 IN LONG, STRUCTURE 71 IN LONG
TRIM PANEL. FIBERGLAS TYPE PF105 2.0 IN THICK + LINING = 1.46 KG/M2

PROPELLER, 0.76 M DIAMETER, 3 BLADES, 4000 RPM, 0.076 M CLEARANCE

TONE TRANSMISSION AT FREQUENCIES AT OR ABOVE 1250.0 HZ IS WITH HIGH FREQUENCY FORMULATION

TONE TRANSMISSION FOR PROPELLER HARMONICS

HARMONIC NO	FREQ	INTERIOR MEAN SQ. PRESSURE PA**2	DB RE 20 MICRO PA
1	200.0	5.8974E-01	91.69
2	400.0	2.6351E-02	78.19
3	600.0	5.3939E-03	71.30
4	800.0	7.6416E-05	52.81
5	1000.0	2.2966E-06	37.59
6	1200.0	7.2388E-07	32.58
7	1400.0	4.5941E-08	20.60
8	1600.0	1.4556E-09	5.61
9	1800.0	1.3173E-09	5.18
10	2000.0	2.9091E-11	-11.38

```
+ ------------------------------------------------------ +
+ ACOUSTIC MODES:                                        +
+ Q = NO. OF AXIAL HALF-WAVES                            +
+ I = ASSIGNED ORDER OF 2-DIMENSIONAL MODAL PATTERN      +
+      IN CYLINDER CROSS-SECTION                         +
+                                                        +
+ STRUCTURAL MODES:                                      +
+ M = NO. OF AXIAL HALF-WAVES                            +
+ N = NO. OF CIRCUMFERENTIAL WAVES AROUND FUSELAGE FOR   +
+      LARGEST SHELL GEN. COORDINATES FOR THIS MODE      +
++++++++++++++++++++++++++++++++++++++++++++++++++++++++++
```

TONE TRANSMISSION FOR FREQUENCY 200.0 HZ, HARMONIC NO. 1

NO	ACOUSTIC FREQ	MODE Q	I	STRUCTURAL NO	FREQ	MODE M	N	ETA R#	M.S.PRESSURE (PA**2)
3	187.6	2	0	13	502.2	1	1	.00000	1.5586E-02
5	217.2	1	1	12	470.5	2	3	.00010	1.8704E-02
3	187.6	2	0	6	301.9	1	2	.00000	8.5077E-02
3	187.6	2	0	1	168.5	1	2	.10685	1.6350E-01
3	187.6	2	0	2	206.2	1	2	.00710	2.1463E-01

TOTAL = 91.69 DB 5.8974E-01

TONE TRANSMISSION FOR FREQUENCY 400.0 HZ, HARMONIC NO. 2

NO	ACOUSTIC FREQ	MODE Q	I	STRUCTURAL NO	FREQ	MODE M	N	ETA R#	M.S.PRESSURE (PA**2)
18	393.8	2	3	8	318.7	1	2	.00001	3.7994E-04
19	414.8	2	4	6	301.9	1	2	.00053	8.1627E-04
13	358.7	1	3	12	470.5	2	3	.00086	8.9625E-04
18	393.8	2	3	21	626.0	3	3	.00016	1.8668E-03
18	393.8	2	3	9	346.7	1	3	.00288	2.0118E-02

TOTAL = 78.19 DB 2.6351E-02

TONE TRANSMISSION FOR FREQUENCY 600.0 HZ, HARMONIC NO. 3

NO	ACOUSTIC FREQ	MODE Q	I	STRUCTURAL NO	FREQ	MODE M	N	ETA R#	M.S.PRESSURE (PA**2)
50	600.3	2	8	22	632.0	1	1	.00003	4.5724E-04
41	572.3	3	6	20	607.5	2	4	.00379	4.9749E-04
49	598.3	1	9	25	646.7	2	4	.00043	6.5737E-04
50	600.3	2	8	17	560.7	1	1	.00012	6.6746E-04
49	598.3	1	9	19	591.9	2	3	.05496	7.4397E-04

TOTAL = 71.30 DB 5.3939E-03

TONE TRANSMISSION FOR FREQUENCY 800.0 HZ, HARMONIC NO. 4

NO	ACOUSTIC FREQ	MODE Q	I	STRUCTURAL NO	FREQ	MODE M	N	ETA R#	M.S.PRESSURE (PA**2)
101	792.6	5	10	27	716.2	4	4	.00010	3.9431E-06
104	801.1	3	14	38	884.0	2	5	.00000	4.4401E-06
102	796.5	4	12	31	779.8	3	3	.00111	4.6114E-06

PROPELLER, 0.76 M DIAMETER, 3 BLADES, 5000 RPM, 0.076 M CLEARANCE

PROPELLER DATA
NUMBER OF BLADES = 3.
PROPELLER RPM = 5000.0
BLADE PASSAGE FREQUENCY (HZ) = 250.0
DISTANCE OF PROPELLER C/L FROM FUSELAGE C/L (M) = .9652
ANGLE BETWEEN VERTICAL AND LINE FROM PROP TO FUSELAGE C/L (DEGREES) = 90.00
DISTANCE OF PROPELLER PLANE FROM FORWARD END OF FUSELAGE (M) = .6620

PROPELLER HARMONIC 1 AT 250.0 HZ

PRESSURE AMPLITUDE, DB RE 20 MICRO PA

CIRCUM. LOCATION L	THETA	K= 1 Z= .041	2 .130	3 .219	4 .307	5 .396	6 .485	7 .573	8 .662	9 .751	10 .839	11 .928	12 1.017	13 1.105	14 1.194	15 1.283	16 1.371
19	180.00	102.0	103.1	104.1	105.1	106.1	107.2	108.2	109.2	110.1	110.6	110.8	110.7	110.4	109.8	109.1	108.1
18	170.00	102.8	104.1	105.1	106.1	107.1	108.1	109.1	110.1	110.9	111.5	111.6	111.4	110.9	110.3	109.3	108.2
17	160.00	103.8	105.3	106.4	107.6	108.5	109.4	110.3	111.3	112.1	112.6	112.7	112.3	111.6	110.7	109.5	108.2
16	150.00	104.7	106.5	108.0	109.4	110.4	111.2	111.8	112.7	113.6	114.0	114.0	113.3	112.3	111.1	109.6	108.0
15	140.00	105.9	108.3	110.3	112.2	113.7	114.5	114.8	115.5	116.3	116.7	116.3	115.2	113.7	112.0	110.1	108.0
14	130.00	108.0	111.0	113.5	116.1	118.2	119.3	119.3	119.3	120.4	120.7	119.8	118.1	115.9	113.8	111.4	109.0
13	120.00	106.9	112.4	115.6	119.0	122.0	123.9	123.8	122.8	124.3	124.4	122.6	120.0	117.1	114.5	111.5	108.7
12	110.00	108.8	112.9	116.7	120.9	125.0	128.1	128.6	126.1	128.6	127.8	124.8	121.2	117.5	114.3	111.0	107.8
11	100.00	108.3	112.8	117.0	121.9	126.9	131.3	133.3	129.0	132.9	130.5	126.3	121.8	117.4	113.8	110.1	106.6
10	90.00	108.2	112.8	117.1	122.1	127.2	131.9	134.2	129.6	133.7	131.0	126.6	121.9	117.4	113.7	109.9	106.4
9	80.00	108.3	112.8	117.0	121.9	126.9	131.3	133.3	129.0	132.9	130.5	126.3	121.8	117.4	113.8	110.1	106.6
8	70.00	108.8	112.9	116.7	120.9	125.0	128.1	128.6	126.1	128.6	127.8	124.8	121.2	117.5	114.3	111.0	107.8
7	60.00	108.9	112.4	115.6	119.0	122.0	123.9	123.8	122.8	124.3	124.4	122.6	120.0	117.1	114.5	111.5	108.7
6	50.00	108.0	111.0	113.5	116.1	118.2	119.3	119.3	119.3	120.4	120.7	119.8	118.1	115.9	113.8	111.4	109.0
5	40.00	105.9	108.3	110.3	112.2	113.7	114.5	114.8	115.5	116.3	116.7	116.3	115.2	113.7	112.0	110.1	108.0
4	30.00	104.7	106.5	108.0	109.4	110.4	111.2	111.8	112.7	113.6	114.0	114.0	113.3	112.3	111.1	109.6	108.0
3	20.00	103.8	105.3	106.4	107.6	108.5	109.4	110.3	111.3	112.1	112.6	112.7	112.3	111.6	110.7	109.5	108.2
2	10.00	102.8	104.1	105.1	106.1	107.1	108.1	109.1	110.1	110.9	111.5	111.6	111.4	110.9	110.3	109.3	108.2
1	0.00	102.0	103.1	104.1	105.1	106.1	107.2	108.2	109.2	110.1	110.6	110.8	110.7	110.4	109.8	109.1	108.1

PHASE (DEGREES)

L	THETA	1	2	3	4	5	6	7	8	9	10	11	12	13	14	15	16
19	180.00	-113.9	-117.6	-118.8	-117.6	-114.0	-108.5	-101.8	-94.9	-88.2	-81.7	-75.2	-68.5	-61.2	-54.2	-45.7	-36.3
18	170.00	-135.2	-139.8	-141.7	-141.0	-137.4	-131.0	-122.9	-114.4	-106.4	-99.0	-92.0	-85.0	-77.6	-70.6	-61.9	-52.5
17	160.00	-158.1	-163.7	-166.6	-166.9	-163.6	-156.5	-146.5	-135.5	-125.4	-116.8	-109.3	-102.1	-94.7	-87.7	-79.1	-69.6
16	150.00	-175.9	177.5	173.5	171.9	174.1	-178.6	-166.3	-151.7	-138.6	-128.5	-120.6	-113.5	-106.4	-99.7	-91.3	-82.0
15	140.00	171.5	164.0	159.2	156.2	157.0	163.3	177.5	-162.7	-145.2	-133.5	-125.6	-119.2	-112.8	-106.7	-98.8	-89.9
14	130.00	165.2	157.2	151.6	147.4	146.5	151.0	165.8	-167.0	-142.9	-130.0	-123.1	-118.0	-112.9	-107.6	-100.5	-92.1
13	120.00	168.8	160.4	154.4	149.3	146.8	148.6	161.6	-160.4	-126.0	-113.8	-109.2	-106.3	-102.8	-98.8	-92.7	-85.0
12	110.00	-179.4	172.1	165.9	160.4	156.8	156.2	165.0	-144.4	-98.8	-90.3	-88.5	-87.5	-85.7	-82.8	-77.7	-70.7
11	100.00	-159.3	-167.8	-174.0	-179.7	176.2	174.1	178.2	-119.0	-65.8	-61.8	-62.1	-62.6	-61.9	-59.7	-55.4	-49.0
10	90.00	-126.8	-135.2	-141.5	-147.1	-151.4	-153.7	-150.4	-85.1	-31.0	-27.8	-28.5	-29.2	-28.7	-26.7	-22.5	-16.1
9	80.00	-94.9	-103.3	-109.6	-115.2	-119.4	-121.5	-117.3	-54.5	-1.3	2.7	2.4	1.9	2.6	4.7	9.1	15.5
8	70.00	-61.8	-70.2	-76.5	-82.0	-85.6	-86.2	-77.4	-26.8	18.8	27.3	29.1	30.1	31.9	34.9	40.0	47.0
7	60.00	-36.3	-44.7	-50.8	-55.8	-58.4	-56.5	-43.6	-5.5	28.8	41.0	45.6	48.6	52.0	56.1	62.2	69.9
6	50.00	-17.5	-25.6	-31.2	-35.3	-36.2	-31.7	-16.9	10.3	34.4	47.3	54.2	59.3	64.4	69.7	76.8	85.2
5	40.00	-.4	-7.8	-12.7	-15.7	-14.9	-8.5	5.6	25.4	42.9	54.6	62.5	69.0	75.3	81.5	89.3	98.3
4	30.00	14.5	7.9	4.0	2.3	4.6	11.8	24.1	38.7	51.8	61.9	69.9	77.0	84.0	90.8	99.1	108.4
3	20.00	28.5	22.9	20.0	19.7	22.9	30.0	40.1	51.1	61.2	69.8	77.3	84.5	91.9	98.9	107.5	117.0
2	10.00	43.0	38.5	36.6	37.2	40.9	47.2	55.3	63.8	71.8	79.2	86.2	93.2	100.6	107.6	116.3	125.8

PROPELLER, 0.76 M DIAMETER, 3 BLADES, 5000 RPM, 0.076 M CLEARANCE

PROPELLER DATA
NUMBER OF BLADES = 3.
PROPELLER RPM = 5000.0
BLADE PASSAGE FREQUENCY (HZ) = 250.0
DISTANCE OF PROPELLER C/L FROM FUSELAGE C/L (M) = .9652
ANGLE BETWEEN VERTICAL AND LINE FROM PROP TO FUSELAGE C/L (DEGREES) = 90.00
DISTANCE OF PROPELLER PLANE FROM FORWARD END OF FUSELAGE (M) = .6620

PROPELLER HARMONIC 2 AT 500.0 HZ

PRESSURE AMPLITUDE, DB RE 20 MICRO PA

CIRCUM. LOCATION L	THETA	K= 1 Z= .041	2 .130	3 .219	4 .307	5 .396	6 .485	7 .573	8 .662	9 .751	10 .839	11 .928	12 1.017	13 1.105	14 1.194	15 1.283	16 1.371
19	180.00	88.6	90.4	91.8	93.3	94.8	96.2	97.6	98.7	99.4	99.8	99.6	99.0	98.0	96.9	95.3	93.5
18	170.00	88.9	90.9	92.5	94.2	95.7	97.1	98.4	99.6	100.3	100.6	100.3	99.5	98.3	96.9	95.0	93.0
17	160.00	89.1	91.5	93.4	95.4	97.0	98.4	99.7	100.8	101.5	101.6	101.1	100.0	98.4	96.7	94.5	92.1
16	150.00	89.0	91.9	94.3	96.8	98.7	100.2	101.3	102.2	102.9	102.8	102.0	100.5	98.4	96.3	93.6	90.8
15	140.00	89.0	92.7	95.8	99.1	101.7	103.5	104.5	105.2	105.6	105.3	103.9	101.7	98.9	96.1	92.8	89.4
14	130.00	89.6	94.1	98.1	102.3	105.9	108.5	109.4	109.5	109.7	109.0	106.9	103.7	100.1	96.6	92.7	88.7
13	120.00	88.6	93.9	98.9	104.4	109.5	113.4	114.9	113.9	114.1	112.6	109.0	104.6	99.8	95.5	90.9	86.3
12	110.00	86.6	92.7	98.5	105.3	112.1	118.0	121.0	118.5	119.4	116.3	110.7	104.6	98.6	93.6	88.3	83.2
11	100.00	84.3	91.1	97.6	105.4	113.7	121.6	126.8	123.1	124.9	119.3	111.7	104.1	97.1	91.4	85.6	80.1
10	90.00	83.9	90.7	97.4	105.4	113.9	122.2	128.0	124.1	126.0	119.9	111.8	103.9	96.8	91.0	85.0	79.6
9	80.00	84.3	91.1	97.6	105.4	113.7	121.6	126.8	123.1	124.9	119.3	111.7	104.1	97.1	91.4	85.6	80.1
8	70.00	86.6	92.7	98.5	105.3	112.1	118.0	121.0	118.5	119.4	116.3	110.7	104.6	98.6	93.6	88.3	83.2
7	60.00	88.6	93.9	98.9	104.4	109.5	113.4	114.9	113.9	114.1	112.6	109.0	104.6	99.8	95.5	90.9	86.3
6	50.00	89.6	94.1	98.1	102.3	105.9	108.5	109.4	109.5	109.7	109.0	106.9	103.7	100.1	96.6	92.7	88.7
5	40.00	89.0	92.7	95.8	99.1	101.7	103.5	104.5	105.2	105.6	105.3	103.9	101.7	98.9	96.1	92.8	89.4
4	30.00	89.0	91.9	94.3	96.8	98.7	100.2	101.3	102.2	102.9	102.8	102.0	100.5	98.4	96.3	93.6	90.8
3	20.00	89.1	91.5	93.4	95.4	97.0	98.4	99.7	100.8	101.5	101.6	101.1	100.0	98.4	96.7	94.5	92.1
2	10.00	88.9	90.9	92.5	94.2	95.7	97.1	98.4	99.6	100.3	100.6	100.3	99.5	98.3	96.9	95.0	93.0
1	0.00	88.6	90.4	91.8	93.3	94.8	96.2	97.6	98.7	99.4	99.8	99.6	99.0	98.0	96.9	95.3	93.5

PHASE (DEGREES)

L	THETA	1	2	3	4	5	6	7	8	9	10	11	12	13	14	15	16
19	180.00	-88.6	-103.5	-113.3	-120.4	-123.3	-122.6	-119.3	-114.2	-107.8	-99.9	-90.5	-79.2	-65.9	-52.3	-35.2	-16.0
18	170.00	-127.9	-144.0	-154.9	-162.9	-166.1	-164.9	-160.4	-153.9	-146.2	-137.4	-127.3	-115.6	-101.9	-87.9	-70.3	-50.7
17	160.00	-170.3	172.3	160.2	150.9	146.9	148.4	154.5	163.3	172.9	-177.1	-166.3	-154.2	-140.2	-126.0	-108.0	-87.9
16	150.00	156.8	138.3	125.0	114.4	109.2	110.5	118.3	130.2	142.7	154.2	165.5	177.6	-168.6	-154.5	-136.5	-116.2
15	140.00	133.9	114.5	100.4	88.7	82.3	82.7	91.8	108.3	125.0	138.1	149.2	160.4	173.4	-173.1	-155.4	-135.2
14	130.00	122.9	103.2	88.9	76.5	69.1	68.1	77.7	100.5	124.2	138.4	147.8	156.9	168.1	-179.5	-162.8	-143.1
13	120.00	131.4	111.9	97.8	85.5	77.5	74.9	83.1	115.7	151.1	164.2	169.6	175.1	-176.7	-166.3	-151.0	-132.1
12	110.00	155.9	136.9	123.3	111.6	103.6	99.7	104.7	149.1	-161.8	-153.7	-152.8	-151.1	-146.0	-137.7	-124.0	-106.1
11	100.00	-163.4	178.2	165.2	154.1	146.3	141.7	143.2	-160.7	-102.6	-100.1	-102.2	-103.2	-100.4	-93.8	-81.5	-64.5
10	90.00	-98.2	-116.6	-129.5	-140.4	-148.1	-152.6	-152.0	-93.4	-34.4	-32.8	-35.3	-36.7	-34.4	-28.1	-16.0	.8
9	80.00	-34.5	-52.9	-65.9	-77.0	-84.7	-89.4	-87.9	-31.8	26.3	28.8	26.7	25.8	28.5	35.1	47.4	64.4
8	70.00	31.1	12.1	-1.5	-13.2	-21.2	-25.0	-20.0	24.3	73.5	81.5	82.5	84.1	89.2	97.6	111.3	129.2
7	60.00	81.1	61.6	47.4	35.2	27.2	24.6	32.8	65.4	100.8	113.8	119.3	124.7	133.0	143.4	158.7	177.6
6	50.00	117.5	97.8	83.4	71.1	63.6	62.7	72.2	95.1	118.7	133.0	142.3	151.5	162.7	175.0	-168.2	-148.5
5	40.00	150.1	130.8	116.7	105.0	98.5	99.0	108.1	124.5	141.3	154.4	165.4	176.7	-170.3	-156.8	-139.2	-119.0
4	30.00	177.7	159.1	145.9	135.3	130.1	131.4	139.2	151.1	163.6	175.1	-173.6	-161.5	-147.7	-133.6	-115.6	-95.3
3	20.00	-157.2	-174.6	173.3	164.1	160.1	161.6	167.7	176.4	-174.0	-163.9	-153.2	-141.0	-127.0	-112.8	-94.9	-74.8
2	10.00	-131.5	-147.6	-158.5	-166.4	-169.7	-168.5	-164.0	-157.5	-149.8	-141.0	-130.9	-119.1	-105.4	-91.5	-73.9	-54.2
1	0.00	-115.5	-130.4	-140.2	-147.3	-150.2	-149.5	-146.2	-141.1	-134.6	-126.8	-117.3	-106.1	-92.8	-79.2	-62.1	-42.9

PROPELLER, 0.76 M DIAMETER, 3 BLADES, 5000 RPM, 0.076 M CLEARANCE

PROPELLER DATA
NUMBER OF BLADES = 3.
PROPELLER RPM = 5000.0
BLADE PASSAGE FREQUENCY (HZ) = 250.0
DISTANCE OF PROPELLER C/L FROM FUSELAGE C/L (M) = .9652
ANGLE BETWEEN VERTICAL AND LINE FROM PROP TO FUSELAGE C/L (DEGREES) = 90.00
DISTANCE OF PROPELLER PLANE FROM FORWARD END OF FUSELAGE (M) = .6620

PROPELLER HARMONIC 3 AT 750.0 HZ

PRESSURE AMPLITUDE, DB RE 20 MICRO PA

CIRCUM. LOCATION L	THETA	K= 1 Z= .041	2 .130	3 .219	4 .307	5 .396	6 .485	7 .573	8 .662	9 .751	10 .839	11 .928	12 1.017	13 1.105	14 1.194	15 1.283	16 1.371
19	180.00	75.8	78.3	80.4	82.5	84.3	86.0	87.4	88.6	89.2	89.3	88.7	87.6	85.9	84.1	81.7	79.1
18	170.00	75.6	78.5	80.8	83.1	85.1	86.9	88.3	89.4	90.0	90.0	89.2	87.8	85.8	83.7	80.9	77.9
17	160.00	75.0	78.4	81.2	83.9	86.2	88.1	89.6	90.6	91.2	90.9	89.8	88.0	85.5	82.9	79.7	76.2
16	150.00	73.9	78.0	81.4	84.8	87.6	89.8	91.2	92.2	92.5	91.9	90.4	88.0	84.9	81.7	77.8	73.7
15	140.00	72.6	77.7	82.0	86.5	90.2	93.0	94.5	95.2	95.2	94.1	91.8	88.5	84.5	80.5	75.9	71.0
14	130.00	71.7	77.8	83.1	88.9	94.0	97.8	99.7	99.8	99.3	97.5	94.1	89.6	84.5	79.7	74.2	68.7
13	120.00	68.8	76.0	82.5	89.9	97.0	102.9	105.8	104.9	103.9	100.9	95.6	89.3	82.8	77.0	70.5	64.2
12	110.00	64.9	73.0	80.7	89.8	99.2	107.8	113.1	111.1	110.2	104.8	96.6	88.1	80.0	73.2	65.9	58.9
11	100.00	60.9	69.8	78.4	88.9	100.3	111.6	120.1	117.3	116.9	108.1	97.0	86.4	76.9	69.2	61.3	53.9
10	90.00	59.9	69.0	77.8	88.7	100.4	112.3	121.5	118.6	118.3	108.7	97.1	86.1	76.3	68.6	60.6	53.3
9	80.00	60.9	69.8	78.4	88.9	100.3	111.6	120.1	117.3	116.9	108.1	97.0	86.4	76.9	69.2	61.3	53.9
8	70.00	64.9	73.0	80.7	89.8	99.2	107.8	113.1	111.1	110.2	104.8	96.6	88.1	80.0	73.2	65.9	58.9
7	60.00	68.8	76.0	82.5	89.9	97.0	102.9	105.8	104.9	103.9	100.9	95.6	89.3	82.8	77.0	70.5	64.2
6	50.00	71.7	77.8	83.1	88.9	94.0	97.8	99.7	99.8	99.3	97.5	94.1	89.6	84.5	79.7	74.2	68.7
5	40.00	72.6	77.7	82.0	86.5	90.2	93.0	94.5	95.2	95.2	94.1	91.8	88.5	84.5	80.5	75.9	71.0
4	30.00	73.9	78.0	81.4	84.8	87.6	89.8	91.2	92.2	92.5	91.9	90.4	86.0	84.9	81.7	77.8	73.7
3	20.00	75.0	78.4	81.2	83.9	86.2	88.1	89.6	90.6	91.2	90.9	89.8	88.0	85.5	82.9	79.7	76.2
2	10.00	75.6	78.5	80.8	83.1	85.1	86.9	88.3	89.4	90.0	90.0	89.2	87.8	85.8	83.7	80.9	77.9
1	0.00	75.8	78.3	80.4	82.5	84.3	86.0	87.4	88.6	89.2	89.3	86.7	87.6	85.9	84.1	81.7	79.1

PHASE (DEGREES)

L	THETA	1	2	3	4	5	6	7	8	9	10	11	12	13	14	15	16
19	180.00	-56.7	-83.8	-103.4	-119.9	-130.6	-135.7	-136.3	-133.1	-126.9	-117.4	-104.8	-88.7	-69.2	-49.0	-23.1	6.0
18	170.00	-114.6	-143.2	-164.0	178.3	167.0	162.0	162.4	166.8	174.3	-175.2	-161.8	-145.0	-124.7	-103.8	-77.1	-47.1
17	160.00	-177.1	152.8	130.6	111.3	99.0	93.9	95.5	101.9	111.3	123.1	137.5	154.9	175.7	-162.8	-135.4	-104.5
16	150.00	134.4	102.9	79.4	56.8	45.2	39.7	42.6	51.8	64.0	77.3	92.2	109.8	130.7	152.3	-179.9	-148.5
15	140.00	100.3	68.0	43.7	22.2	7.7	1.6	5.5	18.7	34.9	49.7	64.3	80.9	101.0	122.1	149.7	-178.9
14	130.00	84.0	51.4	27.2	5.8	-8.9	-15.6	-11.1	7.7	30.7	46.4	58.6	72.3	90.1	109.9	136.6	167.6
13	120.00	96.8	64.6	41.4	21.2	7.4	.6	4.6	32.3	68.2	81.9	88.1	96.3	109.9	127.1	152.0	-177.8
12	110.00	133.4	102.6	80.6	62.2	49.8	43.1	45.1	84.1	136.0	143.2	142.8	144.9	153.6	167.8	-169.4	-140.1
11	100.00	-166.6	164.3	144.0	127.3	116.2	109.4	108.7	159.2	-138.9	-138.0	-142.1	-144.0	-139.2	-127.5	-106.1	-77.1
10	90.00	-66.6	-98.1	-118.2	-134.4	-145.2	-151.9	-153.1	-100.1	-37.1	-37.3	-41.8	-44.2	-39.8	-28.5	-7.8	19.5
9	80.00	26.8	-2.3	-22.6	-39.3	-50.4	-57.2	-57.9	-7.4	54.5	55.4	51.3	49.3	54.2	65.9	87.3	116.3
8	70.00	126.2	95.5	73.5	55.0	42.7	35.9	38.0	76.9	128.8	136.0	135.7	137.8	146.5	160.7	-176.5	-147.2
7	60.00	-158.7	169.3	145.9	125.7	111.9	105.1	109.2	136.9	172.7	-173.6	-167.3	-159.1	-145.6	-128.3	-103.4	-73.3
6	50.00	-104.1	-136.7	-161.0	177.6	162.9	156.3	160.8	179.5	-157.4	-141.7	-129.6	-115.8	-98.0	-78.3	-51.6	-20.5
5	40.00	-55.3	-87.6	-111.9	-133.4	-147.9	-154.0	-150.1	-136.9	-120.7	-105.9	-91.3	-74.7	-54.7	-33.5	-5.9	25.5
4	30.00	-14.3	-45.8	-69.3	-89.9	-103.5	-108.9	-106.1	-96.9	-84.7	-71.4	-56.4	-38.9	-18.0	3.6	31.4	62.8
3	20.00	22.6	-7.5	-29.7	-48.9	-61.3	-66.4	-64.8	-58.4	-48.9	-37.2	-22.8	-5.4	15.4	36.9	64.4	95.3
2	10.00	60.0	31.5	10.7	-7.0	-18.3	-23.4	-23.0	-18.6	-11.0	-.6	12.9	29.7	49.9	70.8	97.6	127.6
1	0.00	83.0	55.9	36.3	19.7	9.1	3.9	3.4	6.5	12.8	22.2	34.9	50.9	70.5	90.7	116.6	145.6

NASA LANGLEY SCALE MODEL FUSELAGE WITH FLOOR
STIFFENED 0.032 IN CYLINDER, STIFFENED FLOOR AT 56.6 DEGREES, RIGID JUNCTION
CAVITY 72 IN LONG, STRUCTURE 71 IN LONG
TRIM PANEL. FIBERGLAS TYPE PF105 2.0 IN THICK + LINING = 1.46 KG/M2

PROPELLER, 0.76 M DIAMETER, 3 BLADES, 5000 RPM, 0.076 M CLEARANCE

TONE TRANSMISSION AT FREQUENCIES AT OR ABOVE 1250.0 HZ IS WITH HIGH FREQUENCY FORMULATION

TONE TRANSMISSION FOR PROPELLER HARMONICS

HARMONIC NO	FREQ	INTERIOR MEAN SQ. PRESSURE PA**2	DB RE 20 MICRO PA
1	250.0	1.7319E-01	66.37
2	500.0	5.1079E-01	91.06
3	750.0	1.4923E-02	75.72
4	1000.0	1.8005E-04	56.53
5	1250.0	8.0997E-07	33.06
6	1500.0	1.0712E-08	14.28
7	1750.0	2.6961E-09	8.29
8	2000.0	5.0761E-09	11.04
9	2250.0	1.0425E-09	4.16
10	2500.0	9.5063E-11	-6.24

```
+  ACOUSTIC MODES:                                          +
+  Q = NO. OF AXIAL HALF-WAVES                              +
+  I = ASSIGNED ORDER OF 2-DIMENSIONAL MODAL PATTERN        +
+       IN CYLINDER CROSS-SECTION                           +
+                                                           +
+  STRUCTURAL MODES:                                        +
+  M = NO. OF AXIAL HALF-WAVES                              +
+  N = NO. OF CIRCUMFERENTIAL WAVES AROUND FUSELAGE FOR     +
+       LARGEST SHELL GEN. COORDINATES FOR THIS MODE        +
+++++++++++++++++++++++++++++++++++++++++++++++++++++++++++++
```

ORIGINAL PAGE IS OF POOR QUALITY

TONE TRANSMISSION FOR FREQUENCY 250.0 HZ, HARMONIC NO. 1

ACOUSTIC NO	MODE FREQ	Q	I	STRUCTURAL MODE NO	FREQ	M	N	ETA R#	M.S.PRESSURE (PA**2)
19	414.8	2	4	6	301.9	1	2	.00053	1.1732E-02
7	254.8	1	2	4	231.0	2	4	.04073	1.4242E-02
9	281.3	3	0	4	231.0	2	4	.00335	1.6509E-02
10	302.2	2	2	6	301.9	1	2	.01324	2.3474E-02
8	271.2	2	1	8	318.7	1	2	.00729	3.4398E-02

TOTAL = 86.37 DB 1.7319E-01

TONE TRANSMISSION FOR FREQUENCY 500.0 HZ, HARMONIC NO. 2

ACOUSTIC NO	MODE FREQ	Q	I	STRUCTURAL MODE NO	FREQ	M	N	ETA R#	M.S.PRESSURE (PA**2)
30	508.2	5	1	12	470.5	2	3	.00004	7.3100E-03
32	510.5	4	3	21	626.0	3	3	.00025	1.1707E-02
29	507.1	1	6	20	607.5	2	4	.00141	2.4621E-02
29	507.1	1	6	16	556.4	2	3	.00359	1.3187E-01
29	507.1	1	6	12	470.5	2	3	.00001	2.9197E-01

TOTAL = 91.06 DB 5.1079E-01

TONE TRANSMISSION FOR FREQUENCY 750.0 HZ, HARMONIC NO. 3

ACOUSTIC NO	MODE FREQ	Q	I	STRUCTURAL MODE NO	FREQ	M	N	ETA R#	M.S.PRESSURE (PA**2)
84	744.6	2	13	34	837.1	1	5	.00000	6.4648E-04
90	755.9	1	14	38	884.0	2	5	.00000	6.9320E-04
91	756.9	3	12	28	717.3	2	2	.00001	1.4788E-03
84	744.6	2	13	30	761.9	3	4	.00013	2.2717E-03
87	751.6	6	6	35	855.4	5	4	.00011	2.4074E-03

TOTAL = 75.72 DB 1.4923E-02

TONE TRANSMISSION FOR FREQUENCY 1000.0 HZ, HARMONIC NO. 4

ACOUSTIC NO	MODE FREQ	Q	I	STRUCTURAL MODE NO	FREQ	M	N	ETA R#	M.S.PRESSURE (PA**2)

Appendix C

MODAL CHARACTERISTICS

- Business Aircraft
- Small Body Aircraft
- Narrow Body Aircraft

```
 MERLIN IVC STRUCTURE SYMMETRIC MODES OUTPUT ON MRFSM4
END
INPUT DATA
GENERAL
     FREELY SUPPORTED                      RIGID                          SYMMETRIC
                50.0
         1    10    1    0    14    1    0    5    1
         T    T     F
SHELL
          7.240E+10     7.240E+10           0.33          0.33
            0.00164          4.54           0.84          9.27
           2.712E+3      1.756E+4
PLATE
          7.240E+10     7.240E+10           0.33          0.33
            0.00151         13.66
            1.57E+5       7.48E+4
END
GENERATE MATRICES
CONSTRAINT
SHELL
PLATE
END
SOLVE
PUNCH
FREQUENCIES
EIGENVECTORS
        20
MODE SHAPES
TRAN                                 20    36    10    T    T
END
END OF JOB
```

ORIGINAL PAGE IS
OF POOR QUALITY

```
 MERLIN IVC STRUCTURE ANTISYMMETRIC MODES OUTPUT ON MRFAM4
END
INPUT DATA
GENERAL
     FREELY SUPPORTED                RIGID                                    ANTISYMMETRIC
              50.0
          1    10     1    0   14     1     0     5     1
          T     T     F
SHELL
            7.240E+10      7.240E+10          0.33           0.33
              0.00164           4.54          0.84           9.27
             2.712E+3       1.756E+4
PLATE
            7.240E+10      7.240E+10          0.33           0.33
              0.00151          13.66
              1.57E+5        7.48E+4
END
GENERATE MATRICES
CONSTRAINT
SHELL
PLATE
END
SOLVE
PUNCH
FREQUENCIES
EIGENVECTORS
        20
MODE SHAPES
TRAN                                  20   36   10    T    T
END
END OF JOB
```

ORIGINAL PAGE IS
OF POOR QUALITY

```
 SMALL DIAMETER NO. 1 STRUCTURE SYMMETRIC MODES OUTPUT ON MRPSM3
END
 INPUT DATA
GENERAL
    FREELY SUPPORTED                   RIGID                            SYMMETRIC
              62.6
        1    10    1    0    14    1    0    5    1
        T    T     F
SHELL
          7.240E+10     7.240E+10          0.33          0.33
            0.00193          5.34         1.145          13.0
          1.892E+3      4.362E+4
PLATE
          7.240E+10     7.240E+10          0.33          0.33
            0.00191         19.68
          1.892E+3      4.362E+4
END
GENERATE MATRICES
CONSTRAINT
SHELL
PLATE
END
SOLVE
PUNCH
FREQUENCIES
EIGENVECTORS
     20
MODE SHAPES
TRAN                           20    36    10    T    T
END
END OF JOB
```

ORIGINAL PAGE IS
OF POOR QUALITY

SMALL DIAMETER NO. 1 STRUCTURE ANTISYMMETRIC MODES OUTPUT ON MRFAM3

```
END
INPUT DATA
GENERAL
      FREELY SUPPORTED                   RIGID                         ANTISYMMETRIC
                  62.6
           1    10    1    0    14    1    0    5    1
           T     T    F
SHELL
              7.240E+10    7.240E+10         0.33          0.33
                0.00193         5.34        1.145          13.0
              1.892E+3     4.362E+4
PLATE
              7.240E+10    7.240E+10         0.33          0.33
                0.00191        19.68
              1.892E+3     4.362E+4
END
GENERATE MATRICES
CONSTRAINT
SHELL
PLATE
END
SOLVE
PUNCH
FREQUENCIES
EIGENVECTORS
        20
MODE SHAPES
TRAN                              20    36    10    T    T
END
END OF JOB
```

NARROW BODY STRUCTURE ANTISYMMETRIC MODES OUTPUT ON MRFAM2

```
END
INPUT DATA
GENERAL
      FREELY SUPPORTED                 RIGID                        ANTISYMMETRIC
                  73.7
         1    10     1     0    14     1     0     5     1
         T     T     F
SHELL
           7.240E+10       7.240E+10          0.33          0.33
             0.00243            6.73         1.875          23.0
            1.271E+4        1.118E+5
PLATE
           7.240E+10       7.240E+10          0.33          0.33
             0.00283           23.64
            1.271E+4         6.98E+5
END
GENERATE MATRICES
CONSTRAINT
SHELL
PLATE
END
SOLVE
PUNCH
FREQUENCIES
EIGENVECTORS
        20
MODE SHAPES
TRAN                                 20    36    10     T     T
END
END OF JOB
```

ORIGINAL PAGE IS
OF POOR QUALITY

```
 NARROW BODY STRUCTURE SYMMETRIC MODES OUTPUT ON MRFSM2
END
INPUT DATA
GENERAL
      FREELY SUPPORTED            RIGID                         SYMMETRIC
                  73.7
            1    10    1    0    14    1    0    5    1
            T     T    F
SHELL
          7.240E+10     7.240E+10          0.33          0.33
            0.00243          6.73         1.875          23.0
          1.271E+4      1.118E+5
PLATE
          7.240E+10     7.240E+10          0.33          0.33
            0.00283         23.64
          1.271E+4      6.98E+5
END
GENERATE MATRICES
CONSTRAINT
SHELL
PLATE
END
SOLVE
PUNCH
FREQUENCIES
EIGENVECTORS
      20
MODE SHAPES
TRAN                                  20   36   10    T    T
END
END OF JOB
```

MERLIN IVC

15	6
10	
5	3
50.0	
9.27	0.84
4.54	13.66

TAPE 7 SYMMETRIC MODES
TAPE 8 ANTISYMMETRIC MODES

SMALL DIAMETER NO. 1

15	6
10	
5	3
62.6	
13.0	1.145
5.34	19.68

TAPE 7 SYMMETRIC MODES
TAPE 8 ANTISYMMETRIC MODES

NARROW BODY

15	6
10	
5	3
73.7	
23.0	1.875
6.73	23.64

TAPE 7 SYMMETRIC MODES
TAPE 8 ANTISYMMETRIC MODES

Business Aircraft

MODAL INFORMATION

FREQUENCY (HZ)	STRUCTURE NO OF MODES IN BAND	STRUCTURE FIRST MODE IN BAND	CAVITY NO OF MODES IN BAND	CAVITY FIRST MODE IN BAND
	1		3	
50.0	0	0	0	0
63.0	2	2	1	4
80.0	2	4	1	5
100.0	2	6	1	6
125.0	9	8	7	7
160.0	10	17	9	14
200.0	12	27	15	23
250.0	14	39	24	38
315.0	18	53	57	62
400.0	34	71	99	119
500.0	36	105	140	218
630.0	28	141	43	358
800.0	46	169	0	0
1000.0	58	215	0	0
1250.0	58	273	0	0
1600.0	56	331	0	0
2000.0	14	387	0	0
2500.0	0	0	0	0
3150.0	0	0	0	0
4000.0	0	0	0	0
5000.0	0	0	0	0

ACOUSTIC MODES

MODE NO	FREQ (HZ)	MODE TYPE	Q	I	LOSS FACTOR	EPSILON
1	.00	SYMM	0	0	0.00000	9.6723E-01
2	22.13	SYMM	1	0	.77700	1.9345E+00
3	44.26	SYMM	2	0	.19425	1.9345E+00
4	66.39	SYMM	3	0	.07716	1.9345E+00
5	88.52	SYMM	4	0	.03574	1.9345E+00
6	110.65	SYMM	5	0	.01675	1.9345E+00
7	115.65	ANTI	0	1	.02132	2.4890E+00
8	117.75	ANTI	1	1	.02057	4.9780E+00
9	123.83	ANTI	2	1	.01860	4.9780E+00
10	132.77	SYMM	6	0	.01043	1.9345E+00
11	133.35	ANTI	3	1	.01604	4.9780E+00
12	135.64	SYMM	0	2	.01303	3.2770E+00
13	137.43	SYMM	1	2	.01269	6.5539E+00
14	142.67	SYMM	2	2	.04809	6.5539E+00
15	145.64	ANTI	4	1	.05491	4.9780E+00
16	151.01	SYMM	3	2	.04292	6.5539E+00
17	154.90	SYMM	7	0	.03130	1.9345E+00
18	160.05	ANTI	5	1	.04546	4.9780E+00
19	161.96	SYMM	4	2	.03732	6.5539E+00
20	175.04	SYMM	5	2	.03195	6.5539E+00
21	176.08	ANTI	6	1	.03756	4.9780E+00
22	177.03	SYMM	8	0	.02397	1.9345E+00
23	189.81	SYMM	6	2	.06842	6.5539E+00
24	193.31	ANTI	7	1	.07849	4.9780E+00
25	199.16	SYMM	9	0	.04769	1.9345E+00
26	200.40	ANTI	0	3	.08292	3.7504E+00
27	201.61	ANTI	1	3	.08192	7.5008E+00
28	205.22	ANTI	2	3	.07906	7.5008E+00
29	205.89	SYMM	7	2	.05815	6.5539E+00
30	211.11	ANTI	3	3	.07472	7.5008E+00
31	211.46	ANTI	8	1	.06559	4.9780E+00
32	214.55	SYMM	0	4	.06708	3.7039E+00
33	215.69	SYMM	1	4	.06637	7.4077E+00
34	219.07	SYMM	2	4	.06434	7.4077E+00
35	219.07	ANTI	4	3	.06938	7.5008E+00
36	221.29	SYMM	10	0	.03863	1.9345E+00
37	223.02	SYMM	8	2	.04956	6.5539E+00
38	224.59	SYMM	3	4	.06446	7.4077E+00
39	228.91	ANTI	5	3	.06691	7.5008E+00
40	230.30	ANTI	9	1	.05822	4.9780E+00
41	232.09	SYMM	4	4	.06036	7.4077E+00
42	240.39	ANTI	6	3	.06068	7.5008E+00
43	240.96	SYMM	9	2	.04470	6.5539E+00
44	241.40	SYMM	5	4	.05579	7.4077E+00
45	253.42	SYMM	11	0	.03361	1.9345E+00

383	600.84	SYMM	16	17	.00565	1.5947E+01
384	608.76	ANTI	17	16	.01036	1.5893E+01
385	609.13	SYMM	19	14	.00844	1.2605E+01
386	609.55	SYMM	16	18	.01095	1.3714E+01
387	612.53	SYMM	15	19	.00730	1.2510E+01
388	613.60	ANTI	19	15	.00816	1.5125E+01
389	614.18	SYMM	17	17	.00541	1.5947E+01
390	622.66	SYMM	17	18	.01050	1.3714E+01
391	622.68	ANTI	18	16	.00991	1.5893E+01
392	624.80	SYMM	16	19	.00702	1.2510E+01
393	627.97	SYMM	18	17	.00518	1.5947E+01
394	636.28	SYMM	18	18	.01005	1.3714E+01
395	637.06	ANTI	19	16	.00946	1.5893E+01
396	637.60	SYMM	17	19	.00674	1.2510E+01
397	642.24	SYMM	19	17	.00495	1.5947E+01
398	650.36	SYMM	19	18	.00962	1.3714E+01
399	650.90	SYMM	18	19	.00647	1.2510E+01
400	664.67	SYMM	19	19	.00620	1.2510E+01

STRUCTURAL MODES

MODE NO	FREQ (HZ)	MODE TYPE	LOSS FACTOR	SHELL M	SHELL NS	SHELL CMNS	PLATE NP	PLATE CMNP	GENERALIZED MASS (KG) TOTAL	SHELL U	PLATE W	JREVB
1	39.60	SYMM	.27445	1	1	.7309	0	.8908	137.89	32.072	72.202	2.4003E-03
2	56.82	ANTI	.62419	1	2	.6761	1	.4457	59.66	34.632	8.319	5.0546E-03
3	67.73	SYMM	.62905	1	2	.5748	1	-.2677	40.14	24.817	7.333	5.7677E-04
4	75.41	SYMM	.31897	2	2	.6169	0	-.5435	85.14	25.932	52.371	1.6405E-04
5	86.13	ANTI	.39695	1	1	-.7027	1	.3168	154.56	40.572	4.127	9.2364E-03
6	102.44	SYMM	.10652	3	2	.2442	1	-.5824	48.03	4.324	42.649	7.3237E-05
7	103.28	ANTI	.62288	2	2	.7326	1	.4426	56.29	33.764	8.319	2.2328E-03
8	112.22	SYMM	.16575	1	3	.2490	1	.9554	45.60	7.353	37.301	6.1924E-05
9	112.86	SYMM	.05130	4	4	.1078	1	.7309	41.43	1.585	39.672	1.1800E-05
10	113.35	SYMM	.18462	2	3	-.2687	1	-1.1167	45.92	8.336	36.151	1.1578E-04
11	121.26	SYMM	.04402	5	4	.0920	1	.7732	40.30	1.285	38.916	5.0032E-06
12	123.49	SYMM	.68750	3	2	.5946	1	1.2011	46.13	34.371	3.806	1.1155E-03
13	125.32	ANTI	.54897	1	3	.7648	1	-.4707	55.93	35.213	13.826	4.8541E-04
14	125.32	SYMM	.44423	2	2	.3620	0	.3677	36.85	17.266	10.190	1.2875E-03
15	132.27	ANTI	.57840	2	3	-.8450	1	.4567	63.14	42.277	14.756	5.2235E-04
16	132.90	SYMM	.03786	6	5	-.0929	1	.7934	39.66	1.085	38.507	2.9764E-06
17	143.80	SYMM	.16714	4	2	-.3670	0	1.0190	52.67	10.037	39.594	6.3605E-04
18	146.15	ANTI	.57997	3	3	.7048	1	-.2535	41.78	31.617	5.817	5.5631E-04
19	149.00	SYMM	.02889	7	5	-.0944	1	.8060	39.24	.958	38.234	2.0648E-06
20	150.78	ANTI	.12554	1	3	.5128	1	.6387	213.89	28.575	11.685	1.0169E-03
21	156.00	SYMM	.04244	5	2	-.1386	0	.8016	37.89	1.679	35.683	9.9538E-05
22	165.17	SYMM	.41284	3	3	.3884	2	.3041	27.03	17.415	6.072	6.5892E-04
23	166.00	ANTI	.39586	3	2	-.9052	1	-.7287	102.88	50.406	30.884	4.4685E-03
24	167.15	SYMM	.02275	6	2	-.0745	0	.7305	35.34	.667	34.484	2.8714E-05
25	170.10	SYMM	.02363	8	5	-.0947	1	.8148	38.96	.880	38.036	6.8297E-07
26	173.15	ANTI	.40346	4	3	.8165	1	-.3815	57.09	38.691	13.126	9.0734E-04
27	181.01	SYMM	.01408	7	4	.0535	0	.6932	34.34	.340	33.903	1.0575E-05
28	181.57	SYMM	.34737	1	3	.4519	2	.4872	39.10	25.632	7.027	5.1416E-04
29	193.11	ANTI	.24370	2	1	1.0020	1	-.1550	215.76	57.389	1.444	4.6052E-03
30	195.84	SYMM	.35276	2	4	.4674	1	-.2102	33.94	27.056	.152	5.9981E-04
31	196.37	SYMM	.01680	9	5	-.0943	1	.8214	38.77	.833	37.900	1.0097E-06
32	199.04	SYMM	.36641	4	3	.4370	2	.1115	21.80	18.895	.139	6.0556E-04
33	199.12	SYMM	.01156	8	4	.0421	0	.6703	33.82	.195	33.565	4.3900E-06
34	208.73	ANTI	.26996	5	3	.9062	1	-.4768	75.86	46.218	23.393	2.1590E-03
35	213.37	SYMM	.17968	1	4	.5003	2	-.6208	61.78	28.927	28.162	6.6218E-04
36	216.11	SYMM	.24966	3	4	.5637	2	-.3089	48.90	33.775	10.625	6.9200E-04
37	222.21	SYMM	.01068	9	4	.0338	0	.6549	33.50	.123	33.345	2.1374E-06
38	222.50	SYMM	.12314	2	1	.3422	2	-.7172	57.13	19.195	29.001	6.1555E-04
39	224.73	ANTI	.18976	4	2	.6230	1	.4602	63.57	33.392	22.018	1.2327E-03
40	227.73	SYMM	.01223	10	5	-.0938	1	.8269	38.65	.806	37.810	6.3569E-07
41	231.09	SYMM	.03501	1	4	-.3083	2	-.3477	1802.69	19.749	4.557	7.2734E-04
42	232.82	ANTI	.19854	1	4	.6729	2	.4970	41.16	27.670	9.002	3.3879E-04
43	232.94	ANTI	.19423	2	4	.8027	2	.5139	60.94	37.579	15.530	4.1159E-04
44	233.42	SYMM	.25895	5	3	.4479	1	-.0798	23.85	20.958	.666	5.6214E-04
45	240.37	SYMM	.18582	4	2	-.4877	2	-.3788	41.61	27.057	9.866	7.0865E-04
46	243.02	ANTI	.18732	3	4	.8064	2	.5136	55.08	37.964	11.467	5.4492E-04

53	282.66	ANTI	.08394	7	3	-.5016	2	.5885	72.95	24.945	45.468	7.6643E-04
54	287.55	ANTI	.14832	1	5	.7525	1	.3242	55.80	45.054	2.522	4.6215E-04
55	287.98	SYMM	.13782	5	2	-.5847	2	-.3439	38.92	27.131	6.097	7.7099E-04
56	288.96	ANTI	.07956	2	5	.5526	1	.6714	62.00	25.845	5.063	3.1812E-04
57	290.95	ANTI	.07847	3	1	-.7158	1	.1649	123.97	34.190	.583	9.5966E-04
58	291.91	SYMM	.11483	3	1	-.9791	2	.9356	147.02	53.414	35.934	1.6147E-03
59	297.61	ANTI	.08956	2	5	.6930	2	.0833	77.11	37.805	.055	4.5314E-04
60	300.77	SYMM	.14934	7	4	.4928	2	-.1026	26.24	23.244	.963	6.0560E-04
61	306.65	ANTI	.14637	7	4	.4446	1	-.1020	24.55	22.424	.048	5.8947E-04
62	307.81	ANTI	.12622	3	5	.6732	1	.3852	42.53	34.160	.940	4.5077E-04
63	309.29	ANTI	.12194	5	2	.5533	1	.2907	32.95	24.689	1.858	6.0641E-04
64	309.60	ANTI	.06412	8	4	.5252	2	.6402	66.95	21.173	44.081	5.6021E-04
65	325.28	ANTI	.11023	4	5	-.7908	2	.5199	51.41	38.661	.849	5.8222E-04
66	335.93	ANTI	.04840	9	4	.4993	2	.6704	61.96	17.402	43.308	3.9326E-04
67	337.38	SYMM	.11566	8	4	.5054	2	-.0975	25.24	22.674	.739	4.8768E-04
68	345.20	SYMM	.09926	6	2	-.4907	2	-.2356	30.96	24.246	2.468	5.0029E-04
69	345.59	ANTI	.10495	5	5	.8515	2	-.9068	58.11	43.028	3.247	7.7527E-04
70	346.11	ANTI	.10172	8	3	.4567	1	-.1918	27.40	22.395	2.970	4.8758E-04
71	357.22	ANTI	.08652	6	5	-.5341	2	.4636	33.85	24.761	6.555	4.7498E-04
72	363.39	ANTI	.03423	10	4	.4453	2	.6950	57.28	13.587	42.790	2.6129E-04
73	365.32	SYMM	.09767	2	5	.6104	3	.1136	39.88	34.883	2.367	5.4638E-04
74	365.88	SYMM	.09857	1	5	.6198	3	.1163	39.49	35.058	2.426	5.4925E-04
75	367.66	SYMM	.09691	3	5	.6127	3	.1169	39.01	34.487	2.109	5.3813E-04
76	368.85	SYMM	.08705	4	5	.6130	2	.2672	44.35	34.325	6.851	5.2984E-04
77	370.50	ANTI	.09038	6	2	-.8386	1	-.9775	66.82	43.861	4.762	8.3076E-04
78	373.70	ANTI	.07940	7	5	-.6123	2	.8297	42.46	30.389	9.426	5.0256E-04
79	374.09	SYMM	.09051	9	4	.5008	2	-.0825	23.54	21.524	.451	3.9138E-04
80	375.60	ANTI	.03648	1	6	-.3983	2	.8302	62.29	20.092	40.394	2.0232E-04
81	376.62	ANTI	.03611	2	6	-.3944	2	.7989	62.16	19.786	40.428	2.0495E-04
82	378.18	SYMM	.08838	5	5	.6708	2	.2236	46.51	37.810	6.239	5.8411E-04
83	378.91	ANTI	.03548	3	6	-.3688	2	.7564	53.95	17.564	33.759	1.8636E-04
84	383.39	ANTI	.07211	9	4	.3751	2	-.2067	27.81	20.582	5.714	3.7021E-04
85	383.79	ANTI	.03424	4	6	-.3622	2	.6765	57.52	17.679	33.205	2.0448E-04
86	387.84	SYMM	.08152	7	5	.4228	3	.0671	23.11	21.181	.127	3.3620E-04
87	390.02	ANTI	.07563	8	5	.5289	2	-.8165	35.40	28.161	4.806	4.2289E-04
88	391.46	SYMM	.07378	6	5	.6091	2	.2657	41.17	30.742	8.053	4.6715E-04
89	397.43	SYMM	.05376	4	1	-.5728	2	.3797	47.55	24.333	5.521	3.8940E-04
90	397.55	ANTI	.03313	5	6	-.2857	2	.4351	38.43	13.383	22.137	1.6564E-04
91	404.17	ANTI	.06413	4	1	-.8520	1	-.2826	135.23	46.862	13.439	7.4988E-04
92	407.94	ANTI	.03281	3	5	.3953	1	-.7739	43.95	20.176	20.558	3.1295E-04
93	409.43	SYMM	.07298	10	4	.4774	2	-.0592	21.71	20.246	.165	3.0725E-04
94	410.34	SYMM	.07183	8	5	.5336	3	.1187	27.63	24.378	1.823	3.5498E-04
95	411.36	ANTI	.07262	9	3	-.4628	2	-.7025	28.36	25.278	.482	3.6613E-04
96	413.53	ANTI	.05248	7	2	-.4936	1	-.6207	38.67	21.910	12.083	3.4113E-04
97	414.14	ANTI	.06239	10	4	.3911	2	-.3024	26.41	20.334	4.900	3.1003E-04
98	417.22	ANTI	.03440	6	6	.2349	2	-.2874	30.93	12.451	16.112	1.6787E-04
99	420.64	SYMM	.05652	7	2	-.4982	2	-.3546	42.25	26.269	12.089	3.7834E-04
100	431.31	SYMM	.06572	9	5	.5653	3	.1466	31.34	26.493	3.387	3.6110E-04
101	433.59	SYMM	.02378	2	5	.2559	3	.1244	29.82	8.742	1.263	9.7037E-05
102	439.05	ANTI	.05741	10	3	-.6290	1	.9152	40.83	27.894	9.614	3.7638E-04
103	442.06	ANTI	.03795	7	2	.2313	2	-.2190	23.89	12.653	9.448	1.5839E-04
104	443.30	ANTI	.04220	8	3	-.3954	1	-.6440	44.13	20.938	20.377	2.8472E-04
105	451.00	SYMM	.04294	3	5	.2176	3	.1378	11.28	8.358	1.778	9.0382E-05
106	453.55	SYMM	.04346	1	5	.2169	3	.1441	11.17	8.486	1.959	9.1896E-05
107	454.79	SYMM	.05835	10	5	.5445	3	.1625	32.67	26.721	4.463	3.3064E-04
108	455.34	SYMM	.04289	4	5	.2065	3	.1357	10.75	8.175	1.581	8.6196E-05
109	455.72	ANTI	.04516	4	5	-.4209	3	.5070	35.16	22.012	5.625	2.5014E-04
110	461.81	SYMM	.03230	2	5	.2060	3	.1574	16.79	9.085	2.522	9.6115E-05
111	[illegible]	SYMM	[illegible]	5	5	.1887	3	.1367	10.95	8.273	1.705	8.7327E-05

122	494.90	SYMM	.03929	7	6	-.2042	3	.1351	9.82	8.219	.826	7.8693E-05
123	498.32	ANTI	.03938	9	5	-.3396	2	-.2099	21.64	15.558	4.814	1.6018E-04
124	501.16	ANTI	.05326	3	6	-.6006	2	-.3092	47.62	35.623	1.955	3.5598E-04
125	501.86	SYMM	.03902	9	3	.3551	2	.2082	28.49	19.120	7.477	1.8455E-04
126	504.47	ANTI	.03685	5	1	-.6560	3	-.1781	80.51	28.796	3.804	3.0149E-04
127	506.56	ANTI	.05173	7	6	-.4613	2	-.2251	28.93	26.001	.568	2.6060E-04
128	519.73	SYMM	.03906	8	2	.2594	3	-.1408	11.17	9.826	.441	8.9840E-05
129	522.52	ANTI	.03730	10	5	.3318	2	.2037	23.17	16.448	5.624	1.5168E-04
130	525.34	ANTI	.04113	4	6	-.5940	3	-.3515	47.59	27.921	13.304	2.6059E-04
131	528.52	ANTI	.05199	8	6	.5391	2	.1804	34.08	30.165	1.600	2.8197E-04
132	530.11	SYMM	.03439	10	3	.2968	3	.1974	18.85	13.327	4.584	1.1549E-04
133	530.99	ANTI	.03215	1	6	.5706	3	.7097	61.85	23.978	32.924	2.2060E-04
134	537.05	ANTI	.02773	2	6	.5312	3	.7502	59.90	20.022	33.238	1.8263E-04
135	543.30	SYMM	.02034	1	1	.4865	3	-.2051	488.47	21.023	6.537	1.8639E-04
136	545.25	ANTI	.03678	5	6	-.5259	3	-.4427	42.25	23.850	13.654	2.1188E-04
137	551.78	SYMM	.04231	9	2	.4181	3	-.1707	19.89	17.919	.279	1.5349E-04
138	553.33	ANTI	.05325	9	6	.5907	2	.1340	39.51	34.842	2.202	3.0411E-04
139	560.67	ANTI	.03873	6	6	.7035	3	.7479	92.20	35.346	32.118	2.9566E-04
140	560.91	ANTI	.01694	3	6	.4187	3	.8709	68.41	11.968	35.172	1.0039E-04
141	563.88	SYMM	.03493	6	6	.3863	2	-.2759	37.58	22.716	10.445	1.8335E-04
142	566.98	SYMM	.04616	3	6	.6551	3	-.3970	49.41	35.497	8.041	2.8213E-04
143	570.07	SYMM	.04866	4	6	-.6523	3	.3977	47.78	37.038	7.400	2.9283E-04
144	570.62	SYMM	.04927	2	6	.6435	3	-.3866	46.73	37.101	7.354	2.9380E-04
145	571.54	SYMM	.04843	1	6	.6221	3	-.3705	44.66	35.759	6.894	2.8120E-04
146	574.18	SYMM	.04726	5	6	.6085	3	-.3777	43.27	34.532	5.634	2.6765E-04
147	579.36	ANTI	.05022	10	6	.5671	3	.1191	38.46	34.193	2.002	2.7247E-04
148	580.27	SYMM	.04609	7	6	.5553	3	-.3284	49.32	36.496	10.623	2.7186E-04
149	585.07	SYMM	.04207	10	2	.4158	3	-.1788	23.89	21.852	.277	1.6576E-04
150	590.86	SYMM	.05216	8	7	.5636	3	-.3468	61.38	46.721	12.053	3.3343E-04
151	591.40	SYMM	.03884	6	1	-.3903	3	-.2659	31.88	24.303	.491	1.7791E-04
152	592.85	ANTI	.03683	7	6	-.5709	3	-.6703	72.70	33.496	21.887	2.4732E-04
153	602.96	ANTI	.03912	6	1	.7333	3	-.1016	63.20	33.671	.616	2.4900E-04
154	604.65	SYMM	.04101	9	7	.4733	3	-.2382	38.57	29.485	7.377	2.0159E-04
155	624.61	SYMM	.03357	10	7	.3674	2	-.1740	24.50	18.509	4.736	1.1951E-04
156	628.02	SYMM	.02359	3	7	-.4984	2	-.0973	231.50	28.748	.130	1.8349E-04
157	631.43	ANTI	.03607	8	6	.4237	3	.5376	57.21	31.663	12.818	2.0159E-04
158	649.63	ANTI	.01017	4	6	.2477	3	.9574	156.49	9.575	37.173	5.5777E-05
159	650.85	SYMM	.03934	7	1	-.7021	2	.4632	54.38	33.933	7.270	2.0953E-04
160	658.16	ANTI	.01955	1	1	-.5778	3	-.1208	819.85	26.175	.555	1.5647E-04
161	672.60	ANTI	.03657	9	2	.4579	3	-.4042	45.13	29.927	6.856	1.6348E-04
162	677.15	SYMM	.02376	1	7	-.7380	2	.3629	501.05	32.411	1.664	1.8505E-04
163	681.78	ANTI	.03753	7	1	-.7900	3	-.0735	72.63	36.441	.247	2.1037E-04
164	685.10	SYMM	.02780	2	7	-.7487	2	.3791	153.10	33.220	1.410	1.8497E-04
165	685.92	SYMM	.02258	2	1	.5587	3	-.1211	270.97	28.593	.629	1.6143E-04
166	695.53	SYMM	.03359	3	7	-.7678	3	-.4268	97.63	36.625	.824	1.9848E-04
167	704.57	SYMM	.03927	8	1	.7301	2	-.5160	58.92	36.180	11.621	1.9085E-04
168	706.20	SYMM	.03891	4	7	.7999	3	.5377	86.87	41.993	1.053	2.1861E-04
169	711.13	ANTI	.03656	10	2	-.4608	3	.2841	35.44	27.474	3.052	1.3010E-04
170	717.65	SYMM	.04148	5	7	.7763	3	.6649	71.92	43.445	3.439	2.1540E-04
171	727.70	SYMM	.04096	6	7	.7085	3	.7566	62.82	41.396	8.177	1.9354E-04
172	736.12	SYMM	.03984	7	7	-.6521	3	-.8352	62.57	40.973	14.192	1.8134E-04
173	740.61	ANTI	.02751	2	7	-.5094	3	.1758	59.80	26.046	4.049	1.2112E-04
174	740.79	SYMM	.03762	1	7	.5699	3	.9817	73.40	41.193	24.726	1.8197E-04
175	743.61	SYMM	.03939	8	7	.6148	3	.9074	67.03	42.238	20.051	1.8046E-04
176	746.97	SYMM	.03296	9	1	.6198	2	-.4164	50.97	29.266	16.365	1.3532E-04
177	748.32	SYMM	.03106	2	8	.5641	3	.9664	83.76	35.263	35.125	1.5420E-04
178	749.73	ANTI	.02988	8	1	-.6176	3	-.1943	53.19	26.324	3.046	1.2600E-04
179	750.82	ANTI	.04275	3	7	.6312	3	-.1717	43.31	35.164	5.531	1.6495E-04
180	751.51	SYMM	.03388	9	7	.4711	3	.8558	43.84	28.893	11.013	1.2223E-04
181	751.66	ANTI	.04476	1	7	-.6496	4	.1754	44.52	37.518	5.363	1.7511E-04

185	759.30	SYMM	.03552	10	7	.5041	3	.6934	66.40	37.069	26.736	1.5528E-04
186	759.50	ANTI	.04227	6	7	.6453	4	-.1902	42.88	34.628	6.721	1.5865E-04
187	761.24	SYMM	.02327	4	8	.5032	3	.7273	72.59	24.578	40.608	1.0203E-04
188	762.37	ANTI	.03076	2	7	-.5598	4	.1723	57.38	28.534	3.393	1.2998E-04
189	764.14	ANTI	.04086	7	7	-.6242	4	.1912	40.19	32.267	6.616	1.4592E-04
190	771.26	ANTI	.03820	8	7	.5385	4	-.1740	33.40	26.962	4.735	1.1964E-04
191	772.73	SYMM	.01800	5	8	.3793	3	.5214	46.59	14.687	24.226	6.0032E-05
192	775.14	ANTI	.04195	9	7	-.7062	3	.2702	53.66	38.691	11.797	1.7063E-04
193	776.58	ANTI	.01601	5	1	-.3980	3	-.7955	201.61	22.195	33.511	8.9833E-05
194	780.19	SYMM	.01444	4	0	-.2516	3	.4051	72.14	14.055	5.100	5.6512E-05
195	781.88	SYMM	.03930	10	1	.7427	2	-.6375	62.63	39.025	15.101	1.6839E-04
196	784.86	ANTI	.03793	10	7	-.6226	3	.2552	43.99	31.503	10.454	1.3438E-04
197	785.60	SYMM	.01670	6	8	-.2926	3	-.3760	33.72	11.463	16.292	4.1582E-05
198	801.35	SYMM	.01770	7	8	.2307	3	.2808	26.54	10.472	11.615	3.5693E-05
199	813.01	ANTI	.03836	9	1	.8316	3	.1765	69.01	39.752	1.147	1.6249E-04
200	816.64	SYMM	.01526	1	7	-.1894	2	.3023	32.26	10.252	17.510	3.2230E-05
201	818.44	SYMM	.01946	8	1	-.2254	3	-.2221	22.43	10.365	8.855	3.3737E-05
202	835.26	SYMM	.02117	9	1	.2429	3	.1871	20.07	10.533	7.257	3.2487E-05
203	837.09	SYMM	.02866	3	0	.4469	4	.1853	88.31	33.135	.911	1.2452E-04
204	837.70	SYMM	.01403	2	7	.1900	4	-.3627	37.45	10.344	17.761	3.0495E-05
205	849.45	ANTI	.01921	3	1	-.4543	4	.2486	192.22	26.234	1.022	9.2809E-05
206	850.95	SYMM	.02239	10	1	.2500	3	.1658	18.81	10.734	6.427	3.1054E-05
207	863.00	ANTI	.04093	10	1	.8858	3	.2756	78.88	46.769	5.676	1.6793E-04
208	870.27	SYMM	.03870	5	0	.4258	4	.3152	43.34	33.775	.507	1.0976E-04
209	870.58	SYMM	.01177	3	1	.2079	4	.5040	53.99	11.001	21.507	2.7252E-05
210	883.41	ANTI	.02032	6	8	-.3692	3	-.2567	51.22	18.546	11.373	5.7532E-05
211	884.79	SYMM	.03876	6	0	.3235	4	.3518	30.37	27.447	.960	8.1831E-05
212	885.75	SYMM	.03277	4	8	.3059	4	.5404	33.21	24.292	6.478	7.2975E-05
213	890.87	SYMM	.03849	7	0	.2927	4	.3301	27.27	25.248	.767	7.4345E-05
214	892.46	SYMM	.03844	1	7	.3358	4	.3792	28.73	26.164	.613	7.7032E-05
215	894.45	SYMM	.03798	2	7	.3390	4	.3624	29.09	26.418	.387	7.7513E-05
216	896.63	SYMM	.03782	8	0	-.2760	4	-.2992	25.23	23.717	.530	6.9514E-05
217	902.96	SYMM	.03776	9	1	.2737	4	.2660	23.69	22.540	.329	6.5897E-05
218	905.28	SYMM	.03793	3	8	-.4296	3	.3830	39.28	31.865	.165	9.5828E-05
219	905.62	ANTI	.02866	1	8	-.3107	4	-.2934	19.21	14.245	3.207	4.2265E-05
220	905.80	ANTI	.02185	4	8	-.2784	4	-.2899	26.20	13.342	2.075	4.0305E-05
221	907.70	ANTI	.02872	2	8	-.3212	4	-.2969	19.63	14.536	3.277	4.2747E-05
222	909.92	SYMM	.03776	10	1	-.2980	4	-.2346	22.59	21.715	.186	6.3321E-05
223	912.66	SYMM	.01537	4	0	-.2442	4	.3942	67.01	17.120	15.585	4.4767E-05
224	914.01	ANTI	.02880	3	8	.3549	4	.3103	21.60	15.773	3.697	4.4996E-05
225	916.29	SYMM	.03857	5	8	-.5609	4	-.7891	71.36	45.241	15.904	1.3513E-04
226	918.68	ANTI	.02649	7	8	.3977	4	.3055	26.85	16.858	5.683	4.8837E-05
227	922.55	ANTI	.02727	5	8	-.3443	4	-.3231	21.80	14.845	2.364	4.3392E-05
228	928.28	SYMM	.01586	1	8	-.4702	3	.2277	430.59	29.801	3.242	8.4815E-05
229	933.02	ANTI	.02787	8	8	.4249	4	.3284	25.33	17.072	5.050	4.8294E-05
230	943.29	ANTI	.01885	4	8	-.4644	4	-.3243	72.01	20.833	6.706	6.0759E-05
231	943.45	SYMM	.03465	4	8	.4100	3	-.1983	33.27	25.989	1.803	7.3861E-05
232	946.18	ANTI	.02821	9	8	.4599	4	.3549	26.44	17.857	4.948	4.9421E-05
233	947.66	SYMM	.04270	6	0	-.4484	4	.2219	40.36	36.242	.231	1.0653E-04
234	952.25	SYMM	.02431	5	8	.5106	4	-.4658	77.09	30.419	23.951	7.7334E-05
235	956.61	ANTI	.02196	6	8	-.3967	4	-.4038	36.39	17.059	1.710	4.6117E-05
236	956.62	SYMM	.04174	7	8	-.4339	3	.1719	34.65	32.121	1.064	9.2862E-05
237	960.54	SYMM	.04075	8	8	-.4336	3	.1702	33.83	30.891	1.989	8.8271E-05
238	962.36	ANTI	.02862	10	8	.5198	4	.4034	31.12	20.247	5.045	5.5943E-05
239	963.43	SYMM	.04017	9	8	.4319	3	-.1716	33.55	30.309	2.498	8.5807E-05
240	966.20	SYMM	.03971	10	8	.4301	3	-.1760	33.38	29.895	2.855	8.3872E-05
241	969.23	SYMM	.02695	2	8	-.4686	4	.2459	65.46	29.632	7.058	8.2530E-05
242	971.81	SYMM	.01997	6	8	.4584	4	-.6706	73.67	23.167	33.213	6.1518E-05
243	[illegible]	SYMM	.03643	5	0	.5237	4	-.1476	124.08	38.502	.267	1.0487E-04

ORIGINAL PAGE IS
OF POOR QUALITY

251	1037.56	ANTI	.02966	6	9	-.6536	4	-.2750	70.08	35.135	9.158	8.6431E-05
252	1037.83	ANTI	.03781	1	9	-.6485	4	-.2846	44.84	35.333	7.531	8.6759E-05
253	1038.16	ANTI	.03810	2	9	.6862	4	.3151	53.54	39.715	8.333	9.6962E-05
254	1041.09	ANTI	.04018	3	9	.7046	4	.2971	49.94	40.394	7.890	9.7986E-05
255	1044.39	ANTI	.04011	4	9	-.7110	4	-.2807	48.91	39.984	7.176	9.5909E-05
256	1044.93	ANTI	.02853	7	9	.4947	4	.3757	46.65	27.148	1.406	6.4440E-05
257	1049.43	SYMM	.01915	9	8	-.3621	4	.8510	90.75	25.772	34.717	5.8025E-05
258	1049.70	ANTI	.01342	2	9	.4036	3	.1563	247.73	23.369	2.196	5.5334E-05
259	1049.89	ANTI	.03825	5	9	-.7013	4	-.2496	47.50	37.565	5.775	8.8679E-05
260	1054.41	ANTI	.02779	7	9	-.7335	3	-.5437	81.59	36.521	18.667	8.3335E-05
261	1055.74	ANTI	.03840	8	9	.7078	4	.2391	46.09	37.098	5.411	8.6992E-05
262	1057.97	SYMM	.01777	4	8	-.3988	4	.5507	67.45	21.145	14.839	4.3926E-05
263	1062.65	ANTI	.03888	9	9	.7306	4	.2095	46.36	37.861	5.290	8.7816E-05
264	1068.97	ANTI	.02324	6	9	.6739	4	.1663	103.74	33.285	2.467	7.6393E-05
265	1070.68	ANTI	.03936	10	9	.7674	4	.1798	49.15	39.918	5.465	9.1410E-05
266	1078.14	SYMM	.02046	10	8	-.3651	4	.8424	92.45	29.493	32.537	5.9254E-05
267	1079.81	SYMM	.03415	1	0	.6087	4	-.7841	100.01	50.285	27.084	1.1201E-04
268	1097.48	ANTI	.01878	3	1	.7304	3	.2211	336.10	37.150	.778	8.3007E-05
269	1098.33	SYMM	.01907	3	8	.4377	4	-.5808	141.86	35.542	16.298	6.1636E-05
270	1099.83	SYMM	.03489	2	0	-.6429	4	.7227	106.36	53.702	22.539	1.1504E-04
271	1100.24	SYMM	.02102	6	0	.5826	4	-.4347	728.37	46.997	7.850	1.0380E-04
272	1116.07	ANTI	.01298	7	9	.6147	3	.1042	687.49	27.356	.557	5.8745E-05
273	1124.65	SYMM	.01651	5	8	-.3101	4	.4987	69.15	23.014	11.170	3.4937E-05
274	1143.95	ANTI	.01032	8	1	-.3714	3	-.8378	90.96	14.774	25.017	2.7594E-05
275	1155.75	ANTI	.01920	4	1	.7559	3	.2802	191.22	35.988	2.049	7.2547E-05
276	1159.05	SYMM	.03525	3	0	-.7573	4	.5826	172.53	67.731	14.508	1.3352E-04
277	1171.45	ANTI	.00985	8	9	.5074	3	.5488	1445.04	23.282	7.877	4.4220E-05
278	1176.43	ANTI	.01014	1	2	-.5037	4	.1323	46571.97	24.671	.177	4.7922E-05
279	1178.96	SYMM	.01961	4	1	.3870	4	.2679	104.10	34.136	2.748	5.3534E-05
280	1187.48	SYMM	.01651	6	10	.3354	4	-.3846	73.06	25.760	6.273	3.2421E-05
281	1211.61	SYMM	.00994	1	2	-.5689	4	-.2982	1775.46	24.149	5.698	4.3693E-05
282	1214.16	ANTI	.00909	2	2	-.4510	4	.2327	2961.27	22.049	.701	3.9779E-05
283	1217.73	ANTI	.00941	9	1	-.3747	3	-.9294	100.10	13.810	33.118	2.3795E-05
284	1219.81	ANTI	.02018	5	1	.7985	3	.3705	171.50	38.925	5.315	7.0319E-05
285	1228.09	SYMM	.02112	7	10	.4470	4	-.2751	66.97	30.555	2.468	4.4105E-05
286	1230.58	ANTI	.01027	9	1	.4414	3	.9147	961.63	26.049	21.351	4.3040E-05
287	1246.61	SYMM	.02033	7	10	.5571	5	.1079	103.12	35.462	.395	5.5194E-05
288	1253.10	SYMM	.02775	5	9	.5029	5	.1499	49.56	32.815	3.930	5.2914E-05
289	1260.29	SYMM	.03324	8	10	.5581	5	.1564	42.17	35.718	2.567	5.7620E-05
290	1261.19	SYMM	.01691	2	9	-.5035	4	-.2350	89.42	26.537	7.866	4.2844E-05
291	1267.35	SYMM	.03300	9	10	.5540	5	.1854	44.37	36.771	5.081	5.8748E-05
292	1268.99	ANTI	.02629	3	10	.7530	4	-.8049	93.32	43.385	29.563	7.0629E-05
293	1270.47	SYMM	.03247	1	9	.5840	5	.2160	47.08	37.499	7.771	6.0219E-05
294	1270.90	SYMM	.02891	6	9	.5771	4	.2539	49.60	34.295	10.599	5.5034E-05
295	1271.32	ANTI	.02992	4	10	-.7963	4	.8392	82.88	47.157	34.102	7.6369E-05
296	1271.34	SYMM	.03073	3	9	-.5754	5	-.2172	46.09	34.901	8.604	5.6090E-05
297	1271.39	ANTI	.02789	1	10	.7463	4	-.7701	74.69	41.570	32.053	6.7230E-05
298	1271.57	ANTI	.02869	2	10	-.7680	4	.7992	76.43	43.916	33.133	7.1025E-05
299	1272.04	ANTI	.03007	5	10	-.8051	4	.8459	84.65	47.973	35.319	7.7463E-05
300	1272.45	SYMM	.03252	10	9	.5679	5	.2011	46.55	37.406	6.835	5.9569E-05
301	1273.13	ANTI	.03039	6	10	-.8211	4	.8604	88.15	49.565	37.306	7.9694E-05
302	1274.23	SYMM	.02713	4	9	.5504	4	.2531	46.83	30.993	10.430	4.9515E-05
303	1274.71	ANTI	.02978	7	10	-.8167	4	.8467	88.22	48.654	38.501	7.7877E-05
304	1275.41	ANTI	.02557	10	10	-.6099	4	.8657	51.45	30.952	2.570	4.9114E-05
305	1276.01	SYMM	.02483	2	9	.5176	5	.2005	56.63	31.833	5.368	5.0323E-05
306	1276.90	ANTI	.02850	8	10	-.7970	4	.8151	85.60	45.927	38.713	7.3071E-05
307	1280.05	ANTI	.02620	9	10	-.7587	4	.7538	81.79	41.262	39.135	6.5121E-05
308	1280.11	ANTI	.01526	3	10	-.6570	4	.6424	213.96	33.795	27.963	5.1502E-05
309	1284.55	ANTI	.01435	10	10	.5789	4	-.4759	104.79	24.469	41.265	3.7388E-05
310	1290.61	ANTI	.01767	6	1	.7707	3	.4433	179.20	36.377	11.503	5.8389E-05
311	1291.16	SYMM	.02034	7	9	.5872	4	.4141	86.21	33.784	22.478	4.8987E-05
[illegible]	[illegible]	[illegible]	[illegible]	10	10	[illegible]	3	[illegible]	167.70	19.472	42.253	2.7861E-05

ORIGINAL PAGE IS OF POOR QUALITY

317	1342.39	ANTI	.01312	2	1	-.7086	5	-.7167	272.34	30.867	34.940	4.5974E-05
318	1344.76	SYMM	.01312	3	2	.6478	4	.2128	350.57	32.579	1.340	4.7999E-05
319	1352.96	ANTI	.00664	4	1	-.2591	5	-.4071	335.94	17.414	23.503	1.9988E-05
320	1353.01	ANTI	.01315	1	1	-.6842	5	-.4600	401.84	34.537	5.238	4.8800E-05
321	1353.70	ANTI	.00552	3	1	.4009	5	.6663	368.87	16.166	40.690	2.0158E-05
322	1372.75	ANTI	.01343	7	1	.7286	5	.6198	247.21	32.735	21.438	4.6203E-05
323	1374.20	ANTI	.01440	2	1	-.6129	5	-.5568	106.21	28.650	9.859	3.9210E-05
324	1375.73	SYMM	.00478	8	9	.2434	5	.2305	453.17	12.075	6.811	1.3148E-05
325	1377.05	ANTI	.01006	4	2	-.5506	5	.6279	880.94	29.693	40.612	3.7981E-05
326	1379.26	SYMM	.01332	1	1	-.3945	5	.1501	34.10	14.987	2.444	1.8998E-05
327	1384.79	ANTI	.00607	5	9	.2933	5	.3714	224.86	14.248	20.005	1.6449E-05
328	1388.57	SYMM	.01238	9	9	.2502	5	.2570	32.44	14.092	8.100	1.5838E-05
329	1391.30	SYMM	.00977	6	1	-.3126	5	-.2228	51.41	14.197	3.155	1.6861E-05
330	1409.13	SYMM	.01231	2	1	-.2929	5	.2004	30.02	13.301	2.851	1.5732E-05
331	1414.43	ANTI	.00742	6	9	.3195	4	.2374	169.27	17.440	9.897	2.0878E-05
332	1416.11	ANTI	.01189	3	1	-.4610	5	-.7369	82.02	22.983	17.488	2.8020E-05
333	1424.61	SYMM	.01396	10	10	-.2804	5	.2875	27.32	14.461	6.017	1.6735E-05
334	1430.33	SYMM	.00924	4	2	.4233	4	.1616	122.59	19.185	4.265	2.4409E-05
335	1445.08	SYMM	.01498	3	10	-.3220	5	.2942	25.83	14.163	3.698	1.5731E-05
336	1450.64	ANTI	.01222	7	11	.4285	4	.3296	118.02	27.169	2.897	3.0194E-05
337	1461.85	ANTI	.01186	5	2	-.6889	5	-.4414	693.34	34.565	9.116	4.3600E-05
338	1465.67	ANTI	.01403	4	11	.4303	5	-.8025	63.93	23.705	16.352	2.5713E-05
339	1466.87	SYMM	.01372	7	10	-.2363	5	.2685	21.41	10.858	1.908	1.1745E-05
340	1466.99	ANTI	.00922	8	1	-.5856	5	-.7348	437.35	26.498	36.507	3.0781E-05
341	1468.55	SYMM	.01612	4	10	.3101	5	-.3055	19.59	12.012	2.777	1.3536E-05
342	1471.81	SYMM	.01508	5	10	-.3865	5	.3379	29.05	15.226	3.533	1.7748E-05
343	1482.73	ANTI	.02002	8	11	.5474	4	.3747	55.45	33.808	.954	3.8030E-05
344	1495.67	SYMM	.01422	6	10	-.4208	5	.3618	26.51	15.308	3.521	1.7371E-05
345	1495.72	ANTI	.02398	9	11	.6367	4	.3950	55.45	42.864	1.908	4.7932E-05
346	1495.94	ANTI	.02249	5	11	.5950	5	-.5161	47.27	36.272	3.554	4.1552E-05
347	1499.68	SYMM	.00841	5	10	-.3310	5	.2744	79.43	15.793	3.249	1.8043E-05
348	1503.45	ANTI	.02567	10	11	.6456	4	.3871	49.64	42.719	2.129	4.7568E-05
349	1503.57	SYMM	.00517	9	10	-.3672	5	.3690	2361.47	16.414	2.808	1.6551E-05
350	1506.52	ANTI	.02412	1	11	-.6391	4	-.3359	54.68	41.608	10.201	4.6147E-05
351	1508.92	SYMM	.01346	8	10	-.3159	5	.3171	20.48	11.435	1.988	1.2107E-05
352	1508.99	ANTI	.02531	6	11	-.6202	4	-.3606	45.29	38.518	1.181	4.3067E-05
353	1509.20	ANTI	.02406	2	11	.6309	4	.3270	53.44	40.350	9.785	4.4556E-05
354	1513.99	ANTI	.02366	3	11	.6218	4	.3112	54.39	39.004	11.008	4.2681E-05
355	1522.55	ANTI	.02339	7	11	-.5981	4	-.3138	48.64	35.484	1.400	3.9648E-05
356	1523.73	ANTI	.01982	4	11	.5877	5	.3751	61.75	34.786	18.560	3.7780E-05
357	1529.30	SYMM	.00916	5	2	.4703	4	.2984	107.66	17.277	2.195	1.8951E-05
358	1543.59	SYMM	.01595	7	10	-.6747	5	.5386	104.42	36.385	7.669	3.6665E-05
359	1545.83	ANTI	.01101	5	11	-.4405	5	-.7347	75.48	20.376	36.464	2.1869E-05
360	1551.23	ANTI	.01611	8	11	-.5382	4	-.2263	70.50	30.204	6.809	3.2876E-05
361	1554.78	SYMM	.01188	9	10	-.4148	5	.4131	36.52	16.149	3.041	1.6134E-05
362	1557.41	ANTI	.00493	6	11	.2556	5	.8068	86.50	8.822	35.212	9.2341E-06
363	1563.72	ANTI	.01190	9	11	-.5531	4	-.2394	211.11	31.966	.829	3.4326E-05
364	1574.17	ANTI	.00675	1	1	-.4065	5	.9335	76.20	11.931	33.959	1.2739E-05
365	1584.37	ANTI	.00612	6	10	-.2916	5	-.8213	110.27	12.539	35.359	1.2342E-05
366	1585.65	ANTI	.00666	2	1	-.4211	5	.9350	89.45	12.483	34.222	1.3090E-05
367	1600.64	ANTI	.00430	7	10	-.1866	5	-.8624	53.92	5.687	35.125	5.3837E-06
368	1602.31	SYMM	.01911	10	11	.5107	5	-.5036	54.29	34.635	5.744	3.2535E-05
369	1603.49	ANTI	.00761	9	10	.3477	5	.8190	102.76	17.290	35.604	1.6251E-05
370	1608.56	SYMM	.01898	8	11	.6210	5	-.3041	51.91	32.348	6.477	3.1819E-05
371	1611.55	ANTI	.00704	3	1	-.4761	5	.9452	121.64	15.960	34.872	1.6207E-05
372	1611.88	SYMM	.01242	6	11	-.5559	4	.3127	90.19	28.071	6.738	2.7981E-05
373	1612.89	ANTI	.01424	10	10	-.5497	5	-.7765	186.65	42.550	36.314	3.9973E-05
374	1626.55	SYMM	.01326	10	11	.7289	5	-.2973	32130.93	37.220	6.994	3.6317E-05
[illegible]	[illegible]	[illegible]	[illegible]	[illegible]	[illegible]	[illegible]	[illegible]	[illegible]	52.24	38.312	8.423	3.7659E-05

ORIGINAL PAGE IS
OF POOR QUALITY

375	[illegible]	[illegible]	[illegible]	[illegible]	[illegible]	[illegible]	[illegible]	[illegible]	[illegible]	[illegible]	[illegible]	[illegible]
376	1635.78	SYMM	.01839	6	11	.7156	5	-.3173	55.78	34.021	5.719	3.3187E-05
377	1638.29	SYMM	.02114	7	11	.7752	5	-.2104	53.33	37.037	7.666	3.6264E-05
378	1643.71	ANTI	.00411	8	1	-.2405	5	.9059	65.82	6.304	35.821	5.6335E-06
379	1659.06	SYMM	.01573	10	11	.6522	4	-.3765	53.02	26.995	8.791	2.5891E-05
380	1659.68	ANTI	.00933	4	1	-.5666	5	.9439	231.63	26.765	34.326	2.5038E-05
381	1681.82	SYMM	.01431	8	11	.7830	4	-.2861	123.57	36.711	7.207	3.4689E-05
382	1685.20	ANTI	.00782	7	2	.4385	5	-.3933	372.68	26.417	7.692	2.1588E-05
383	1699.65	ANTI	.00258	10	10	.1519	5	.9390	126.18	4.349	37.412	3.1650E-06
384	1714.06	SYMM	.01078	7	2	.6668	4	.3635	265.67	34.227	3.444	3.0339E-05
385	1715.50	ANTI	.00506	9	1	-.4043	5	.9556	127.81	11.412	38.240	1.0119E-05
386	1728.91	ANTI	.00703	5	1	-.3611	5	.5354	238.33	22.315	11.029	1.7038E-05
387	1789.20	SYMM	.00716	9	11	-.4910	4	.2366	232.50	23.096	2.712	1.8378E-05
388	1800.55	ANTI	.00690	8	12	-.4057	5	-.0905	202.97	24.469	.434	1.6232E-05
389	1802.73	ANTI	.00722	6	12	.4210	5	-.2330	194.79	25.426	2.199	1.6871E-05
390	1808.49	SYMM	.00871	8	2	.6461	4	.4204	302.67	29.673	5.260	2.3753E-05
391	1825.02	ANTI	.00663	10	1	.5719	5	-.8785	292.88	21.416	33.223	1.7000E-05
392	1859.56	ANTI	.01514	7	12	.7245	5	-.1024	97.31	42.379	.619	3.0596E-05
393	1885.21	ANTI	.01890	9	12	.7388	5	-.1255	49.33	39.567	1.037	2.8724E-05
394	1887.17	ANTI	.01743	8	12	.7714	5	-.1239	68.88	43.273	1.080	3.1249E-05
395	1903.50	ANTI	.01968	10	12	.7831	5	-.1988	49.99	42.288	2.506	3.0713E-05
396	1905.82	SYMM	.00779	9	2	.5737	4	.4445	354.90	30.245	8.209	2.0272E-05
397	1906.32	SYMM	.01328	10	12	-.7298	5	-.6335	90.84	36.983	15.716	2.6473E-05
398	1920.80	SYMM	.00854	10	12	.5840	5	.5314	92.99	23.523	17.702	1.6278E-05
399	1939.21	ANTI	.00926	9	12	-.6160	5	.1719	152.43	28.975	2.267	2.0497E-05
400	2054.62	ANTI	.00663	10	12	.3521	4	-.1592	317.08	27.748	2.135	1.5273E-05

Small Body Aircraft

MODAL INFORMATION

FREQUENCY (HZ)	STRUCTURE NO OF MODES IN BAND	STRUCTURE FIRST MODE IN BAND	CAVITY NO OF MODES IN BAND	CAVITY FIRST MODE IN BAND
	21		3	
50.0	1	22	1	4
63.0	3	23	1	5
80.0	3	26	4	6
100.0	12	29	5	10
125.0	14	41	10	15
160.0	14	55	21	25
200.0	22	69	29	46
250.0	27	91	65	75
315.0	33	118	106	140
400.0	31	151	139	246
500.0	47	182	16	385
630.0	38	229	0	0
800.0	53	267	0	0
1000.0	58	320	0	0
1250.0	22	378	0	0
1600.0	1	400	0	0
2000.0	0	0	0	0
2500.0	0	0	0	0
3150.0	0	0	0	0
4000.0	0	0	0	0
5000.0	0	0	0	0

ACOUSTIC MODES

MODE NO	FREQ (HZ)	MODE TYPE	O	I	LOSS FACTOR	EPSILON
1	.00	SYMM	0	0	0.00000	9.6858E-01
2	14.91	SYMM	1	0	.87331	1.9372E+00
3	29.83	SYMM	2	0	.21833	1.9372E+00
4	44.74	SYMM	3	0	.09703	1.9372E+00
5	59.65	SYMM	4	0	.04474	1.9372E+00
6	74.57	SYMM	5	0	.02230	1.9372E+00
7	83.88	ANTI	0	1	.02630	2.4750E+00
8	85.19	ANTI	1	1	.02550	4.9501E+00
9	89.02	ANTI	2	1	.02335	4.9501E+00
10	89.48	SYMM	6	0	.01817	1.9372E+00
11	95.06	ANTI	3	1	.02403	4.9501E+00
12	102.93	ANTI	4	1	.02050	4.9501E+00
13	104.39	SYMM	7	0	.01335	1.9372E+00
14	110.81	SYMM	0	2	.01671	3.6587E+00
15	111.81	SYMM	1	2	.06119	7.3175E+00
16	112.23	ANTI	5	1	.06427	4.9501E+00
17	114.75	SYMM	2	2	.05809	7.3175E+00
18	119.30	SYMM	8	0	.03810	1.9372E+00
19	119.50	SYMM	3	2	.05356	7.3175E+00
20	122.65	ANTI	6	1	.05382	4.9501E+00
21	125.84	SYMM	4	2	.04830	7.3175E+00
22	133.56	SYMM	5	2	.04288	7.3175E+00
23	133.91	ANTI	7	1	.04514	4.9501E+00
24	134.22	SYMM	9	0	.03010	1.9372E+00
25	142.42	SYMM	6	2	.09373	7.3175E+00
26	145.84	ANTI	8	1	.09460	4.9501E+00
27	149.13	SYMM	10	0	.06061	1.9372E+00
28	152.24	SYMM	7	2	.08203	7.3175E+00
29	157.74	ANTI	0	3	.09806	3.8533E+00
30	158.27	ANTI	9	1	.08032	4.9501E+00
31	158.45	ANTI	1	3	.09719	7.7066E+00
32	159.58	SYMM	0	4	.07582	3.7995E+00
33	160.28	SYMM	1	4	.07517	7.5990E+00
34	160.54	ANTI	2	3	.09468	7.7066E+00
35	162.34	SYMM	2	4	.07326	7.5990E+00
36	162.83	SYMM	8	2	.07171	7.3175E+00
37	163.97	ANTI	3	3	.09076	7.7066E+00
38	164.04	SYMM	11	0	.05009	1.9372E+00
39	165.73	SYMM	3	4	.07030	7.5990E+00
40	168.65	ANTI	4	3	.08579	7.7066E+00
41	170.37	SYMM	4	4	.06653	7.5990E+00
42	171.10	ANTI	10	1	.06873	4.9501E+00
43	174.05	SYMM	9	2	.06276	7.3175E+00
44	174.48	ANTI	5	3	.08015	7.7066E+00
45	176.14	SYMM	5	4	.06223	7.5990E+00
46	178.96	SYMM	12	0	.04735	1.9372E+00
47	181.35	ANTI	6	3	.08347	7.7066E+00
48	182.95	SYMM	6	4	.06490	7.5990E+00

383	446.53	ANTI	14	19	.00964	1.4324E+01
384	447.07	SYMM	17	17	.00839	1.4972E+01
385	447.76	ANTI	18	15	.00952	1.0286E+01
386	450.28	SYMM	15	18	.01104	1.2120E+01
387	453.69	ANTI	15	19	.00913	1.4324E+01
388	454.08	ANTI	18	16	.01432	1.4916E+01
389	455.69	SYMM	18	17	.00787	1.4972E+01
390	456.86	ANTI	19	15	.00915	1.0286E+01
391	457.87	SYMM	16	18	.01068	1.2120E+01
392	461.23	ANTI	16	19	.00884	1.4324E+01
393	463.05	ANTI	19	16	.01377	1.4916E+01
394	464.63	SYMM	19	17	.00757	1.4972E+01
395	465.82	SYMM	17	18	.01031	1.2120E+01
396	469.12	ANTI	17	19	.00854	1.4324E+01
397	474.10	SYMM	18	18	.00996	1.2120E+01
398	477.34	ANTI	18	19	.00825	1.4324E+01
399	482.70	SYMM	19	18	.00961	1.2120E+01
400	485.88	ANTI	19	19	.00796	1.4324E+01

STRUCTURAL MODES

MODE NO	FREQ (HZ)	MODE TYPE	LOSS FACTOR	SHELL M	SHELL NS	SHELL CMNS	PLATE NP	PLATE CMNP	GENERALIZED MASS (KG) TOTAL	SHELL d	PLATE W	JREVB
1	23.50	SYMM	.17621	1	1	.5055	0	.7413	239.40	32.773	171.254	6.3251E-04
2	35.57	SYMM	.05561	2	2	-.0988	1	.4554	117.68	2.211	114.899	8.1640E-06
3	36.79	SYMM	.09036	1	2	-.1605	1	.9052	118.59	6.827	109.260	7.8894E-05
4	37.46	SYMM	.04586	3	2	-.0494	1	.5285	111.17	.808	110.230	3.0016E-07
5	38.35	SYMM	.04342	4	4	.0482	1	.5570	108.92	.465	108.403	1.9902E-08
6	38.36	ANTI	.51558	1	2	.7405	1	.5249	171.16	83.218	52.324	4.2831E-03
7	38.91	SYMM	.04262	5	4	.0451	1	.5584	107.81	.353	107.425	4.0519E-09
8	39.42	SYMM	.04199	6	4	.0393	1	.5375	106.95	.265	106.662	1.4095E-09
9	39.61	SYMM	.55832	2	1	-.4935	1	6.6112	121.23	67.516	12.808	1.9306E-03
10	39.93	SYMM	.04140	7	4	.0323	1	.4965	106.17	.187	105.975	5.6025E-10
11	40.43	SYMM	.04091	8	4	.0252	1	.4373	105.49	.121	105.360	1.8701E-10
12	40.43	SYMM	.07569	3	4	.1460	1	2.2791	108.36	4.531	102.689	2.7226E-05
13	40.72	SYMM	.05047	4	4	-.0817	1	-1.4138	103.51	1.323	101.991	8.3065E-07
14	40.89	SYMM	.04765	5	4	-.0707	1	-1.3394	102.53	.965	101.468	8.7013E-08
15	40.93	SYMM	.04056	9	4	.0190	1	.3675	104.94	.073	104.866	7.7534E-11
16	41.07	SYMM	.05074	6	4	.0824	1	1.6934	102.01	1.338	100.578	3.8460E-09
17	41.28	SYMM	.07624	7	4	-.1459	1	-3.2503	102.75	4.396	98.084	7.3829E-09
18	41.44	SYMM	.04033	10	4	-.0141	0	-.3495	104.55	.044	104.504	3.8688E-11
19	41.59	SYMM	.64071	8	4	-.4757	1	*******	74.30	49.862	21.727	6.7177E-08
20	42.00	SYMM	.06348	9	4	.1149	1	3.1123	112.29	3.156	108.973	2.7002E-09
21	42.54	SYMM	.04723	10	4	.0601	1	1.8337	106.94	.951	105.945	7.0092E-10
22	53.65	SYMM	.36925	1	1	.6224	2	-.8281	186.07	57.814	72.810	4.7113E-03
23	59.88	ANTI	.43147	1	1	-.8758	1	.2898	485.20	107.491	19.255	1.4340E-02
24	63.16	ANTI	.37046	2	2	-.8696	1	-.7475	300.80	106.664	155.584	1.9999E-03
25	68.91	SYMM	.56481	1	2	.5828	2	.2941	106.73	65.304	27.876	1.9546E-04
26	77.01	SYMM	.58387	2	2	.5791	2	.2786	101.74	65.592	21.876	4.2030E-04
27	82.20	ANTI	.31595	1	3	-.7829	2	.6389	253.04	82.497	136.314	7.8648E-04
28	82.93	ANTI	.19493	3	3	-.4192	1	.5100	179.52	34.158	138.937	4.7811E-04
29	89.46	ANTI	.44307	2	3	-.6621	2	.6202	136.76	67.320	53.576	8.2200E-04
30	93.32	ANTI	.19808	1	2	-.5462	1	1.4786	534.38	84.598	16.600	2.2029E-03
31	93.50	ANTI	.11831	4	3	-.3528	2	.5237	153.66	18.042	133.023	1.5464E-04
32	100.97	SYMM	.56826	3	2	.5562	2	.2518	95.59	64.022	17.406	1.2230E-03
33	100.98	ANTI	.06383	5	3	-.2256	2	.4852	134.85	7.485	126.366	4.9739E-05
34	105.44	ANTI	.03873	6	3	-.1366	2	.4315	124.89	3.124	121.389	1.8076E-05
35	105.81	SYMM	.36051	2	1	-.6633	2	.5260	168.22	60.816	40.688	2.8528E-03
36	106.01	ANTI	.61637	3	3	.5042	2	-.7419	78.17	59.318	.951	1.2694E-03
37	107.90	ANTI	.02932	7	3	-.0869	1	.4472	120.44	1.561	118.705	7.7085E-06
38	109.35	ANTI	.02538	8	3	-.0591	1	.4701	118.11	.913	117.110	2.8944E-06
39	110.31	ANTI	.02341	9	3	-.0424	1	.4929	116.71	.589	116.072	6.0049E-07
40	111.02	ANTI	.02230	10	3	.0354	1	.5139	115.77	.405	115.339	1.0423E-07
41	112.33	ANTI	.34623	4	3	.7027	2	-2.5514	197.31	86.952	86.542	8.3844E-04
42	113.80	ANTI	.36112	2	2	.5431	1	-.9147	133.56	58.235	57.517	1.7134E-03
43	114.02	ANTI	.46680	5	3	.5436	2	-3.1356	96.45	62.363	23.859	2.0422E-04
44	115.02	ANTI	.42127	6	3	-.4314	2	3.4569	94.40	55.597	33.203	1.4842E-04

375	1104.25	ANTI	.03330	9	11	[illegible]	4	[illegible]	[illegible]	[illegible]	[illegible]	[illegible]
376	1108.85	ANTI	.01973	8	11	-.3888	4	.1181	157.88	66.767	4.194	3.0923E-05
377	1110.99	ANTI	.01881	7	11	-.4542	4	.1385	204.35	74.423	4.884	3.2526E-05
378	1120.86	ANTI	.01007	4	11	.2433	4	-.0754	133.80	30.052	.928	1.3144E-05
379	1121.01	ANTI	.02488	10	11	.5126	5	.1426	124.93	77.497	11.685	3.5512E-05
380	1142.79	SYMM	.01223	8	2	.4349	4	.2911	1153.55	74.685	20.243	3.3348E-05
381	1162.66	ANTI	.00828	5	2	-.2904	4	-.0514	187.56	29.399	1.520	1.2467E-05
382	1166.22	SYMM	.01714	9	11	-.5398	4	-.1413	350.47	91.578	3.741	3.6405E-05
383	1176.27	ANTI	.01011	8	1	.5023	5	-.1885	1360.18	61.873	12.663	2.6564E-05
384	1190.63	SYMM	.01528	6	11	.4402	4	.1007	108.52	46.073	1.718	1.8488E-05
385	1195.55	ANTI	.00980	9	1	.5683	5	-.1682	604.53	52.254	9.227	2.2541E-05
386	1198.35	SYMM	.01090	9	11	.4791	4	.2042	816.52	65.875	8.214	2.6625E-05
387	1205.92	SYMM	.02652	10	11	.6387	4	.1104	103.90	82.784	1.850	3.2644E-05
388	1209.03	ANTI	.00803	6	2	.3375	5	-.0893	239.72	32.903	3.194	1.3141E-05
389	1212.27	SYMM	.02715	7	11	.6578	5	-.0697	94.20	79.671	.423	3.1807E-05
390	1219.65	SYMM	.02767	8	11	.6806	5	-.0729	95.33	82.494	.420	3.2724E-05
391	1234.72	SYMM	.02471	9	11	.6908	5	-.0740	107.94	79.963	.533	3.1446E-05
392	1247.02	ANTI	.00980	9	1	.5793	5	-.2280	3304.65	64.727	17.330	2.5727E-05
393	1259.84	ANTI	.00741	7	2	.3408	5	-.1126	262.44	33.242	4.646	1.1792E-05
394	1263.18	SYMM	.00847	10	11	.3635	4	.1673	3598.59	58.983	5.009	2.1305E-05
395	1287.35	SYMM	.01398	10	11	-.6597	4	.0715	307.80	73.726	4.080	2.6717E-05
396	1294.07	ANTI	.00824	10	1	-.5459	5	.1827	937.29	50.651	10.758	1.8190E-05
397	1315.79	ANTI	.00698	8	2	-.3193	5	.1234	273.84	34.052	5.490	1.0427E-05
398	1315.87	ANTI	.00782	10	1	.5516	5	-.2088	3884.32	52.996	14.213	1.8608E-05
399	1376.24	ANTI	.03907	9	12	.3632	5	-.1103	256.11	47.656	4.755	1.3196E-05
400	1414.83	ANTI	.02122	10	12	.5632	4	.0632	87.94	71.978	.729	2.1001E-05

Narrow Body Aircraft

MODAL INFORMATION

FREQUENCY (HZ)	STRUCTURE NO OF MODES IN BAND	STRUCTURE FIRST MODE IN BAND	CAVITY NO OF MODES IN BAND	CAVITY FIRST MODE IN BAND
	16		5	
50.0	11	17	4	6
63.0	4	28	5	10
80.0	10	32	11	15
100.0	21	42	24	26
125.0	22	63	32	50
160.0	22	85	70	82
200.0	34	107	96	152
250.0	36	141	140	248
315.0	43	177	13	388
400.0	55	220	0	0
500.0	65	275	0	0
630.0	49	340	0	0
800.0	12	389	0	0
1000.0	0	0	0	0
1250.0	0	0	0	0
1600.0	0	0	0	0
2000.0	0	0	0	0
2500.0	0	0	0	0
3150.0	0	0	0	0
4000.0	0	0	0	0
5000.0	0	0	0	0

ACOUSTIC MODES

MODE NO	FREQ (HZ)	MODE TYPE	Q	I	LOSS FACTOR	EPSILON
1	296.49	SYMM	19	19	0.00000	1.3132E+01
2	8.17	SYMM	1	0	1.11685	1.9508E+00
3	16.33	SYMM	2	0	.27921	1.9508E+00
4	24.50	SYMM	3	0	.12409	1.9508E+00
5	32.67	SYMM	4	0	.06980	1.9508E+00
6	40.83	SYMM	5	0	.04467	1.9508E+00
7	49.00	SYMM	6	0	.03102	1.9508E+00
8	51.63	ANTI	0	1	.04144	2.6439E+00
9	52.27	ANTI	1	1	.04043	5.2878E+00
10	54.15	ANTI	2	1	.03767	5.2878E+00
11	57.15	ANTI	3	1	.03084	5.2878E+00
12	57.17	SYMM	7	0	.02078	1.9508E+00
13	61.09	ANTI	4	1	.02698	5.2878E+00
14	65.33	SYMM	8	0	.01591	1.9508E+00
15	65.82	ANTI	5	1	.02324	5.2878E+00
16	71.18	ANTI	6	1	.03294	5.2878E+00
17	73.50	SYMM	9	0	.02083	1.9508E+00
18	74.85	SYMM	0	2	.03056	3.9644E+00
19	75.29	SYMM	1	2	.03020	7.9288E+00
20	76.61	SYMM	2	2	.02917	7.9288E+00
21	77.03	ANTI	7	1	.02813	5.2878E+00
22	78.75	SYMM	3	2	.02760	7.9288E+00
23	81.66	SYMM	4	2	.02567	7.9288E+00
24	81.67	SYMM	10	0	.01688	1.9508E+00
25	83.27	ANTI	8	1	.02407	5.2878E+00
26	85.26	SYMM	5	2	.02355	7.9288E+00
27	89.46	SYMM	6	2	.06116	7.9288E+00
28	89.82	ANTI	9	1	.05915	5.2878E+00
29	89.83	SYMM	11	0	.03988	1.9508E+00
30	94.18	SYMM	7	2	.05518	7.9288E+00
31	96.62	ANTI	10	1	.05112	5.2878E+00
32	98.00	SYMM	12	0	.03351	1.9508E+00
33	99.35	SYMM	8	2	.04959	7.9288E+00
34	100.28	SYMM	0	3	.03876	4.8617E+00
35	100.61	SYMM	1	3	.03851	9.7235E+00
36	101.60	SYMM	2	3	.03776	9.7235E+00
37	103.23	SYMM	3	3	.03658	9.7235E+00
38	103.61	ANTI	11	1	.04445	5.2878E+00
39	104.24	ANTI	0	4	.05465	4.1110E+00
40	104.56	ANTI	1	4	.05432	8.2220E+00
41	104.90	SYMM	9	2	.04448	7.9288E+00
42	105.46	SYMM	4	3	.03504	9.7235E+00
43	105.52	ANTI	2	4	.05334	8.2220E+00
44	106.17	SYMM	13	0	.02855	1.9508E+00
45	107.08	ANTI	3	4	.05179	8.2220E+00
46	108.27	SYMM	5	3	.03325	9.7235E+00
47	109.24	ANTI	4	4	.04977	8.2220E+00
48	110.77	ANTI	12	1	.03889	5.2878E+00
49	110.78	SYMM	10	2	.03989	7.9288E+00
50	111.61	SYMM	6	3	.03129	9.7235E+00

376	269.49	ANTI	12	18	.03409	1.5335E+01
377	270.99	SYMM	12	19	.02367	1.3132E+01
378	272.05	SYMM	17	16	.02030	1.3967E+01
379	272.44	ANTI	16	17	.02380	1.7799E+01
380	272.57	ANTI	13	18	.03333	1.5335E+01
381	273.15	SYMM	19	14	.02809	1.8207E+01
382	273.79	ANTI	19	15	.01388	1.0276E+01
383	274.05	SYMM	13	19	.02315	1.3132E+01
384	275.85	ANTI	14	18	.03254	1.5335E+01
385	276.31	SYMM	18	16	.01968	1.3967E+01
386	276.45	ANTI	17	17	.02311	1.7799E+01
387	277.31	SYMM	14	19	.02261	1.3132E+01
388	279.33	ANTI	15	18	.03173	1.5335E+01
389	280.64	ANTI	18	17	.02118	1.7799E+01
390	280.74	SYMM	19	16	.01800	1.3967E+01
391	280.78	SYMM	15	19	.02062	1.3132E+01
392	283.01	ANTI	16	18	.02919	1.5335E+01
393	284.44	SYMM	16	19	.02029	1.3132E+01
394	285.00	ANTI	19	17	.02054	1.7799E+01
395	286.87	ANTI	17	18	.02841	1.5335E+01
396	288.28	SYMM	17	19	.01975	1.3132E+01
397	290.91	ANTI	18	18	.02763	1.5335E+01
398	292.30	SYMM	18	19	.01921	1.3132E+01
399	295.12	ANTI	19	18	.02684	1.5335E+01
400	296.49	SYMM	19	19	.01867	1.3132E+01

STRUCTURAL MODES

MODE NO	FREQ (HZ)	MODE TYPE	LOSS FACTOR	SHELL M	SHELL NS	SHELL CMNS	PLATE NP	PLATE CMNP	GENERALIZED MASS (KG) TOTAL	SHELL W	PLATE W	JREVB
1	13.12	SYMM	.29045	1	1	.8186	0	.9040	1504.34	307.172	864.146	1.2240E-03
2	24.82	ANTI	.58992	1	2	-.7086	1	-.4026	478.25	272.212	104.505	2.9716E-03
3	27.34	SYMM	.09488	2	3	-.2251	1	.6938	557.72	37.552	512.600	3.6995E-05
4	27.69	SYMM	.14307	1	3	.2948	1	-.9113	561.06	68.352	476.880	1.2000E-04
5	28.97	SYMM	.07341	3	3	-.1748	1	.7874	513.04	22.082	487.973	2.9388E-06
6	30.15	SYMM	.06182	4	3	-.1259	1	.8206	492.90	14.277	477.120	4.0674E-07
7	31.13	SYMM	.05628	5	4	.1111	1	.8377	481.66	10.595	470.133	6.2508E-08
8	32.02	SYMM	.05271	6	4	.1037	1	.8479	473.61	8.239	464.727	1.1318E-08
9	32.86	SYMM	.05014	7	4	.0929	1	.8548	467.23	6.543	460.227	6.5168E-09
10	33.66	SYMM	.04825	8	4	.0813	1	.8600	462.02	5.305	456.385	2.5500E-09
11	34.41	SYMM	.04689	9	4	.0703	1	.8642	457.81	4.414	453.149	1.7527E-09
12	35.15	SYMM	.04592	10	4	.0608	1	.8675	454.36	3.775	450.402	9.1734E-10
13	35.33	SYMM	.37726	2	1	.6910	0	1.4243	987.30	288.866	423.372	5.5821E-03
14	35.89	ANTI	.52300	2	2	-.9034	1	-.4956	690.72	389.553	182.962	1.5343E-03
15	36.35	ANTI	.48251	1	1	-.8150	1	.2309	1336.14	363.899	40.331	1.1627E-02
16	42.20	SYMM	.13911	3	2	-.2416	0	.9052	549.83	67.344	458.813	2.7160E-04
17	44.75	SYMM	.06359	4	3	-.1234	0	.7245	434.47	13.449	416.830	4.1345E-05
18	45.32	SYMM	.65670	1	2	.4026	1	.2492	186.18	148.135	4.148	3.2236E-04
19	45.84	SYMM	.04708	5	3	-.0719	0	.6634	409.14	3.897	404.049	1.0836E-05
20	46.40	SYMM	.04280	6	3	-.0460	0	.6341	400.55	1.540	398.542	2.8310E-06
21	46.75	SYMM	.04134	7	3	-.0312	0	.6164	396.63	.748	395.659	4.2289E-07
22	47.02	SYMM	.04075	8	3	-.0221	0	.6042	394.46	.416	393.924	6.5721E-08
23	47.27	SYMM	.04045	9	3	-.0163	0	.5952	393.12	.251	392.801	3.1124E-08
24	47.54	SYMM	.04029	10	3	.0124	0	-.5883	392.22	.160	392.015	1.1043E-08
25	48.90	ANTI	.39344	1	3	-.6610	1	.2633	533.05	234.937	79.727	8.6385E-04
26	51.49	SYMM	.56685	2	2	.3944	1	.1354	212.79	146.693	31.518	4.3657E-04
27	53.28	ANTI	.49396	3	2	-.7817	1	-.4714	596.21	306.857	204.890	2.4469E-03
28	59.09	ANTI	.22814	1	2	.4052	1	-.6081	731.67	166.534	90.900	8.8593E-04
29	61.09	ANTI	.56040	2	3	-.7682	2	.2460	462.91	314.489	49.612	9.2599E-04
30	61.19	SYMM	.22749	1	1	-.3632	2	.7256	531.12	115.386	342.699	1.0771E-03
31	62.42	SYMM	.54657	3	3	.4075	2	.1994	242.96	164.373	47.319	6.2108E-04
32	71.33	ANTI	.55443	3	3	.5471	2	-.2387	259.82	189.932	38.993	3.9623E-04
33	71.35	SYMM	.30624	2	1	-.6971	2	.8858	880.62	231.820	389.932	2.3892E-03
34	71.37	ANTI	.36633	4	3	.6125	1	-.5245	837.26	324.799	450.129	1.7080E-03
35	76.13	ANTI	.33405	2	1	-.7005	2	-.1382	945.22	283.059	18.681	2.4258E-03
36	77.23	SYMM	.56005	4	3	.4738	2	.1763	227.45	170.147	28.051	6.1987E-04
37	77.48	ANTI	.44487	1	4	.6229	2	-.3586	430.53	254.708	104.741	4.2867E-04
38	81.78	ANTI	.27129	5	3	-.6326	2	.6343	832.06	265.222	533.682	8.0112E-04
39	82.01	ANTI	.32826	2	4	.8450	1	-.3814	854.14	364.394	254.681	5.0504E-04
40	83.00	ANTI	.61095	4	2	.4129	2	-.1560	212.56	178.055	1.465	8.6133E-04
41	89.00	ANTI	.15965	6	3	.3958	2	-.7118	649.76	122.202	514.217	3.8055E-04
42	89.65	SYMM	.10561	1	3	.3448	1	.0661	930.25	105.776	6.247	3.2428E-04
43	93.29	ANTI	.08923	7	3	-.2266	2	.7681	570.86	60.254	505.230	1.4163E-04

ORIGINAL PAGE IS
OF POOR QUALITY

345	585.69	SYMM	.02482	5	0	.4750	4	.0849	1972.35	260.182	4.745	4.4752E-05
346	585.94	SYMM	.02588	6	10	.5639	5	-.2535	800.35	190.408	45.699	3.1448E-05
347	588.29	SYMM	.03645	8	1	.6301	4	-.4319	775.61	272.395	85.714	4.5724E-05
348	589.00	SYMM	.01751	4	2	-.3856	5	.3123	1467.17	173.244	22.055	2.4796E-05
349	598.37	ANTI	.03905	1	11	.3680	4	.0371	389.61	200.020	1.003	2.9091E-05
350	599.28	ANTI	.02524	9	11	-.5084	5	.5767	3009.37	349.012	179.532	4.7764E-05
351	600.34	ANTI	.03495	10	11	.4971	5	.3631	1005.25	321.799	82.930	4.5965E-05
352	601.63	ANTI	.03498	2	11	.3666	4	.0363	386.58	177.499	.670	2.5408E-05
353	606.69	ANTI	.02258	7	1	.4857	5	-.1814	943.92	187.735	17.883	2.7583E-05
354	608.44	ANTI	.01880	5	1	-.5001	5	.2425	1818.07	194.665	33.623	2.9908E-05
355	611.36	ANTI	.03473	3	11	.4058	4	.0367	350.98	167.068	.992	2.2981E-05
356	611.53	SYMM	.01530	9	11	-.4758	5	-.4374	11386.29	217.939	42.825	3.2285E-05
357	611.79	SYMM	.04380	9	11	.4892	5	.4445	379.02	223.445	44.819	3.2984E-05
358	614.32	SYMM	.04646	7	11	.6096	5	.4704	452.45	272.062	114.437	3.9278E-05
359	615.77	SYMM	.05069	5	11	.6206	5	.4735	406.30	277.469	95.714	4.0038E-05
360	615.91	SYMM	.05473	10	11	.6253	5	.4870	385.68	289.856	84.282	4.1949E-05
361	616.83	SYMM	.04752	6	11	.6466	5	.4833	529.61	311.206	98.639	4.4536E-05
362	617.61	SYMM	.05443	8	11	-.7304	5	-.5180	574.65	383.046	163.208	5.3355E-05
363	618.30	ANTI	.02306	1	11	-.5345	5	.0746	1593.10	256.869	3.219	3.4365E-05
364	624.21	SYMM	.02386	6	11	-.4942	5	-.2946	1326.68	246.656	75.664	3.3242E-05
365	624.66	ANTI	.04020	4	11	.4877	4	.0394	324.94	187.493	1.839	2.5923E-05
366	626.29	SYMM	.03269	9	11	-.4710	4	-.2686	544.69	217.033	153.729	2.9303E-05
367	632.01	SYMM	.02701	7	10	-.5449	5	-.2347	1124.46	258.918	24.674	3.6293E-05
368	634.19	ANTI	.03228	2	11	-.6636	5	.0684	1024.67	308.055	2.925	4.1848E-05
369	636.39	ANTI	.04793	5	11	-.5886	4	-.0429	335.94	238.950	2.410	3.1791E-05
370	642.75	ANTI	.00622	10	11	-.2152	5	.5820	1116.12	56.763	214.321	7.4758E-06
371	643.50	ANTI	.03688	8	11	-.6376	5	.1165	578.62	265.964	8.144	3.4915E-05
372	644.38	ANTI	.04295	6	11	-.7009	4	-.0390	560.51	306.540	.939	4.0755E-05
373	647.38	ANTI	.03019	6	11	-.5193	5	-.2066	1141.91	308.119	30.818	4.0677E-05
374	650.60	ANTI	.03385	3	11	.6301	5	-.0541	622.96	255.640	1.900	3.3578E-05
375	652.64	ANTI	.05092	7	11	-.6911	4	-.0418	391.78	294.653	1.601	3.8625E-05
376	655.95	SYMM	.01632	10	1	.4698	4	-.4707	1745.00	188.652	202.442	2.2723E-05
377	656.16	SYMM	.01882	7	2	-.5234	4	-.2052	4441.69	264.318	48.111	3.5191E-05
378	658.23	SYMM	.01682	10	1	.4654	4	-.4701	1518.98	184.841	200.169	2.2490E-05
379	658.56	ANTI	.05051	9	11	.7686	5	-.0671	447.04	323.227	3.087	4.2344E-05
380	666.37	ANTI	.03581	8	11	-.5909	5	-.0687	495.29	242.532	4.381	3.1366E-05
381	667.37	ANTI	.04673	10	11	.7745	5	-.0714	464.47	311.526	3.462	4.0036E-05
382	667.79	ANTI	.03006	4	11	.6068	5	-.0868	678.23	241.975	4.871	3.1355E-05
383	677.76	SYMM	.01945	8	10	-.5357	5	-.0356	1844.04	264.963	2.002	2.7318E-05
384	688.36	ANTI	.01398	7	1	-.3505	5	.2346	2141.84	166.953	42.222	1.9970E-05
385	689.65	ANTI	.02760	5	11	.6078	5	-.1702	1063.13	288.765	22.043	3.5528E-05
386	690.15	SYMM	.01720	8	2	-.5895	4	-.2392	6905.87	268.818	49.225	3.2098E-05
387	705.59	ANTI	.02176	9	1	.4692	5	-.1510	1070.03	234.290	22.206	2.6402E-05
388	709.77	ANTI	.03570	6	12	.4184	4	-.1152	391.56	236.555	16.029	2.5495E-05
389	714.99	ANTI	.04778	8	12	-.5384	4	.1381	333.11	296.475	13.313	3.1941E-05
390	715.19	ANTI	.04725	7	12	-.5518	4	.1408	368.53	315.287	13.378	3.3908E-05
391	717.67	ANTI	.04629	9	12	-.5382	4	.1323	337.03	292.124	9.958	3.0944E-05
392	717.95	ANTI	.05044	10	12	-.6009	4	.1479	376.09	345.518	12.437	3.6758E-05
393	724.28	SYMM	.02148	9	12	.4533	4	.0838	1029.43	272.911	5.271	2.4004E-05
394	729.32	SYMM	.01443	9	2	.4869	4	.1222	6549.03	272.197	12.446	2.5614E-05
395	734.58	ANTI	.01215	8	12	-.3725	5	-.1577	2352.02	173.362	21.150	1.7448E-05
396	758.41	ANTI	.01382	10	1	.5522	5	-.1795	1960.95	192.859	25.209	1.9501E-05
397	759.45	SYMM	.03628	10	12	-.7294	4	-.0755	653.61	395.073	3.022	3.5152E-05
398	773.67	SYMM	.01456	10	12	-.5369	4	.0855	5055.85	274.926	7.867	2.4063E-05
399	779.27	ANTI	.01200	9	2	.4712	5	-.3109	11621.06	215.445	78.555	2.0408E-05
400	823.51	ANTI	.01327	10	2	.5601	5	-.3873	56379.69	268.746	129.039	2.2886E-05

Appendix D

FLIGHT TEST PREDICTIONS

- Input Data (PAIN)
- Run No. 10 (Downsweep)

```
 NASA FLIGHT TEST COMPARISONS: RUN NO. 10
1.1012     1.204      334.08     343.0
  21
50.0       63.0       80.0       100.0      125.0      160.0      200.0      250.0
315.0      400.0      500.0      630.0      800.0      1000.0     1250.0     1600.0
2000.0     2500.0     3150.0     4000.0     5000.0
9.27       0.84       50.0       0.33
CABIN LENGTH = 7.89 METERS? FUSELAGE LENGTH = 9.27 METERS
7.89       0.00
630.0
STRUCTURAL LOSS FACTORS
0.0400     0.0320     0.0250     0.0200     0.0160     0.0125     0.0100     0.0080
0.0063     0.0050     0.0040     0.0032     0.0025     0.0020     0.0016     0.0013
0.0010     0.0008     0.0006     0.0005     0.0004
ACOUSTIC LOSS FACTORS
0.0
0.0
0.0
TRIM PANEL: INSULATION 2.1 INCHES PF105+LINING OF 1.95 KG/M2
0.055      1.95       28.10      2.0
0.0        0.0        0.0        0.0
1.6        2.1        2.7        3.3        5.0        8.0        10.1       20.0
30.0       40.0       55.0       80.0       124.0      165.0      223.0      280.0
325.0      360.0      398.0      428.0      460.0
1.63       1.48       1.32       1.16       0.95       0.75       0.58       0.47
0.38       0.30       0.25       0.21       0.17       0.14       0.115      0.01
0.08       0.065      0.055      0.050      0.045
1180.0     1179.0     1177.0     1175.0     1170.0     1165.0     1150.0     1130.0
1110.0     1070.0     1035.0     980.0      920.0      865.0      805.0      735.0
675.0      620.0      580.0      550.0      525.0
1.7        2.3        2.9        3.5        4.0        4.5        5.8        7.2
9.0        11.5       14.5       18.5       22.0       23.8       25.8       26.8
27.2       27.0       26.3       25.2       23.8
PROPELLER TONES
 FOUR BLADE DOWTY ROTOL: 2.69 M DIA, 1568 RPM, CLEARANCE=0.06 PROP DIA.
2.35        75.0        1.12        4.0         1568.0      +1.0
    5   16    8
   1   1  0.00  1.52  1.02     1      -.91667E+02      .37323E+02
   1   1  0.00  1.52  1.02     2      -.52304E+02      .66143E+01
   1   1  0.00  1.52  1.02     3      -.11721E+02      .11487E+01
   1   1  0.00  1.52  1.02     4       .29884E+02      .19901E+00
   1   1  0.00  1.52  1.02     5       .71876E+02      .34483E-01
   1   2   .15  1.53  1.02     1      -.11272E+03      .37273E+02
   1   2   .15  1.53  1.02     2      -.94720E+02      .67555E+01
   1   2   .15  1.53  1.02     3      -.75439E+02      .12022E+01
   1   2   .15  1.53  1.02     4      -.55057E+02      .21367E+00
   1   2   .15  1.53  1.02     5      -.33556E+02      .37906E-01
   1   3   .29  1.57  1.02     1      -.13034E+03      .36975E+02
```

ORIGINAL PAGE IS
OF POOR QUALITY

FOUR BLADE DOWTY ROTOL: 2.69 M DIA, 1568 RPM, CLEARANCE=0.06 PROP DIA.

PROPELLER DATA
NUMBER OF BLADES = 4.
PROPELLER RPM = 1568.0
BLADE PASSAGE FREQUENCY (HZ) = 104.5
DISTANCE OF PROPELLER C/L FROM FUSELAGE C/L (M) = 2.3500
ANGLE BETWEEN VERTICAL AND LINE FROM PROP TO FUSELAGE C/L (DEGREES) = 75.00
DISTANCE OF PROPELLER PLANE FROM FORWARD END OF FUSELAGE (M) = 1.1200

PROPELLER HARMONIC 1 AT 104.5 HZ

CIRCUM. LOCATION L	THETA	AXIAL LOCATION K= 1	2	3	4	5	6	7	8	9	10	11	12	13	14	15	16
	Z=	.094	.240	.387	.534	.680	.827	.973	1.120	1.267	1.413	1.560	1.706	1.853	2.000	2.146	2.293
		PRESSURE AMPLITUDE, DB RE 20 MICRO PA															
19	165.00	118.5	119.5	120.3	121.1	121.6	122.0	122.3	122.4	122.4	122.3	122.1	121.7	121.1	120.4	119.6	118.7
18	155.00	119.1	120.3	121.2	122.0	122.6	123.0	123.2	123.3	123.3	123.1	122.8	122.3	121.6	120.8	119.9	118.8
17	145.00	119.8	121.1	122.3	123.2	123.9	124.3	124.4	124.4	124.3	124.0	123.6	122.9	122.1	121.1	120.0	118.8
16	135.00	121.5	123.1	124.6	125.7	126.5	127.0	127.0	126.9	126.6	126.2	125.6	124.8	123.8	122.5	121.2	119.7
15	125.00	123.8	125.7	127.5	128.9	130.0	130.5	130.4	130.0	129.6	129.1	128.3	127.3	126.0	124.5	122.8	121.1
14	115.00	125.2	127.4	129.5	131.3	132.6	133.3	133.1	132.4	131.8	131.2	130.2	128.9	127.2	125.4	123.5	121.6
13	105.00	125.9	128.4	130.9	133.1	134.9	135.9	135.6	134.3	133.7	133.1	131.8	130.0	128.0	125.9	123.7	121.6
12	95.00	126.2	129.0	131.8	134.4	136.6	138.1	137.9	136.0	135.5	134.7	133.0	130.8	128.4	126.0	123.7	121.4
11	85.00	126.4	129.3	132.3	135.2	137.7	139.6	139.6	137.1	136.9	135.9	133.8	131.3	128.7	126.1	123.5	121.1
10	75.00	126.4	129.4	132.5	135.4	138.1	140.1	140.3	137.6	137.5	136.3	134.1	131.4	128.7	126.1	123.5	121.0
9	65.00	126.4	129.3	132.3	135.2	137.7	139.6	139.6	137.1	136.9	135.9	133.8	131.3	128.7	126.1	123.5	121.1
8	55.00	126.2	129.0	131.8	134.4	136.6	138.1	137.9	136.0	135.5	134.7	133.0	130.8	128.4	126.0	123.7	121.4
7	45.00	125.9	128.4	130.9	133.1	134.9	135.9	135.6	134.3	133.7	133.1	131.8	130.0	128.0	125.9	123.7	121.6
6	35.00	125.2	127.4	129.5	131.3	132.6	133.3	133.1	132.4	131.8	131.2	130.2	128.9	127.2	125.4	123.5	121.6
5	25.00	123.8	125.7	127.5	128.9	130.0	130.5	130.4	130.0	129.6	129.1	128.3	127.3	126.0	124.5	122.8	121.1
4	15.00	121.5	123.1	124.6	125.7	126.5	127.0	127.0	126.9	126.6	126.2	125.6	124.8	123.8	122.5	121.2	119.7
3	5.00	119.8	121.1	122.3	123.2	123.9	124.3	124.4	124.4	124.3	124.0	123.6	122.9	122.1	121.1	120.0	118.8
2	-5.00	119.1	120.3	121.2	122.0	122.6	123.0	123.2	123.3	123.3	123.1	122.8	122.3	121.6	120.8	119.9	118.8
1	-15.00	118.5	119.5	120.3	121.1	121.6	122.0	122.3	122.4	122.4	122.3	122.1	121.7	121.1	120.4	119.6	118.7
		PHASE (DEGREES)															
19	165.00	-109.5	-118.5	-126.3	-132.6	-137.4	-140.6	-142.4	-143.1	-143.2	-142.9	-142.6	-142.4	-142.2	-141.9	-141.5	-140.7
18	155.00	-124.6	-133.9	-141.8	-148.3	-153.0	-155.8	-156.9	-156.6	-155.6	-154.5	-153.7	-153.2	-152.9	-152.7	-152.3	-151.7
17	145.00	-137.1	-146.7	-154.9	-161.6	-166.3	-168.7	-168.9	-167.3	-164.8	-162.6	-161.1	-160.4	-160.2	-160.2	-160.1	-159.8
16	135.00	-146.1	-156.0	-164.5	-171.5	-176.4	-178.6	-177.7	-174.1	-169.5	-165.9	-163.8	-163.1	-163.3	-163.7	-164.1	-164.2
15	125.00	-150.6	-160.7	-169.6	-177.1	177.6	175.4	177.5	-176.2	-168.5	-163.0	-160.6	-160.4	-161.3	-162.5	-163.5	-164.2
14	115.00	-149.7	-160.0	-169.3	-177.2	176.8	174.1	177.2	-172.6	-160.2	-153.0	-151.0	-151.8	-153.8	-155.9	-157.8	-159.2
13	105.00	-142.9	-153.4	-162.9	-171.3	-178.1	178.3	-178.4	-162.7	-144.1	-136.1	-135.4	-137.7	-141.0	-144.2	-147.0	-149.0
12	95.00	-130.3	-140.9	-150.5	-159.3	-166.7	-171.6	-168.9	-146.8	-121.0	-114.1	-115.5	-119.3	-123.6	-127.7	-131.2	-133.9
11	85.00	-112.7	-123.2	-132.9	-141.9	-149.8	-155.6	-154.1	-126.1	-95.0	-90.2	-93.1	-97.9	-103.0	-107.7	-111.7	-114.7
10	75.00	-91.7	-102.1	-111.9	-120.9	-129.0	-135.1	-134.3	-103.7	-70.7	-67.0	-70.4	-75.6	-80.9	-85.8	-89.9	-93.2
9	65.00	-68.9	-79.4	-89.1	-98.1	-106.0	-111.8	-110.4	-82.3	-51.2	-46.4	-49.3	-54.1	-59.2	-63.9	-67.9	-71.0
8	55.00	-46.9	-57.4	-67.0	-75.8	-83.3	-88.1	-85.4	-63.3	-37.6	-30.7	-32.0	-35.8	-40.2	-44.3	-47.8	-50.5
7	45.00	-26.8	-37.3	-46.8	-55.2	-62.0	-65.6	-62.3	-46.6	-28.0	-19.9	-19.3	-21.6	-24.9	-28.1	-30.8	-32.9
6	35.00	-9.2	-19.5	-28.8	-36.8	-42.8	-45.4	-42.4	-32.1	-19.8	-12.5	-10.5	-11.4	-13.3	-15.5	-17.4	-18.7
5	25.00	6.0	-4.1	-13.1	-20.5	-25.8	-28.0	-26.0	-19.6	-11.9	-6.4	-4.1	-3.8	-4.7	-5.9	-6.9	-7.6
4	15.00	19.1	9.3	.7	-6.3	-11.2	-13.4	-12.5	-8.9	-4.3	-.6	1.4	2.1	1.9	1.5	1.1	1.0
3	5.00	30.4	20.8	12.6	6.0	1.3	-1.2	-1.4	.3	2.7	4.9	6.4	7.1	7.3	7.3	7.4	7.7
2	-5.00	40.0	30.7	22.7	16.3	11.6	8.8	7.7	8.0	9.0	10.1	10.9	11.4	11.7	11.9	12.3	12.9

FOUR BLADE DOWTY ROTOL: 2.69 M DIA, 1568 RPM, CLEARANCE=0.06 PROP DIA.

PROPELLER DATA
NUMBER OF BLADES = 4.
PROPELLER RPM = 1568.0
BLADE PASSAGE FREQUENCY (HZ) = 104.5
DISTANCE OF PROPELLER C/L FROM FUSELAGE C/L (M) = 2.3500
ANGLE BETWEEN VERTICAL AND LINE FROM PROP TO FUSELAGE C/L (DEGREES) = 75.00
DISTANCE OF PROPELLER PLANE FROM FORWARD END OF FUSELAGE (M) = 1.1200

PROPELLER HARMONIC 2 AT 209.1 HZ

AXIAL LOCATION

PRESSURE AMPLITUDE, DB RE 20 MICRO PA

CIRCUM. LOCATION L	THETA	K= 1 Z= .094	2 .240	3 .387	4 .534	5 .680	6 .827	7 .973	8 1.120	9 1.267	10 1.413	11 1.560	12 1.706	13 1.853	14 2.000	15 2.146	16 2.293
19	165.00	108.9	110.5	111.9	113.0	113.9	114.5	114.7	114.7	114.4	113.9	113.1	112.2	111.0	109.6	108.1	106.4
18	155.00	109.1	111.0	112.6	113.9	114.9	115.5	115.8	115.6	115.2	114.6	113.6	112.5	111.1	109.6	107.8	105.9
17	145.00	109.3	111.5	113.4	115.0	116.2	116.9	117.1	116.8	116.2	115.3	114.2	112.8	111.2	109.3	107.3	105.2
16	135.00	110.4	113.0	115.3	117.4	118.9	119.8	120.0	119.5	118.6	117.4	115.9	114.2	112.2	110.0	107.7	105.2
15	125.00	111.9	115.0	117.9	120.4	122.4	123.6	123.8	123.0	121.6	120.0	118.2	116.1	113.7	111.1	108.4	105.6
14	115.00	112.4	116.0	119.5	122.6	125.2	126.9	127.1	125.9	123.9	121.9	119.6	117.0	114.2	111.2	108.1	105.0
13	105.00	112.3	116.4	120.5	124.3	127.6	130.0	130.5	128.5	125.8	123.5	120.7	117.5	114.2	110.7	107.2	103.8
12	95.00	111.9	116.5	121.0	125.5	129.5	132.7	133.7	130.9	127.7	125.1	121.7	117.9	113.9	110.0	106.2	102.5
11	85.00	111.5	116.3	121.2	126.1	130.8	134.6	136.1	132.7	129.3	126.5	122.4	118.0	113.7	109.5	105.4	101.5
10	75.00	111.4	116.3	121.3	126.3	131.2	135.2	137.0	133.3	130.0	127.0	122.7	118.1	113.6	109.3	105.1	101.2
9	65.00	111.5	116.3	121.2	126.1	130.8	134.6	136.1	132.7	129.3	126.5	122.4	118.0	113.7	109.5	105.4	101.5
8	55.00	111.9	116.5	121.0	125.5	129.5	132.7	133.7	130.9	127.7	125.1	121.7	117.9	113.9	110.0	106.2	102.5
7	45.00	112.3	116.4	120.5	124.3	127.6	130.0	130.5	128.5	125.8	123.5	120.7	117.5	114.2	110.7	107.2	103.8
6	35.00	112.4	116.0	119.5	122.6	125.2	126.9	127.1	125.9	123.9	121.9	119.6	117.0	114.2	111.2	108.1	105.0
5	25.00	111.9	115.0	117.9	120.4	122.4	123.6	123.8	123.0	121.6	120.0	118.2	116.1	113.7	111.1	108.4	105.6
4	15.00	110.4	113.0	115.3	117.4	118.9	119.8	120.0	119.5	118.6	117.4	115.9	114.2	112.2	110.0	107.7	105.2
3	5.00	109.3	111.5	113.4	115.0	116.2	116.9	117.1	116.8	116.2	115.3	114.2	112.8	111.2	109.3	107.3	105.2
2	-5.00	109.1	111.0	112.6	113.9	114.9	115.5	115.8	115.6	115.2	114.6	113.6	112.5	111.1	109.6	107.8	105.9
1	-15.00	108.9	110.5	111.9	113.0	113.9	114.5	114.7	114.7	114.4	113.9	113.1	112.2	111.0	109.6	108.1	106.4

PHASE (DEGREES)

L	THETA	1	2	3	4	5	6	7	8	9	10	11	12	13	14	15	16
19	165.00	-105.0	-126.9	-146.8	-164.4	-179.7	167.6	157.3	149.4	143.4	139.0	135.8	133.5	132.2	131.7	132.1	133.5
18	155.00	-133.0	-155.1	-175.1	167.1	151.8	139.2	129.3	122.1	117.0	113.4	110.8	108.9	107.7	107.2	107.6	109.0
17	145.00	-155.5	-177.8	162.0	144.1	128.7	116.3	106.9	100.6	96.7	94.2	92.2	90.6	89.3	88.7	88.8	90.0
16	135.00	-170.9	166.9	146.6	128.6	113.2	100.9	92.1	87.1	84.9	83.9	82.6	80.9	79.2	77.9	77.5	78.1
15	125.00	-177.2	160.7	140.6	122.6	107.2	94.9	86.8	83.6	84.2	85.2	84.4	82.0	79.2	76.8	75.3	75.0
14	115.00	-173.0	165.2	145.4	127.6	112.1	99.7	92.1	91.7	96.9	100.5	99.4	95.3	90.6	86.4	83.5	82.1
13	105.00	-157.5	-178.8	161.8	144.3	128.7	116.0	108.6	111.9	124.6	130.5	127.4	120.7	113.5	107.3	102.8	100.1
12	95.00	-130.9	-151.6	-170.6	172.1	156.5	143.3	135.4	143.5	166.2	171.7	165.4	156.0	146.5	138.5	132.4	128.6
11	85.00	-94.7	-115.2	-133.8	-150.9	-166.6	179.8	171.2	-176.3	-144.7	-142.0	-150.9	-162.2	-173.1	177.6	170.5	165.9
10	75.00	-52.3	-72.6	-91.2	-108.2	-123.9	-137.7	-146.7	-132.2	-97.2	-96.1	-105.9	-117.8	-129.2	-139.0	-146.4	-151.3
9	65.00	-7.2	-27.6	-46.3	-63.4	-79.0	-92.7	-101.3	-88.8	-57.2	-54.5	-63.3	-74.6	-85.6	-94.9	-101.9	-106.6
8	55.00	36.0	15.3	-3.7	-21.0	-36.6	-49.9	-57.7	-49.6	-26.9	-21.4	-27.7	-37.1	-46.6	-54.7	-60.7	-64.5
7	45.00	74.7	53.4	34.0	16.5	.9	-11.8	-19.2	-15.9	-3.2	2.7	-.4	-7.1	-14.3	-20.5	-25.0	-27.7
6	35.00	107.9	86.1	66.3	48.5	33.0	20.6	13.1	12.6	17.8	21.4	20.3	16.2	11.5	7.3	4.4	3.1
5	25.00	135.9	113.8	93.7	75.7	60.3	48.0	39.9	36.7	37.3	38.3	37.5	35.2	32.3	29.9	28.4	28.2
4	15.00	159.6	137.3	117.1	99.1	83.7	71.3	62.6	57.6	55.6	54.3	53.1	51.4	49.6	48.4	47.9	48.5
3	5.00	179.5	157.3	137.0	119.1	103.8	91.3	82.0	75.6	71.7	69.2	67.3	65.6	64.4	63.7	63.9	65.0
2	-5.00	-163.8	174.1	154.0	136.2	120.9	108.3	98.5	91.2	86.1	82.5	79.9	78.0	76.8	76.3	76.8	78.2
1	-15.00	-150.3	-172.2	167.9	150.3	135.0	122.3	112.0	104.1	98.1	93.7	90.5	88.2	86.9	86.4	86.8	88.2

FOUR BLADE ... CLEARANCE=0.08 PROP DIA.

PROPELLER DATA
NUMBER OF BLADES = 4.
PROPELLER RPM = 1568.0
BLADE PASSAGE FREQUENCY (HZ) = 104.5
DISTANCE OF PROPELLER C/L FROM FUSELAGE C/L (M) = 2.3500
ANGLE BETWEEN VERTICAL AND LINE FROM PROP TO FUSELAGE C/L (DEGREES) = 75.00
DISTANCE OF PROPELLER PLANE FROM FORWARD END OF FUSELAGE (M) = 1.1200

PROPELLER HARMONIC 3 AT 313.6 HZ

CIRCUM. LOCATION L	THETA	K= 1 Z= .094	2 .240	3 .387	4 .534	5 .680	6 .827	7 .973	8 1.120	9 1.267	10 1.413	11 1.560	12 1.706	13 1.853	14 2.000	15 2.146	16 2.293
		PRESSURE AMPLITUDE, DB RE 20 MICRO PA															
19	165.00	99.5	101.8	103.8	105.4	106.6	107.4	107.6	107.5	106.9	106.0	104.7	103.2	101.3	99.3	97.0	94.5
18	155.00	99.3	101.9	104.2	106.1	107.5	108.4	108.7	108.5	107.7	106.6	105.1	103.2	101.1	98.8	96.2	93.4
17	145.00	99.0	102.0	104.7	107.0	108.7	109.7	110.1	109.7	108.7	107.2	105.3	103.2	100.7	98.0	95.1	92.0
16	135.00	99.4	103.0	106.2	109.1	111.3	112.7	113.1	112.5	111.1	109.1	106.7	104.1	101.2	98.0	94.6	91.1
15	125.00	100.2	104.4	108.3	111.8	114.7	116.6	117.1	116.2	114.1	111.4	108.5	105.3	101.9	98.3	94.5	90.5
14	115.00	99.8	104.6	109.4	113.7	117.5	120.2	121.0	119.6	116.4	112.9	109.3	105.5	101.5	97.3	93.1	88.8
13	105.00	98.8	104.3	109.8	115.1	120.0	123.7	125.1	122.9	118.4	114.0	109.7	105.2	100.5	95.8	91.1	86.4
12	95.00	97.5	103.6	109.9	116.1	122.0	126.9	129.1	126.2	120.1	115.3	110.2	104.8	99.4	94.2	89.1	84.1
11	85.00	96.5	103.0	109.8	116.6	123.3	129.1	132.2	128.5	121.6	116.7	110.8	104.6	98.7	93.0	87.6	82.4
10	75.00	96.2	102.8	109.7	115.8	123.7	129.8	133.3	129.4	122.3	117.2	111.0	104.5	98.4	92.6	87.1	81.8
9	65.00	96.5	103.0	109.8	116.6	123.3	129.1	132.2	128.5	121.6	116.7	110.8	104.6	98.7	93.0	87.6	82.4
8	55.00	97.5	103.6	109.9	116.1	122.0	126.9	129.1	126.2	120.1	115.3	110.2	104.8	99.4	94.2	89.1	84.1
7	45.00	98.8	104.3	109.8	115.1	120.0	123.7	125.1	122.9	118.4	114.0	109.7	105.2	100.5	95.8	91.1	86.4
6	35.00	99.8	104.6	109.4	113.7	117.5	120.2	121.0	119.6	116.4	112.9	109.3	105.5	101.5	97.3	93.1	88.8
5	25.00	100.2	104.4	108.3	111.8	114.7	116.6	117.1	116.2	114.1	111.4	108.5	105.3	101.9	98.3	94.5	90.5
4	15.00	99.4	103.0	106.2	109.1	111.3	112.7	113.1	112.5	111.1	109.1	106.7	104.1	101.2	98.0	94.6	91.1
3	5.00	99.0	102.0	104.7	107.0	108.7	109.7	110.1	109.7	108.7	107.2	105.3	103.2	100.7	98.0	95.1	92.0
2	-5.00	99.3	101.9	104.2	106.1	107.5	108.4	108.7	108.5	107.7	106.6	105.1	103.2	101.1	98.8	96.2	93.4
1	-15.00	99.5	101.8	103.8	105.4	106.6	107.4	107.6	107.5	106.9	106.0	104.7	103.2	101.3	99.3	97.0	94.5
		PHASE (DEGREES)															
19	165.00	-95.0	-130.1	-162.4	169.3	142.2	119.6	100.6	85.0	72.7	63.3	56.4	51.5	48.6	47.4	47.9	50.1
18	155.00	-136.3	-171.7	155.8	126.3	100.2	77.6	58.8	43.7	32.0	23.3	17.0	12.7	10.0	9.0	9.6	11.9
17	145.00	-169.5	155.0	122.5	93.0	66.8	44.4	25.8	11.2	.4	-7.3	-12.9	-17.0	-19.6	-20.8	-20.3	-18.2
16	135.00	168.0	132.8	100.5	71.3	45.3	23.0	4.8	-8.9	-18.5	-25.1	-30.1	-34.2	-37.3	-39.1	-39.3	-37.7
15	125.00	159.1	124.5	92.8	64.2	38.7	16.8	-.9	-13.6	-21.3	-26.2	-30.7	-35.6	-40.0	-43.2	-44.6	-44.0
14	115.00	165.9	132.2	101.5	73.9	49.2	27.7	10.5	-.5	-4.7	-6.7	-11.4	-18.4	-25.4	-30.9	-34.2	-35.1
13	105.00	-170.4	157.1	127.6	101.1	77.2	56.1	39.2	30.7	33.5	35.6	28.9	18.0	7.3	-1.3	-7.0	-9.6
12	95.00	-129.9	-161.4	170.2	144.6	121.3	100.4	83.4	78.2	92.7	97.1	86.1	70.7	56.0	44.3	36.3	32.0
11	65.00	-75.4	-106.2	-133.9	-158.9	178.2	157.3	140.0	137.9	165.1	167.2	152.3	133.7	116.3	102.5	92.8	87.3
10	75.00	-11.7	-42.2	-69.6	-94.5	-117.3	-138.3	-155.7	-156.4	-123.8	-123.7	-140.0	-159.6	-177.9	167.5	157.2	151.3
9	65.00	55.9	25.1	-2.6	-27.6	-50.5	-71.4	-88.7	-90.8	-63.6	-61.5	-76.4	-95.0	-112.3	-126.2	-135.9	-141.4
8	55.00	120.4	88.9	60.5	34.9	11.6	-9.3	-26.2	-31.5	-17.0	-12.6	-23.6	-39.0	-53.7	-65.4	-73.3	-77.6
7	45.00	178.0	145.4	115.9	89.4	65.5	44.4	27.6	19.0	21.8	23.9	17.2	6.3	-4.4	-13.0	-18.7	-21.3
6	35.00	-132.8	-166.4	162.9	135.2	110.6	89.1	71.9	60.8	56.7	54.7	50.0	43.0	36.0	30.5	27.2	26.3
5	25.00	-91.2	-125.9	-157.5	173.9	148.4	126.5	108.8	96.1	88.3	83.5	78.9	74.1	69.7	66.5	65.1	65.7
4	15.00	-56.3	-91.5	-123.8	-153.1	-179.0	158.7	140.5	126.7	117.1	110.5	105.5	101.5	98.4	96.6	96.4	98.0
3	5.00	-26.9	-62.4	-95.0	-124.5	-150.6	-173.1	168.4	153.8	143.0	135.2	129.6	125.6	123.0	121.8	122.2	124.4
2	-5.00	-2.6	-37.9	-70.5	-99.9	-126.1	-148.7	-167.5	177.4	165.8	157.1	150.8	146.4	143.7	142.7	143.3	145.6
1	-15.00	17.1	-18.1	-50.4	-79.6	-105.7	-128.3	-147.4	-162.9	-175.2	175.4	168.4	163.6	160.6	159.4	159.9	162.1

FOUR BLADE DOWTY ROTOL: 2.69 M DIA, 1568 RPM, CLEARANCE=0.06 PROP DIA.

PROPELLER DATA
NUMBER OF BLADES = 4.
PROPELLER RPM = 1568.0
BLADE PASSAGE FREQUENCY (HZ) = 104.5
DISTANCE OF PROPELLER C/L FROM FUSELAGE C/L (M) = 2.3500
ANGLE BETWEEN VERTICAL AND LINE FROM PROP TO FUSELAGE C/L (DEGREES) = 75.00
DISTANCE OF PROPELLER PLANE FROM FORWARD END OF FUSELAGE (M) = 1.1200

PROPELLER HARMONIC 4 AT 418.1 HZ

CIRCUM. LOCATION		AXIAL LOCATION															
	K=	1	2	3	4	5	6	7	8	9	10	11	12	13	14	15	16
I	THETA	Z= .094	.240	.387	.534	.680	.827	.973	1.120	1.267	1.413	1.560	1.706	1.853	2.000	2.146	2.293
		PRESSURE AMPLITUDE, DB RE 20 MICRO PA															
19	165.00	90.3	93.2	95.8	97.9	99.5	100.5	100.9	100.6	99.8	98.5	96.7	94.5	92.0	89.2	86.2	82.9
18	155.00	89.7	93.0	96.0	98.4	100.3	101.5	101.9	101.6	100.6	99.0	96.9	94.3	91.5	88.3	84.9	81.2
17	145.00	88.8	92.6	96.1	99.1	101.3	102.8	103.3	102.9	101.5	99.5	96.9	93.9	90.6	87.0	83.2	79.1
16	135.00	88.5	93.0	97.2	100.9	103.8	105.7	106.4	105.7	103.9	101.2	98.0	94.4	90.5	86.3	81.9	77.4
15	125.00	88.5	93.8	98.8	103.3	107.0	109.6	110.6	109.7	107.0	103.4	99.3	95.0	90.5	85.7	80.8	75.8
14	115.00	87.2	93.3	99.2	104.8	109.7	113.4	114.8	113.4	109.5	104.4	99.3	94.3	89.1	83.8	78.4	72.9
13	105.00	85.2	92.1	99.1	105.9	112.2	117.3	119.6	117.6	111.5	104.8	98.7	92.9	87.1	81.2	75.3	69.4
12	95.00	83.1	90.8	98.6	106.6	114.3	120.9	124.4	121.6	113.0	105.2	98.4	91.6	85.0	78.6	72.3	66.0
11	85.00	81.5	89.7	98.1	106.9	115.6	123.4	128.1	124.7	114.0	106.3	98.5	90.8	83.5	76.7	70.0	63.4
10	75.00	80.9	89.2	97.9	107.0	116.0	124.2	129.5	125.8	114.4	106.9	98.7	90.5	83.0	76.0	69.2	62.5
9	65.00	81.5	89.7	98.1	106.9	115.6	123.4	128.1	124.7	114.0	106.3	98.5	90.8	83.5	76.7	70.0	63.4
8	55.00	83.1	90.8	98.6	106.6	114.3	120.9	124.4	121.6	113.0	105.2	98.4	91.6	85.0	78.6	72.3	66.0
7	45.00	85.2	92.1	99.1	105.9	112.2	117.3	119.6	117.6	111.5	104.8	98.7	92.9	87.1	81.2	75.3	69.4
6	35.00	87.2	93.3	99.2	104.8	109.7	113.4	114.8	113.4	109.5	104.4	99.3	94.3	89.1	83.8	78.4	72.9
5	25.00	88.5	93.8	98.8	103.3	107.0	109.6	110.6	109.7	107.0	103.4	99.3	95.0	90.5	85.7	80.8	75.8
4	15.00	88.5	93.0	97.2	100.9	103.8	105.7	106.4	105.7	103.9	101.2	98.0	94.4	90.5	86.3	81.9	77.4
3	5.00	88.8	92.6	96.1	99.1	101.3	102.8	103.3	102.9	101.5	99.5	96.9	93.9	90.6	87.0	83.2	79.1
2	-5.00	89.7	93.0	96.0	98.4	100.3	101.5	101.9	101.6	100.6	99.0	96.9	94.3	91.5	88.3	84.9	81.2
1	-15.00	90.3	93.2	95.8	97.9	99.5	100.5	100.9	100.6	99.8	98.5	96.7	94.5	92.0	89.2	86.2	82.9
		PHASE (DEGREES)															
19	165.00	-81.7	-130.3	-175.1	144.0	107.1	74.5	46.5	23.1	4.2	-10.5	-21.5	-29.2	-33.9	-35.9	-35.4	-32.4
18	155.00	-136.7	174.6	129.5	88.3	51.2	18.7	-9.2	-32.3	-50.8	-64.9	-75.3	-82.4	-86.7	-88.3	-87.5	-84.3
17	145.00	179.1	130.4	85.3	44.2	7.3	-25.2	-53.0	-75.9	-93.8	-107.3	-117.0	-123.7	-127.9	-129.4	-128.7	-125.5
16	135.00	149.3	100.9	56.3	15.8	-20.7	-52.8	-80.3	-102.8	-120.1	-132.9	-142.1	-148.8	-153.3	-155.5	-155.4	-152.7
15	125.00	137.4	90.0	46.5	7.2	-28.2	-59.6	-86.5	-108.5	-125.0	-136.9	-146.0	-153.4	-159.2	-162.9	-164.1	-162.4
14	115.00	146.5	100.6	58.8	21.3	-12.5	-42.6	-68.8	-90.0	-104.8	-114.7	-123.8	-133.4	-142.1	-148.5	-151.8	-151.8
13	105.00	178.3	134.2	94.4	58.8	26.9	-2.0	-27.6	-47.3	-57.3	-62.3	-72.6	-87.0	-100.5	-110.8	-117.0	-119.1
12	95.00	-127.9	-170.3	151.9	118.1	87.3	59.1	33.9	16.2	16.8	19.2	4.4	-16.9	-36.4	-51.0	-60.3	-64.6
11	85.00	-55.1	-96.4	-133.1	-165.9	164.2	136.3	111.0	95.3	110.9	115.4	94.7	68.2	44.2	26.2	14.5	8.6
10	75.00	29.9	-11.0	-47.2	-79.7	-109.5	-137.4	-162.7	-177.4	-154.2	-151.3	-174.1	157.7	132.1	112.9	100.5	94.1
9	65.00	120.0	78.7	42.0	9.2	-20.7	-48.6	-73.9	-89.6	-74.0	-69.5	-90.2	-116.7	-140.7	-158.7	-170.4	-176.3
8	55.00	-154.0	163.5	125.7	91.8	61.1	32.8	7.6	-10.0	-9.4	-7.0	-21.8	-43.1	-62.6	-77.2	-86.5	-90.9
7	45.00	-77.3	-121.4	-161.2	163.2	131.3	102.4	76.8	57.1	47.1	42.1	31.8	17.4	3.9	-6.4	-12.5	-14.7
6	35.00	-11.6	-57.6	-59.3	-136.9	-170.6	159.3	133.0	111.8	97.1	87.2	78.0	68.4	59.7	53.4	50.1	50.0
5	25.00	43.7	-3.8	-47.2	-86.6	-122.0	-153.3	179.7	157.8	141.2	129.4	120.3	112.8	107.0	103.3	102.2	103.8
4	15.00	90.2	41.9	-2.9	-43.3	-79.8	-111.9	-139.4	-161.9	-179.2	168.0	158.8	152.1	147.6	145.4	145.5	148.2
3	5.00	129.2	90.5	35.4	-5.8	-42.7	-75.1	-102.9	-125.8	-143.7	-157.2	-166.9	-173.6	-177.7	-179.3	-178.6	-175.4
2	-5.00	161.6	112.9	67.8	26.6	-10.5	-43.0	-70.9	-94.0	-112.5	-126.6	-137.0	-144.1	-148.4	-150.0	-149.2	-146.0
1	-15.00	-172.3	139.1	94.3	53.4	16.5	-16.1	-44.1	-67.4	-86.3	-101.1	-112.1	-119.8	-124.5	-126.5	-125.9	-123.0

FOUR BLADE DOWTY ROTOL: 2.69 M DIA, 1568 RPM, CLEARANCE=0.06 PROP DIA.

PROPELLER DATA
NUMBER OF BLADES = 4.
PROPELLER RPM = 1568.0
BLADE PASSAGE FREQUENCY (HZ) = 104.5
DISTANCE OF PROPELLER C/L FROM FUSELAGE C/L (M) = 2.3500
ANGLE BETWEEN VERTICAL AND LINE FROM PROP TO FUSELAGE C/L (DEGREES) = 75.00
DISTANCE OF PROPELLER PLANE FROM FORWARD END OF FUSELAGE (M) = 1.1200

PROPELLER HARMONIC 5 AT 522.7 HZ

ORIGINAL PAGE IS OF POOR QUALITY

CIRCUM. LOCATION L	THETA	K= 1	2	3	4	5	6	7	8	9	10	11	12	13	14	15	16
	Z=	.094	.240	.387	.534	.680	.827	.973	1.120	1.267	1.413	1.560	1.706	1.853	2.000	2.146	2.293
		PRESSURE AMPLITUDE, DB RE 20 MICRO PA															
19	165.00	81.0	84.7	87.9	90.5	92.4	93.7	94.2	93.9	92.9	91.2	88.9	86.2	83.0	79.4	75.6	71.4
18	155.00	80.0	84.2	87.8	90.8	93.2	94.7	95.3	94.9	93.7	91.6	88.9	85.7	82.1	78.1	73.8	69.2
17	145.00	78.6	83.3	87.5	91.2	94.0	95.9	96.6	96.2	94.6	92.1	88.8	85.0	80.8	76.3	71.5	66.5
16	135.00	77.6	83.1	88.2	92.7	96.3	98.7	99.7	99.1	97.0	93.7	89.6	85.1	80.1	74.9	69.5	63.8
15	125.00	76.8	83.2	89.2	94.7	99.3	102.6	104.0	103.2	100.2	95.7	90.6	85.1	79.4	73.5	67.4	61.2
14	115.00	74.6	81.9	89.1	95.9	101.9	106.5	108.6	107.4	102.9	96.6	90.0	83.5	77.1	70.6	63.9	57.2
13	105.00	71.8	80.0	88.3	96.6	104.3	110.7	114.1	112.3	105.2	96.3	88.2	80.9	73.9	66.9	59.8	52.6
12	95.00	68.8	77.9	87.3	96.9	106.4	114.8	119.7	117.3	106.7	95.2	86.1	78.1	70.6	63.1	55.6	48.1
11	85.00	66.5	76.2	86.4	97.1	107.8	117.6	124.0	121.0	106.9	94.9	85.3	76.4	68.2	60.3	52.4	44.5
10	75.00	65.7	75.7	86.1	97.0	108.2	118.6	125.6	122.4	106.8	95.4	85.4	75.8	67.3	59.3	51.4	43.5
9	65.00	66.5	76.2	86.4	97.1	107.8	117.6	124.0	121.0	106.9	94.9	85.3	76.4	68.2	60.3	52.4	44.5
8	55.00	68.9	77.9	87.3	96.9	106.4	114.8	119.7	117.3	106.7	95.2	86.1	78.1	70.6	63.1	55.6	48.1
7	45.00	71.8	80.0	88.3	96.6	104.3	110.7	114.1	112.3	105.2	96.3	88.2	80.9	73.9	66.9	59.8	52.6
6	35.00	74.6	81.9	89.1	95.9	101.9	106.5	108.6	107.4	102.9	96.6	90.0	83.5	77.1	70.6	63.9	57.2
5	25.00	76.8	83.2	89.2	94.7	99.3	102.6	104.0	103.2	100.2	95.7	90.6	85.1	79.4	73.5	67.4	61.2
4	15.00	77.6	83.1	88.2	92.7	96.3	98.7	99.7	99.1	97.0	93.7	89.6	85.1	80.1	74.9	69.5	63.8
3	5.00	78.6	83.3	87.5	91.2	94.0	95.9	96.6	96.2	94.6	92.1	88.8	85.0	80.8	76.3	71.5	66.5
2	-5.00	80.0	84.2	87.8	90.8	93.2	94.7	95.3	94.9	93.7	91.6	88.9	85.7	82.1	78.1	73.8	69.2
1	-15.00	81.0	84.7	87.9	90.5	92.4	93.7	94.2	93.9	92.9	91.2	88.9	86.2	83.0	79.4	75.6	71.4
		PHASE (DEGREES)															
19	165.00	-66.6	-128.7	174.1	121.6	73.8	31.2	-5.6	-36.8	-62.4	-82.7	-98.0	-108.8	-115.5	-118.4	-118.0	-114.3
18	155.00	-135.5	162.6	105.1	51.9	4.0	-38.4	-75.2	-106.4	-131.9	-151.7	-166.5	-176.6	177.3	174.8	175.7	179.8
17	145.00	169.5	107.5	49.6	-3.2	-50.7	-93.1	-130.1	-161.2	173.7	154.3	140.1	130.4	124.7	122.4	123.5	127.6
16	135.00	132.3	70.5	13.4	-38.4	-85.3	-127.3	-163.9	165.1	140.1	120.9	106.9	97.2	91.1	88.5	89.1	93.0
15	125.00	117.4	56.7	1.3	-48.8	-94.1	-134.8	-170.7	158.4	133.2	113.7	99.3	88.8	91.6	77.6	77.0	79.9
14	115.00	128.7	70.0	16.9	-30.6	-73.1	-111.7	-145.6	-177.4	157.2	137.8	122.7	110.2	100.3	93.7	91.0	92.2
13	105.00	168.0	112.3	61.9	17.2	-22.6	-59.0	-92.7	-122.9	-146.6	-163.1	-178.7	164.4	149.4	138.6	132.7	131.6
12	95.00	-125.3	-178.4	134.5	92.4	54.2	18.9	-14.2	-43.2	-60.4	-66.2	-83.4	-109.0	-131.9	-148.5	-158.5	-162.7
11	85.00	-33.6	-96.0	-131.9	-172.2	151.1	116.4	83.4	55.4	50.2	58.2	33.8	-1.3	-31.3	-52.2	-64.9	-70.9
10	75.00	71.9	20.9	-24.0	-64.1	-101.0	-135.6	-168.3	164.2	167.0	178.4	150.5	112.3	79.3	56.5	43.0	37.5
9	65.00	-174.7	132.9	87.0	46.7	10.0	-24.8	-57.7	-85.8	-90.9	-82.9	-107.3	-142.4	-172.4	166.7	154.0	148.0
8	55.00	-68.1	-121.2	-168.2	149.6	111.4	76.1	43.1	14.1	-3.1	-9.0	-26.2	-51.8	-74.7	-91.3	-101.3	-105.5
7	45.00	28.5	-27.2	-77.6	-122.3	-162.1	161.5	127.8	97.6	73.9	57.4	41.8	24.9	9.9	-.9	-6.8	-7.9
6	35.00	111.0	52.3	-.9	-48.3	-90.9	-129.4	-164.3	164.9	139.5	120.1	105.0	92.5	82.6	76.0	73.2	74.5
5	25.00	-179.8	119.5	64.1	14.0	-31.3	-71.9	-107.9	-138.8	-164.0	176.5	162.2	151.6	144.4	140.4	139.8	142.7
4	15.00	-121.6	176.6	119.5	67.7	20.8	-21.2	-57.8	-88.8	-113.8	-133.0	-147.0	-156.7	-162.8	-165.4	-164.8	-160.9
3	5.00	-72.9	-134.9	167.2	114.4	66.9	24.5	-12.5	-43.6	-68.7	-88.1	-102.3	-111.9	-117.7	-120.0	-118.9	-114.7

NASA FLIGHT TEST COMPARISONS: RUN NO. 10
MERLIN IVC
CABIN LENGTH = 7.89 METERS, FUSELAGE LENGTH = 9.27 METERS
TRIM PANEL: INSULATION 2.1 INCHES PF105+LINING OF 1.95 KG/M2

FOUR BLADE DOWTY ROTOL: 2.69 M DIA, 1568 RPM, CLEARANCE=0.06 PROP DIA.

TONE TRANSMISSION AT FREQUENCIES AT OR ABOVE 630.0 HZ IS WITH HIGH FREQUENCY FORMULATION

```
++++++++++++++++++++++++++++++++++++++++++++++++++++++++++
+  NOTATION FOR MODES OF CYLINDER WITH FLOOR             +
+  ======================================               +
+  ACOUSTIC MODES:                                       +
+  O = NO. OF AXIAL HALF-WAVES                           +
+  I = ASSIGNED ORDER OF 2-DIMENSIONAL MODAL PATTERN     +
+        IN CYLINDER CROSS-SECTION                       +
+                                                        +
+  STRUCTURAL MODES:                                     +
+  M = NO. OF AXIAL HALF-WAVES                           +
+  N = NO. OF CIRCUMFERENTIAL WAVES AROUND FUSELAGE FOR  +
+        LARGEST SHELL GEN. COORDINATES FOR THIS MODE    +
++++++++++++++++++++++++++++++++++++++++++++++++++++++++++
```

TONE TRANSMISSION FOR FREQUENCY 104.5 HZ, HARMONIC NO. 1

ACOUSTIC MODE NO	FREQ	O	I	STRUCTURAL MODE NO	FREQ	M	N	ETA R#	M.S.PRESSURE (PA**2)
4	65.2	3	0	6	102.4	3	2	.00023	1.9973E-01
6	108.7	5	0	11	121.3	5	4	.00116	2.0834E-01
14	142.4	2	2	6	102.4	3	2	.00094	2.5007E-01
8	117.7	1	1	7	103.3	2	2	.00346	5.9139E-01
6	108.7	5	0	6	102.4	3	2	.00017	6.2569E-01
					TOTAL =			99.90 DB	3.9111E+00

TONE TRANSMISSION FOR FREQUENCY 209.1 HZ, HARMONIC NO. 2

ACOUSTIC MODE NO	FREQ	O	I	STRUCTURAL MODE NO	FREQ	M	N	ETA R#	M.S.PRESSURE (PA**2)
35	219.4	4	3	39	224.7	4	2	.08632	6.9210E-02
33	215.6	1	4	38	222.5	2	1	.00148	1.2638E-01
31	210.7	3	3	23	166.0	3	2	.00523	2.5939E-01
31	210.7	3	3	39	224.7	4	2	.03040	2.6261E-01
29	205.1	2	3	23	166.0	3	2	.01236	3.6370E-01
					TOTAL =			96.59 DB	1.8247E+00

TONE TRANSMISSION FOR FREQUENCY 313.6 HZ, HARMONIC NO. 3

ACOUSTIC MODE NO	FREQ	O	I	STRUCTURAL MODE NO	FREQ	M	N	ETA R#	M.S.PRESSURE (PA**2)

TONE TRANSMISSION FOR FREQUENCY 209.1 HZ. HARMONIC NO. 2

ACOUSTIC MODE NO	FREQ	Q	I	STRUCTURAL MODE NO	FREQ	M	N	ETA R#	M.S.PRESSURE (PA**2)
35	218.4	4	3	39	224.7	4	2	.08632	6.9210E-02
33	215.6	1	4	38	222.5	2	1	.00148	1.2638E-01
31	210.7	3	3	23	166.0	3	2	.00523	2.5939E-01
31	210.7	3	3	39	224.7	4	2	.03040	2.6261E-01
29	205.1	2	3	23	166.0	3	2	.01236	3.6370E-01

TOTAL = 96.59 DB 1.8247E+00

TONE TRANSMISSION FOR FREQUENCY 313.6 HZ. HARMONIC NO. 3

ACOUSTIC MODE NO	FREQ	Q	I	STRUCTURAL MODE NO	FREQ	M	N	ETA R#	M.S.PRESSURE (PA**2)
92	323.6	7	6	64	309.6	8	4	.00095	7.6146E-03
86	312.3	5	7	55	288.0	5	2	.00000	8.8725E-03
83	305.6	5	6	53	282.7	7	3	.00355	9.1306E-03
88	314.0	6	6	47	248.3	6	3	.00115	1.0669E-02
88	314.0	6	6	64	309.6	8	4	.02334	1.1205E-01

TOTAL = 88.06 DB 2.5558E-01

TONE TRANSMISSION FOR FREQUENCY 418.1 HZ. HARMONIC NO. 4

ACOUSTIC MODE NO	FREQ	Q	I	STRUCTURAL MODE NO	FREQ	M	N	ETA R#	M.S.PRESSURE (PA**2)
184	419.5	2	13	75	367.7	3	5	.00390	3.0984E-03
190	424.0	4	12	98	417.2	6	6	.00058	3.4825E-03
186	420.0	3	12	92	407.9	3	5	.00456	3.9299E-03
186	420.0	3	12	109	455.7	4	5	.00149	6.5557E-03
182	417.2	2	12	92	407.9	3	5	.01320	7.5219E-03

TOTAL = 83.92 DB 9.8740E-02

TONE TRANSMISSION FOR FREQUENCY 522.7 HZ. HARMONIC NO. 5

ACOUSTIC MODE NO	FREQ	Q	I	STRUCTURAL MODE NO	FREQ	M	N	ETA R#	M.S.PRESSURE (PA**2)
322	523.4	9	17	132	530.1	10	3	.00131	1.6537E-04
314	517.0	9	16	129	522.5	10	5	.01202	1.7478E-04
320	522.1	4	19	141	563.9	6	6	.00017	3.4575E-04
320	522.1	4	19	143	570.1	4	6	.00017	3.4744E-04
325	525.8	8	18	132	530.1	10	3	.00494	3.8636E-04

TOTAL = 71.02 DA 5.0524E-03

NASA FLIGHT TEST COMPARISONS: RUN NO. 10
MERLIN IVC
CABIN LENGTH = 7.89 METERS: FUSELAGE LENGTH = 9.27 METERS
TRIM PANEL: INSULATION 2.1 INCHES PF105+LINING OF 1.95 KG/M2

FOUR BLADE DOWTY ROTOL: 2.69 M DIA. 1568 RPM. CLEARANCE=0.06 PROP DIA.

TONE TRANSMISSION AT FREQUENCIES AT OR ABOVE 630.0 HZ IS WITH HIGH FREQUENCY FORMULATION

TONE TRANSMISSION FOR PROPELLER HARMONICS

HARMONIC NO	FREQ	INTERIOR MEAN SQ. PRESSURE PA**2	DB RE 20 MICRO PA	EXPECTED VALUE
1	104.5	3.9111E+00	99.90	~~113.59~~ Spurious
2	209.1	1.8247E+00	96.59	96.85
3	313.6	2.5558E-01	88.06	86.90
4	418.1	9.8740E-02	83.92	70.81
5	522.7	5.0524E-03	71.02	62.60

1. Report No.	2. Government Accession No.	3. Recipient's Catalog No.
NASA CR-172428		

4. Title and Subtitle Propeller Aircraft Interior Noise Model Utilization Study and Validation	5. Report Date September 1984
	6. Performing Organization Code
7. Author(s) L.D. Pope	8. Performing Organization Report No. 84-001
	10. Work Unit No.
9. Performing Organization Name and Address L.D. Pope, Ph.D., P.E./Consulting Engineer 1776 Woodstead Ct., Suite 111 The Woodlands, TX 77380 P.O. Box 7956, The Woodlands, TX 77387	11. Contract or Grant No. NAS1-17281
	13. Type of Report and Period Covered Contractor report
12. Sponsoring Agency Name and Address National Aeronautics and Space Administration Washington, DC 20546	14. Sponsoring Agency Code

15. Supplementary Notes

Langley Technical Monitor: William H. Mayes

16. Abstract

Utilization and validation of a computer program designed for aircraft interior noise prediction is considered. The program, entitled PAIN (an acronym for Propeller Aircraft Interior Noise), permits (in theory) predictions of sound levels inside propeller driven aircraft arising from sidewall transmission. The objective of the work reported was to determine the practicality of making predictions for various airplanes and the extent of the program's capabilities. The ultimate purpose was to discern the quality of predictions for tonal levels inside an aircraft occurring at the propeller blade passage frequency and its harmonics. The effort involved three tasks:

1) program validation through comparisons of predictions with scale-model test results,
2) development of utilization schemes for large (full scale) fuselages, and
3) validation through comparisons of predictions with measurements taken in flight tests on a turboprop aircraft.

Findings should enable future users of the program to efficiently undertake and correctly interpret predictions.

17. Key Words (Suggested by Author(s))	18. Distribution Statement
Aircraft Interior Noise Propeller Noise Sound Transmission	[redacted]

19. Security Classif. (of this report)	20. Security Classif. (of this page)	21. No. of Pages	22. Price
Unclassified	Unclassified	237	

[redacted]